UNIVERSITA' DEGLI STUDI DI NAPOLI "FEDERICO II"

Dottorato di Ricerca in Morfologia Clinica e Patologica
XXIV ciclo
Coordinatore Prof.ssa Stefania Montagnani

TESI DI DOTTORATO

CASCATE DI SEGNALAZIONE INNESCATE DAI RECETTORI PER FORMIL PEPTIDI IN CELLULE NON FAGOCITICHE

Relatore

Prof. Rosario Ammendola

Correlatore

Prof. Germano Guerra

Dottorando

Dott. Fabio Cattaneo

ANNO ACCADEMICO 2010-2011

Indice

PREMESSA

Il recettore per N-Formil peptidi (FPR) e le sue varianti FPRL1 (FPR-like-1) e FPRL2 (FPR-like-2) appartengono alla famiglia dei recettori a sette tratti transmembrana accoppiati a proteine Gi sensibile all'azione della tossina della pertosse (PTX) (1, 2). Infatti, per tutte e tre le isoforme del recettore è possibile osservare una totale assenza di risposta delle cellule al rispettivo agonista quando queste sono preincubate con PTX (2-3). Le varianti FPR e FPRL1 sono state per la prima volta individuate in cellule fagocitiche, mentre FPRL2 è stato inizialmente individuato in monociti ed in cellule dendritiche (4-5).

Successivamente, le tre varianti di recettori per N-formil peptidi sono state identificate anche in altri tipi cellulari e tessuti sia a livello trascrizionale che traduzionale (2,3,5-7) suggerendo che tali recettori abbiano ulteriori funzioni rispetto a quelle esercitate nelle cellule polimorfonucleate (PMN).

Inizialmente si riteneva che tali recettori legassero esclusivamente peptidi N-formilati e poiché le proteine batteriche (8,9) e mitocondriali (10) sono le uniche fonti di peptidi N-formilati in natura, è stato ipotizzato che FPR e FPRL1 mediassero la migrazione dei fagociti presso i siti di infezione batterica e/o di danno tissutale. Tale ipotesi era supportata dall'osservazione che i peptidi N-formilati sono in grado di indurre il rilascio di peptidi antibatterici e specie ossidanti da parte dei fagociti (3, 11-13). Nel corso degli ultimi anni è stata identificata un'ampia varietà di ligandi non formilati, sia di natura peptidica che lipidica, in grado di interagire con i recettori FPR e FPRL1 attivando meccanismi cellulari più complessi.

I recettori per N-formil peptidi, una volta stimolati dai rispettivi agonisti, attivano un'ampia varietà di cascate di segnalazione in grado di regolare i processi di angiogenesi, proliferazione e sopravvivenza cellulare.

Risulta ormai evidente il ruolo biologico che i recettori per N-formil peptidi ricoprono nella risposta immune innata, vista la responsività che possiedono, non solo nei confronti dei metaboliti batterici e dei mediatori endogeni dell'infiammazione, ma anche per alcuni domini peptidici derivati dall'envelope del ceppo virale HIV-1. Molto probabile è inoltre un loro coinvolgimento nei meccanismi molecolari responsabili del morbo di Alzheimer e nelle malattie da prioni, vista la reattività di questi recettori verso la proteina amiloide sierica A (SAA), l'isoforma amminoacidica di 42 amminoacidi derivata dalla proteina amiloide β (A β_{42}) e verso un frammento peptidico derivato dalla proteina prionica umana (PrP 106-126) (1, 3, 14).

Infine, è stato osservato un coinvolgimento di questi recettori nelle invasioni neoplastiche di alcuni tessuti tumorali maligni, come nelle cellule di glioma e cancro anaplastico del polmone umano, dove tali recettori sembrano mediare la motilità, la crescita e anche l'angiogenesi del tessuto tumorale, grazie all'instaurarsi di loop autocrini con agonisti endogeni (15) e alla transattivazione di recettori tirosin-kinasici come EGFR (5) o c-Met.

L'espressione dei recettori per N-formil peptidi, sia a livello trascrizionale che proteico, è stata osservata anche in cellule mesenchimali staminali (MSC) dove il legame con N-fMLP induce variazioni nell'adesività cellulare alla matrice extracellulare, homing e migrazione cellulare in risposta ad un gradiente chemiotattico, spesso associato al danno tissutale.

1 INTRODUZIONE

1.1 Recettori per N-formil peptidi.

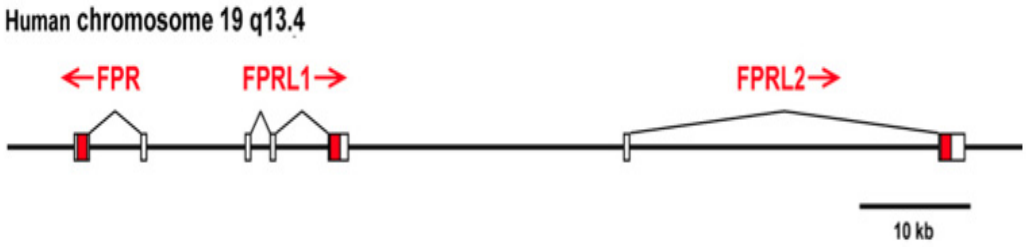

Figura 1. Organizzazione cromosomica dei geni FPR, FPRL1 e FPRL2. In bianco e in rosso sono indicate rispettivamente le porzioni non codificanti e codificanti.

I recettori per N-formil peptidi FPR, FPRL1 e FPRL2 appartengono alla famiglia dei recettori a sette tratti trans-membrana accoppiati a proteine G (GPCR) (16).

FPR è stato definito a livello biochimico per la prima volta nel 1976 come recettore ad alta affinità per il peptide N-formil-metionin-leucil-fenialanina (N-fMLF), sulla superficie dei neutrofili, ed è stato successivamente clonato nel 1990 da una libreria di cDNA di cellule leucemiche mieloidi differenziate HL-60 (2). FPR è attivato da concentrazioni picomolari di peptidi formilati, che mediano l'attività chemiotattica e la mobilizzazione intracellulare del calcio (2).

Dal punto di vista molecolare FPR è codificato da un singolo gene di circa 6 Kb con una open reading frame priva di introni, ma la regione 5' UTR è localizzata in tre esoni. Il sito d'inizio della trascrizione è separato da circa 5 Kb dal sito d'inizio della traduzione, mentre l'ipotetico promotore contiene una TATA box non consenso e un sequenza CCAAT invertita. Questo recettore è espresso non solo in cellule polimorfonucleate, dove inizialmente è stato

individuato, ma anche in una varietà di cellule non linfoidi come epatociti, cellule dendritiche, astrociti, cellule della microglia e della tunica media delle arterie coronarie (3).

Due ulteriori geni umani, noti come FPRL1 e FPRL2, sono stati successivamente isolati mediante ibridazioni a bassa stringenza, utilizzando il c-DNA di FPR come sonda (16-18). È stato osservato che i tre geni codificanti per le tre diverse isoforme sono organizzati in cluster sul braccio lungo del cromosoma 19 in posizione 19q 13.3 (16, 18) (Figura 1).

Tra FPR e FPRL1 si osserva un'omologia di circa il 69% a livello amminoacidico; in particolar modo un alto grado di identità è stato trovato nei tre loop citosolici , mentre la coda carbossilica (citosolica) e i domini extracellulari hanno un minor grado di identità. Questo suggerisce che i siti di legame al ligando (localizzati nei domini extracellulari) e le proprietà di signaling (nella coda carbossilica) differiscono tra i due recettori (19). È stato anche dimostrato che FPRL1, dopo stimolazione con alte concentrazioni di N-fMLP, favorisce solo la mobilizzazione di Ca^{2+}, ma non la chemiotassi e che FPRL1 è espresso in una più ampia varietà di cellule e tessuti rispetto a FPR.

FPRL1 è stato definito come un recettore a bassa affinità per N-fMLP, come osservato dalla sua attivazione *in vitro* solo in presenza di alte concentrazioni di N-fMLP (range μM) (12, 13). Tuttavia, non è ancora chiaro se tali concentrazioni di N-fMLP si possano generare *in vivo* nei siti di infezione e/o danno tissutale.

FPRL2 codifica per una presunta proteina che presenta una percentuale di omologia amminoacidica pari al 56% con il recettore FPR e dell' 83% con il recettore FPRL1. FPRL2 è espresso sulla membrana dei monociti e delle cellule

dendridiche, ma non dei neutrofili (4). FPRL2 non lega alcun peptide N-formilato, ma sembra legare alcuni peptidi chemiotattici non formilati in comune con FPRL1 (20, 21).

È stato inoltre dimostrato che il recettore FPRL1 può riconoscere anche molecole non correlate ai formil-peptidi e non necessariamente indicanti la presenza di microrganismi patogeni, ma piuttosto segnalanti un danno o un pericolo dal self (22). In particolare, il primo specifico agonista ad alta affinità descritto per il recettore FPRL1 è la lipossina A_4 (LXA_4), un mediatore lipidico derivante dal metabolismo dell'acido arachidonico, per cui il recettore è stato anche denominato LXA_4 receptor (22). Pertanto, FPRL1 rappresenta l'unico recettore della famiglia dei GPCR chemiotattici ad avere ligandi sia peptidici che lipidici (7, 23). LXA4 è capace di promuovere la migrazione di cellule CHO trasfettate con FPRL1 e la mobilitazione di Ca^{2+} nei monociti, ma la sua più importante attività biologica è quella di inibire le risposte infiammatorie stimolate dall'attivazione di FPRL1 da parte dei suoi agonisti, comportandosi come un mediatore antinfiammatorio (24).

La massiva presenza di questi recettori su cellule del compartimento linfocitario ne sottolinea l'importanza nella risposta immune innata, infatti, topi knok-out per tali geni presentano una maggiore suscettibilità alle infezioni, ma anche una ridotta mobilità cellulare dei neutrofili murini (2). I recettori per N-formil peptidi svolgono un ruolo importante nella risposta immune innata, visto anche il pathway di trasduzione che attivano. La via di segnalazione prevede, infatti, l'attivazione di una serie di secondi messaggeri come PI3K (fosfatidil inositolo 3 chinasi) e PLC (fosfolipasi-C), nonché le MAPK. Queste, a loro volta,

promuovono non solo uno stimolo mitogenico, ma sono anche responsabili della fosforilazione della subunità citosolica p47phox della NADPH ossidasi, che cosi genera specie reattive dell'ossigeno, contribuendo in modo significativo alla risposta immune innata.

1.2 Struttura dei recettori FPR.

La struttura dei recettori FPR, FPRL1 e FPRL2 è caratterizzata dalla presenza di tre domini extracellulari (e1-e3), importanti nel riconoscimento del ligando, tre domini intracellulari (i1-i3) coinvolti nella trasduzione del segnale all'interno della cellula, una porzione N-terminale extracellulare e una porzione C-terminale intracellulare (19, 25) (Figura 2).

Tutti i recettori chemoattrattanti GPCR dei neutrofili condividono sequenze simili nei domini transmembrana, così come in alcuni domini citosolici associati al signaling. Al contrario, le regioni dei recettori GPCR esposte sulla superficie, che conferiscono la specificità al ligando, mostrano un basso grado di similarità di sequenza. Il sito di legame extracellulare coinvolge parti diverse del recettore, in funzione del tipo di agonista riconosciuto, ma il legame degli stessi agonisti a FPR e FPRL1 non coinvolge siti strutturali identici, anche se alcuni agonisti sono comuni ai due recettori omologhi (25).

I recettori FPR sono associati a livello citoplasmatico ad una proteina G etero-trimerica (α-β-γ), sensibile a PTX, che interagisce con il recettore attivo e che si disassembla per inviare il segnale all'interno della cellula: α-GTP si dissocia dal complesso βγ ed entrambe le subunità trasducono il segnale.

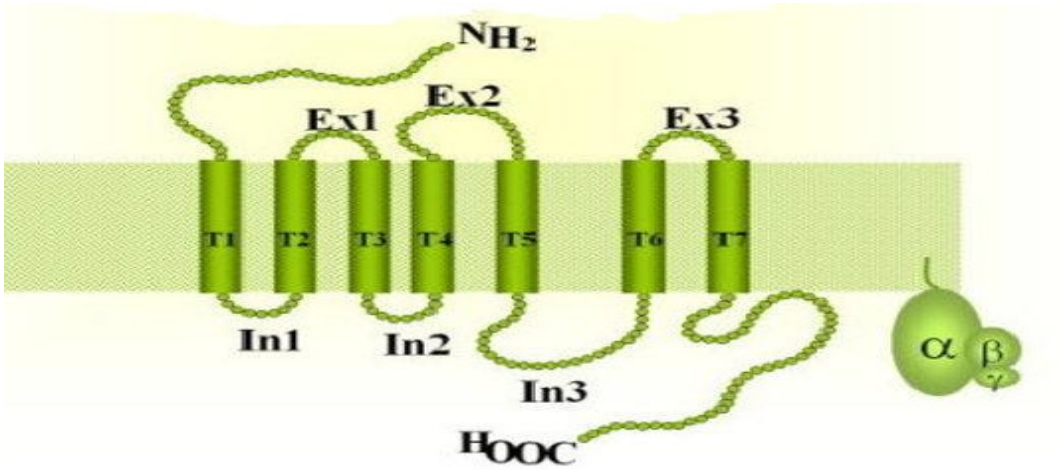

Figura 2. Struttura tipo di un recettore a sette tratti trans-membrana

I bersagli dei componenti dissociati della proteina G sono enzimi o canali ionici collocati sulla membrana plasmatica che trasmettono a valle il segnale. Si innescano così una serie di segnali molecolari e vie di trasduzione, condivise da molti altri recettori leucocitari chemoattrattanti (19). La conferma che sia FPR che FPRL1 trasducono segnali attraverso la proteina G è fornita dall'osservazione che le loro risposte sono sensibili a PTX che inattiva le proteine G attraverso ribosilazione dell'adenosina 5'-difosfato (26).

1.3 Ligandi dei recettori per N-formil peptidi

1.3.1 Agonisti

Oltre ai peptidi formilati di origine batterica (N-fMLP), anche una varietà di peptidi sintetici si è mostrata in grado di attivare i recettori FPR e FPRL1. Le prime dimostrazioni, che individuavano esclusivamente in un peptide N-formilato un agonista ottimale per tali recettori, sono state successivamente ampliate dalla

scoperta di nuovi ligandi non formilati, capaci di legare i recettori per formil-peptidi ed attivare la risposta cellulare (12, 13). Numerosi studi continuano ad individuare nuovi agonisti in grado di attivare i recettori per N-formil peptidi. Per esempio, WKYMVm, noto come peptide W, è un esapeptide modificato basato su una sequenza isolata da una libreria di peptidi random. Inizialmente è stato definito come potente stimolante di molte linee cellulari leucocitarie umane, ma anche dei neutrofili presenti nel sangue periferico (27-29). Successivamente è stato dimostrato che questo peptide utilizza il recettore FPRL1, per stimolare la risposta dei fagociti (30).

Domini capaci di interagire con i recettori per N-formil peptidi sono stati individuati anche nelle proteine dell'envelope del virus HIV-1. Tra questi i tre domini peptidici derivanti dalla proteina HIV-1 gp41 (T20/DP178, T21/DP107 e N36) rappresentano potenti agonisti con funzione chemiotattica per i recettori per N-formil peptidi. Più precisamente, T20/DP178 attiva specificamente FPR (31), T21/DP107 agisce sia su FPR che su FPRL1, verso cui ha una maggiore affinità e N36, che presenta una parziale omologia di sequenza con T21/DP107, ma che utilizza come recettore funzionale solo FPRL1(32). Altri due domini peptidici, capaci di stimolare in maniera specifica il recettore FPRL1, sono stati individuati nella proteina gp120 dell'envelope di HIV-1 (33, 34). Uno di questi, posizionato nella regione C4-V4 di gp120 (HIV-1 LAI), è costituito da una sequenza di 20 aa (peptide F), mentre l'altro dominio deriva dalla regione V3 (HIV-1 MN) ed è costituito da una sequenza di 33 aa (peptide V3).

Oltre all'individuazione di numerosi agonisti esogeni, importanti progressi sono stati fatti per identificare molecole di origine endogena capaci di interagire

con i recettori per N-formil peptidi. Tra i ligandi di origine endogena, sicuramente da menzionare sono i peptidi formilati di origine mitocondriale, che vengono rilasciati a seguito del danno cellulare, ma anche un peptide regolato dai glucocorticoidi, chiamato annessina I (lipocortina I), il cui dominio N-terminale è in grado di legare e di attivare la risposta cellulare attraverso FPR. Questi studi hanno rappresentato le prime prove della presenza di agonisti endogeni per FPR (3).

A differenza di FPR, FPRL1 sembra interagire con un maggior numero di agonisti endogeni, compreso la proteina amieloide sierica A (SAA) (35), il peptide di 42 aa derivante dall'amiloide β ($A\beta_{42}$) (36), il frammento della proteina prionica PrP106-126 (37), un frammento peptidico mitocondriale MYFINILTL, derivato dalla subunità 1 della NADH deidrogenasi (38) e LL-37 un frammento di clivaggio della proteina antibatterica catelicidina in grado di legare l'endotossina batterica (39). Tutte queste molecole sono stimoli chemiotattici e proinfiammatori per i leucociti umani.

SAA, $A\beta_{42}$ e PrP106-126 sono proteine endogene che quando si aggregano tendono a precipitare, formando depositi amiloidei responsabili di stati patologici, come l'amiloidosi sistemica (SAA), l'Alzehimer ($A\beta_{42}$) ed il morbo di Creutzfeld-Jakob (PrP106-126).

Oltre alle proteine chemioatrattanti o ai ligandi proteici, FPRL1 può interagire anche con metaboliti lipidici. Infatti, la lipossina A4 (LXA4), è in grado di legare FPRL1 e innescare una via di segnalazione apparentemente inibitoria attraverso questo recettore (40, 41). Successivamente è stato dimostrato che in neutrofili e cellule tumorali epiteliali LXA4 per arrestare la risposta pro-

infiammatoria coinvolge, non solo agonisti di FPRL1, ma anche mediatori che non usano questo recettore, come TNF-α (38).

È da evidenziare la notevole eterogeneità dei ligandi per i recettori per N-formil peptidi, visto che la maggior parte di questi agonisti, sia che siano di origine endogena o esogena, non mostrano alcuna significativa omologia fra di loro o con N-fMLP.

1.3.2 Antagonisti

Il possibile coinvolgimento dei recettori per N-formil peptidi nelle infezioni microbiche e nelle risposte infiammatorie ha promosso numerosi studi per individuare antagonisti, che risultano importanti per delineare la cascata di trasduzione del segnale associata all'attivazione del recettore, ma che rappresentano anche un punto di partenza per lo sviluppo di nuovi agenti terapeutici.

Numerosi antagonisti sono stati individuati per il recettore ad alta affinità FPR. La sostituzione del gruppo N-formilato con un t-butilossicarbonile (tBOC) o con il gruppo isopropilureido rende i peptidi capaci di bloccare l'attivazione da parte di N-fMLP dei fagociti umani, presumibilmente attraverso un legame al recettore FPR, competitivo con quello dei peptidi agonisti (42, 43). L'IC50 (inhibitory concentration 50%) per N-t-Boc-Phe-Leu-Phe-Leu-Phe-OH (tBoc-FLFLF) e per isopropilureido-FLFLF, necessaria per il blocco del legame delle cellule al ligando, è nel range di 0.44-3.7 μM. Sono stati sviluppati peptidi antagonisti per FPR più potenti, con un peso molecolare relativamente piccolo,

che mostrano valori di IC50 nel range di concentrazioni submicromolari. Tali antagonisti potrebbero avere un grosso potenziale a scopo terapeutico (44, 45).

La ciclosporina H (CsH), un peptide ciclico, è un potente e selettivo antagonista di FPR, che inibisce il legame di fMLP ai leucociti e abolisce la risposta cellulare, mediata da FPR, inclusa la chemiotassi, la mobilizzazione di Ca^{2+}, l'attivazione GTPasica e il rilascio di mediatori proinfiammatori (46-48). Recentemente sono stati descritti due ulteriori antagonisti per FPR e la sua variante per FPRL1: l'acido deossicolico (DCA) e l'acido chenodeossicolico (CDCA), che attenuano l'attivazione sia di FPR che di FPRL1 da parte dei loro agonisti (49). DCA e CDCA si legano alla membrana cellulare e potrebbero rappresentare un ostacolo sterico ed impedire l'accesso ai recettori FPR da parte dei loro agonisti. Sia DCA che CDCA sono sali biliari, la cui concentrazione è considerevolmente elevata durante la chemiotassi. Inoltre, è stato osservato che anche piccoli peptidi ricchi dell'amminoacido W, come il peptide WRW4, fungono da antagonista sulla trasduzione del segnale mediata dal recettore FPRL1 (5). Gli antagonisti endogeni o sintetici dei recettori FPR potrebbero contribuire alla soppressione della risposta antibatterica e fornire le basi per lo sviluppo di antagonisti terapeutici per contrastare l'eccessiva attivazione dei recettori FPR che può risultare essere estremamente dannosa a livello tissutale (14).

1.4 Pathway di trasduzione del segnale.

La trasduzione del segnale innescata dai recettori per N-formil peptidi è stata recentemente rivisitata (26). FPR, FPRL1 e FPRL2 sono tutti associati alla famiglia delle proteine $G_{i,}$ come dimostrato dalla totale perdita della responsività

cellulare ai loro specifici agonisti, dopo esposizione alla tossina della pertosse (50-52). I vari recettori della famiglia FPR attivano pathway di trasduzione distinti e molecole di segnalazione differenti, rendendo altamente specifiche le risposte cellulari (53).

Nei neutrofili umani, FPR e FPRL1, dopo il legame con il proprio agonista, subiscono un rapido cambio conformazionale che consente l'interazione con il complesso eterotrimerico della proteina G inattiva αβγ. Questa si dissocia nella subunità α e nel complesso βγ, capace di attivare la fosfolipasi C (PLC) (54, 55) e la fosfatidilinositolo 3-chinasi (PI3K) (3, 56, 57).

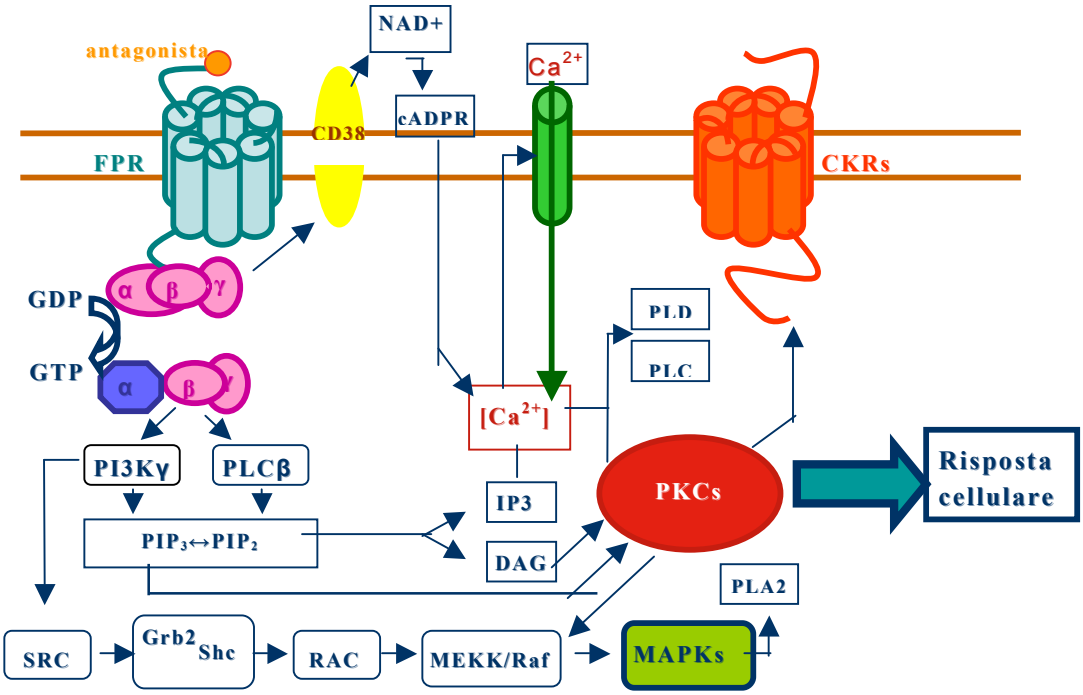

Figura 3. Pathway di segnalazione intracellare di un recettore per N-formil peptidi.

L'idrolisi dal fosfatidilinositolo 4,5 bisfosfato (PIP2), ad opera dalla PLC, genera inositolo 3-fosfato (IP_3), che rilascia il calcio conservato nel reticolo endoplasmatico e diacilglicerolo (DAG), che attiva varie isoforme della protein

chinasi C (PKC). Anche il pathway fosfatidilinositolo 3 chinasi (PI3K)- Akt/PKB risulta essere attivato, in particolar modo la PI3Kγ, che è l'isoforma maggiormente associata ai recettori per chemoattrattanti (55). Altri effettori intracellulari sono: la fosfolipasi A2 e D; le protein-chinasi attivate dai mitogeni (MAPK) ERK1/ERK2, JNK e p38MAPK, ma anche alcune proteine tirosin-chinasi (51, 55) (Figura 3).

1.4.1 Incremento del calcio citosolico e migrazione cellulare

Uno dei secondi messaggeri più importanti, a valle dei recettori FPR, è il calcio. L'incremento del livello del Ca^{2+} citosolico, infatti, sembra essere una condizione necessaria per la risposta dei neutrofili alla presenza di peptidi formilati ed è anche uno degli eventi più precocemente distinguibili quando una cellula è esposta a N-fMLP (26, 59). In neutrofili a riposo, la concentrazione citosolica del Ca^{2+} si mantiene a livelli bassi (~ 100 nM) comparata a quella extracellulare. Dopo stimolazione chemotattica la concentrazione citosolica dello ione aumenta sino a raggiungere livelli μM, per ritornare, poi, rapidamente, allo stato basale. Questo transiente aumento di calcio ha un ruolo determinante nel rimodellamento citoscheletrico di alcune proteine come l'actina, sulla quale non ha effetto polimerizzante, ma induce la formazione e la stabilizzazione dei cross-link tra i filamenti (26). Le modificazioni citoscheletriche inducono la polarizzazione dei neutrofili, le modificazioni della membrana, la fagocitosi e la chemiotassi (59).

L'aumento del calcio intracellulare è determinato, principalmente, dalla fosfolipasi β (PLC-β) uno dei bersagli molecolari della proteina G attivata dal

recettore FPR. Questa agisce sul fosfatidilinositolo 4,5-bifosfato di membrana, generando due prodotti: l'inositolo 1,4,5-trifosfato (IP_3) e il diacilglicerolo (DAG). IP_3 diffonde dalla membrana nel citosol, si lega ai canali di rilascio del Ca^{2+} a livello del reticolo endoplasmatico e li apre, determinando quindi un aumento della concentrazione del Ca^{2+} intracitoplasmatico. Il rilascio di Ca^{2+} dai depositi interni induce, inoltre, l'apertura dei canali per il Ca^{2+} sulla membrana plasmatica e, quindi, un ulteriore influsso ed un incremento dello ione all'interno della cellula.

L'aumento della concentrazione di calcio potrebbe essere conseguente anche all'azione di altri effettori. Il segnale di attivazione della proteina G sembrerebbe agire, con meccanismi non ancora ben chiari, su una glicoproteina di membrana, CD38, che catalizza la produzione di cADP ribosio, dal suo substrato NAD^+. Questa glicoproteina sembra essere un essenziale e specifico trasduttore di N-fMLF nei neutrofili murini. Infatti, i neutrofili $CD38^{-/-}$ non riescono a migrare in risposta a N-fMLF *in vitro* e ad accumularsi in un sito di infezione di *in vivo*. Il secondo messaggero cADP ribosio induce il rilascio di ioni calcio dai depositi intracitoplasmatici ed il loro influsso extracellulare, con l'effetto biologico finale di migrazione neutrofila (60).

1.4.2 Cascata delle MAPK

La cascata delle MAPK (Mitogen-activated protein kinase) è uno dei meccanismi di trasduzione cellulare maggiormente studiati. Questo pathway si ritrova in tutte le cellule eucariotiche e risulta essere implicato in diversi meccanismi fisiologici, come la crescita cellulare, il differenziamento, la

trasformazione oncogenica, la risposta immune, l'apoptosi (61), ma anche la migrazione cellulare (62).

La cascata delle MAPK è caratterizzata da un modulo centrale costituito da tre proteine chinasi che sono: una MAPK-chinasi chinasi (MAPKKK o Raf); una MAPK-chinasi (MAPKK o MEK) e una MAPK. I segnali sono trasmessi attraverso questo modulo grazie a fosforilazioni e attivazione sequenziale di questi componenti. La MAPKKK è la prima ad essere attivata in seguito all'interazione con il complesso Ras-GTP (63-66), e/o con altre proteine chinasi che connettono il modulo di attivazione delle MAPK ai recettori di membrana. Il diverso tipo di stimolo, inoltre, può determinare l'attivazione di differenti MAPK. Una volta attivata, la MAPKKK fosforila la MAPKK, una chinasi a specificità doppia che fosforila, contemporaneamente, un residuo di treonina ed uno di tirosina della MAPK. Le MAPK attivate migrano dal citosol al nucleo dove, a loro volta, attivano per fosforilazione substrati a valle, che comprendono altre proteine chinasi e fattori di trascrizione, per ottenere la risposta appropriata allo stimolo extracellulare. La cascata delle MAPK, oltre a determinare un forte stimolo mitogenico, è responsabile dell'attivazione di numerosi bersagli, tra i quali extracellular response kinases 1 e 2 (ERK 1/2), Jun N-terminal Kinases (JNK) e p38MAPK, che determinano modificazioni dell'espressione genica.

ERK 1 e 2 sono proteine di 44 e 42 kDa, con un'identità di sequenza di circa l'85% soprattutto nella regione di binding, localizzata nel core della proteina. Le ERK sono attivate dalle chinasi MEK (mitogen and extracellular signal-regulated kinases), che sono regolate, a loro volta, da recettori per fattori di crescita e tirosine chinasi, attivate attraverso Ras (67).

A seguito della traslocazione nel nucleo, le ERK sono responsabili della fosforilazione di diversi substrati, che variano in funzione dello stimolo iniziale (68).

Le JNK rispondono ad una varietà di stimoli: shock termico, shock osmotico, stimolo pro-infiammatorio mediato da citochine ed esposizione a raggi UV (69). Le JNK sono codificate da tre geni diversi, JNK-1; JNK-2 e JNK-3, i quali, a seguito di eventi di splicing alternativo, danno origine alle diverse isoforme. Le JNK sono attivate da una doppia fosforilazione a livello del motivo Thr-Pro-Tyr, ad opera di proteine leganti GTP, appartenenti alla famiglia delle proteine Rho. Diversi fattori trascrizionali nucleari, come Myc, Smad3 e p53 rappresentano alcuni dei target delle JNK (70).

Le p38 MAPK risultano essere attivate a seguito della doppia fosforilazione a carico del motivo Thr-Gly-Tyr mediante uno stimolo innescato da stress ambientali, come quello termico, osmotico, ossidativo, radioattivo ed ischemico, ma anche da citochine pro-infiammatorie e TNF. Ad oggi sono note quattro isoforme, che mostrano un'omologia di circa il 60%. Due di queste isoforme (p38α , p38β) sono espresse in modo ubiquitario. L'isoforma p38γ è espressa prevalentemente a livello del muscolo scheletrico, mentre l'isoforma p38δ è espressa nei polmoni, nei reni, nel pancreas e nel piccolo intestino (68).

La famiglia delle p38 MAPK è responsabile anche degli eventi di migrazione cellulare e rimodellamento della cromatina (71).

1.4.3 Attivazione delle proteine kinasi C

Le proteine kinasi C (PKC) sono un gruppo eterogeneo di almeno undici serine/treonine chinasi, dipendenti da fosfolipidi e caratterizzate da un'elevata similarità a livello dei loro domini catalitici, tipicamente ricchi di cisteine (72, 73). Le PKC sono costituite da una singola catena polipeptidica, su cui si ritrovano due importanti domini funzionali: un dominio C-terminale con attività chinasica, costituita da una sequenza altamente conservata e comune a tutte le proteine chinasi, e un dominio regolatore N-terminale, che interagisce con fosfatidilserina (PS), Ca^{2+}, diacilglicerolo (DAG) e altri lipidi (74). La famiglia delle PKC è costituita da isoforme tipiche (α, β_1, β_2 e γ), che sono regolate in maniera Ca^{2+}, DAG e PS dipendente, isoforme nuove (δ, ε, η e θ), che sono regolate solo dal DAG e dalla PS ed infine le isoforme atipiche (ζ, λ e ι) che sono insensibili sia al Ca^{2+} che al DAG (75).

La distribuzione intracellulare delle isoforme delle PKC suggerisce una relazione isoforma/funzione biologica specifica, ma questo livello di specializzazione è stato solo parzialmente osservato. La PKC può essere usata da diversi tipi di recettori per regolare l'attivazione delle MAPK, la cui fosforilazione ha un importante impatto sui processi citoplasmatici, nucleari, citoscheletrici e di membrana (68).

Vista l'ubiquitaria espressione della PKC e la diversità del citoscheletro nei differenti tipi cellulari (76), non sorprende che la PKC mostri associazione e attività fosforilante con un'ampia gamma di componenti citoscheletriche. Infatti, il cross-linking tra la PKC e le proteine citoscheletriche di membrana è importante nel contesto di numerose funzioni cellulari. La PKC, insieme alle PI3K, attiva

integrine e altre molecole di adesione, così da stabilizzare le connessioni strutturali ai filamenti di actina (77).

L'attivazione delle isoforme della PKC è generalmente associata alla traslocazione da un compartimento cellulare ad un altro (78, 79).

Infine, il coinvolgimento di membri della famiglia di PKC nell'attivazione e nella regolazione della NADPH ossidasi è stato proposto da numerosi studi che dimostrano che p47phox è un substrato di PKC e che partecipa alla cascata di segnale tra il recettore per formil-peptidi e l'attivazione della NADPH ossidasi. Recentemente è stato anche dimostrato che neutrofili di topi knock-out per la PKC beta presentano un decremento del 50% nel livello di produzione di superossido comparato ai neutrofili di topi normali (79). È chiaro, quindi, che PKC ha un ruolo determinante nell'attivazione della NADPH ossidasi e nella generazione di specie reattive dell'ossigeno.

1.4.4 Attivazione della NADPH ossidasi

L'attivazione del complesso multimerico della NADPH ossidasi e la conseguente generazione di specie reattive dell'ossigeno (ROS) (80, 81) rappresenta una delle più importanti risposte biochimiche innescate dalla stimolazione dei recettori per N-formil peptidi.

Inizialmente il complesso della NADPH ossidasi è stato isolato e caratterizzato nei fagociti, ma successivamente è stato identificato anche in numerose altre popolazioni cellulari. Questo complesso multimerico sfrutta gli elettroni provenienti dall'ossidazione del NADPH intracellulare, per generare anione superossido, secondo la reazione:

$$2\ O_2 + NADPH \rightarrow 2\ O_2^- + NADP^+ + H^+$$

Successivamente, l'anione superossido dismuta in perossido di idrogeno (H_2O_2) e altre specie reattive durante il cosiddetto oxidative burst. Tali molecole vengono generalmente utilizzate come primo mezzo di difesa nei confronti di batteri e funghi patogeni, visto il loro elevato potere microbicida (80).

La NADPH ossidasi, nei fagociti, è costituita da almeno sei subunità: gp91phox, una glicoproteina che costituisce la subunità catalitica, p40phox, p47phox, p67phox, p22phox (phox indica PHagocyte OXidase) ed infine da una piccola GTP-asi come Rac1 o Rac2 (82).

Nelle cellule resting l'ossidasi è inattiva e le subunità p40phox, p47phox e p67phox sono localizzate nel citosol. Le subunità p22phox e gp91phox sono, invece, espresse a livello della membrana cellulare, di vescicole secretorie e granuli specifici, dove costituiscono una flavoemeproteina, nota come citocromo b_{558} (80). Questo possiede due distinti gruppi eme ed un gruppo flavinico (FAD), che funge da intermedio nel trasporto di elettroni. Infatti, l'attività ossidasica risulta essere assente sia in seguito alla rimozione del FAD dall'enzima, che in seguito ai trattamenti con antagonisti flavinici, come il difenilene iodonio (DPI) (81).

Il flusso di elettroni che porta alla riduzione finale dell'ossigeno e alla formazione dell'anione superossido prevede un meccanismo a due stadi: dal NADPH al FAD (stadio1); dal FAD al gruppo eme del cyt b_{558} (stadio 2) ed infine all'ossigeno molecolare (82).

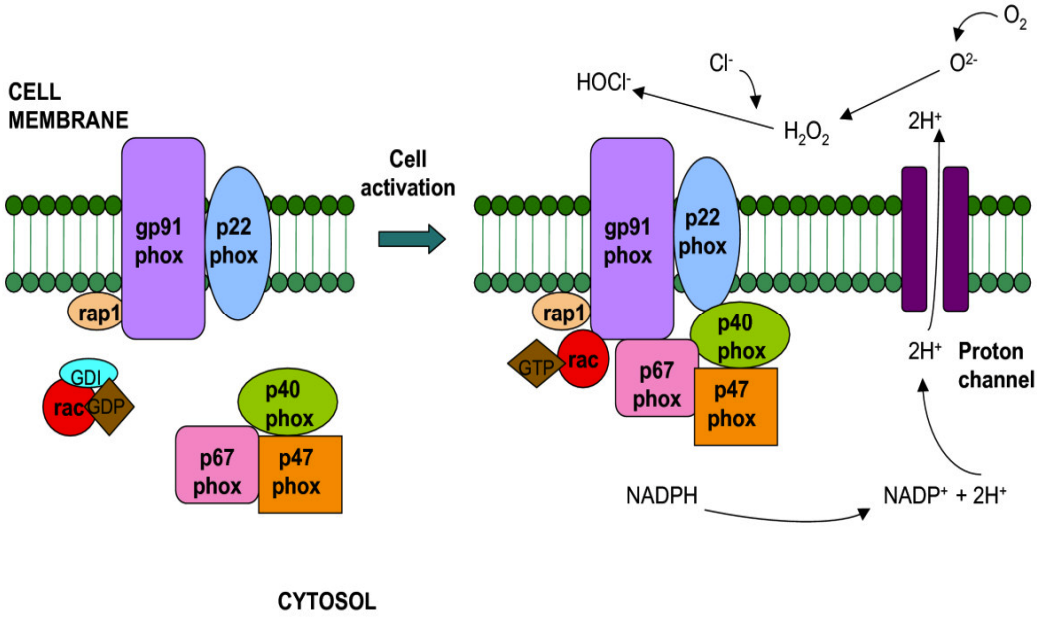

Figura 4. Attivazione della NADPH ossidasi e generazione di anione superossido

Quando una cellula resting viene esposta ad una serie di stimoli, le subunità p47phox, p40phox e p67phox vengono fosforilate e successivamente traslocano sulla membrana (Figura 4).

La fosforilazione a carico di tali subunità è responsabile di un cambiamento conformazionale, che porta ad un riarrangiamento del complesso p47phox-p40phox-p67phox che trasloca a livello della membrana, dove si verifica la sua associazione con Rac-GTP ed il citocromo b_{558} e permettono l'attivazione della NADPH ossidasi (82).

Il ruolo di p67phox, sembra essere quello di piattaforma molecolare che collega la subunità p47phox con la p40phox (83).

La subunità citosolica p47phox, invece, può essere considerata una subunità regolatoria del complesso enzimatico, poiché la sua fosforilazione consente la traslocazione delle componenti citosoliche del complesso della NADPH ossidasi; inoltre, p47phox è presente, a livello cellulare, sia in forma

libera che complessata alle altre subunità citosoliche dell'ossidasi, quali p40phox e p67phox (79). La subunità p47phox è fosforilata su siti multipli grazie all'azione di varie chinasi (80, 84).

Evidenze, sia biochimiche che genetiche, suggeriscono che la fosforilazione di p47phox induce dei cambiamenti conformazionali, che eliminano un'interazione intramolecolare con funzione inibitoria tra i domini SH3 interni (82) (Figura 5).

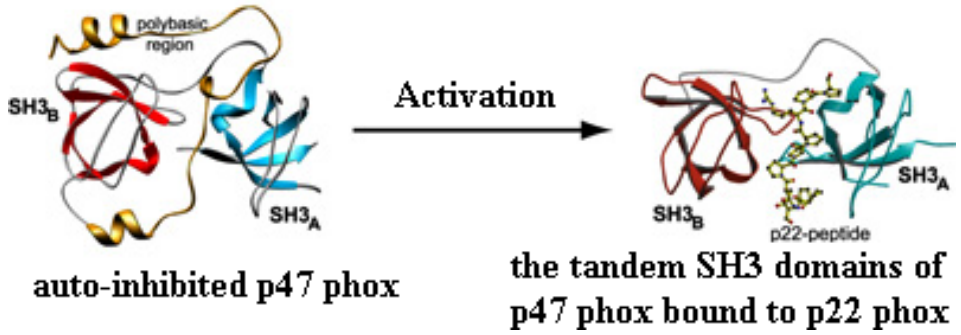

Figura 5. Cambiamento conformazionale di p47phox dallo stato inattivo auto-inibito allo stato attivo

p40phox presenta domini PX (PHOX) che legano fosfatidilinositoli, cruciali per il reclutamento di p47phox dal citosol alla membrana. Molti domini PX contengono anche un motivo Pro-X-X-Pro, che lega i moduli del dominio SH3. Ciò suggerisce che i domini PX siano bifunzionali, in quanto coordinano sia la localizzazione delle subunità a livello della membrana, che l'evento dell'assemblaggio. Durante l'attivazione della NADPH ossidasi, circa 8-9 residui di serina, presenti all'estremità C-terminale di p47phox, vengono fosforilati. Tra questi, la fosforilazione della serina 379 è condizione necessaria sia per la traslocazione di p47phox, che per l'attivazione dell'enzima. Recentemente è stato

dimostrato come anche la fosforilazione delle serine 303, 304 e 328 rappresentino un evento importante per l'attivazione della subunità p47phox, in quanto questi residui, nello stato non fosforilato, contribuiscono sostanzialmente al mantenimento della conformazione auto-inibita della molecola. La fosforilazione di molteplici residui di serina di p47phox è, quindi, necessaria a destabilizzare la conformazione auto-inibita fornendo un importante meccanismo di controllo che previene un'inappropriata attivazione dell'attività ossidasica.

Le ERK sono coinvolte nella fosforilazione di p47phox e rappresentano uno dei bersagli della PKC nella via di trasduzione attivata da FPR. Questo spiega come la stimolazione del recettore per formil-peptidi porti all'attivazione dell'enzima NADPH ossidasi e alla generazione di specie reattive dell'ossigeno.

Un ulteriore controllo nel processo di attivazione della NADPH ossidasi è determinato dalla graduale dissociazione e successiva traslocazione sulla membrana della GTPasi Rac (Rac1 nel 4% o Rac2 nel 96% dei casi circa) e dai complessi citosolici formati con Rho GDP dissociation Inhibitor (GDI), a cui è legata quando la cellula è a riposo. La traslocazione di Rac avviene secondo un meccanismo indipendente dalla traslocazione del complesso p47phox-p67phox, ma comunque ad esso coordinato (85-87). È stato dimostrato che la transiente espressione di Rac, costitutivamente attivato, è sufficiente ad indurre la traslocazione sulla membrana delle componenti citosoliche dell'ossidasi ed a determinare l'assemblaggio di un'ossidasi attiva. Questi dati rafforzano l'idea sul compito di Rac GTPasi di coordinare la traslocazione del complesso p47phox-p67phox, in associazione alla simultanea traslocazione cinetica osservata per i tre fattori citosolici (88). È possibile, inoltre, che Rac abbia anche un'attività

regolatoria sull'attivazione di p47phox. Questo potrebbe avvenire grazie alla capacità di Rac di controllare l'attivazione di chinasi bersaglio come p21-activated kinases (PAK), a loro volta capaci di modulare la fosforilazione di p47phox. Questa ipotesi deve ancora essere opportunamente dimostrata.

p67phox si ritrova complessato con p47phox a livello citosolico e tale interazione è richiesta per la traslocazione di p47phox a livello della membrana. Una volta che il complesso si è posizionato sulla membrana, p67phox interagisce con Rac e con il citocromo b_{558} per sostenere la catalisi, tramite un meccanismo non ancora conosciuto; ma p67phox è sicuramente essenziale per il funzionamento del complesso enzimatico. Analisi di mutanti di delezione, infatti, hanno identificato un dominio di attivazione (aa 199-210 e forse anche aa 187-193), che è richiesto per la formazione del complesso enzimatico sul citocromo $b_{558.}$ Questo dominio, inoltre, regola il trasferimento di elettroni dall'NADPH al FAD, legato al citocromo (80).

La funzione di p40phox, invece, non è ancora ben chiara, in quanto può agire come attivatore o come inibitore, a seconda del sistema sperimentale; probabilmente ha un ruolo di adattatore molecolare, che facilita l'assemblaggio del complesso. Inoltre, ci sono alcune evidenze che inducono a supporre che p40phox può stabilizzare p67phox ed agire come modulatore generale dell'attività della NADPH ossidasi (23).

1.4.5 Generazione di radicali liberi

La generazione di ROS ad azione battericida da parte delle cellule polimorfonucleate, in sede di infiammazione, è fondamentale per la risoluzione

dell'infezione e per l'inattivazione dell'agente patogeno che causa l'evento lesivo. Le specie coinvolte comprendono: l'anione superossido prodotto dalla NADPH ossidasi attiva; il perossido di idrogeno, che si forma per trasformazione del superossido; l'ipoclorito di sodio, altamente tossico per i batteri, che si forma dal perossido di idrogeno, in presenza di alogenuri ad opera dell'enzima mieloperossidasi, e che è rilasciato dai granuli azzurrofili del fagocita. Questi intermedi e i loro prodotti di reazione possono iniziare e amplificare la risposta infiammatoria, generando fattori chemotattici per i fagociti, indirettamente (ad esempio il leucotriene B4, attraverso la via lipossigenasica) o direttamente, reagendo con i lipidi insaturi. Essi, inoltre, possono potenziare la lesione tissutale attraverso l'aumento dell'attività proteasica lisosomiale dei leucociti attivati (legata alla fagocitosi) e attraverso le alterazioni della matrice extracellulare (gli anioni superossido, ad esempio, sono in grado di depolimerizzare l'acido ialuronico). Pertanto, nei focolai infiammatori la matrice strutturale del tessuto può essere danneggiata dai radicali dell'ossigeno, in presenza o in assenza di proteasi lisosomiali. L'integrità del meccanismo di produzione di superossido da parte dei fagociti, difesa primaria contro le infezioni batteriche, può essere enfatizzata in alcune condizioni patologiche di cronicizzazione infiammatoria, per cui i mediatori dell'effetto battericida diventano mediatori degli effetti citotossici e istotossici dei leucociti attivati.

Le cellule, per proteggersi, dal danno ossidativo si servono di una serie di sistemi enzimatici antiossidanti quali:

- la superossido dismutasi (SOD) che rimuove il radicale superossido trasformandolo in H_2O_2.

- la catalasi che da due molecole di H_2O_2 forma H_2O e O_2.
- la perossidasi che ha la stessa azione della precedente ma richiede la presenza di un cosubstrato riducente(RH_2) diverso dall'H_2O_2 come donatore di elettroni.

Simile ruolo protettivo è svolto anche da tutti i composti contenenti gruppi sulfidrilici (-SH), come ad esempio il glutatione e la cisteamina, che cedono facilmente alle molecole ossidanti l'idrogeno, che in queste è fissato da un legame debole allo zolfo. La reazione è catalizzata dall'enzima glutatione-S-trasferasi, che trasferisce un atomo di idrogeno dal gruppo sulfidrilico delle molecole che lo contengono agli agenti ossidanti. Unitamente a questi sistemi enzimatici sono presenti molecole con caratteristiche intrinseche antiossidanti, come l'α-tocoferolo, che impedisce la propagazione delle reazioni radicaliche nell'autossidazione dei lipidi insaturi sulle membrane cellulari; l'ascorbato, presente nel citosol e nel liquido extracellulare; l'urato e la bilirubina, che sono coinvolte principalmente nell'eliminazione dei radicali liberi dal plasma.

Nonostante la presenza di queste molecole con proprietà antiossidante e protettiva dei tessuti, la generazione di radicali liberi da parte delle cellule, durante i processi infiammatori, ma anche in numerosi altri processi cellulari, come la respirazione mitocondriale, può condurre ad un loro progressivo accumulo che può compromettere importanti funzioni fisiologiche e danneggiare i tessuti. I radicali liberi sono, infatti, per la loro forte reattività, in grado di interagire praticamente con tutte le macromolecole presenti nelle cellule, determinando ossidazione dei gruppi tiolici, modificazioni chimiche degli acidi nucleici, perossidazione dei lipidi insaturi delle membrane biologiche,

autossidazione degli zuccheri, interazione tra perossidazione dei lipidi, dei glucidi e dei protidi, alterazioni cellulari dello stato redox e di quello energetico. Più in generale, è stato messo in evidenza che condizioni ossidanti elevate sono di per sé un fattore potenziale di lesione cellulare. Considerando il coinvolgimento eziologico dei radicali liberi in numerosissime patologie e considerando il substrato infiammatorio comune in diversi stati morbosi, il ruolo dei recettori FPR, in alcuni stati patologici, potrebbe essere quello di esacerbare la risposta infiammatoria, portando all'aumento del reclutamento leucocitario ed alla produzione di mediatori infiammatori, ma anche all'eccessiva produzione di radicali liberi, con esteso danno tissutale (22).

Tuttavia, nel complesso delle ricerche eseguite, risulta che i ROS non sono soltanto mediatori del danno tessutale, ma possono anche fungere da intermedi metabolici o secondi messaggeri in percorsi cellulari di segnalazione. Essi, infatti, esercitano un'importante azione regolatoria di diverse funzioni cellulari, che comprendono l'espressione genica, la crescita cellulare, la trasduzione di segnali biologici e, naturalmente, la difesa contro patogeni esterni. La loro generazione, entro determinati limiti, è essenziale per mantenere l'omeostasi cellulare. Inoltre, è stato dimostrato che i ROS sono coinvolti nell'attivazione di recettori tirosina kinasi (RTK) (89, 90). Infatti, i ROS mediano l'inibizione dell'attività delle fosfotirosine fosfatasi (PTPase) sbilanciando l'equilibrio dello stato di fosforilazione degli RTK verso uno stato fosforilato (5).

1.5 I recettori per N-formil peptidi e i tumori

L'espressione dei recettori per N-formil peptidi è stata osservata anche in alcune linee cellulari tumorali.

In linee cellulari di astrocitoma, è stata dimostrata l'espressione di recettori ad alta e a bassa affinità per N-fMLP ed esperimenti di RT-PCR hanno confermato l'espressione dei trascritti di FPR e di FPRL-1. FPR è espresso selettivamente nella linea cellulare di glioblastoma altamente maligna U-87, ma anche in quelle di glioblastoma multiforme e di astrocitoma anaplasitco. In queste linee cellulari N-fMLP induce una forte mobilizzazione del Ca^{2+}, ma anche un aumento della secrezione di IL-6, la cui variazione risulta essere sensibile alla tossina della pertosse. Le cellule U-87 rispondono agli agonisti dei recettori per N-formil peptidi, aumentando la motilità, la proliferazione cellulare e la produzione di VEGF. Inoltre, la stimolazione con fMLP determina anche un aumento dei livelli di fosforilazione delle ERK, delle p38MAPK e delle JNK, ma anche di Akt, che è localizzato a valle del pathway della PI_3K e che contribuisce alla sopravvivenza delle cellule tumorali e alla loro proliferazione[1].

La stimolazione di FPR con N-fMLP induce anche la traslocazione nucleare del fattore trascrizionale HIF-α e la formazione del complesso di NF-kB, costituito dalle subunità p50 e p65. HIF-α è un fattore trascrizionale, capace di aumentare l'espressione del gene VEGF, che recluta le cellule endoteliali vascolari e, quindi, promuove l'angiogenesi.

Anche il fattore trascrizionale STAT3 risulta implicato nell'angiogenesi dei tumori maligni ed è associato al signaling di alcuni GPCR per chemoattrattanti. Nelle cellule di glioblastoma, N-fMLP induce una rapida e transiente

fosforilazione di STAT3 sia a livello del residuo di Tyr 705 che di Ser 727; inoltre, il trattamento con inibitori delle tirosin chinasi AG490 blocca il signaling Jak/STAT e previene la crescita delle cellule U-87 stimolata da N-fMLP. È stato osservato anche che l'attivazione dei pathway innescati da FPR può aumentare la sopravvivenza delle cellule di glioblastoma aumentando i livelli di Bcl-2, che interferisce con il rilascio del citocromo c dai mitocondri e con l'attivazione delle procaspasi 9. L'espressione dei recettori per N-formil peptidi nelle linee cellulari U-87 di glioblastoma maligno e BT325 è correlata con il progredire della malignità delle cellule tumorali (1).

Questi dati indicano che i recettori per N-formil peptidi possono rappresentare un eventuale target farmacologico, perché in grado di mediare la proliferazione, la sopravvivenza e la migrazione di cellule tumorali.

1.6 Transattivazione di RTK mediata da GPCR

Sulla superficie cellulare sono presenti diversi tipi di recettori trans-membrana, tra i quali i GPCR e i recettori tirosin-kinasici (RTK) sono maggiormente espressi.

La stimolazione di un GPCR determina l'attivazione di una serie di cascate di segnalazione che culminano con la modulazione dei secondi messageri: adenosina monofosfato ciclica (cAMP), proteina kinasi C (PKC), Ca^{2+} ed una serie di molecole intermedie come fosfatidilinositolo 3-kinasi (PI3K), specie reattive dell'ossigeno (ROS), MAPK, Pyk2 e Src (91).

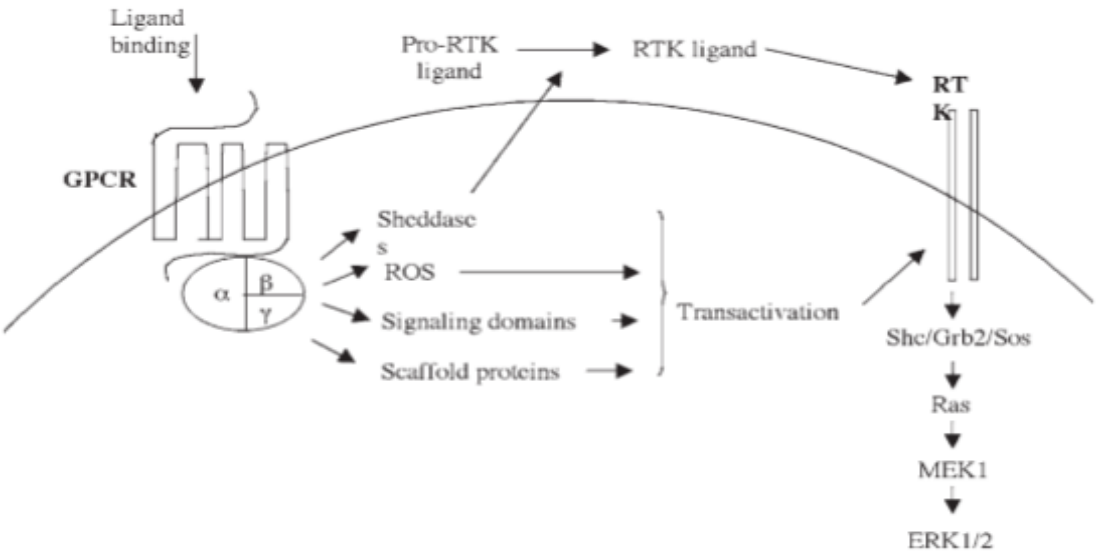

Figura 6. Rappresentazione schematica della transattivazione di un RTK mediata da un GPCR

I recettori tirosin kinasi sono proteine trans-membrana che attraversano la membrana una volta sola, i cui ligandi comprendono fattori di crescita e insulina. Dopo opportuna stimolazione da parte del proprio agonista, il recettore dimerizza, attivando il proprio dominio tirosina kinasi che autofosforila il recettore a livello dei residui di tirosina citosolici. Questi, a loro volta, fungono da siti di legame per una serie di proteine coinvolte nelle relative cascate di segnalazione intracellulare. Queste vedono coinvolte le proteine Shc, Grb2 e Sos che mediano l'attivazione di Ras e del pathway delle MAPK (92, 93).

Inizialmente si riteneva che GPCR e RTK ed i loro rispettivi effettori del segnale, attivassero cascate di segnalazione lineari e distinte tra loro e che convergevano su target comuni a valle della cascata di segnalazione, come ad esempio le MAPK. È stato successivamente osservato che i pathway attivati da GPCR e RTK non sono mutuamente esclusivi tra loro e che spesso agiscono in maniera sinergica presentando numerosi punti di interazione non solo a monte e a

valle della cascata di segnalazione (94, 95). In questo modo, il coinvolgimento di molecole comuni a più cascate di segnalazione, determina un'integrazione dei diversi stimoli attraverso una complessa cross-comunicazione definendo un sistema di controllo più intricato dei meccanismi che regolano la proliferazione, il differenziamento, la crescita e la sopravvivenza cellulare.

I GPCR possono instaurare crosstalk con un RTK in differenti modi. In alcuni casi è stato dimostrato che la stimolazione diretta di un GPCR determina la fosforilazione delle tirosine di un RTK e la sua conseguente attivazione mediante un fenomeno conosciuto come "transattivazione" (96, 97). L'aumentata dimerizzazione dei RTK determina il reclutamento di proteine regolatrici come Shc, Grb2 e Sos che attraverso il dominio di omologia Src 2 (SH2) interagiscono con le tirosine citosoliche fosforilate del recettore venendo a loro volta attivate.

Negli ultimi anni, sono stati identificati diversi meccanismi in grado di indurre la transattivazione di un RTK ad opera di un GPCR (Figura 6). È stato dimostrato, infatti, che molecole come PKC, Src e ROS possono mediare la transattivazione di un RTK. Inoltre, uno dei più recenti meccanismi molecolari di transattivazione individuati è quello che vede l'attivazione da parte di un GPCR di proteine chiamate "shaddasi" che clivano il ligando di un RTK nella sua forma attiva rendendolo in grado di legare e stimolare il recettore bersaglio (98).

1.6.1 EGFR: struttura e pathway di trasduzione

Il gene umano per EGFR è collocato sul braccio corto del cromosoma 7 in posizione 7p11.2 e codifica per un recettore per fattori di crescita transmembrana di tipo 1 con attività tirosin kinasica del peso di 170 kDa (99). EGFR appartiene

alla famiglia degli RTK HER/erbB, che comprende HER1 (EGFR/erbB1), HER2 (neu, erbB2), HER3 (erbB3) e HER4 (erbB4). Questi recettori possiedono una struttura molecolare molto simile, infatti, hanno un sito di legame ricco in cisteine; un domino transmembrana a singola α-elica; un dominio citoplasmatico con attività tirosin kinasica e un dominio carbossi-terminale di segnalazione intracellulare (100).

La stimolazione di EGFR determina la sua omodimerizzazione e/o eterodimerizzazione con altri membri della famiglia, seguita dall'attivazione del dominio tirosin kinasico che autofosforilando i domini citosolici rende possibile l'interazione con proteine adattatrici che mediano l'attivazione delle cascate di segnalazione intracellulari (101). Le cascate di segnalazione intracellulare vedono attivati principalmente il pathway RAS-RAF-MEK-MAPK, PI3K-PTEN-Akt e l'attivazione del fattore trascrizionale STAT (signal transducer and activator of transcription) (102). Le cascate di segnalazione intracellulare attivate da EGFR regolano principalemente la proliferazione, l'angiogenesi, la metastatizzazione e la sopravvivenza cellulare (Figura 7) (103).

L'attività tirosin kinasica di EGFR può essere alterata da diversi meccanismi oncogenici che comprendono mutazioni geniche di EGFR, incremento del numero di copie del gene e iper-espressione della proteina EGFR (104). L'attivazione impropria di EGFR inibisce l'apoptosi delle cellule tumorali favorendone la progressione (105). EGFR può anche interagire con il pathway delle integrine (106, 107) e attivare le metalloproteasi della matrice alterando i meccanismi di adesione cellulare, stimolando la motilità cellulare e promuovendo i processi di metastatizzazione (108).

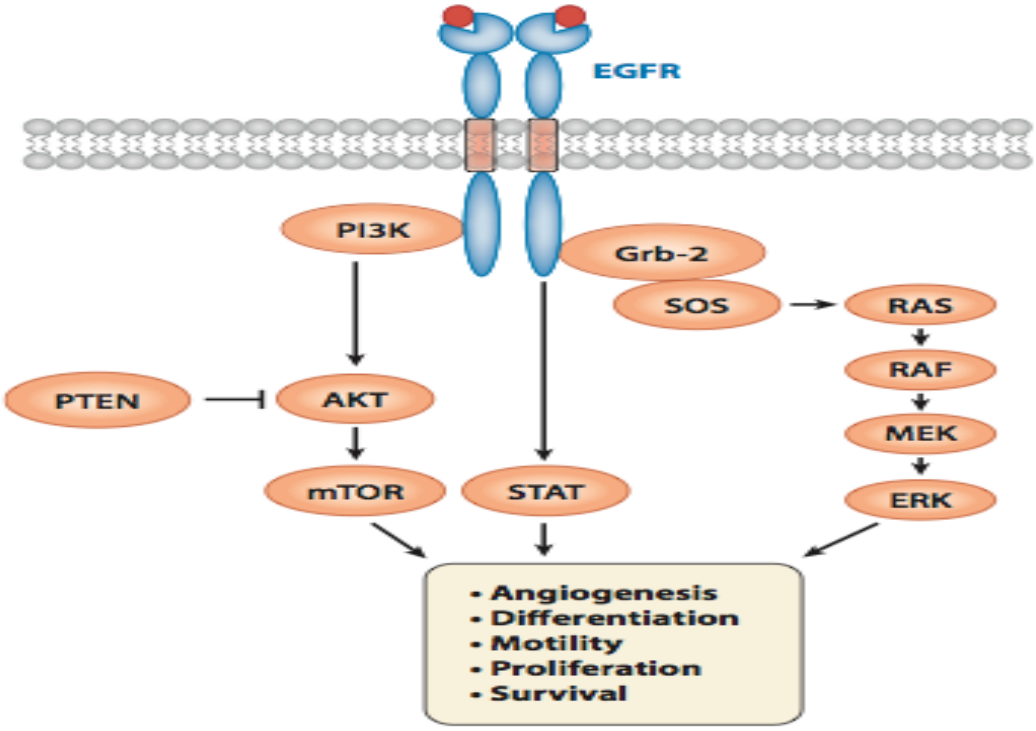

Figura 7. Schema rappresentativo delle cascate di segnalazione intracellulare associate ad EGFR.

L'acquisizione di funzione o mutazioni attivanti il gene di EGFR ricorrono in alcuni NSCLC (non Small Cancer Lung Cell), determinando un'attivazione costitutiva dell'attività tirosin kinasica di EGFR. Queste evidenze suggeriscono un ruolo strategico di EGFR nei processi di angiogensi, migrazione, sopravvivenza e proliferazione cellulare eleggendolo target farmacologico in numerosi processi tumorali.

1.6.2 C-Met: struttura e pathway di trasduzione

Il recettore per il fattore di crescita epatico (HGF) o scatter factor (SF), noto anche come c-Met, fu definito inizialmente come un proto-oncogene. Il gene Met è stato mappato sul braccio lungo del cromosoma 7 in posizione q21-31 e codifica

per una proteina di 1408 aa che manca di una significativa omologia di sequenza con gli altri recettori tirosin kinasici per fattori di crescita fino ad ora conosciuti (106).

Tale recettore è costituito da una catena di 50 kDa (α) unita tramite un ponte disolfuro ad una catena di 145 kDa (β) con cui forma un complesso αβ di 190 kDa. La catena α non attraversa la membrana cellulare ed è esposta all'ambiente extracellulare, mentre la catena β attraversa la membrana cellulare e possiede domini intracellulari tirosin kinasici (106-109). Il segmento intracellulare della catena β è composto da tre porzioni: una sequenza juxtamembrana che downregola l'attività tirosin kinasica in seguito alla fosforilazione del residuo di Ser in posizione 975; una regione catalitica che regola positivamente l'attività kinasica in seguito alla fosforilazione dei residui di Tyr in posizione 1234 e 1235; e un sito di legame multifunzionale in posizione carbossi-terminale che presenta due Tyr in posizione 1349 e 1356, che se fosforilate possono reclutare diverse proteine adattatrici e trasduttori del segnale (110).

L'osservazione che il ligando HGF/SF possa agire da fattore di crescita (HGF), da scatter factor (SF) e da regolatore morfogenico dimostra che tale ligando può comportarsi in differenti modi, attivando diversi processi cellulari che tuttavia non sono mutualmente esclusivi tra di loro.

Il legame di HGF/SF al recettore c-Met induce l'autofosforilazione delle tirosine citosoliche della catena β (111). Le proteine coinvolte nell'attivazione delle cascate di segnalazione intracellulare si complessano al recettore attivato attraverso un Src homology domain (SH) di tipo 2, come ad esempio PLC-γ; Ras-GAP, PI3K, $pp60^{c\text{-}src}$ e GRB2-Sos (112-115). Infatti, è stato dimostrato che la

sequenza amminoacidica contenuta nei domini SH2 di numerose proteine è in grado di legare le fosfotirosine del recettore c-Met (112,116,117). Poiché, una volta attive, le proteine dotate di un dominio SH2 possono attivare a loro volta differenti fosfopeptidi di segnalazione intracellulare, è possibile comprendere l'eterogenità di risposte cellulari a cui una cellula, che esprime un recettore c-Met, può andare incontro (Figura 8).

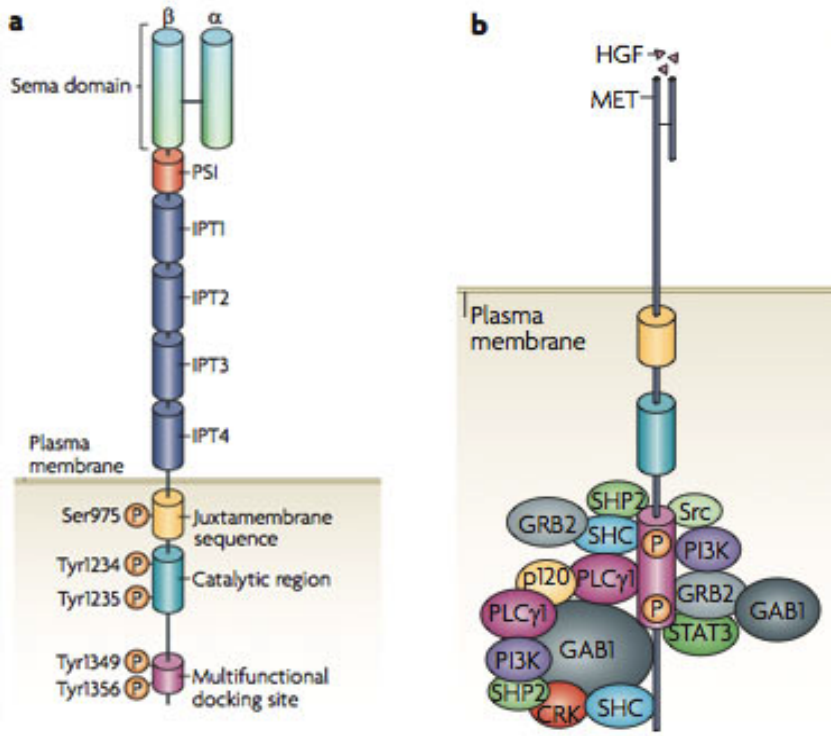

Figura 8. Struttura del recettore c-Met (A). Eterogeneità dei mediatori e trasduttori del segnale associati a c-Met (B).

2 OBIETTIVI DELLA TESI

Gli studi condotti nel corso del Dottorato sono stati rivolti al ruolo del recettore per N-formil peptidi FPRL1 in cellule non appartenenti al compartimento polimorfonucleato (PMN). In particolar modo sono state analizzate:

I. L'espressione sia trascrizionale che traduzionale dei recettori per N-formil peptidi in cellule epiteliali polmonari (IMR-90), di cancro anaplastico del polmone (CaLu-6) e cellule epiteliali di prostata (PNT1A).
II. Le cascate di segnalazione intracellulare innescate da FPRL1 in seguito alla stimolazione con gli agonisti sintetici WKYMVm e N-fMLP oppure con la catelicidina LL-37.
III. Il contributo di FPRL1 nella proliferazione cellulare tumorale delle linee cellulari di glioblastoma U-87 e di cancro anaplastico del polmone CaLu-6.
IV. La capacità di FPRL1 di transattivare alcuni recettori tirosin kinasci (EGFR e c-Met) nonché i meccanismi molecolari responsabili della transattivazione.
V. Le cascate di segnalazione associate ai recettori tirosin kinasici in seguito alla loro transattivazione mediata da FPRL1.

I risultati hanno dimostrato l'espressione di un recettore FPRL1 funzionalmente attivo nelle linee cellulari IMR-90, CaLu-6 e PNT1A. La stimolazione di FPRL1 con il suo agonista sintetico selettivo WKYMVm oppure con LL-37 e l'utilizzo di specifici inibitori hanno consentito di dissezionare i pathway di

trasduzione attivati nelle linee cellulari IMR-90, CaLu-6 e PNT1A. In cellule IMR-90 è stato dimostrato che il legame della catelicidina LL-37 con FPRL1 innesca il pathway delle ERK, e l'attivazione della NADPH ossidasi, espressa in queste cellule, attraverso un meccanismo molecolare associato alla mobilizzazione del Ca^{2+}.

Il contributo di FPRL1 nella regolazione della proliferazione e del ciclo celulare è stata studiata nella linea cellulare di glioblastoma U-87, analizzando l'espressione degli inibitori dei complessi ciclina/CDK (CKI), $p21^{waf1/cip1}$ e $p16^{INK4A}$.

Lo studio della capacità di FPRL1 di transattivare recettori tirosin kinasici è stato effettuato sulle linee cellulari CaLu-6 e PNT1A. In particolar modo, nella linea cellulare CaLu-6 è stato dimostrato che la stimolazione di FPRL1 con WKYMVm innesca la transattivazione di EGFR, espresso in maniera abbondante in queste cellule, in assenza di EGF. Il meccanismo molecolare osservato prevede, la fosforilazione di STAT3 e di Src, nonché la generazione di anione superossido mediato dalla NADPH ossidasi. L'incremento del rate di proliferazione cellulare rappresenta una delle risposte cellulari a valle.

In cellule PNT1A è stata osservata l'espressione di un recettore FPRL1 funzionalmente attivo. La stimolazione con WKYMVm determina la transattivazione del recettore c-Met, espresso significativamente in queste cellule, in assenza del suo ligando HGF.

La transattivazione dei recettori c-Met ed EGFR indotta dalla stimolazione di FPRL1 dipende dalla generazione di ROS. Infatti, nel lavoro di tesi, è stato dimostrato che inibitori specifici della NADPH ossidasi, o il silenziamento della subunità catalitica della NADPH ossidasi p22phox mediante specifici siRNA

previene la transfosforilazione dei domini tirosina kinasi citosolici di entrambi i recettori.

I risultati ottenuti nel corso del dottorato dimostrano nuove funzioni per FPRL1 diverse da quelle che li vedono coinvolti nella risposta immune innata, suggerendo il loro coinvolgimento in diversi processi fisiopatologici che includono il controllo del ciclo cellulare. Ulteriori studi saranno necessari per identificare nuovi approcci farmacologici volti a prevenire l'attivazione di FPRL1 e le relative cascate di segnalazione intracellulare.

3 MATERIALI E METODI

3.1 Colture cellulari e trattamenti

I peptidi WKYMVm (PW), WRWWWW (WRW4), LL-37, fMLP sono stati sintetizzati e purificati mediante HPLC dalla PRIMM (Milano, Italia). I reagenti per SDS-PAGE sono stati forniti dalla Bio-Rad (Hercules, CA, USA). Gli anticorpi, anti-fosfo-ERK1/2, anti-tubulina, anti-c-Src, anti-$p21^{waf1/cip1}$ anti-$p16^{INK4A}$, anti-$p27^{kip1}$, anti-p47phox, anti-PKC-α, anti-PKC-δ, anti-FPRL1, anti-EGFR, anti-cMet, anti-STAT3, anti-ciclina A, anti-p-Y, anti-Rabbit e la proteina A/G Plus agarose sono stati procrastinati dalla Santa Cruz Biotechnology (Santa Cruz, CA, USA). Gli anticorpi anti-p-c-Src (Tyr416), anti-p-Akt (Ser473), anti-p-STAT3 (Tyr705) e anti-p-STAT3 (Ser727) sono stati forniti da Cell Signaling Technology (Danvers, MA, USA). La proteina A–horseradish peroxidase e l'anticorpo anti-mouse Ig–horseradish peroxidase sono stati ordinati presso Amersham Pharmacia Biotech (Little Chalfont, 171 Buckinghamshire, UK). DPI, BAPTA-AM, GF109203X, Go6983, PD098059, AG1478, SU11273, Wortmanina, LY294002, PP2, PP3, e la genisteina sono stati forniti dalla Calbiochem (La Jolla, CA, USA). La tossina della pertosse (PTX), apocinina, l'anticorpo anti-p-Ser e 3-(4,5-dimethylthiazol-2-yl)-2,5-diphenylte- trazolium bromide (MTT) sono stati procrastinati dalla Sigma (St. Louis, MO, USA).

Il siRNA p22phox (SI03078523) ed il relativo controllo negativo (SI03650318) sono stati forniti dalla Qiagen (Hiden, Germany).

Le linee cellulari umane Hek293, IMR-90, U-87, CaLu-6 e PNT1A sono state fornite dalla ATCC (Rockville, MD, USA). Le cellule CaLu-6 sono state cresciute in Dulbecco's modified Eagle's medium (DMEM) contenente il 10% di siero fetale

bovino (FBS), 100 U/ml penicillina, 100 μg/ml streptomicina, 1% L-glutammina, e 1% modified Eagle's medium (MEM).

Le linee cellulari Hek293, IMR-90 e U-87 sono state cresciute in mezzo DMEM contenente il 10% di FBS e 100 U/ml penicillina, 100 μg/ml streptomicina.

Le cellule PNT1A sono state coltivate in mezzo di coltura RPMI contenente il 10% di FBS, 100 U/ml penicillina, 100 μg/ml streptomicina, 1% L-glutammina. Le culture cellulari, una volta raggiunta una confluenza dell'80% sono state incubate in mezzo deprivato di siero per 24 h, e successivamente sono state stimolate o con il peptide WKYMVm alla concentrazione finale di 10 μM, o con LL-37 alle concentrazioni di 1, 10 e 100 nM per tempi differenti, o con fMLP 1 μM per 1, 2 e 4 ore, così come indicato nelle figure. In altri esperimenti, cellule deprivate di siero, sono state preincubate con 100 ng/ml di PTX per 16 h oppure con 50 μM di PD098059 per 90min, 10 μM di PP2 per 45min, 10 μM di PP3 per 45min, 60 μM di genisteina per 1h, 2 μM di AG1478 per 1h, 100 mM apocinina per 2h, 2 μM SU11274 per 16h, 50 μM LY294002 per 1h, 100 μM DPI per 15min, 25 μM BAPTA-AM per 1h, 10 μM GF109203X per 10min, 10 μM Go6983 per 10min, 0,5 μM wortmannina per 1h o 10 μM WRW4 per 15min prima della stimolazione o con WKYMVm per 2 min alla concentrazione finale di 10 μM, o con LL-37 10 nM per 1min o con fMLP 1 μM per 2h.

Negli esperimenti di silenziamento, 4×10^5 cellule sono state incubate per 12 h con i siRNA ad una concentrazione finale di 5 nM in DMEM contenente il 10% di FBS, in presenza di 20 ml di HiPerFect (Qiagen). Le cellule sono state successivamente deprivate di siero prima di essere stimolate con WKYMVm per 2 min alla concentrazione finale di 10 μM.

3.2 Estrazione RNA ed analisi di RT-PCR

L'RNA totale è stato estratto dalle cellule CaLu-6, PNT1A e da PMN con il RNAeasy Mini kit (Qiagen) seguendo le istruzioni fornite dalla casa produttrice. Sono stati utilizzati 0,1 μg di RNA come templato per gli esperimenti di RT-PCR. Per amplificare i cDNA di FPRL1 è stato disegnato un oligonucleotide senso 5'-AATTCACATCGTGGTGGACA-3' ed un oligonucleotide antisenso 5'-GAGGCAGCTGTTGAAGAAGG-3', in accordo con la sequenza della regione codificante del gene umano FPRL1. Questi primer generano un amplificato di 688-bp. Invece, per il gene umano codificante per la proteina FPR, è stato disegnato un primer senso 5'-CTCCAGTTGGACTAGCC-3' ed un primer antisenso 5'-CCATCACCCAGGGCCCA-3' che amplificano un frammento di 500-bp. Per il gene GAPDH, è stato utilizzato un primer senso con sequenza 5'-CCATGGAGAAGGCTGGG-3' ed un primer antisenso con 5'-CGCCACAGTTTCCCGGA-3' il cui prodotto di amplificazione genera un frammento di 280-bp.

3.3 *Western Blot e saggio di immunoprecipitazione*

Cellule deprivate di siero sono state stimolate per differenti tempi con il peptide WKYMVm alla concentrazione finale di 10 μM in presenza o assenza di specifici inibitori. Cellule CaLu6 e PNT1A sono state lavate con phospate-buffered saline (PBS) freddo e lisate con 0,5 ml di RIPA buffer (50 mM Tris–HCl, pH 7.4, 150 mM NaCl, 1% NP-40, 1 mM EDTA, 0.25% sodium deoxycholate, 1 mM NaF, 10 μM Na3VO4, 1 mM phenylmethylsulfonyl fluoride, 10 μg/ml

aprotinin, 10 μg/ml pepstatin, 10 μg/ml leupeptin), incubandole per 45 min a 4°C. La concentrazione proteica degli estratti ottenuti è stata determinata utilizzando il Bio-Rad protein assay. L'analisi di western blot è stata eseguita separando uguali quantità di proteine mediante elettroforesi su gel denaturante di poliacrilammide (SDS-PAGE) ad un voltaggio di 120mV per circa 2,5 – 3 ore. Dato il peso molecolare delle proteine in esame si è utilizzato un gel al 10%, per aumentarne il potere di setaccio molecolare.

Dopo la migrazione elettroforetica, le proteine sono state trasferite elettricamente (80mV per 2 ore o 25 mV per 12 h a freddo) dal gel ad una membrana di nitrocellulosa (*blotting*). I filtri sono stati incubati con una soluzione al 5% latte-0,1% Tween in TBS per 1h a temperatura ambiente e quindi incubati il tempo necessario, con l'opportuna concentrazione di anticorpo primario diluita nell'appropriata soluzione.

I complessi antigene anticorpo sono stati rilevati con il sistema di chemioluminescenza ECL chemiluminescence reagent kit (Amersham Pharmacia Biotech).

Gli estratti nucleari sono stati ottenuti con il Qproteome nuclear protein kit (Qiagen) seguendo le istruzioni riportate dal fornitore. Negli esperimenti di immunorpecipitazione, i lisati cellulari contenenti uguali quantità di proteine sono stati incubati, con 3 μg di anticorpo anti-EGFR o anti-p47phox, overnight a 4°C. Gli immunocomplessi così generati, sono stati incubati con 30 μl di Protein A/G Plus agarose su un rotore per 45 min a 4°C. Successivamente, gli immunoprecipitati sono stati lavati per tre volte con PBS freddo, risospesi in 40 μl di Laemmli buffer, bolliti per 5 min a 94°C, pellettati per breve centrifugazione e separati mediante SDS-

PAGE al 10%. Il livello di fosforilazione delle proteine è stato stimato quantitativamente analizzando la densitometria delle bande utilizzando uno scanner Discover Pharmacia equipaggiato con una workstation densitometrica Sun Spark Classic.

3.4 Saggio produzione anione superossido

Per determinare la produzione di $O_2^{\bullet -}$, membrane e citosol sono stati isolati da cellule di cancro del polmone deprivate di siero per 24 h prima di essere stimolate con il peptide WKYMVm alla concentrazione finale di 10 μM per differenti tempi. La generazione di superossido da parte del complesso della NADPH ossidasi è stato determinato come tasso di riduzione del citocromo C sensibile alla superossido dismutasi. Una combinazione di 10 μg di proteine di membrana e di 200 μg di proteine citosoliche sono state incubate a temperatura ambiente in una soluzione di PBS del volume finale di 1 ml, in presenza di 15 μM GTPγ-S, 100 μM citocromo C e 10 μM FAD. Successivamente è stato aggiunto NADPH (100 μM) ed è stata monitorata la produzione di superossido leggendo l'assorbanza a 550 nm. La riduzione specifica del citocromo C è stata controllata aggiungendo ai campioni di controllo 200 U/ml di superossido dismutasi. I livelli di $O_2^{\bullet -}$ sono stati calcolati analizzando il coefficiente di estinzione molare del citocromo C, $\Delta E_{550}/\Delta t$=21.1 mM^{-1} cm^{-1}, considerando che 1 mole di $O_2^{\bullet -}$ riduce 1 mole di citocromo C. Lo Student T test è stato utilizzato per comparare i risultati ottenuti dai vari trattamenti ed rispettivi controlli ed i valori il cui rapporto presentava $p<0.05$ sono stati considerati significativi.

3.5 Saggio in vitro dell'attività kinasica

Il saggio di attività kinasica di c-Src è stato effettuato utilizzando l'enolosai muscolare denaturata di coniglio (Sigma) come substrato esogeno. La proteina c-Src è stata immunoprecipitata incubando overnight a 4°C 5 μg di anticorpo anti-c-Src e la proteina A/G-Sepharose. Gli immunoprecipitati sono stati lavati per tre volte con un buffer all'1% di Nonidet P-40 e due volte con una soluzione 25 mM Tris-HCl, pH 7,4 , 10 mM $MnCl_2$. La proteina c-Src immunoprecipitata è stata successivamente incubata con 20 μl di kinase buffer (50 mM Tris–HCl, pH 7.4, 10 mM MnCl2, 1 mM dithiothreitol) contenente 2 μg di enolasi denaturata acida e 10 mCi di [γ-^{32}P] ATP (PerkinElmer Life Sciences, Waltham, MA, USA) per reazione di 10 min a 37°C. le reazioni sono state stoppate aggiungendo Laemmli sample buffer e risolte mediante SDS-PAGE e i segnali sono stati rilevati mediante autoradiografia. L'enolasi muscolare di coniglio è stata denaturata incubandola in una soluzione di acido acetico 25 mM per 10 min a 30°C ed è stato aggiunto in rapporto 1/10 rispetto al volume della soluzione finale della reazione di kinasi.

3.6 Analisi statistica

Tutti i dati riportati sono espressione delle deviazioni standard e sono rappresentativi dei risultati ottenuti da tre o più esperimenti indipendenti. L'analisi statistica è stata effettuata utilizzando lo Student's T test e solo i risultati con $p<0,05$ sono stati considerati significativi.

3.7 Saggio di vitalità cellulare

In una piastra da 96 pozzetti sono state piastrate $4x10^4$ cellule in un volume di mezzo completo pari a 200 μl prima di essere stimolate con WKYMVm 10 μM, in presenza o assenza di 100 ng/ml di PTX o WRW4 10 μM per 12, 24 e 36 h a 37°C. MTT (5 mg/ml in PBS) è stato aggiunto per ciascun pozzetto ed è stato incubato per 4 h. Dopo aver rimosso con attenzione il mezzo, 200 μl di dimethyl sulfossido (DMSO) è stato aggiunto in ogni pozzetto. L'assorbanza dei sali di formalzano generatosi è stata analizzata mediante spettrofotometria alla lunghezza d'onda di 540 nm. L'effetto di WKYMVm sulla crescita cellulare e stato valutato come viatalità cellulare. Quattro esperimenti indipendenti sono stati effettuati per ciascun trattamento.

4 RISULTATI

4.1 LL-37 induce la fosforilazione delle ERK e l'attivazione della NADPH ossidasi in cellule IMR-90 mediante un meccanismo FPRL1-dipendente

In studi precedenti, nel laboratorio dove ho svolto la tesi, è stato dimostrato che cellule IMR-90 esprimono un recettore FPRL1 funzionalmente attivo e che la sua stimolazione con WKYMVm induce l'attivazione del complesso della NADPH ossidasi attraverso un meccanismo ERK (p42 e p44 MAPK) dipendente (5, 7). La catelicidina LL-37 agisce come un antibiotico endogeno, ma mostra ruoli addizionali che comprendono la regolazione delle risposte immuni e infiammatorie, la promozione del wound healing, la riepitelizzazione e un'attività chemiotattica rivolta verso neutrofili, monociti e cellule T attraverso il legame con FPRL1. LL-37 può anche indurre la generazione di ROS ed il rilascio di α-defensine dai neutrofili. È stata pertanto analizzata la cascata di segnalazione innescata dal legame di LL-37 con FPRL1 in cellule IMR-90. Abbiamo dimostrato che la stimolazione con LL-37 induce la fosforilazione delle ERK attraverso un meccanismo concentrazione dipendente (Figura 9A) e tempo dipendente (Figura 9B).

L'attivazione della NADPH ossidasi richiede la fosforilazione di p47phox su diversi residui di serina. Tale fosforilazione è catalizzata da diverse kinasi tra le quali le ERK giocano un ruolo importante. Abbiamo dimostrato che LL-37 induce la fosforilazione di p47phox già dopo 30" dalla stimolazione (Figura 9C) e che tale evento dipende dall'attivazione del pathway Ras-MAPK e dal legame di LL-37 con FPRL1, come osservato dall'effetto di PD098059, un inibitore di MEK, nonché di

PTX e WRW4 sulla fosforilazione di p47phox (Figura 9E). La fosforilazione delle ERK risulta essere uno degli effetti a valle della cascata di segnalazione innescata da FPRL1. Infatti, il pretrattamento con PTX e WRW4 previene tale attivazione (Figura 9D). Di conseguenza l'esposizione per tempi crescenti con LL-37 induce un incremento della produzione di ROS (Figura 9F).

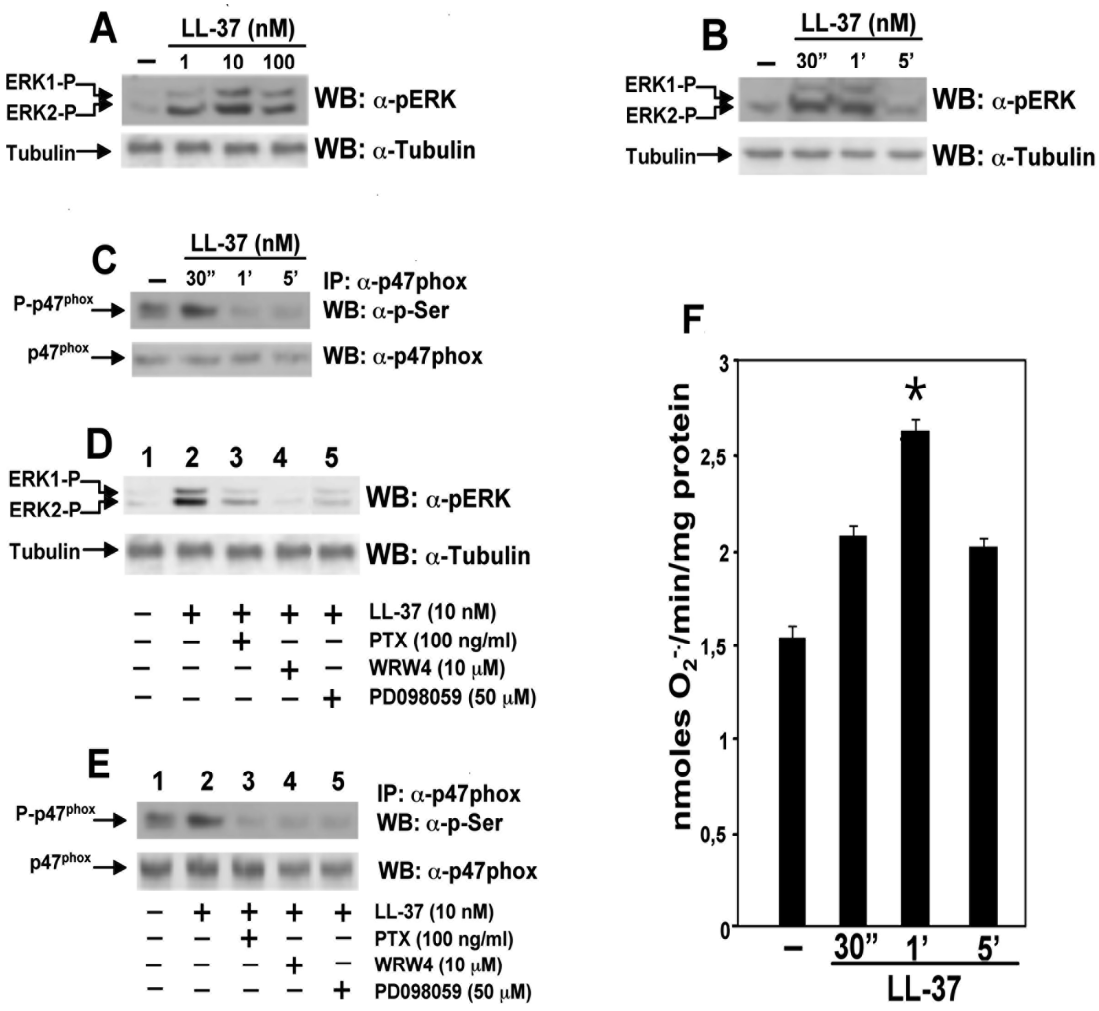

Figura 9. Attivazione delle ERK, fosforilazione di p47phox e generazione di ROS associata all'attivazione del complesso della NADPH ossidasi in seguito alla stimolazione di cellule IMR-90 con LL-37. (A) Lisati cellulari ottenuti da cellule IMR-90 deprivate di siero e stimolate con concentrazioni crescenti di LL-37 o (B e C) per tempi crescenti alla concentrazione di 10nM o (D e E) preincubate alle concentrazioni indicate con PTX o WRW4 o PD098059, prima della stimolazione con LL-37 per 30" alla concentrazione riportata. Venti microgrammi di estratti toali sono stati risolti mediante SDS-PAGE 10% e la fosforilazione delle ERK è stata rilevata utilizzando un anticorpo anti-fosfo-ERK (α-p-ERK). Un anticorpo anti-tubulin (α-tubulin) è stato utilizzato per la normalizzazione degli estratti caricati. La fosforilazione di p47phox è stata rilevata immunoprecipitando un milligrammo di estratti totali con un anticorpo anti-p47phox (α-p47phox), e la fosforilazione di p-47phox (p-p47phox) è stata saggiata utlizzando un anticorpo anti-fosfo-Serina (α-p-Ser). I filtri sono stati successivamente reincubati con un anticorpo α–p47phox per verificare la quantità di proteine caricate. (F) Per monitorare la generazione di specie reattive dell'ossigeno (ROS), 10 μg di membrane e 200 μg di proteine citosoliche sono state purificate da cellule IMR-90 cresciute in mezzo deprivato di siero e stimolate con LL-37 per i tempi indicati. La riduzione specifica del citocromo C è stata monitorata a 550 nm come descritto in materiali e metodi.

4.2 La fosforilazione delle ERK e l'attivazione della NADPH ossidasi indotta da LL-37 è un evento mediato dal Ca^{2+}

Altri pathway che attivano kinasi sono innescati da recettori a sette tratti transmembrana e possono essere coinvolti nella generazione di specie reattive dell'ossigeno. In studi precedenti abbiamo dimostrato che in fibroblasti umani stimolati con WKYMVm, l'attivazione delle ERK e di p47phox è prevenuta dai pretrattamenti con inibitori selettivi o generali della PKC (7). Pertanto abbiamo analizzato in cellule IMR-90 stimolate con LL-37 il coinvolgimento di isoforme di PKC sensibili a GF109203X o a Go6983 nella cascata di segnalazione che porta alla generazione di anione superossido NADPH-dipendente.

Abbiamo osservato che la preincubazione con GF109203X, che agisce come competitore inibitorio del sito di legame all'ATP della PKC, o con Go6983, che inibisce le isoforme di PKC α, β, γ, δ, ζ, prima della stimolazione con LL-37 non attenua la fosforilazione delle ERK (Figura 10A). In diversi tipi cellulari LL-37 induce la mobilizzazione del calcio che rappresenta anche uno degli effetti a valle dell'attivazione di FPRL1. Abbiamo pertanto utilizzato il chelante del calcio BAPTA-AM per analizzare gli effetti della deplezione del calcio sull'attivazione delle ERK e sulla generazione di ROS. I risultati hanno mostrato che BAPTA-AM previene significativamente la fosforilazione delle ERK e di p47phox indotta da LL-37 (Figura 10A e 10B). Come atteso, la generazione di ROS NADPH-dipendente è inibita dalla preincubazione con il chelante del calcio, con apocinina, con DPI, con PTX o con PD098059 (Figura 10C).

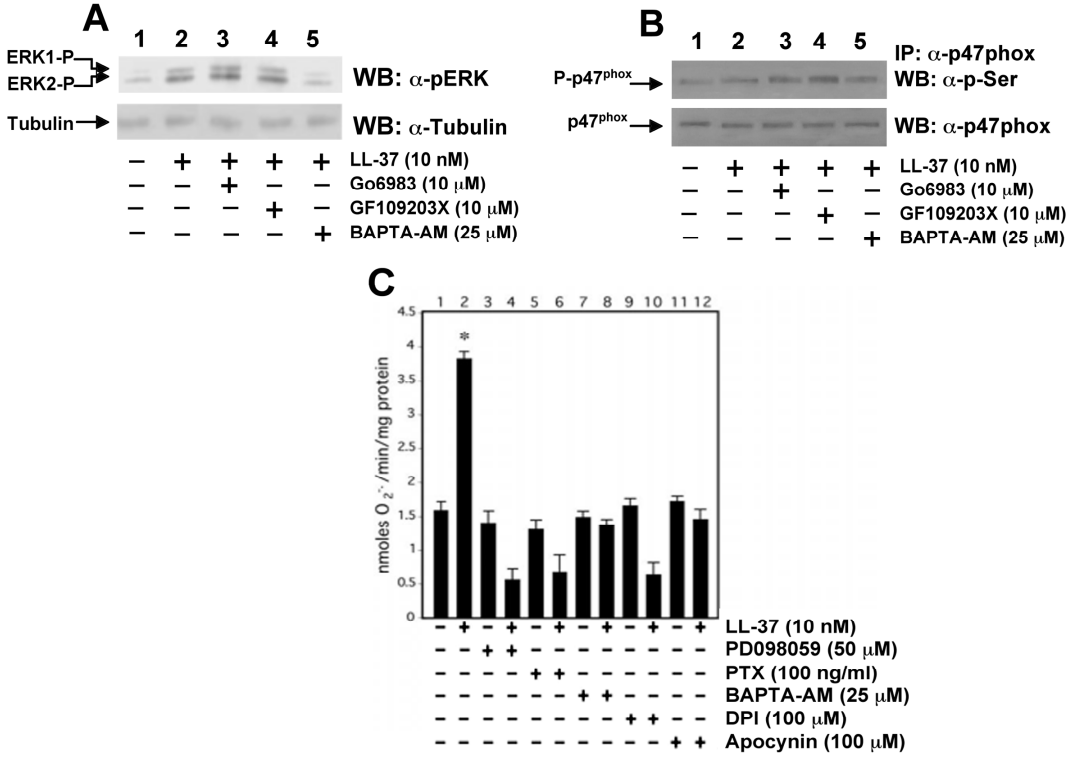

Figura 10. La stimolazione di FPRL1 con LL-37 attiva le ERK, p47phox e la NADPH ossidasi secondo un meccanismo Ca^{2+} dipendente. (A e B) Cellule IMR-90 sono state deprivate di siero e stimolate per 30" con LL-37 in presenza o assenza degli inibitori Go6983, GF109203X e BAPTA-AM alle concentrazioni riportate. La fosforilazione delle ERK è stata rilevata utilizzando un anticorpo anti-fosfo-ERK (α-p-ERK). Un anticorpo anti-tubulin (α-tubulin) è stato utilizzato per la normalizzazione degli estratti caricati. La fosforilazione di p47phox è stata rilevata immunoprecipitando un milligrammo di estratti totali con un anticorpo anti-p47phox (α-p47phox), e la fosforilazione di p-47phox (p-p47phox) è stata saggiata utlizzando un anticorpo anti-fosfo-Serina (α-p-Ser). I filtri sono stati successivamente reincubati con un anticorpo α–p47phox per verificare la quantità di proteine caricate. (C) La generazione di specie reattive dell'ossigeno è stata monitorata come descritto in materiali e metodi stimolando le cellule IMR-90 con LL-37 per 30" in presenza o assenza dei composti PD098059, PTX, BAPTA-AM, DPI e apocinina alle concentrazioni riportate.

4.3 LL-37 è espresso in fibroblasti umani IMR-90

La catelicidina hCAP18/LL-37 è sintetizzata sotto forma di precursore (pro-peptide) e la sua piena funzione biologica richiede il clivaggio ad opera della proteinasi-3 che taglia il pro-peptide tra l'alanina 103 e la leucina 104, originando un frammento di 37 aa che presenta due leucine all'NH_2-terminale (LL-37). Abbiamo analizzato nelle linee cellulari IMR-90 ed HEK-293 i trascritti della catelicidina hCAP18/LL-37 mediante RT-PCR ed i risultati hanno dimostrato che in queste due linee cellulari è espressa l'intera regione codificante (Figura 11A). Abbiamo anche valutato mediante esperimenti di western blot, condotti con un anticorpo monoclonale specifico, il pattern di clivaggio e i livelli di espressione della proteina hCAP18/LL-37. I risultati ottenuti mostrano che sia il pro-peptide che la forma attiva, rappresentata da una banda immunoreattiva di 3.7 KDa, è espressa in entrambe le linee cellulari (Figura 11B).

Recentemente è stato dimostrato che in macrofagi, monociti, neutrofili e cellule epiteliali alveolari l'espressione e il rilascio di LL-37 nella sua forma attiva può essere indotto dalla stimolazione di alcuni Toll-like receptor (TLR) come TLR-2, TLR-4 e TLR-9. La famiglia dei TLR gioca un ruolo chiave nel riconoscimento dei patogeni e nell'attivazione della risposta immune innata. Infatti, i TLR, riconoscendo i pattern molecolari associati ai patogeni generalmente espressi dagli agenti infettivi, mediano la produzione di citochine necessarie per il corretto sviluppo della risposta immune. Pertanto abbiamo analizzato l'espressione di questi recettori in fibroblasti umani e gli esperimenti condotti mediante RT-PCR dimostrano che i livelli di espressione dei trascritti di TLR-2, TLR-4 e TLR-9 non sono rilevabili in cellule IMR-90 (Figura 11C).

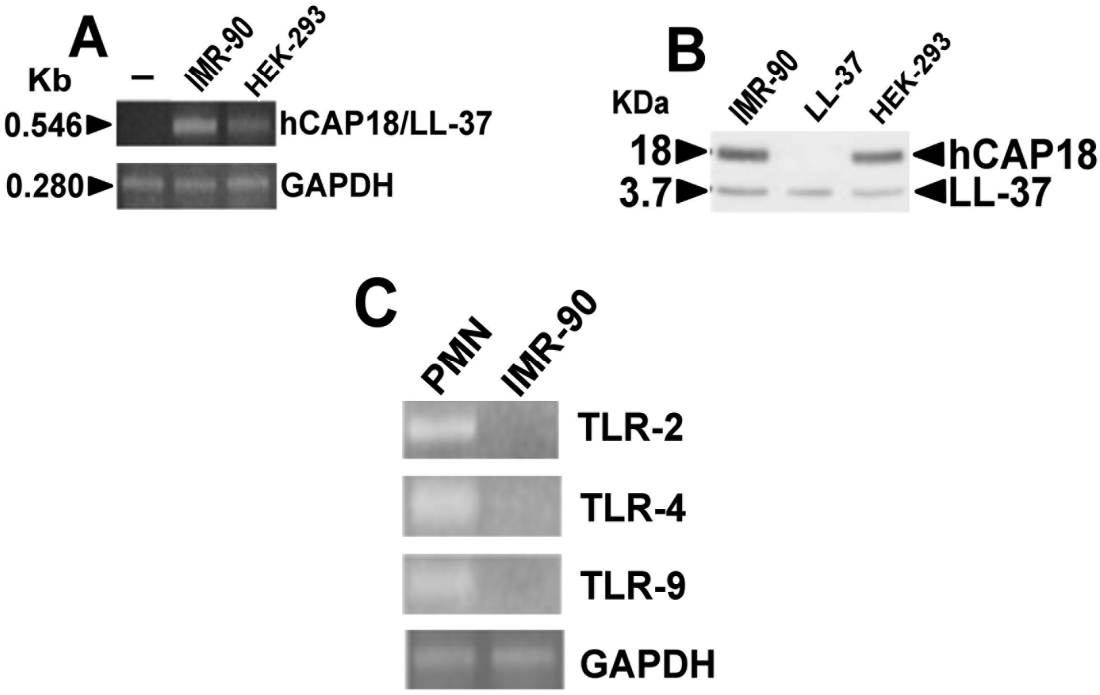

Figura 11. Espressione di LL-37 e di TLR in cellule IMR-90 e HEK-293. RNA totale e proteine sono state purificate da cellule polimorfonucleate (PMN), IMR-90 e HEK293. (A) L'espressione di hCAP/LL-37 è stata determinata mediante RT-PCR e coamplificando con coppie di primer specifici per la regione codificante di hCAP/LL-37 e per la GAPDH. I segnali attesi degli amplificati di hCAP/LL-37 e GAPDH sono rispettivamente di 546bp e 280bp. (B) L'espressione e il clivaggio di hCAP/LL-37 è stata determinata mediante western blot utilizzando un anticorpo specifico anti-hCAP/LL-37. Un SDS-PAGE 10-20% è stato utilizzato per separare 50 μg di estratti totali e 20 ng di peptide LL-37. Le freccie indicano il pro-peptide hCAP/LL-37 (18KDa) e la forma matura del peptide LL-37 (3.7KDa). (C) L'espressione dei TLR è stata determinata mediante RT-PCR e coamplificando con coppie di primer specifici per le regioni codificanti dei TLR e per la GAPDH. I prodotti di PCR sono stati separati su un gel di agarosio all'1,5%.

4.4La stimolazione dei recettori per N-formil peptidi con N-fMLP regola il ciclo cellulare in cellule di glioblastoma U-87

In cellule umane di glioblastoma U-87, la stimolazione per tempi crescenti con N-fMLP induce un accumulo degli inibitori delle kinasi ciclina-dipendneti $p21^{waf1/cip1}$ e $p16^{INK4A}$ secondo un evento regolato nel tempo (Figura 12A). La proteina $p21^{waf1/cip1}$ può promuovere o arrestare la proliferazione e la progressione del ciclo cellulare in funzione della sua localizzazione. Infatti, $p21^{waf1/cip1}$ inibisce la proliferazione se localizzata a livello nucleare, mentre se si accumula a livello citosolico promuove la progressione del ciclo e la proliferazione cellulare (1). È stata quindi analizzata la localizzazione di $p21^{waf1/cip1}$ in cellule stimolate con N-fMLP ed è stato osservato un suo accumulo prevalentemente a livello nucleare (Figura 12B). N-fMLP induce in cellule U-87 la fosforilazione delle ERK e tale evento è prevenuto dal pretrattamento con l'inibitore di MEK-1, PD098059, e richiede la generazione di ROS come dimostrato dall'osservazione che l'apocinina ne inibisce la fosforilazione (Figura 12C). Questi eventi dipendono dall'attivazione del recettore FPR. Infatti, il pretrattamento con la tossina della pertosse, che ADP-ribosila le proteine Gi accoppiate al recettore, previene sia la fosforilazione delle ERK che l'accumulo di $p21^{waf1/cip1}$ (Figura 12D). Questi suggeriscono che in cellule di glioblastoma U-87, l'interazione FPR/N-fMLP induce un arresto nella progressione del ciclo cellulare attraverso l'aumento di espressione di $p16^{INK4A}$ e di $p21^{waf1/cip1}$ e che l'accumulo a livello nucleare di $p21^{waf1/cip1}$ è un evento regolato da MEK e dalla generazione di superossido NADPH-dipendente.

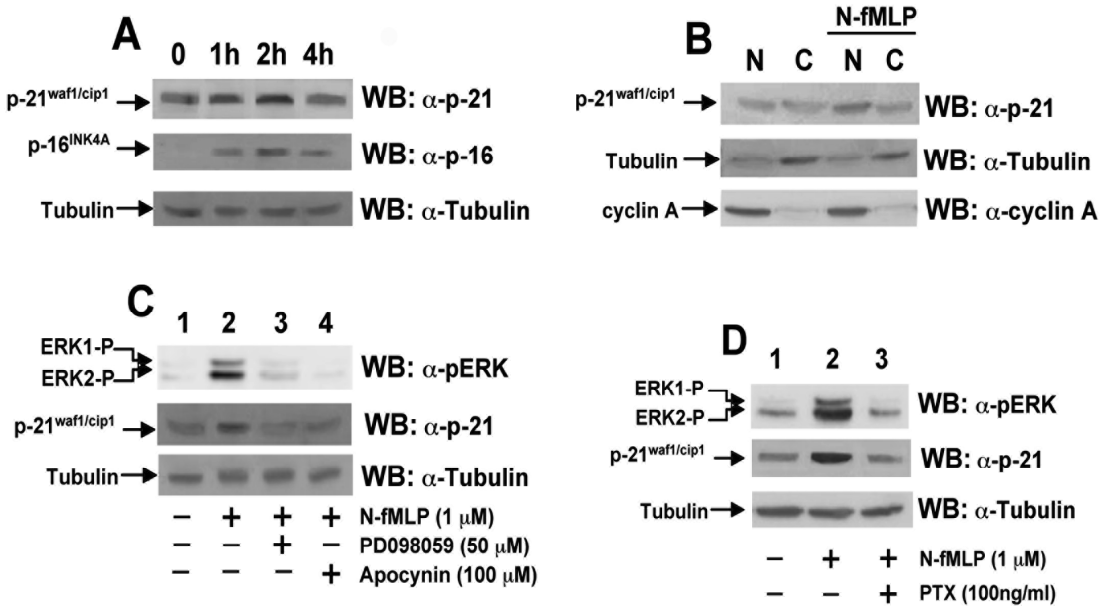

Figura 12. La stimolazione di FPR con N-fMLP, in cellule U-87, induce l'accumulo di CKI secondo un meccanismo MEK/NADPH ossidasi dipendente. (A) Le cellulle umane di glioblastoma U-87 sono state deprivate di siero e stimolate con N-fMLP 1 μM per 1h, 2h e 4h. (B) Le cellule U-87 deprivate di siero sono state esposte a N-fMLP 1 μM per 2h oppure a PBS, come controllo negativo, e le frazioni nucleari (N) e citosoliche (C) sono state isolate come riportato in materiali e metodi. Nei pannelli C e D le cellule U-87 deprivate di siero sono state stimolate con N-fMLP 1 μM per 2h in presenza o assenza di PD098059, apocinina e PTX alle concnetrazioni indicate. Venti microgrammi di estratti opportunamente purificati sono stati risolti mediante SDS-PAGE 10% e successivamente ibridizzati con un anticorpo anti-$p16^{INK4A}$ (α-$p16^{INK4A}$), oppure anti-$p21^{waf1/cip1}$ (α-$p21^{waf1/cip1}$) oppure anti-fosfo-ERK (α-p-ERK). Un anticorpo anti-tubulin (α-tubulin) è stato utilizzato per la normalizzazione della frazione citosolica e degli estratti totali caricati, mentre, la frazione nucleare è stata normalizzata utilizzato un anticorpo anti-ciclina A (α-ciclina A).

4.5 FPRL1 è un recettore funzionalmente espresso in cellule CaLu-6 e PNT1A

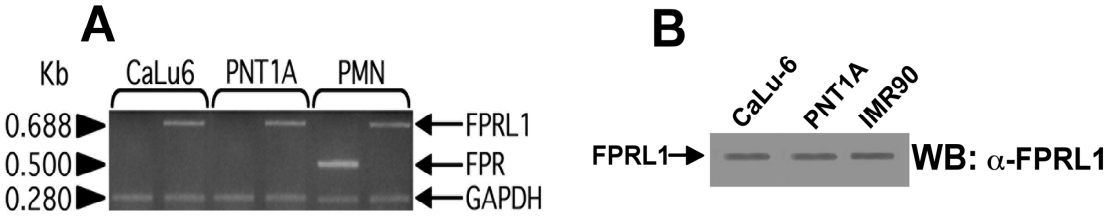

Figura 13. Espressione del recettore FPRL1 in cellule CaLu6 e PNT1A. (A) Gli RNA totali sono stati retrotrascritti e i cDNA sono stati coamplificati con coppie di *primer* specifici per il recettore FPR o FPRL1 e per la GAPDH (gene *housekeeping*). I segnali attesi degli amplificati di FPR, FPRL1 e GAPDH sono rispettivamente di 688bp, 500bp e 280bp. (B) Cinquanta microgrammi di estratti proteici di membrana sono stati isolati da cellule CaLu-6, PNT1A e IMR-90 come controllo, sono stati separati mediante SDS-PAGE al 10% e ibridizzati con un anticorpo anti-FPRL1 (α-FPRL1).

Nelle linee cellulari CaLu-6 e PNT1A è stata analizzata l'espressione trascrizionale e traduzionale dei recettori FPR e FPRL1 mediante analisi di RT-PCR, effettuata utilizzando coppie di primer specifici che amplificano una regione codificante dei due recettori, ed esperimenti di western blot, condotti con anticorpi anti-FPRL1. I risultati ottenuti dimostrano che in queste linee cellulari sono trascritti solo gli mRNA codificanti per il recettore FPRL1 e non quelli per il recettore FPR (Figura 13A). Tali dati sono stati confermati anche dall'osservazione che anticorpi anti-FPRL1 evidenziano l'espressione del recettore FPRL1 in cellule CaLu-6 e PNT1A (Figura 13B). Abbiamo quindi analizzato la funzionalità di questo recettore e la sua capacità di indurre la fosforilazione delle ERK e l'attivazione della NADPH ossidasi in cellule stimolate con WKYMVm.

Gli esperimenti hanno dimostrato che il trattamento per tempi crescenti con l'agonista induce la fosforilazione delle ERK la quale è sostenuta fino a 10 min dalla

stimolazione (Figura 14A). Inoltre, la preincubazione delle cellule CaLu-6 e PNT1A con PD098059 o con PTX, prima della stimolazione con WKYMVm, previene la fosforilazione delle ERK (Figura 14B), suggerendo che tale evento è MEK-dipendente e richiede l'attivazione di FPRL1.

La fosforilazione e la traslocazione sulla membrana delle subunità citosoliche della NADPH ossidasi sono considerate eventi chiave per l'assemblaggio e l'attivazione della NADPH ossidasi fagocitica e non fagocitica (7). Poiché p47phox è un substrato dell'attività kinasica delle ERK, e la fosforilazione di p44MAPK/p42MAPK è considerata un prerequisito per l'attivazione della NADPH ossidasi, sono stati analizzati i meccanismi molecolari che determinano la produzione di anione superossido NADPH-dipendente nelle due linee cellulari stimolate con WKYMVm. I risultati ottenuti dimostrano che p47phox è rapidamente fosforilata a livello dei residui di Serina (Figura 14C) e che questa è significativamente prevenuta dal pretrattamento con PTX o con PD098059 (Figura 14D). Inoltre, come conseguenza dell'attivazione della subunità regolatoria della NADPH ossidasi, la stimolazione di FPRL1 con WKYMVm induce la generazione di superossido NADPH-dipendente con un picco di produzione a 2 min dalla stimolazione (Figura 14E). Questi dati suggeriscono che, nelle linee cellulari CaLu-6 e PNT1A, FPRL1 è un recettore biologicamente funzionale.

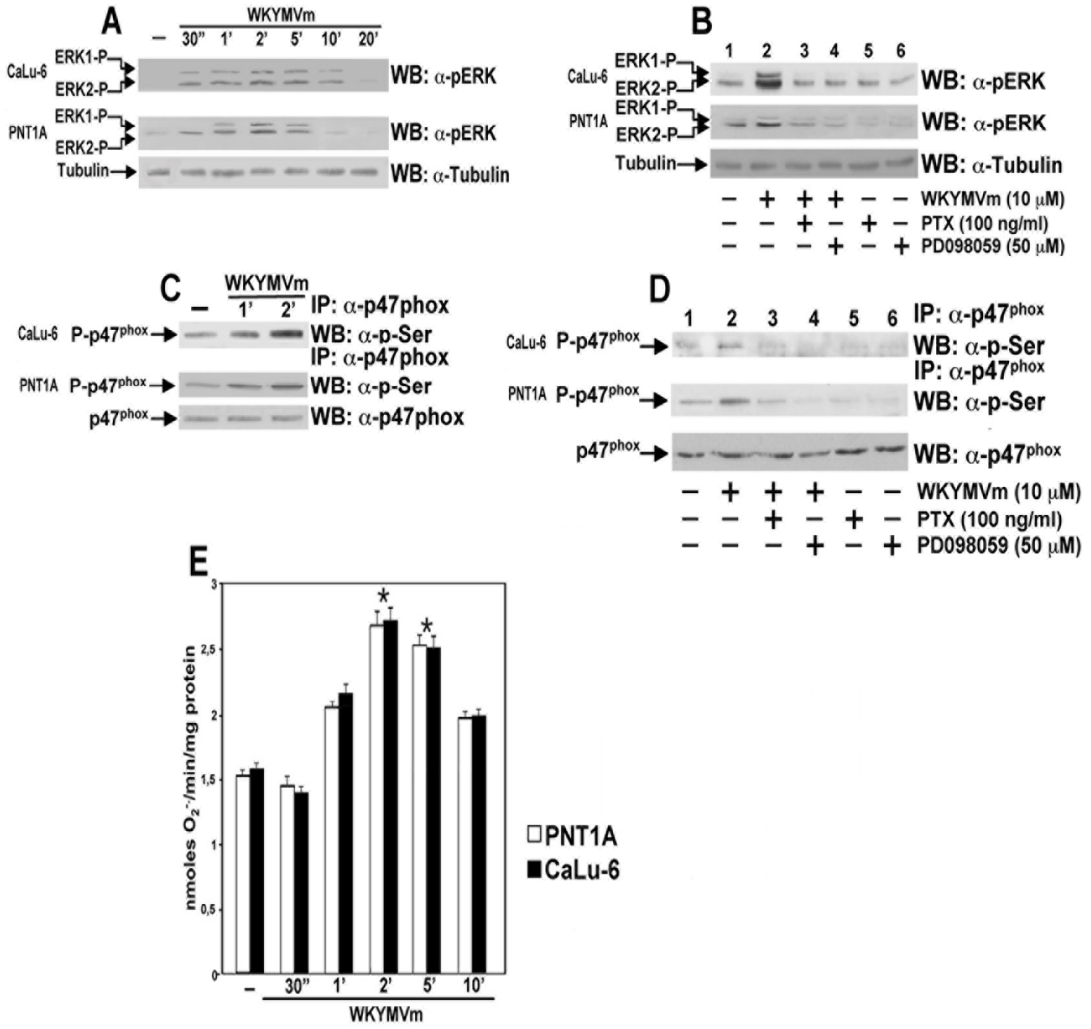

Figura 14. Attivazione delle ERK, fosforilazione di p47phox e generazione di ROS associata all'attivazione del complesso della NADPH ossidasi in seguito alla stimolazione di cellule CaLu-6 e PNT1A con WKYMVm. (A) Lisati cellulari di CaLu-6 e PNT1A deprivate di siero e stimolate per tempi crescenti con WKYMVm (10μM) o (B) preincubate alle concentrazioni indicate con PTX o PD098059, prima della stimolazione. Venti microgrammi di estratti toali sono stati risolti mediante SDS-PAGE 10% e la fosforilazione delle ERK è stata rilevata utilizzando un anticorpo anti-fosfo-ERK (α-p-ERK). Un anticorpo anti-tubulin (α-tubulin) è stato utilizzato per la normalizzazione degli estratti caricati. (C) Cellule CaLu-6 e PNT1A deprivate di siero sono state stimolate con WKYMVm per i tempi riportati o (D) preincubate con PTX e PD098059 prima della stimolazione. Un milligrammo di estratti totali è stato immunoprecipitato con un anticorpo anti-p47phox (α-p47phox), e la fosforilazione di p-47phox (p-p47phox) è stata saggiata utlizzando un anticorpo anti-fosfo-Serina (α-p-Ser). I filtri sono stati successivamente reincubati con un anticorpo α–p47phox per verificare la quantità di proteine caricate. Dieci microgrammi di membrane e 200 μg di proteine citosoliche sono state purificate da cellule CaLu-6 e PNT1A cresciute in mezzo deprivato di siero e stimolate con WKYMVm per i tempi indicati. La riduzione specifica del citocromo C è stata monitorata a 550 nm come descritto in materiali e metodi.

4.6 La generazione di superossido è necessaria per la transattivazione di EGFR e c-Met mediata da FPRL1

È stato dimostrato che recettori a sette tratti trans-membrana accoppiati a proteina G possono transattivare recettori tirosin kinasici esercitando un'azione sinergica che contribuisce ad esacerbare il fenotipo tumorale e a favorire la produzione di fattori angiogenici (94, 95). Poiché i recettori EGFR e c-Met sono costitutivamente espressi rispettivamente in cellule CaLu-6 e PNT1A, è stata esaminata la capacità di FPRL1 di transattivare tali recettori. Come mostrato in Figura 15A e 16A, la stimolazione per tempi crescenti con WKYMVm induce la fosforilazione regolata nel tempo di EGFR in CaLu-6 e di c-Met in PNT1A con un picco di fosforilazione dei residui di tirosina citosolici dei recettori a 2 min dalla stimolazione. Inoltre, la preincubazione con PTX, prima della stimolazione di FPRL1 con il suo agonista, determina una significativa riduzione del livello di fosforilazione delle tirosine citosoliche di EGFR e di c-Met come conseguenza dell'inibizione selettiva delle proteine Gi (Figura 15B e 16B).

Molte evidenze sperimentali dimostrano che i ROS sono intermedi della segnalazione coinvolti nell'attivazione dei recettori tirosin kinasi. L'inibizione mediata dai ROS dell'attività delle fosfotirosine fosfatasi (PTPasi), risulta in uno shift dell'equilibrio dallo stato non fosforilato a quello fosforilato dei recettori tirosina kinasi (89, 90). Allo scopo di determinare il ruolo dei ROS generati dalla NADPH ossidasi nella transattivazione di EGFR e c-Met, le linee cellulari CaLu-6 e PNT1A sono state preincubate con l'apocinina, un inibitore selettivo della NADPH ossidasi, o con siRNA per silenziare selettivamente l'espressione della subunità p22phox, prima della stimolazione con WKYMVm.

I risultati dimostrano che il blocco delle funzioni della NADPH ossidasi previene la fosforilazione delle tirosine citosoliche dei recettori EGFR e c-Met indotta da FPRL1 (Figure 15C, 15D, 16C e 16D), suggerendo che l'attivazione della NADPH ossidasi ricopre un ruolo chiave nella transattivazione di tali RTK.

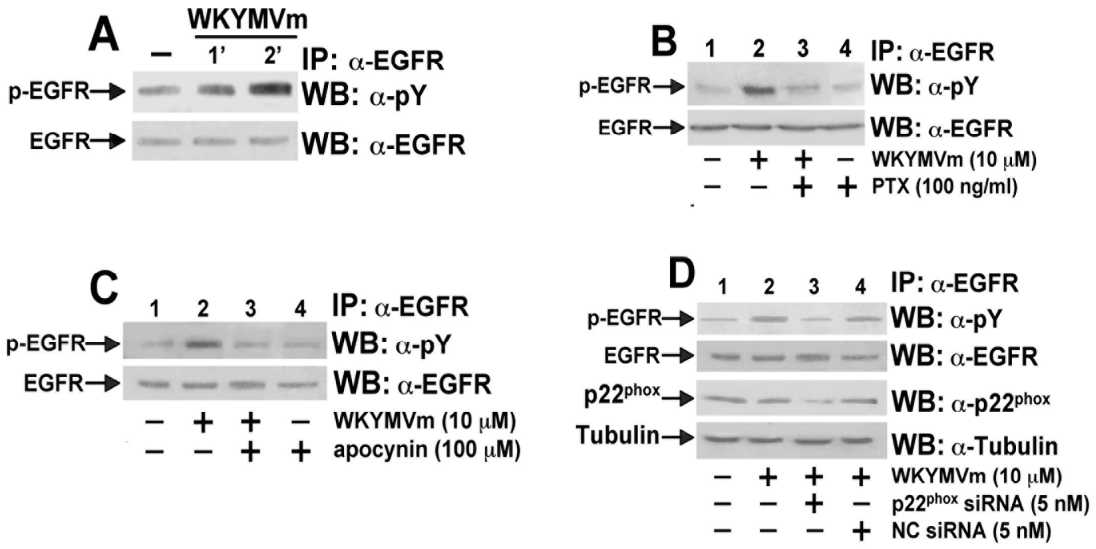

Figura 15. FPRL1 induce la transattivazione di EGFR secondo un meccanismo NADPH ossidasi dipendente. (A) Cellule CaLu-6 deprivate di siero sono state incubate con WKYMVm 10 μM per i tempi indicati o preincubati con (B) PTX 100ng/ml o (C) apocynin 100 μM prima della stimolazione. (D) Cellule deprivare di siero sono state incubate per 12 h con siRNA specifici per i trascritti di p22phox (p22phox siRNA), alla concentrazione finale di 5 nM, o con un siRNA aspecifico come controllo negativo (NC siRNA) in mezzo DMEM contente il 10% di FBS in presenza di 20μl di HiPerfect. Le cellule sono state deprivate di siero per 24 h prima della stimolazione con WKYMVm per 2 min. Ottocento microgrammi di lisati totali, sono stati incubati con 3μg di anti-EGFR (α–EGFR) e gli immunocomplessi sono stati mixati con 30μl di resina Protein A/G Plus agarose. Gli immunoprecipitati sono stati risolti con SDS-PAGE 10% e la fosforilazione di EGFR (p-EGFR) è stata rilevata utilizzando un anticorpo anti-fosfo-Tirosina (α-p-Y). Gli anticorpi α–EGFR e α–tubulin sono stati utilizzati per controllare la quantità di proteine caricata. Un anticorpo α–p22phox è stato utilizzato per controllare il silenziamento di p22phox.

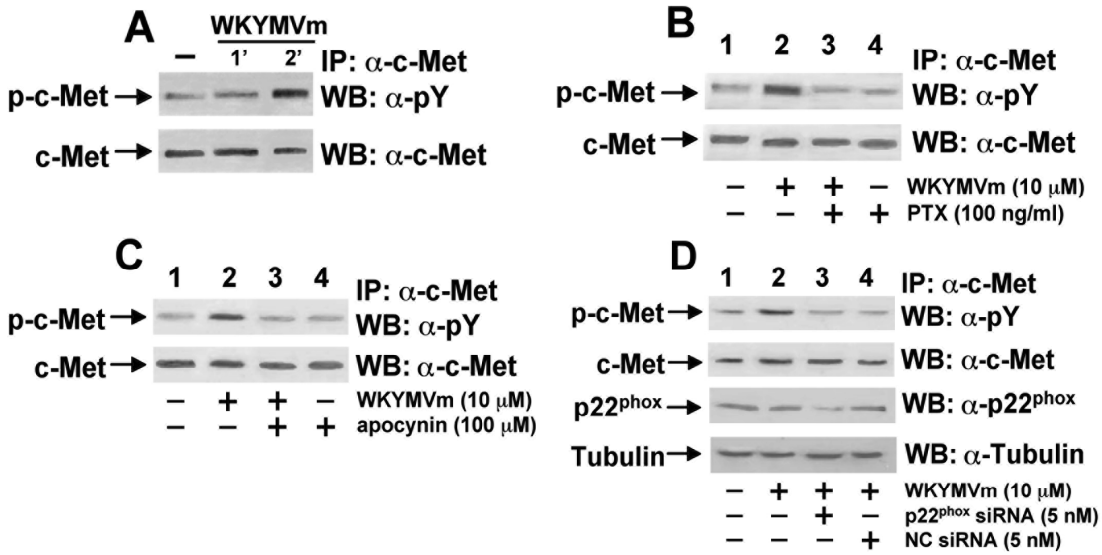

Figura 16. FPRL1 induce la transattivazione di c-Met secondo un meccanismo NADPH ossidasi dipendente. (A) Cellule PNT1A deprivate di siero sono state incubate con WKYMVm 10 μM per i tempi indicati o preincubati con (B) PTX 100ng/ml o (C) apocynin 100 μM prima della stimolazione. (D) Cellule deprivare di siero sono state incubate per 12 h con siRNA specifici per i trascritti di p22phox (p22phox siRNA), alla concentrazione finale di 5 nM, o con un siRNA aspecifico come controllo negativo (NC siRNA) in mezzo RPMI contente il 10% di FBS in presenza di 20μl di HiPerfect. Le cellule sono state deprivate di siero per 24 h prima della stimolazione con WKYMVm per 2 min. Ottocento microgrammi di lisati totali, sono stati incubati con 3μg di anti-c-Met (α–c-Met) e gli immunocomplessi sono stati mixati con 30μl di resina Protein A/G Plus agarose. Gli immunoprecipitati sono stati risolti con SDS-PAGE 10% e la fosforilazione di c-Met (p-c-Met) è stata rilevata utilizzando un anticorpo anti-fosfo-Tirosina (α-p-Y). Gli anticorpi α–c-Met e α–tubulin sono stati utilizzati per controllare la quantità di proteine caricata. Un anticorpo α–p22phox è stato utilizzato per controllare il silenziamento di p22phox.

4.7 L'attivazione di c-Src è necessaria per la transattivazione di EGFR e di c-Met indotta da FPRL1

Molte proteine citosoliche sono coinvolte nel mediare i processi di transattivazione. La famiglia delle tirosin kinasi c-Src può agire come mediatore del segnale sia a monte che a valle degli eventi che regolano la transattivazione di un RTK. Pertanto, è stato analizzato il ruolo di c-Src nella transattivazione dei recettori EGFR e c-Met, nelle linee cellulari CaLu-6 e PNT1A, stimolate con WKYMVm. I risultati hanno dimostrato che la preincubazione con genisteina, un inibitore generico

delle tirosin kinasi, o con AG1478, un inibitore selettivo dell'attività tirosin kinasica di EGFR, o con SU11274, un inibitore selettivo dell'attività tirosin kinasica di c-Met, o con PP2, un inibitore selettivo dell'attività tirosin kinasica di c-Src prevengono la fosforilazione in tirosina di EGFR e c-Met (Figura 17). Tali risultati suggeriscono che nelle due linee cellulari c-Src gioca un ruolo chiave nel mediare i segnali da FPRL1 a EGFR o a c-Met.

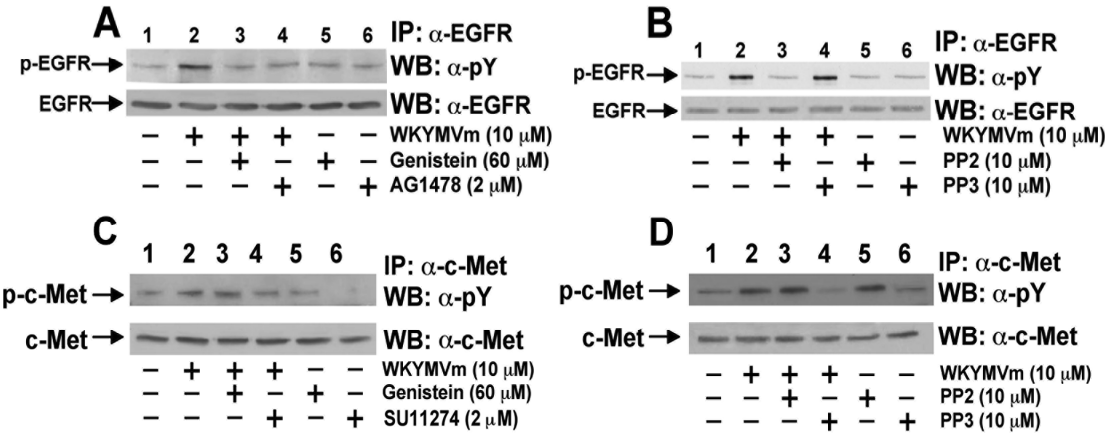

Figura 17. La fosforilazione di EGFR in cellule CaLu-6 e di c-Met in cellule PNT1A, mediata da FPRL1, è prevenuta dal pretrattamento con inibitori generici e specifici delle tirosin kinasi. (A) Cellule CaLu-6 deprivate di siero sono state preincubate con genistein o AG1478 o (B) con PP2 o PP3 alle concentrazioni indicate, prima della stimolazione con WKYMVm. (C) Cellule PNT1A deprivate di siero sono state preincubate con genistein o SU11274 (D) o con PP2 o PP3 alle concnetrazioni riportate prima della stimolazione con WKYMVm. Ottocento microgrammi di estratti totali isolati da cellule CaLu-6 e PNT1A sono stati incubati rispettivamente con anticorpi anti-EGFR (α–EGFR) e anti-c-Met (α–c-Met). Le proteine sono state risolte su SDS-PAGE al 10% e la fosforilazione di EGFR (p-EGFR) e di c-Met (p-c-Met) sono state rilevate con un anticorpo anti-fosfo-Tirosina (α–p-Y). Gli anticorpi α–EGFR e α–c-Met sono stati utilizzati come controllo delle proteine caricate.

È stato dimostrato che in cellule U-87 e in cellule FPRL1/CHO, la stimolazione di FPRL1 con WKYMVm induce un aumento dell'attività kinasica di c-Src. Pertanto, abbiamo valutato la capacità dell'agonista sintetico di attivare c-Src in cellule CaLu-6 e PNT1A mediante un saggio di kinasi in vitro, utilizzando enolasi e [^{32}P]ATP come substrato. Come riportato in figura 18A, l'attività kinascia di c-Src

risulta essere aumentata nelle due linee cellulari esposte a WKYMVm per 2 min (canale 2), mentre è completamente prevenuta dalla preincubazione con PTX (canale 3).

L'attività della proteina c-Src è regolata dalla fosforilazione a carico di due distinti residui di tirosina. L'autofosforilazione del residuo di tirosina in posizione 416, localizzata nel dominio kinasico, attiva c-Src, mentre la fosforilazione del residuo di tirosina in posizione 527 blocca l'attività di c-Src. Abbiamo analizzato i livelli di fosforilazione del residuo di tirosina 416 di c-Src in cellule CaLu-6 e PNT1A deprivate di siero e stimolate per tempi crescenti con WKYMVm utilizzando un anticorpo fosfospecifico in grado di rilevare la fosforilazione di tale residuo di tirosina.

I risultati ottenuti mostrano che il livello di fosforilazione della tirosina 416 di c-Src, in cellule stimolate con WKYMVm, è un evento regolato nel tempo con un picco di fosforilazione registrato a 2 min dalla stimolazione (Figura 18B). Inoltre, in esperimenti effettuati pretrattando le due linee cellulari con PTX, prima della stimolazione con WKYMVm, si osserva che il blocco specifico delle proteine Gi previene significativamente la fosforilazione di c-Src a carico della sua tirosina 416 (Figura 18C).

La proteina c-Src è sensibile alle condizioni redox intracellulari, come dimostrato dall'inattivazione ROS-dipendente delle PTPasi che controllano il suo stato di fosforilazione. Abbiamo pertanto analizzato il ruolo dei ROS, generati dalla NADPH ossidasi, nel mediare l'attivazione di c-Src indotta da FPRL1. Abbiamo osservato che i pretrattamenti con l'apocinina o la preincubazione con siRNA

selettivi per il trascritto della subunità p22phox, prima della stimolazione per 2 min con WKYMVm, prevengono la fosforilazione del residuo di tirosina 416 di c-Src

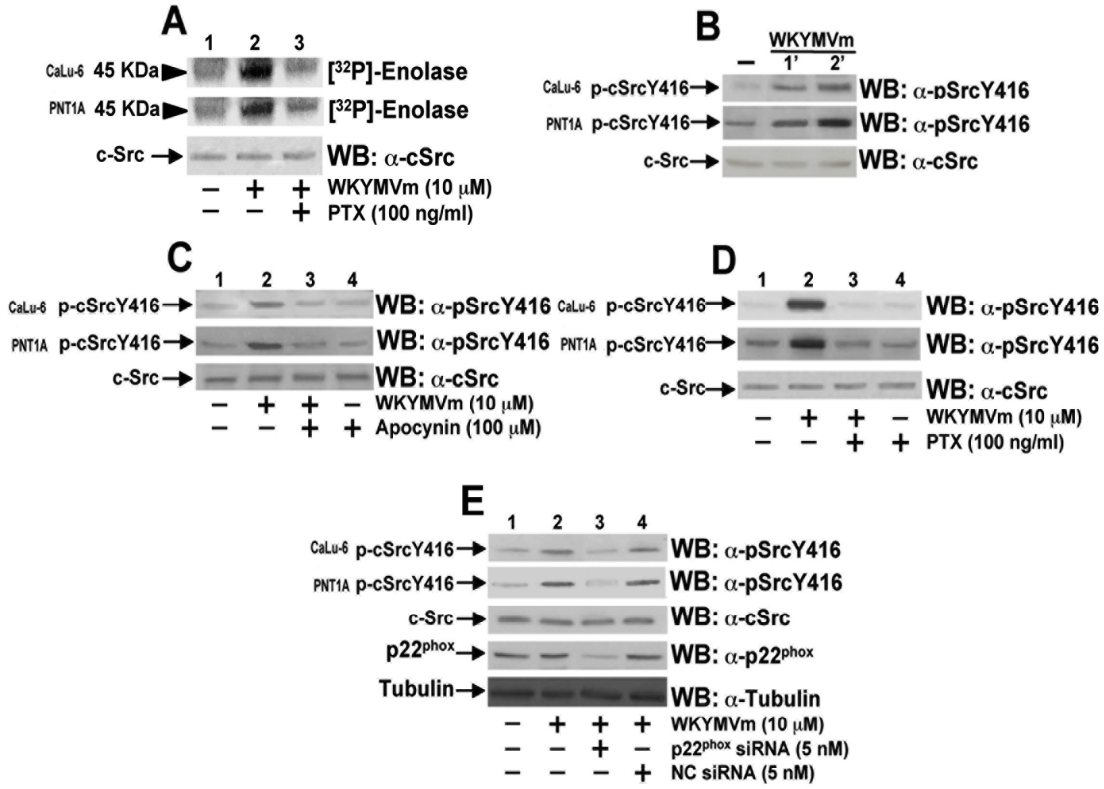

Figura 18. L'attivazione di c-Src associata alla stimolazione di FPRL1 dipende dall'attivazione della NADPH ossidasi. (A) L'attività cellulare di c-Src è stata rilevata mediante un saggio di attività kinasica in vitro. Le cellule CaLu-6 e PNT1A sono state esposte a WKYMVm 10 μM in presenza e assenza di PTX 100ng/ml. Dagli estratti totali ottenuti dalle due linee cellulari è stata immunoprecipitata la proteina c-Src con un anticorpo anti-cSrc e l'attività kinasica di c-Src è stata misurata direttamente sulle sfere della resina A/G agarose incubando in vitro gli immunocomplessi leganti c-Src con il substrato dell'enolasi e [γ^{32}P]ATP. I campioni sono stati successivamente risolti su SDS-PAGE 10% ed i segnali sono stati rilevati mediante autradiografia. (B) Le cellule sono state stimolate con WKYMVm per i tempi indicati oppure sono state preincubate con (C) PTX 100 ng/ml o (D) apocinin 100 μM prima della stimolazione. Cinquanta microgrammi di estratti proteici totali sono stati caricati e separati mediante SDS-PAGE 10% e la fosforilazione di c-Src sulla tirosina 416 (Y416) è stata rilevata utilzzando un anticorpo anti-fosfo-SrcY416 specifico (α–p-SrcY416). Un anticorpo α–cSrc è stato utilizzato per normalizzare gli estratti caricati. (E) Cellule CaLu-6 e PNT1A deprivate di siero sono state incubate per 12 h con siRNA specifici per i trascritti di p22phox (p22phox siRNA), alla concentrazione finale di 5 nM, o con un siRNA aspecifico come controllo negativo (NC siRNA) in mezzo RPMI contente il 10% di FBS in presenza di 20μl di HiPerfect. Le cellule sono state deprivate di siero per 24 h prima della stimolazione con WKYMVm per 2 min. Cinquanta microgrammi di estratti sono stati caricati e separati mediante SDS-PAGE 10% e la fosforilazione di c-Src sulla tirosina 416 (Y416) è stata rilevata utilzzando un anticorpo anti-fosfo-SrcY416 specifico (α–p-SrcY416). Un anticorpo α–cSrc è stato utilizzato per normalizzare gli estratti caricati. Gli anticorpi α–cSrc e α–tubulin sono stati utilizzati per controllare la quantità di proteine caricata. Un anticorpo α–p22phox è stato utilizzato per controllare il silenziamento di p22phox.

(Figura 18D e 18E), suggerendo che l'attività kinasica di c-Src indotta da FPRL1 richiede l'attivazione della NADPH ossidasi.

4.8 WRW4 previene la cascata di segnalazione indotta dalla stimolazione di FPRL1

Il peptide WRW4 antagonizza il legame dello specifico ligando WKYMVm al recettore FPRL1 inibendo gli eventi di segnalazione cellulare associati che includono l'aumento del flusso intracellulare del calcio e la fosforilazione delle ERK (5). Per investigare ulteriormente il ruolo di FPRL1 nell'attivazione delle cascate di segnalazione intracellulare analizzate, le linee cellulari CaLu-6 e PNT1A sono state esposte a WRW4. Abbiamo osservato che, la preincubazione con WRW4, prima della stimolazione con WKYMVm, previene l'attivazione delle ERK (Figura 19A) e la fosforilazione del residuo di tirosina 416 di c-Src (Figura 19B), con un massimo effetto alla concentrazione di 10 μM. La preincubazione con WRW4 previene anche la transattivazione di EGFR in cellule CaLu-6 (Figura19C), di c-Met in cellule PNT1A (Figura 19D), e la fosforilazione di p47phox (Figura 19E).

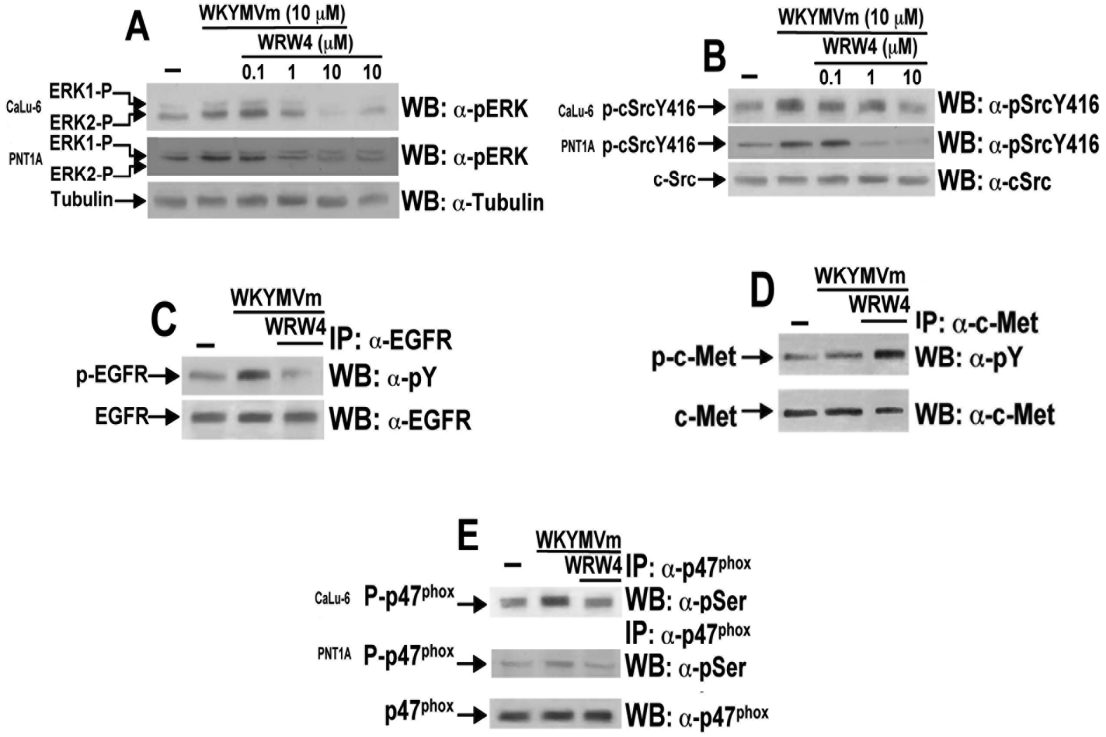

Figura 19. WRW4 previene l'attivazione delle cascate di segnalazione cellulare indotte dalla stimolazione di FPRL1. Lisati cellulari ottenuti da cellule CaLu-6 e PNT1A stimolate per 2 min con WKYMVm in presenza o assenza di concentrazioni crescenti di WRWWWW (WRW4), come riportato. (A) Cinquanta microgrammi di proteine sono state separate mediante SDS-PAGE 10% e saggiati con un anticorpo anti-fosfo-ERK (α–p-ERK) o (B) anti-fosfo-SrcY416 (α–p-SrcY416). Gli estratti sono stati normalizzatti reincubando i filtri o con α–tubulin o con α–c-Src. (C) Cellule CaLu-6 deprivate di siero sono state stimolate con WKYMVm per 2 min o preincubate per 15 min con WRW4 10 μM prima della stimolazione. Ottocento microgrammi di lisati totali sono stati immunoprecipitati con un anticorpo anti-EGFR (α–EGFR) e risolti su SDS-PAGE 10% e la fosforilazione di EGFR (p-EGFR) è stata rilevata utilizzando un anticorpo anti-fosfo-Tirosina (α-p-Y). Un anticorpo α–EGFR è stato utilizzato per controllare la quantità di proteine caricata. (D) Cellule PNT1A deprivate di siero sono state stimolate con WKYMVm per 2 min o preincubate per 15 min con WRW4 10 μM prima della stimolazione. Ottocento microgrammi di lisati totali sono stati immunoprecipitati con un anticorpo anti-cMet (α–c-Met) e risolti su SDS-PAGE 10%. La fosforilazione di c-Met (p-c-Met) è stata rilevata utilizzando un anticorpo anti-fosfo-Tirosina (α-p-Y). Un anticorpo α–c-Met è stato utilizzato per controllare la quantità di proteine caricata. (E) Cellule CaLu-6 e PNT1A sono state deprivate di siero e stimolate con WKYMVm per 2 min o preincubate per 15 min con WRW4 10 μM prima della stimolazione. Ottocento microgrammi di lisati totali sono stati immunoprecipitati con un anticorpo anti-p47phox (α–p47phox) e risolti su SDS-PAGE 10% e la fosforilazione di p47phox (p-p47phox) è stata rilevata utilizzando un anticorpo anti-fosfo-Serina (α-p-Ser). Un anticorpo α–p47phox è stato utilizzato per controllare la quantità di proteine caricata.

4.9 La transattivazione di EGFR e c-Met mediata da FPRL1 induce l'attivazione dei pathway JAK/STAT3 e PI3K/Akt

Le proteine STAT sono attivate in seguito alla stimolazione di un recettore per citochine o per fattori di crescita come EGFR e c-Met. STAT 2, 4, e 6 sono attivate da alcune citochine. STAT 1, 3, 5a e 5b, invece, possono essere attivate anche da fattori di crescita. L'attivazione di un recettore per fattori di crescita e la sua dimerizzazione determina la fosforilazione della proteina adattatrice JAK (receptor-associated Janus kinases) che a sua volta può mediare il reclutamento e la fosforilazione di STAT3 sul residuo di tirosina in posizione 705 necessaria alla dimerizzazione di STAT3. Tali eventi rappresentano l'innesco della cascata di segnalazione JAK/STAT. Una volta attivo, STAT3 trasloca nel nucleo dove regola la trascrizione di geni specifici ed è bersaglio di un'ulteriore fosforilazione a livello del residuo di serina in posizione 727, che incrementa la capacità di binding al DNA e l'attività trascrizionale.

Un altro evento che si osserva in seguito all'autofosforilazione di un recettore tirosin kinasico, è l'attivazione del pathway PI3K/Akt. La PI3K (fosfatidilinositolo3kinasi) catalizza la fosforilazione del fosfatidilinositolo4,5bisfosfato (PIP2) in fosfatidil3,4,5trifosfato (PIP3) che è capace di legare la proteina kinasi B (PKB) nota anche come Akt. Il legame di PIP3 ad Akt è necessario per la successiva attivazione della kinasi che avviene per una fosforilazione a carico del residuo di serina in posizione 473, catalizzata da PDK1. Tale fosforilazione determina l'attivazione di Akt che, attraverso l'interazione con una serie di proteine bersaglio, promuove la sopravvivenza cellulare.

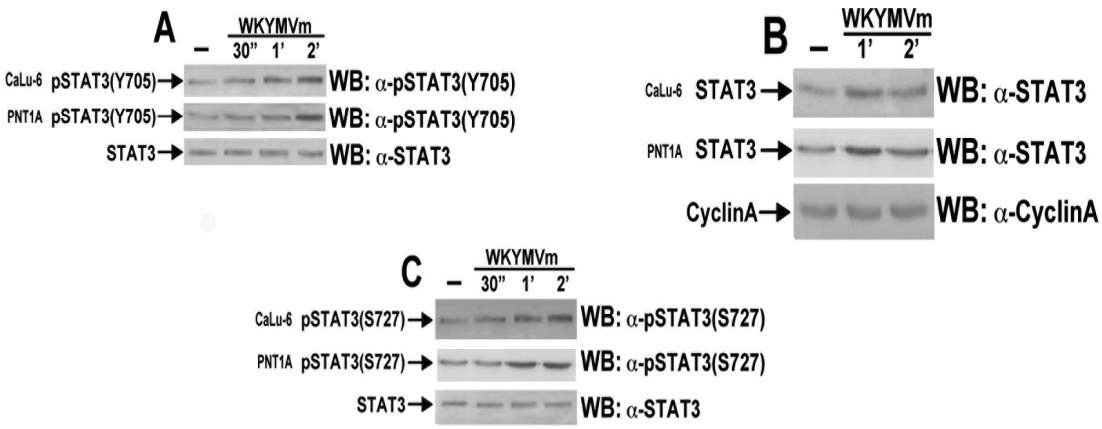

Figura 20. La transattivazione di EGFR mediata da FPRL1 induce l'attivazione del pathway di STAT3. Estratti totali e nucleari sono stati isolati da cellule CaLu-6 e PNT1A stimolate con WKYMVm per tempi crescenti. (A) Cinquanta microgrammi di proteine totali sono stati separati mediante SDS-PAGE 10% e la fosforilazione di STAT3 è stata rilevata con anticorpi specifici anti-fosfo-STAT3 Y705 (α-p-STAT3(Y705)) o (C) anti-fosfo-STAT3 S727 (α-p-STAT3(S727)). Un anticorpo anit-STAT3 (α-STAT3) è stato utilizzato come controllo della quantità degli estratti caricati. (B) Cinquanta microgrammi di estratti nucleari sono stati separati mediante SDS-PAGE al 10% e la migrazione nucleare di STAT3 è stata valutata mediante saggio di western blot con un anticorpo α-STAT3. Lo stesso filtro è stato ibridizzato con un anticorpo anti-cyclin A (α-CyclinA) per controllare la quantità degli estratti caricati.

Mediante esperimenti di western blot, abbiamo osservato nelle linee cellulari CaLu-6 e PNT1A che la stimolazione per tempi diversi, con l'agonista WKYMVm induce la fosforilazione di STAT3 sul suo residuo di tirosina 705 (Figura 20A), la migrazione nucleare di STAT3 (Figura 20B) e la fosforilazione del residuo di serina 727 di STAT3 (Figura 20C). Questi risultati suggeriscono che l'attivazione, la dimerizzazione e la migrazione nucleare di STAT3 sono associati alla cascata di segnalazione dipendente dalla stimolazione di FPRL1.

Sono stati analizzati i meccanismi molecolari coinvolti nell'attivazione FPRL1-dipendente di STAT3 pretrattando le linee cellulari con PTX, genisteina, AG1478 (nelle cellule CaLu-6) e SU11274 (nelle cellule PNT1A). Questi esperimenti dimostrano che la fosforilazione del residuo di tirosina in posizione 705

di STAT3 è un evento che dipende non solo dall'attivazione di FPRL1, ma anche dalla transattivazione di EGFR e c-Met, essendo prevenuta da PTX e da inibitori sia generici che specifici dei due recettori (Figura 21A). Inoltre, abbiamo osservato che la fosforilazione di STAT3 sulla tirosina 705 è regolata dall'attivazione di c-Src, essendo prevenuta dal pretrattamento con PP2, ma non dipende dall'attivazione di MEK, come dimostrato dall'assenza di variazioni dello stato di fosforilazione di STAT3 su tale residuo in seguito al pretrattamento con PD098059, l'inibitore selettivo di MEK (Figura 21B).

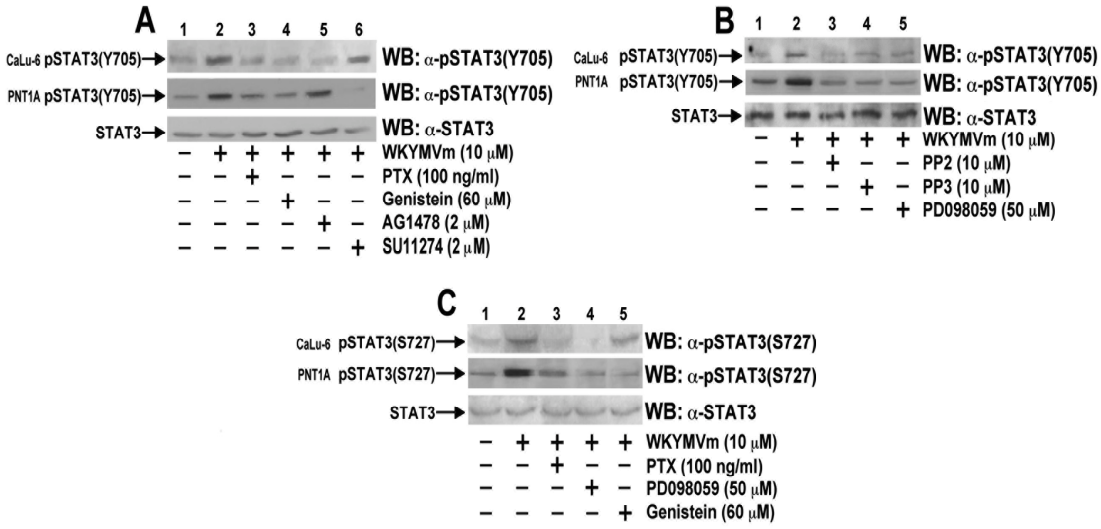

Figura 21. L'attivazione del pathway di STAT3 mediata da FPRL1 richiede l'attivazione di EGFR, c-Src e MEK1. Cellule CaLu-6 e PNT1A deprivate di siero sono state stimolate con WKYMVm per 2 min o preincubate con le appropriate concentrazioni di inibitori prima della stimolazione così come riportato in materiali e metodi. Cinquanta microgrammi di estratti totali sono sati separati e trasferiti su filtro di PVDF elettroforeticamente. (A) Le linee cellulari CaLu-6 e PNT1A sono state preincubate per 16 h con PTX, oppure per 1 h con genistein oppure per 1 h con AG1478 o per 16 h con SU11274, prima della stimolazione con WKYMVm. Il filtro è stato ibridizzato con un anticorpo primario specifico per la rilevazione della fosforilazione del residuo di tirosina in posizione 705 di STAT3 (α-p-STAT3(Y705)). (B) Cellule CaLu-6 e PNT1A deprivate di siero sono state pretrattate per 45 min con PP2, o per 45 min con PP3, o per 90 min con PD098059 alle concentrazioni indicate, prima della stimolazione con WKYMVm. Un anticorpo α-p-STAT3(Y705) è stato utilizzato per rilevare la fosforilazione di STAT3 in posizione 705. (C) Cellule CaLu-6 e PNT1A deprivate di siero sono state pretrattate con PTX, PD098059 e genistein alle concentrazioni riportate, prima di essere stimolate con l'agonista di FPRL1. Il filtro è stato incubato con un anticorpo specifico per rilevare la fosforilazione di STAT3 sul residuo di serina in posizione 727 (α-p-STAT3(S727)). Per controllare la quantità di estratti caricati i filtri sono stati reincubati con un anticorpo α-STAT3.

Anche la fosforilazione del residuo di serina in posizione 727 di STAT3 è completamente prevenuta dal pretrattamento con PTX in entrambe le linee cellulari (Figura 21C). Come atteso, tale fosforilazione è prevenuta dal pretrattamento con PD098059, ma non dal pretrattamento con la genisteina, che essendo un inbitore dell'attività tirosin kinasica non sortisce alcun effetto sui meccanismi di fosforilazione delle serine (Figura 21C). L'attivazione delle ERK è quindi richiesta per la fosforilazione del residuo di serina 727 di STAT3 nelle cellule stimolate con WKYMVm.

Nella linea cellulare PNT1A, la stimolazione per tempi diversi con WKYMVm determina la fosforilazione tempo-regolata del residuo di serina di Akt in posizione 473 (Figura 22A). Tale fosforilazione è prevenuta da PTX ed SU11274, suggerendo il coinvolgimento di proteine G attivate e di c-Met transfosforilato, e dal pretrattamento con wortmannina e LY294002, due inibitori selettivi della PI3K (Figura 22B).

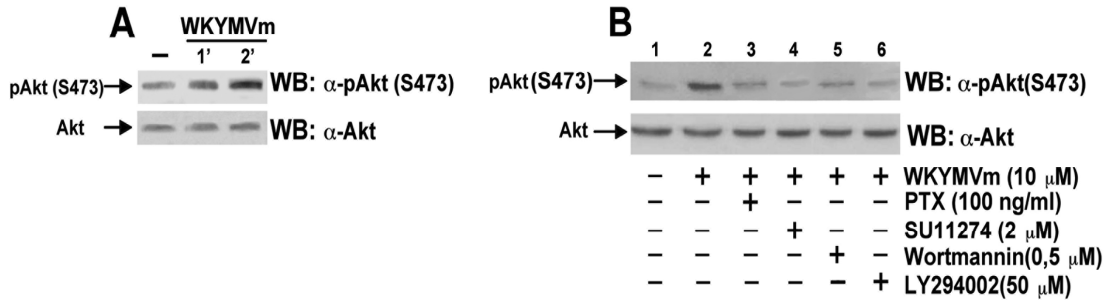

Figura 22. L'attivazione del pathway di Akt mediato da FPRL1 richiede l'attivazione di c-Met e della PI3K. Cellule PNT1A deprivate di siero sono state stimolate per tempi crescenti con WKYMVm. (A) Cinquanta microgrammi di proteine totali sono stati separati mediante SDS-PAGE 10% e la fosforilazione di Akt è stata rilevata con anticorpi specifici anti-fosfo-Akt S473 (α-p-Akt(S473)). (B) Cellule PNT1A deprivate di siero sono state pretrattate per 16 h con PTX, o per 16 h con SU11274, o per 1 h con Wortmanin o per 1 h con LY294002, prima di essere stimolate con stimolate con WKYMVm per 2 min. Cinquanta microgrammi di estratti sono stati separati mediante SDS-PAGE 10 % e saggiati con un anticorpo α-p-Akt(S473). La quantità di estratti caricata è stata normalizzata reincubando i filtri con un anticorpo anti-Akt (α-p-Akt).

Questi dati suggeriscono che la fosforilazione PI3K-dipendente di Akt è un evento associato alla transattivazione di c-Met mediata dall'attivazione di FPRL1.

4.10 Le cascate di segnalazione attivate dalla stimolazione di FPRL1 promuovono la proliferazione cellulare

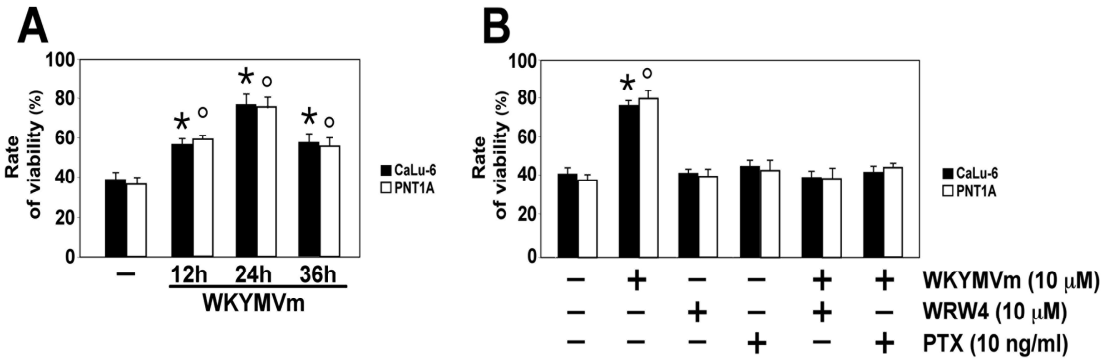

Figura 23. Le cascate di segnalazione intracellulare attivate dalla stimolazione di FPRL1 in cellule CaLu-6 e PNT1A promuovono un incremento dell'indice di proliferazione cellulare. (A) In una multi-well da 96 sono state piastrate 4x 10^4 cellule CaLu-6 o PNT1A in 200 μl di mezzo di coltura con WKYMVm 10μM per 12, 24 e 36 h a 37°C. (B) Le linee cellulari CaLu-6 e PNT1A sono state incubate per 24 h con l'agonista di FPRL1 in presenza o assenza di PTX o WRW4 alle concentrazioni indicate. MTT (5mg/ml in PBS) è stato aggiunto per ciascuna well ed è stato incubato per 4 h a 37°C. Dopo aver rimosso il mezzo di coltura, sono stati aggiunti in ciascun pozzetto 200 μl di DMSO per solubilizzare i sali di formalzano generati. L'assorbanza dei sali di formalzano sono stati letti con un microplate reader alla lunghezza d'onda di 540 nm. L'effetto di WKYMVm sulla crescita cellulare è stato indicato come percentuale di vitalità cellulare.

Gli effetti delle cascate di segnalazione, attivate in seguito alla stimolazione di FPRL1 con WKYMVm, sono stati analizzati valutando la variazione dell'indice di proliferazione cellulare delle linee cellulari CaLu-6 e PNT1A. Abbiamo osservato che la stimolazione per tempi diversi con WKYMVm determina un incremento dell'indice di proliferazione cellulare, che raggiunge il massimo livello dopo 24 ore di stimolazione (Figura 23A). L'inibizione delle proteine Gi, oppure il pretrattamento

con WRW4, l'antagonista selettivo di FPRL1, prevengono in maniera significativa l'incremento della proliferazione delle linee cellulari CaLu-6 e PNT1A (Figura 23B).

Questi dati suggeriscono che le cascate di segnalazione intracellulare attivate dalla stimolazione di FPRL1 con WKYMVm promuovono un incremento dell'indice di proliferazione cellulare nelle due linee cellulari che può essere prevenuto antagonizzando l'attività del recettore FPRL1.

5 DISCUSSIONE

I risultati ottenuti nel corso del dottorato dimostrano che i recettori per N-formil peptidi sono funzionalmente espressi in un'ampia varietà di tipi di cellulari non correlati al compartimento polimorfonucleato, dove inizialmente sono stati identificati. Tali recettori sono promiscui per l'eterogenità di cascate di segnalazione intracellulare attivate, per la loro espressione tessuto specifica o per la natura del ligando con il quale i recettori interagiscono.

Tra i ligandi analizzati abbiamo dimostrato che in fibroblasti polmonari umani IMR90 deprivati di siero, la stimolazione con LL-37 induce la fosforilazione delle ERK e di p47phox mediante un meccanismo MEK-dipendente e Ca^{2+}-dipendente, nonché la generazione MEK-dipendente di ROS. Questa cascata di segnalazione è mediata dall'interazione di LL-37 con FPRL-1 come dimostrano i risultati ottenuti preincubando le cellule con PTX o con WRW4, l'antagonista selettivo di FPRL1, che prevengono significativamente l'attivazione delle ERK, la fosforilazione di p47phox e l'attivazione LL-37-dipendente della NADPH ossidasi.

La generazione di anione superossido NADPH-dipendente in cellule fagocitiche stimolate con LL-37 è stata osservata in diversi studi. Questi hanno dimostrato che in macrofagi umani i peptidi antimicrobici promuovono un burst ossidativo (118) e che in neutrofili il peptide LL-37 media la generazione di ROS, attraverso un meccanismo NADPH ossidasi-dipendente. Tuttavia, i meccanismi molecolari che sono alla base della generazione di superossido da parte della NADPH ossidasi in cellule stimolate con LL-37, non sono stati descritti, anche se la capacità di LL-37 di indurre la fosforilazione delle ERK in diversi tipi cellulari è

stata riportata in alcuni lavori (119-122). I risultati ottenuti nel nostro laboratorio per la prima volta dimostrano che in fibroblasti umani, stimolati con LL-37, l'attivazione delle ERK è un evento necessario per la fosforilazione e l'attivazione di p47phox, nonché per la generazione di superossido NADPH-dipendente. Inoltre, l'osservazione che la deplezione del calcio intracellulare, ottenuta pretrattando le cellule con il chelante del calcio BAPTA-AM, riduce significativamente la fosforilazione delle ERK e l'attivazione della NADPH ossidasi mediata da LL-37, suggerisce che in queste cellule la generazione di ROS dipende anche dalla mobilizzazione intracellulare del Ca^{2+}.

LL-37 utilizza FPRL1 come recettore per mediare la sua azione in monociti, neutrofili del sangue periferico, cellule T (123) e cellule endoteliali (124). Nella linea cellulare di cheratinociti umani HaCaT, l'interazione FPRL1/LL-37 induce la migrazione cellulare, l'attivazione di fattori trascrizionali e di metalloproteasi della matrice, innescando i pathway di segnalazione delle MAPK e di PI3K/Akt, che risultano essere mediati anche dalla transattivazione di EGFR (125). In HUVECs, è stato osservato che la migrazione e la proliferazione cellulare indotta dalla stimolazione con LL-37 è prevenuta dal pretrattamento con F2L (126), un peptide che deriva dalla proteina legante l'eme, che è stata indentificata come un ligando endogeno di FPRL2 (127). È stato anche dimostrato che LL-37 promuove la produzione e il rilascio dell'interleuchina-1β (IL-1β) nei monociti attraverso l'attivazione del recettore nucleotidico $P2X_7$ (128) e induce, in neutrofili, l'arresto dell'apoptosi attraverso l'attivazione di FPRL1 e $P2X_7$ (122). La capacità che LL-37 ha nell'interagire con differenti recettori è ulteriormente supportata dagli studi condotti in cellule epiteliali polmonari, dove è stata osservata l'espressione sia di

recettori ad alta che a bassa affinità per LL-37. FPRL1 sembra essere un recettore a bassa affinità in queste cellule (129). Inoltre, in monociti primari umani (130) ed in cellule epiteliali delle vie aeree (131), la fosforilazione delle ERK indotta da LL-37 non è prevenuta dalla preincubazione con PTX, indicando che le cascate di segnalazione intracellulare attivate non sono associate al recettore FPRL1 (130, 131). In queste cellule, oltre ad un recettore GPCR insensibile a PTX, la fosforilazione delle ERK mediata da LL-37 richiede l'attivazione dei domini tirosin kinasici di EGFR, attraverso il clivaggio del ligando di EGFR (131), mediata da un meccanismo metalloproteasi-dipendente. Queste osservazioni suggeriscono che LL-37 può agire su differenti cellule bersaglio attraverso l'interazione con differenti recettori ed innescare diversi pathway di trasduzione del segnale.

Un problema irrisolto è la provenienza del NADPH necessario alla generazione di anione superossido. La via del pentosio fosfato, attraverso la glucosio-6-fosfato deidrogenasi, è la fonte principale di NADPH. In cellule endoteliali il NADPH e richiesto come cofattore per la NADPH ossidasi e i suoi livelli riflettono un aumentato stato di stress ossidativo che, in parte, è attribuibile alla NADPH ossidasi e/o all'ossido nitrico sintasi endoteliale (133, 134). Il NADPH è anche richiesto come fonte di equivalenti riducenti per mantenere ridotte le risorse di glutatione. In cellule endoteliali vascolari, specifici componenti ossidati delle particelle LDL, come ox-PAPC, inducono la generazione di superossido che sembra essere mediata dall'attività della NADPH ossidasi (135). Il pretrattamento di queste cellule con 2-deossiglucosio, un antimetabolita che blocca la produzione di NADPH attraverso la via del pentosio fosfato, riduce significativamente il livello di produzione di superossido (135), suggerendo che, in cellule endoteliali stimolate con ox-PAPC, la

via del pentosio fosfato è la fonte principale di NADPH necessario per l'attività della NADPH ossidasi. Studi per stabilire il ruolo della via pentosio fosfato del metabolismo del glucosio in fibroblasti umani stimolati con LL-37 sono in corso.

I nostri studi, dimostrano che la fosforilazione delle ERK è richiesta per la generazione di superossido NADPH-dipendente in fibroblasti umani stimolati con LL-37, ma lasciano aperta la questione sul significato biologico del legame di LL-37 con FPRL1 in questa linea cellulare. Si potrebbe ipotizzare un ruolo nella difesa immune innata da parte dei fibroblasti umani che potrebbero essere attratti in sede di danno tissutale per rilasciare ROS in seguito all'interazione di LL-37 con FPRL1, oppure, dare inizio al processo di riparazione del danno tissutale stesso. Una conoscenza più dettagliata delle cascate di segnalazione intracellullare mediate da LL-37 e dei suoi meccanismi di interazione, potrebbero permettere la progettazione di nuovi farmaci in grado di modulare le cascate di segnalazione associate a FPRL1 e l'interazione LL-37/FPRL1.

Nei nostri studi abbiamo anche dimostrato che la stimolazione di cellule CaLu-6 e PNT1A, opportunamente deprivate di siero e stimolate con un agonista selettivo per il recettore FPRL1, determina la generazione NADPH-dipendente di specie reattive dell'ossigeno (ROS), le quali mediano la transattivazione dei recettori tirosin kinasici EGFR e c-Met. I nostri dati suggeriscono che i ROS svolgono un ruolo chiave nel collegare i segnali che partono da FPRL1 e giungono a EGFR o c-Met modulando l'attività kinasica di c-Src, come dimostrato dagli effetti di PP2, apocinina, e di siRNA contro p22phox, sulla fosforilazione di c-Src e sulla transattivazione di EGFR e c-Met. Inoltre, i risultati ottenuti dimostrano che in seguito alla transattivazione di EGFR e c-Met i residui di tirosina fosforilati

forniscono siti di legame per il reclutamento e l'attivazione dei pathway di JAK/STAT3 e di PI3K/Akt. Inoltre, le cascate di segnalazione innescate dalla stimolazione di FPRL1 nelle due linee cellulari culmina con un significativo incremento dell'indice di proliferazione cellulare.

EGFR è un recettore di membrana che appartiene alla famiglia dei recettori tirosin kinasici c-erb-B, noto per essere iperespresso in una varietà di cellule tumorali, compresa la linea cellulare di cancro anaplastico del polmone CaLu-6 (136).

Il recettore per il fattore di crescita epatico (HGF) o scatter factor (SF), noto anche come c-Met, è un recettore dotato di attività tirosin kinasica. Definito inizialmente come un proto-oncogene, c-Met se stimolato innesca cascate di segnalazione responsabili dell'aumentata angiogenesi, proliferazione e sopravvivenza cellulare. Il recettore c-Met è spesso coinvolto in diversi processi tumorali, anche se il suo ligando HGF è scarsamente espresso nel corso della vita adulta (110).

I recettori EGFR e c-Met, oltre ad essere attivati dai propri ligandi EGF e HGF rispettivamente, possono essere transattivati anche da alcuni recettori accoppiati a proteine G (GPCR). Il cross-talk che si instaura tra i due recettori è cruciale per espandere la rete di comunicazione cellulare. Infatti, i recettori per l'angiotensina (137), LPA (138), CXCL12 (139), bombesina (140), trombina (141) ed endotelina-1 (142) possono transattivare EGFR rafforzando, in questo modo, la trasmissione del segnale di crescita. In cellule di glioblastoma, la transattivazione di EGFR è determinata dall'interazione di N-fMLP con FPR (143) e l'inibizione della fosforilazione di EGFR riduce significativamente la chemiotassi e la proliferazione

cellulare tumorale mediata dalla stimolazione di FPR (143, 144). Quindi, il recettore FPR espresso in cellule di glioblastoma può amplificare la capacità di EGFR di promuovere la proliferazione cellulare tumorale. In linea con questi risultati, nei nostri studi abbiamo dimostrato che come conseguenza della trasduzione del segnale mediata dalla stimolazione di FPRL1 con WKYMVm si osserva un incremento dell'indice di proliferazione cellulare delle cellule CaLu-6 e PNT1A, il quale è prevenuto dal blocco del recettore FPRL1.

Non sempre la stimolazione dei recettori per N-formil peptidi e la conseguente attivazione delle ERK è riconducibile ad un incremento della proliferazione cellulare. I nostri dati mostrano che, nella linea cellulare umana di glioblastoma U-87, la stimolazione con N-fMLP, un agonista selettivo di FPR, promuove l'accumulo degli inibitori di CDK (CKI) $p16^{INK4A}$ e di $p21^{waf1/cip1}$. L'accumulo di $p21^{waf1/cip1}$ osservato dipende dall'attivazione delle ERK e di MEK la quale è prevenuta dal pretrattamento con l'apocinina, un inibitore selettivo della NADPH ossidasi, suggerendo il coinvolgimento dei ROS come mediatori del segnale in questo evento. I dati ottenuti in cellule di glioblastoma U-87 sottolineano la complessità dei meccanismi di trasduzione del segnale innescati in seguito alla stimolazione di un recettore per N-formil peptidi.

La transattivazione di un RTK ad opera di un GPCR è un evento ampiamente descritto in letteratura e può essere mediato da diverse molecole di segnalazione, come tirosin kinasi non recettoriali, metalloproteasi e ROS (145). In cellule di glioblastoma, la fosforilazione N-fMLP-dipendente di EGFR richiede la presenza del recettore FPR e delle proteine Gi associate al recettore ed è controllata dalla tirosin kinasi c-Src (146, 147). I nostri risultati dimostrano che il signaling indotto da

FPRL1 induce un aumento dell'attività kinasica di c-Src e che quest'ultima ha un ruolo chiave nella transattivazione di EGFR e c-Met.

Un ulteriore meccanismo molecolare che può contribuire alla transattivazione dei RTK è la generazione di ROS, che inattivando le PTPasi, controllano la loro attività, modificando l'equilibrio tra stato non fosforilato e stato fosforilato a favore di quest'ultimo (149-154). L'ossidazione e la riduzione dei gruppi sulfidrilici delle cisteine delle PTPasi può quindi rappresentare l'interruttore responsabile dell'accensione o dello spegnimento delle cascate di segnalazione intracellulare.

Una delle macchine enzimatiche deputata alla generazione dei ROS è la famiglia delle NADPH ossidasi (Nox). Questi, sono enzimi associati alla membrana, che catalizzano e regolano la produzione di ROS. A differenza dei livelli citotossici di superossido prodotti dai fagociti, la famiglia delle proteine Nox non-fagocitiche si distingue per la produzione di bassi livelli di ROS, che giocano un ruolo cruciale nel controllo dei normali processi fisologici e che stimolano le cascate di segnalazione intracellulare attivando le kinasi ed inibendo le PTPasi (155). In condizioni fisiologiche, la produzione intracellulare di ROS non altera lo stato redox della cellula grazie alle riserve di agenti riducenti che questa normalmente possiede. L'ambiente riducente intracellulare permette ai ROS, generati in seguito ad uno stimolo, di funzionare da secondi messaggeri limitando il loro effetto nello spazio e nel tempo (156). La principale caratteristica della NADPH ossidasi nonfagocitica è che oltre ad essere costitutivamente attiva, è particolarmente sensibile ad una varietà di stimoli fisio-patologici. Infatti, diverse condizioni patologiche sono associate ad una iper-produzione di ROS da parete dei membri della famiglia dei Nox. Queste comprendono malattie croniche che tendono ad apparire tardivamente nel corso della

vita, come ad esempio l'Alzheimer, l'aterosclerosi, l'ipertensione, la nefropatia diabetica, la fibrosi epatica e il cancro. In molte di queste malattie, l'iper-produzione di ROS è spesso associata all'aumentata espressione degli enzimi Nox e/o delle loro subunità regolatore (157).

I ROS possono anche influenzare lo stato di attivazione di c-Src modulando direttamente la sua attività kinasica o indirettamente, modulando fattori che a loro volta regolano l'attività kinasica di c-Src (158, 159). Nei nostri studi abbiamo dimostrato che il signaling indotto da FPRL1 innesca la generazione di superossido NADPH-dipendente che gioca un ruolo cruciale nella transattivazione di EGFR, modulando l'attività tirosin kinasica di c-Src. Va, però, considerato che una concomitante transattivazione di EGFR ligando-dipendente non può essere esclusa.

I recettori tirosin kinasici possono innescare una serie di pathway di trasduzione del segnale generalmente coinvolti nella proliferazione e nella sopravvivenza cellulare come quello di STAT3 e di PI3K/Akt. STAT3 è un fattore trascrizionale che appartiene alla famiglia delle proteine STAT. Per poter essere attivato richiede una fosforilazione del residuo di tirosina in posizione 705 e questo evento è mediato da un RTK, da tirosin kinasi citosoliche come c-Src o da componenti della famiglia delle proteine JAK. Una seconda fosforilazione sul residuo di serina 727 stabilizza ed incrementa l'attività trascrizionale di STAT3 (160-162).

La proteina Akt, nota anche come PKB, svolge un ruolo chiave nel controllo della sopravvivenza e dell'apoptosi cellulare. La proteina Akt presenta un sito maggiore di fosforilazione nella regione carbossi-terminale a livello del residuo di serina in posizione 473. Nelle due linee cellulari analizzate abbiamo dimostrato che

la stimolazione di FPRL1 con WKYMVm determina la fosforilazione di STAT3 sia sul residuo di tirosina 705, che di serina 727, suggerendo che l'attivazione di STAT3 è collegata alla cascata di segnalazione attivata da FPRL1. Inoltre, abbiamo osservato che il pathway delle MAPK innescato da FPRL1 ricopre un ruolo importante nella regolazione della fosforilazione del residuo di serina 727 di STAT3. Infatti, i risultati ottenuti pretrattando le cellule con PD098059, prima della stimolazione con WKYMVm, dimostrano che la fosforilazione delle ERK è cruciale per l'attivazione di STAT3. Inoltre, in cellule PNT1A, la stimolazione di FPRL1 con il suo agonista induce l'attivazione di Akt mediata dalla PI3K, come dimostrato dall'osservazione che i pretrattamenti con wortmannina e LY294002, due inibitori selettivi della PI3K, ne prevengono l'attivazione.

Negli ultimi anni sono stati identificati diversi ligandi che hanno reso FPRL1 il più promiscuo della famiglia dei recettori per N-formil peptidi. La maggior parte degli agonisti identificati non presenta una sostanziale omologia di sequenza, suggerendo che FPRL1 può essere attivato da un'ampia varietà di ligandi non correlati tra loro. Numerosi studi sono focalizzati alla comprensione dell'interazione ligando/FPRL1, anche per il potenziale ruolo di FPRL1 come target farmacologico.

Infatti, sia gli agonisti che gli antagonisti di FPRL1 svolgono un ruolo terapeutico. WKYMVm incrementa l'attività battericida dei neutrofili in pazienti in chemioterapia (163) ed aumenta l'espressione endogena di TRAIL, un nuovo potenziale agente antitumorale, in monociti e neutrofili umani (164). Inoltre, WKYMVm, interagendo con FPRL1, inibisce l'infezione virale Env-dipendente del virus HIV attraverso la desensitizzazione eterologa dei recettori per le chemokine

CCR5 e CXCR4, suggerendo un nuovo approccio per lo sviluppo di farmaci anti-HIV-1 (165).

L'interazione di FPRL1 con SAA, Aβ42 e peptidi prionici umani suggerisce che questo recettore può giocare un ruolo proinfiammatorio nell'amiloidosi, nel morbo di Alzheimer e nelle malattie da prioni. Anche se ad oggi sono stati identificati diversi antagonisti per FPRL1, ulteriori studi sono necessari per identificare nuovi antagonisti che consentano di delineare le cascate di trasduzione del segnale associate all'attivazione del recettore e che forniscano le basi per lo sviluppo di nuove molecole anti-infiammatorie. Gli antagonisti di FPRL1 comprendono la proteina inibitrice della chemiotassi dello *Staphylococcus Aureus,* la proteina inibitrice di FPRL1 FLIpr, l'acido biliare deossicocilico e chenodeossicocilico, e Quin-c7, un nonpeptide sintetico sviluppato attraverso modificazioni chimiche di QuinC-7 (166-168). Inoltre, peptidi ricchi in triptofano (W), come ad esempio WRW4, esercitano un effetto antagonistico sulla trasduzione del segnale di FPRL1 mediata da WKYMVm, suggerendo un loro impiego nel trattamento di diverse malattie nelle quali è noto il coinvolgimento attivo di FPRL1 (169).

La transattivazione di EGFR e di c-Met mediata da FPRL1, può avere importanti risvolti fisiopatologici. Le cascate di segnalazione attivate da FPRL1 possono essere innescate non solo da WKYMVm, ma anche da altri agonisti generalmenti presenti nei processi infiammatori e in sede di danno tissutale, condizioni che generalmente si riscontrano nel microambiente necrotico tumorale. Come risultato dell'interazione tra queste molecole e FPRL1 si può determinare l'attivazione di una serie di molecole di segnalazione come ROS, ERK e c-Src che

rappresentano i mediatori della transattivazione di EGFR e c-Met e dell'attivazione dei pathway di STAT3 e Akt, favorendo la proliferazione e la sopravvivenza cellulare.

I risultati ottenuti forniscono un contributo nel chiarire la complessità dei meccanismi di trasduzione del segnale che possono essere attivati dai recettori per N-formil peptidi nei processi fisiologici ed in quelli tumorali. Inoltre, offrono nuove prospettive sul ruolo dei recettori per N-formil peptidi in cellule non fagocitiche, proponendo nuove terapie basate sull'interazione FPRL1/agonista e sul relativo pathway di segnalazione. L'identificazione di un nuovo target farmacologico da accoppiare alle terapie antitumorali già esistenti rivolte verso i recettori EGFR e c-Met, potrebbe, infatti, contrastare più efficacemente la proliferazione e la sopravvivenza cellulare tumorale.

BIBLIOGRAFIA

1. Cattaneo F., Guerra G., Ammendola R. (2010). *Expression and signalling of Formyl Peptide Receptor in the Brain*. Neurochem. Res. 35(12):2018-2026, Review.
2. Le Y., Philip M. M., Wang J. M. (2002). *Formyl-peptide receptors revisited*. TRENDS in Immunology 23(11):541-548.
3. Le Y., Joost J., Oppenheim X., Wang J. M. *(2001). Pleiotropic roles of formyl peptide receptors.* Citokine and Growth Factor Reviews 12:91-105.
4. Durstin M., Gao J., Tiffany H., Mc Dermott D., Murphy P. M. (1994). *Differential expression of the N-formylpeptide receptor gene cluster in human phagocytes.* Biochem. Biophys. Res. Commun. 201:174-179.
5. Cattaneo F., Iaccio A., Guerra G., Montagnani S., Ammendola R. (2011). *NADPH-oxidase-dependent reactive oxygen species mediate EGFR transactivation by FPRL1 in WKYMVm-stimulated human lung cancer cells.* Free Radic. Biol. Med. 51(6):1126-1136.
6. Harada M., Habata Y., Hosoya M., Nishi K., Fujii R., Kobayashi M., Hinuma S. (2004). *N-formylated humanin activates both formyl peptide receptor-like 1 and 2*. Biochem. Biophys. Res. Commun. 324:255-261.
7. Ammendola R., Russo L., De Felice C., Esposito F., Russo T., Cimino F. (2004). *Low-affinity-receptor mediated inducuction of superoxide by N-Formyl-Methionyl-Leucyl-Phenylalanine and WKYMVm in IMR90 Human Fibroblast*, Free Radic. Biol. Med. 36:189-200.

8. Schiffman E., Showell H. V., Corcoran B. A., Ward P.A., Smith E., Becker E. L. (1975). *The isolation and partial characterization of neutrophil chemotactic factors from Escherichia coli.* J. Immunol. 114:1831-7.
9. Marasco W. A., Phan S. H., Krutzsch H., Showell H. J., Feltner D. E., Nairn R., Becker E. L., Ward P. A. (1984). *Purification and identification of formyl-methionyl-leucyl-phenylalanine as the major peptide neutrophil chemiotactic factor produced be Escherichia coli.* J. Biol. Chem. 259:5430-9.
10. Carp H. (1982). *Mitochondrial N-formylmethionyl proteins as chemoattractants for neutrophils.* J. Exp. Med. 155:264-75.
11. Panaro M. A., Mitolo V. (1999). *Cellular responses to FMLP challenging: a mani review.* Immunopharmacol. Immunotoxicol. 21:397-419.
12. Murphy P. M. (1997). *The N-formyl peptide chemotactic receptors. In: Horuk R, editor. Chemoattractant ligands and their receptors. Boca Raton*, FL: CRC Press 269–99.
13. Prossnitz E. R., Ye R. D. (1997). *The N-formyl peptide receptor: a model for the study of chemoattractant receptor structure and function.* Pharmacol. Ther. 74:73–102.
14. Le Y., Yang Y, Cui Y, Yazawa H., Gong W., Qiu C., Wang J. M. (2002). *Receptors for chemotactic formyl peptides as pharmacological targets.* International Immunopharmacology 2:1-13.
15. Zhou Y., Bian X., Le Y., Gong W., Hu J. Y., Zhang X., Wang L., Iribarren P., Salcedo R., Howard O. M. Z., Farrar W, Wang J. M. (2005). *Formylpeptide Receptor FPR and the Rapid Growth of malignant Human Gliomas*. Journal of the National Cancer Institute 97:1298-1308.

16. Bao L., Gerard N. P., Eddy R. L., Shows T. B., Gerard C. (1992). *Mapping of genes for the human C5a receptor (C5AR), human FMLP receptor (FPR), and two FMLP receptor homologue orphan receptors (FPRH1, FPRH2) to chromosome 19.* Genomics 13:437-440.

17. Ye R.D., Cavanagh S. L., Quehenberger O., Prossnitz E.R., Cochrane C. G. (1992). *Isolation of a cDNA that encodes a novel granulocyte N-formyl peptide receptor.* Biochem. Biophys. Res. Commun. 184:582-589.

18. Murphy P.M., Ozçelik T., Kenney R. T., Tiffany H. L., McDermott D., Francke U. (1992). *A structural homologue of the N-formyl-peptide receptor. Characterization and chromosome mapping of a peptide chemoattractant receptor family.* J. Biol. Chem. 267:7637-7643.

19. Fu H., Karlsson J., Bylund J., Movitz C., Karlsson A, Dahlgren C. (2006). *Ligand recognition and activation of formyl peptide receptors in neutrophilis*. J. Leukoc. Biol. 79:247-256.

20. Christophe T., Karlsson A., Dugave C., Rabiet M. J., Boulay F., Dahlgren C. (2001). *The synthetic peptide Trp-Lys-Tyr-Met-Val-Met-NH2 specifically activates neutrophils throught FPRL1/lipoxin A4 receptors and is an agonist of orphan monocyte-expressed chemoattractant receptor FPRL2.* J. Biol. Chem. 276:21585-93.

21. Betten A., Bylund J., Christophe T., Boulay F., Romero A., Hellstrand K., Dahlgren C. (2001). *A proinflammatory peptide from Helicobacter pylori activates monocytes to induce lymphocyte dysfunction and apoptosis.* J. Clin. Invest. 108:1221-1228.

22. Pontieri G.M, Russo M.A., Frati L. (2005). *Patologia generale*, Tomo I, III Edizione, Piccin cap. 13 pp. 347-353, cap. 11 pp. 306-308, cap. 7 pp.205-228.

23. Ammendola R., Ruocchio M., Chirico G., Russo L., De Felice C., Esposito F., Russo T., Cimino F. (2002). *Inhibition of NADH/NADPH oxidase effects signal transduction by growth factor receptor in normal fibroblast.* Arch. Biochem. Biophys. 397:253 – 257.

24. Shiose A, Sumimoto H. (2000). *Arachidonic acid and phosphorylation synergistically induce a conformational change of p47phox to activate the phagocyte NADPH oxidase.* J. Biol. Chem. *275*:13793-18801.

25. Roland Seifert, Katharina Wenzel-Seifert (2003). *The human formyl peptide receptor as model system for constitutively active G-protein-coupled receptors.* Life Sciences 73, 2263-2280.

26. Selvatici R., Falzarano S., Mollica A., Spisani S. (2006). *Signal transduction pathways triggered by selective formylpeptide analogues in human neutrophils.* Eur. J. Pharmacol. 534:1-11.

27. Seo J. K., Choi S. Y., Kim Y., Baek S. H., Kim K. T., Chae C. B., et al. (1997). *A peptide with unique receptor specificity. Stimulation of phosphoinositide hydrolysis and induction of superoxide generation in human nertrophils.* J. Immunol. 158:1895-901.

28. Seo J. K., Bae Y. S., Song H., Baek S. H., Kim B. S., Choi W. S., et al. (1998). *Distribution of the receptor for a novel peptide stimulating phosphoinositide hydrolysis in human leukocytes.* Clin. Biochem. 31:137-41.

29. Bae Y. S., Ju S. A., Kim J. Y., Seo J. K., Baek S. H., Kwak J. Y., et al. (1999). *Trp-Lys-Tyr-Met-Val-D-Met stimulates superoxide generation and killing of*

Staphylococcus aureus via phospholipase D activation in human monocytes. J. Leuko. Bio. 65:241-8.

30. Le Y., Gong W., Li B., Dunlop N. M., Shen W., Su S. B., et al. (1999). *Utilization of two seven-transmembrane, G protein-coupled receptors, formyl peptide receptor-like 1 and formyl peptide receptor, by the synthetic hexapeptide WKYMVm for human phagocyte activation.* J. Immunol. 163:6777-84.

31. Su S. B., Gong W. H., Gao J. L., Shen W. P., Grimm M. C., Deng X., et al. (1999). *T20:DP178, an ectodomain peptide of human immunodeficiency virus type 1 gp41, is an activator of human phagocyte N-formyl peptide receptor.* Blood 93:3885-92.

32. Le Y., Jiang S., Hu J., Gong W., Su S., Dunlop N. M., et al. (2000). *N36, a synthetic N-terminal heptad repeat domain of the HIV-1 envelope protein gp41, is an activator of human phagocytes.* Clin. Immunol. 96:236-42.

33. Deng X., Ueda H., Su S. B., Gong W., Dunlop N. M., Gao J. L., et al. (1999). *A synthetic peptide derived from HIV-1 gp120 down-regulates the expression and function of chemokine receptors CCR5 and CXCR4 in monocytes by activating the seventransmembrane G protein-coupled receptor FPRL1:LXA4R.* Blood 94:1165-73.

34. Shen W., Proost P., Li B., Gong W., Le Y., Sargeant R., et al. (2000). *Activation of the chemotactic peptide receptor FPRL1 in monocytes phosphorylates the chemokine receptor CCR5 and attenuates cell responses to selected chemokines.* Biochem. Biophys. Res. Commun. 272:276-83.

35. Carp H. (1982). *Mitochondrial N-formylmethionyl proteins as chemoattractants for neutrophils.* J. Exp. Med. 155:264-75.

36. Le Y., Gong W., Tiffany H. L., Tumanov A., Nedospasov S., Shen W., et al. (2000). *Amyloid b42 activates a G protein-coupled chemoattractant receptor FPR-like 1.* J. Neurosci. 21(RC123):1–5.

37. Le Y., Yazawa H., Gong W., Yu Z., Ferrans V. J., Murphy P. M., et al. (2001). *The neurotoxic prion peptide fragment PrP106–126 is a chemotactic agonist for the g protein-coupled receptor fprl1.* J. Immunol. 166:1448-51.

38. Chiang N., Fierro I. M., Gronert K., Serhan C. N. (2000). *Activation of lipoxin A4 receptors by aspirin-triggered lipoxins and select peptides evokes ligand-specific responses in inflammation*. J. Exp. Med. 191:1197-207.

39. Yang D., Chen Q., Schmidt A. P., Anderson G. M., Wang J. M., Wooters J., et al. (2000). *LL-37, the neutrophil granule- and epithelial cell-derived cathelicidin, utilizes formyl peptide receptor-like 1 (FPRL1) as a receptor to chemoattract human peripheral blood neutrophils, monocytes, and T cells.* J. Exp. Med. 192:1069–74.

40. Fiore S., Maddox J. F., Perez H. D., Serhan C. N. (1994). *Identification of a human cDNA encoding a functional high affinity lipoxin A4 receptor.* J. Exp. Med. 180:253-60.

41. Takano T., Fiore S., Maddox J. F., Brady H. R., Petasis N. A., Serhan C. N. (1997). *Aspirin-triggered 15-epi-lipoxin A4 (LXA4) and LXA4 stable analogues are potent inhibitors of acute inflammation: evidence for anti-inflammatory receptors.* J. Exp. Med. 185:1693-704.

42. Freer R. J., Day A. R., Radding J. A., Schiffmann E., Aswanikumar S., et al. (1980). *Further studies on the structural requirements for synthetic peptide chemoattractants*. Biochemistry. 19:2404-10

43. Dalpiaz A., Pecoraro R., Vertuani G., Spisani S., Rizzuti O., et al. (1999). *Formylpeptide receptor antagonists: structure and activity.* Boll. Chim. Farm. 138:44-8.

44. Higgins 3rd JD, Bridger GJ,Derian CK, Beblavy MJ, Hernandez PE, et al. (1996). *N-terminus urea-substituted chemotactic peptides: new potent agonists and antagonists toward the neutrophil fMLP receptor.* J. Med. Chem. 39:1013-1015.

45. Derian C. K., Solomon H. F., Higgings 3rd J. D., Bedlavy M. J., Santulli R. J., et al. (1996). *Selective inhibition of N-formylpeptide analogues.* Biochemisrty. 35:1265-1269.

46. Wenzel-Seifert K., Grűnbaum L., Seifert R. (1991). *Differential inhibition of human neutrophil activation by cyclosporins A, D, and H: cyclosporine H is a potent and effective inhibitor of formyl peptide-induced superoxide formation.* J. Immunol. 147:1940-1946.

47. Wenzel-Seifert K., Seifert R. (1993), *Cyclosporin H is a potent and selective formyl peptide receptor antagonist: comporison with N-t-Butoxylcarbonyl-L-phenylalanyl-L-leucyl- L- phenylalanyl-L-leucyl-L-phenylalanine and Cyclosporins A,B, C, D and E.* J. Immunol. 150:4591-4599.

48. De Paulis A., Ciccarelli A., De Crescenzo G., Crillo R., Patella V., Marone G. (1996). *Cyclosporin H is a potent and selective competitive antagonist of*

human basophil activation by N-formyl-methionyl-leucyl-phenylalanine. J. Allergy Clin. Immunlo. 98:152-164.

49. Chen X., Yang D., Shen W., Dong H. F., Wang J. M., Oppenhein J. J., et al. (2000). *Characterization of chenodeoxycholic acid as an endogenous antagonist of the G-coupled formyl peptide receptors,* Inflammation Res. 49:744-755.
50. Sahagun-Ruiz A., Colla J.S., Juhn J., Gao J.L., Murphy P.M., McDermott D.H. (2001). *Contrasting evolution of the human leukocyte N-formylpeptide receptor subtypes FPR and FPRL1R.* Genes Immun. 2:335-342.
51. Le Y., Oppenheim J.J., Wang J.M., Boulay F., Tardif M., Bormann B.J., et all (1998). *Broad immunocytochemical localization of the formylpeptide receptor in human organs, tissues and cells.* Cell Tissue Res. 292:129-135.
52. Christophe T., Karlasson A., Dugave C., Rabiet M.J., Boulay F., Dahlgren C. (2001). *The synthetic peptide Trp-Lys-Tyr-Met-Val-Met-NH_2 specifically activates neutrophils through FPRL1/Lipoxin A(4) receptors and is an agonist for the orphan monocyte-expressed chemoattractant receptor FPRL2.* J. Boil. Chem. 276:21585-21593.
53. Nick J. A., Avdi N.J., Young S.K., Knall C., Gerwins P., Johnson, G.L., Worthen G.S., (1997). *Common and distinct intracellular signaling pathways in human neutrophils utilized by platelet activating factor and fMPL*. J. Clin. Invest. 99:975-986.
54. Del Prete A., Vermi W., Dander E., Otero K., Barberis L., Luini W., et all (2004). *Defective dendritic cell migration and activation of adaptive immunity in PI3K gamma deficient mice.* Embo. J. 23:3505-3515.

55. Bea Y.S., Song J.Y., He R., Ye R.D., Kwak J.Y., et all. (2003). *Differential activation of formyl peptide receptor signaling by peptide ligands.* Mol. Pharmacol. 64:841-7.

56. Leopoldt D., Hanck T., Exner T., Maier U., Wetzeker R., Nurnberg B. (1998). *Gbetagamma stimulates phosphoinositide 3-kinase-gamma by direct interaction with two domains of the catalytic p110 subunit.* J. Biol. Chem. 273:7024-7029.

57. Pan Z.K., Chen L.Y., Cochrane C.G., Zuraw B.L. (2000). *fMet-Leu-Phe stimulates proinflammatory cytokine gene expression in human peripheral blood monocytes: the role of phosphatidyl-inositol 3-kinase.* J. Immunol. 164:404-411.

58. Takai Y., Sasaki T., Matozaki T. (2001). *Small GTP-binding proteins.* Phisiol. Rev. 81:153-208.

59. Zaffran Y., Lepidi H., Bongrand P., Mege J. L., Capo C. (1993). *F-actin content and spatial distribution in restino and chemoattractant-stimulated human polymorphonuclear leucocytes. Which role for intracellular-free calcium?* J. Cell. Sci. 105:675-684.

60. Partida-Sanchez S. et al. (2001). *Cyclic ADP-ribose production by CD38 regulates intracellular calcium release, extracellular calcium influx and chemotaxis in neutrophils and is required for bacterial clearance in vivo.* Nat. Med. 7:1209-1216.

61. Schaeffer H. J., Webe M. J., (1999). *Mitogen-activated protein kinases: specific messages from ubiquitous messengers.* Moll. Cell Biol. 19, 2435-2444.

62. Niggli V. (2003). *Signalling to migration in neutrophils: importance of localized pathways.* Int. J. Biochem .Cell. Biol. 35:1619-1638.

63. Feig L.A., (2003). *Rall GTPases: approaching thir 15 minutes of fame.* Cell Biol. 13:419-425.

64. Ridley A.J. (2001). *Rho family proteins: coordinating cell responses.* Trends Cell Biol. 11:471-477.

65. Van Aelst L., D'Souza-Schorey C. (1997). *Rho GTPases and signaling networks.* Genes Dev. 11:2295-2322.

66. Hall A. (1998). *Rho GTPases and actin cytoskeleton.* Science 279:509-514.

67. Moodie S.A., Wolfman A. (1994). *The 3Rs of life: Ras, Raf and growth regulation.* Trend Genet. 10:44-48.

68. Selvatici R., Falzarano S., Mollica A., Spisani S. (2006). *Signal transduction pathways trigged by selective formylpeptide analogues in human neutrophils.* Europ. J. Pharmacol. 534:1-11.

69. Irving E.A., Bamford M. (2002). *Role of mitogen- and stress-activated kinases in ischemic injury.* J. Cereb. Blood Flow Metab. 22, 631-647.

70. Ali A., Hoeflich K. P., Woodgett J. R. (2001). *Glycogen synthase kinase-3: properties, function and regulation.* Chem. Rev. 101:2527-2540.

71. Kyriakis J. M., Avurch J. (2001). *Mammalian mitogen-activated protein kinase signal transduction pathways activated by stress and inflammation.* Physiol. Rev. 8:807-869.

72. Dekker L. V., Parker P. J. (1997). *PKC isozymes and myeloid cell differentiation.* R. G. Austin, Texas, USA, pp. 121-129.

73. Jaken S. (1996). *Protein kinases C isozymes and substrates.* Curr. Opin. Cell Biol. 8:168-173.

74. Fabbro D., Buchdunger E., Wood J., Mestan J., Hofmann F., Ferrari S., Mett H., O'Reilly T. (1999). *Inhibitor with potential as an anticancer agent.* Pharmacol. Ther. 82:293-301.

75. Spitaler M., Cantrell D. A. (2004). *Protein kinase C and beyond.* Nat. Immunol. 5:785-790.

76. Keenan C., Kellehe D. (1998). *Protein kinase C and cytoskeleton.* Cell Singnal. 10:225-232.

77. Ridley A. J., Schwartz M. A., Burridge K., Firtel R. A., Ginsberg M. H., Borisy G., Parson J. T., Horwitz A. R. (2003). *Cell migration: integrating signals from front to back.* Science 302:1704-1709.

78. Newton A. C. (1995). *Protein kinase C: structure, function, and regulation,* J. Biol. Chem. 270, p.28495.

79. Blobe G. C., et al (1996). *Protein kinase C isoenzymes: regulation and function*. Cancer Surv. 27, p.213.

80. Babior B. M. (1999*). NADPH Oxidase: un update*. Blood. 93:1464-1476.

81. Lambert J. D. (2000). *Regulation of phagocytic oxygen radical production by protein interactions*. Biochem. Mol. Biol. Int. 33:427-439.

82. Bokoch G. M., Knaus U. G.(2003). *NADPH oxidases: not just for leukocytes anymore*. TRENDS in Biochemical Sciences; 28(9):502-508.

83. Lapouge K., et al (2002). *Architecture of the p40pohx-p47phox-p67phox complex in the resting state of the NADPH oxidase. A central role for p67phox.* J. Biol. Chem. 277:10121-10128.

84. De Leo F. R., Quinn M. T. (1996). *Assembly of the phagocyte NADPH oxidase: molecular interaction of oxidase proteins.* J. Leukoc. Biol. 60:677-691.

85. Heyworth P. G. et al. (1994). *Rac translocates independently of the neutrophil NADPH oxidase components p47phox and p67phox.* J. Biol. Chem. 296:30749-30752.

86. Dorseuil O., et al. (1995). *Dissociation of Rac translocation from p47phox-p67phox movements in human neutrophils by tyrosine kinase inhibitors.* J. Leukoc. Biol. 58:108-113.

87. Price M. O., et al. (2002). *Rac activation induces NADPH oxidase activity in transgenic COSphox cells, and the level of superoxide production is exchange factor-dependent.* J. Biol. Chem. 277:19220-19228.

88. Quinn M. T., et al. (1993). *Translocation of Rac correlates with NADPH oxidase activation.* J. Biol. Chem. 268:20983-20987.

89. Fischer O. M., Giordano S., Comoglio P. M., Ullrich A. (2004). *Reactive oxygen species mediate Met receptor transactivation by G protein-coupled receptors and epidermal growth factor receptor in human carcinoma cells.* J. Biol. Chem. 279:28970-28978.

90. Catarzi S., Biagioni C., Giannoni E., Favalli F., Marcucci T., Iantommasi T., Vincenzini M. T. (2005). *Redox regulation of platelet-derived-growth-factor-receptor: role of NADPH oxidase and c-Src tyrosine kinase.* Biochem. Biophys. Acta. 1745:166-175.

91. Bunemann M., Hosey M. M. (1999). *G-protein coupled receptor kinases as modulators of G-protein signalling*. J. Physiol. 517:5–23.

92. McCormick F. (1993). *Signal transduction. How receptors turn Ras on*. Nature 363:15–16.

93. Pierce K. L., Luttrell L. M., Lefkowitz R. J. (2001). *New mechanisms in heptahelical receptor signaling to mitogen activated protein kinase cascades*. Oncogene 20:1532–1539.

94. Waters C., Pyne S., Pyne N. J. (2004). *The role of G-protein coupled receptors and associated proteins in receptor tyrosine kinase signal transduction*. Semin. Cell Dev. Biol. 15:309–323.

95. Lowes V. L., Ip. N. Y., Wong Y. H. (2002). *Integration of signals from receptor tyrosine kinases and g protein-coupled receptors*. Neurosignals 11:5–19.

96. Luttrell L. M., Della Rocca G. J., Van Biesen T., Luttrell D. K., Lefkowitz R. J. (1997). *Gbetagamma subunits mediate Src-dependent phosphorylation of the epidermal growth factor receptor. A scaffold for G protein-coupled receptor-me- diated Ras activation*. J. Biol. Chem. 272:4637–4644.

97. Daub H., Weiss F. U., Wallasch C., Ullrich A. (1996). *Role of transactivation of the EGF receptor in signalling by G-protein-coupled receptors*. Nature 379:557–560.

98. Natarajan K., Berk C. B. (2006). *Crosstalk Coregulation Mechanisms of G Protein- Coupled Receptors and Receptor Tyrosine Kinases.* Methods Mol. Biol. 332:51-77.

99. Yarden Y., Sliwkowski M. X. (2001). *Untangling the ErbB signaling network.* Nat. Rev. Mol. Cell Biol. 2:127–37.

100. Wells A. (1999). *EGF receptor*. Int. J. Biochem. Cell Biol. 31:637–43.

101. De Luca A., Carotenuto A., Rachiglio A., Gallo M., Maiello M. R., et al. 2008. *The role of the EGFR signaling in tumor microenvironment*. J. Cell Physiol. 214:559–67.

102. Jimeno A., Hidalgo M. (2006). *Pharmacogenomics of epidermal growth factor receptor (EGFR) tyrosine kinase inhibitors*. Biochim. Biophys. Acta 1766:217–29.

103. Mosesson Y., Yarden Y. (2004). *Oncogenic growth factor receptors: implications for signal transduction therapy*. Semin. Cancer Biol. 14:262–70.

104. Ciardiello F., Tortora G. (2008). *EGFR antagonists in cancer treatment.* N. Engl. J. Med. 358:1160–74.

105. Woodburn J. R. (1999). *The epidermal growth factor receptor and its inhibition in cancer therapy*. Pharmacol. Ther. 82:241–50.

106. Park M., Dean M., Kaul K., et al. (1987). *Sequence of MET protoonco- gene cDNA has features characteristic of the tyrosine family of growth factor receptors*. Proc. Natl. Acad. Sci. USA. 84:6379-83.

107. Naldini L., Weidner K. M., Vigna E., et al. (1991). *Scatter factor and hepatocyte growth factor are indistinguishable ligands for the MET receptor.* EMBO J. 10:2867–78.

108. Bottaro D. P., Rubin J. S., Faletto D. L., et al. (1991). *Identification of the hepatocyte growth factor as the c-met protooncogene product.* Science 258:802-4.

109. Giordano S., Zhen Z., Medico E., et al. (1993). *Transfer of motogenic and invasive response to scatter factor/hepatocyte growth fac- tor by transfection of human MET protooncogene.* Proc. Natl. Acad. Sci. USA. 90:649-53.

110. Trusolino L., Bertotti A., Comoglio P. M. (2010). *MET signalling: principles and functions in development, organ regeneration and cancer.* Nat. Rev. Mol. Cell. 11:834-48.

111. Faletto D. L., Kaplan D. R., Halverson D. O., et al. (1993). *Signal transduction in c-met mediated motogenesis. In: Goldberg ID, Rosen EM, editors. Hepatocyte Growth Factor – Scatter Factor (HGF – SF) and the c -met receptor.* Birkhauser 107–30.

112. Ponzetto C., Bardelli A., Zhen Z., et al. (1994). *A multifunctional docking site mediates signaling and transformation by the hepatocyte growth-factor scatter factor-receptor family.* Cell. 77:261-71.

113. Ponzetto C., Bardelli A., Maina F., et al. (1993). *A novel recognition motif for phosphatidylinositol 3-kinase binding mediates its association with the hepatocyte growth- factor scatter factor-re- ceptor.* Mol. Cell. Biol. 13:4600-8.

114. Pawson T., Gish C. D. (1992). *SH2 and SH3 domains: from structure to function.* Cell. 171:359-62.

115. Koch C. A., Anderson D., Moran M. F., et al. (1991). *SH2 and SH3 domains, elements that controll interactions of cytoplasmic signalling proteins*. Science. 252:668-74.

116. Songyang Z., Shoelson S. E., Chaudhuri M., et al. (1993). *SH2 domains recognise specific phophopeptide sequences.* Cell. 72:767-78.

117. Songyang Z., Gish G., Mbamalu G., et al. (1995). *A single-point muta- tion switches the specificity of group-iii src homology (SH) 2 domains to that of group-i sh2 domains.* J. Biol. Chem. 270:26029-32.

118. Zughaier S. M., Shaker W. M., Stephens D. S. (2005). *Antimicrobial peptides and endotoxin inhibit cytokine and nitric oxide release but amplify respiratory*

burst response in human and murine macrophages. Cell. Microbiol. 7:1251-1262.

119. Chen X., Niyonsaba F., Ushio H., Nagaoka I., Ikeda S., Okumura K., Ogawa H. (2006). *Synergistic effect of antibacterial agents human beta-defensins, cathelicidin LL-37 and lysozyme against Staphylococcus aureus and Escherichia coli*. Dermatol J. Sci. 43:63–66.

120. Niyonsaba F., Ushio H., Nagaoka I., Okumura K., Ogawa H. (2005). *The human beta-defensins (-1, -2, -3, -4) and cathelicidin LL-37 induce IL-18 secretion through p38 and ERK MAPK activation in primary human keratinocytes.* J. Immunol. 175:1776–1784.

121. Zheng Y., Niyonsaba F., Ushio H., Nagaoka I., Ikeda S., Okamura R., Ogawa H. (2007). *Cathelicidin LL-37 induces the generation of reactive oxygen species and release of human alpha-defensins from neutrophils*. Brit. J. Dermatol. 157:1124–1131.

122. Nagaoka I., Tamura H., Hirata M. (2006). *An antimicrobial cathelicidin peptide, human CAP18/LL-37, suppresses neutrophil apoptosis via the activation of formyl-peptide receptor-like 1 and P2X7.* J. Immunol. 176:3044–3052.

123. Yang D., Chen Q., Schmidt A.P., Anderson G.M., Wang J.M., Wooters J., Oppenheim J. J., Chertov O. (2000). *LL-37, the neutrophil granule- and epithelial cell-derived cathelicidin, utilizes formyl peptide receptor-like 1 (FPRL1) as a receptor to chemoattract human peripheral blood neutrophils, monocytes, and T cells.* J. Exp. Med. 192:1069–1074.

124. Koczulla R., Von Degenfeld G., Kupatt C., Krötz F., et al. (2003). *An angiogenic role for the human peptide antibiotic LL-37/hCAP-18.* J. Clin. Invest. 111:1665–1672.

125. Carretero M., Escàmez M.J., Garcìa M., Duarte B., Holguìn A., Retamosa L., Lorcano J.L., Del Rìo M., Larcher F. (2008). *In vitro and in vivo wound healing-promoting activities of human cathelicidin LL-37.* J. Invest. Dermatol. 128:223–236.

126. Lee S.Y., Lee M.S., Lee H.Y., Kim S.D., Shim J. W., Jo S.H.,. Lee J.W, et al. (2008). F2L, a peptide derived from heme-binding protein, inhibits LL-37-induced cell proliferation and tube formation in human umbilical vein endothelial cells. FEBS Lett. 582:273–278.

127. Migeotte I., Riboldi E., Franssen J.D., Grégoire F., Loison C., et al. (2005). *Identification and characterization of an endogenous chemotactic ligand specific for FPRL2*. J. Exp. Med. 201:83–93.

128. Elssner A., Duncan M., Gavrilin M., Wewers M.D. (2004). *A novel P2X7 receptor activator, the human cathelicidin-derived peptide LL37, induces IL-1 beta processing and release.* J. Immunol. 172:4987–4994.

129. Lau Y.E., Rozek A., Scott M.G., Goosney D.L., Davidson D.J., Hancock R.E. (2005). *Interaction and cellular localization of the human host defense peptide LL-37 with lung epithelial cells.* Infect. Immun. 73:583–591.

130. Bowdish D.M.E., Davidson D.J., Speert D.P., Hancock R.E.W. (2004). *The human cationic peptide LL-37 induces activation of the extracellular signal-regulated kinase and p38 kinase pathways in primary human monocytes*. J. Immunol. 172:3758–3765.

131. Tjabringa G.S., Aarbiou J., Ninaber D.K., Drijfhout J.W., Sørensen O.E., et al. *The antimicrobial peptide LL-37 activates innate immunity at the airway epithelial surface by transactivation of the epidermal growth factor receptor.* (2003). J. Immunol. 171:6690–6696.

132. Shaykhiev R., Beisswenger C., Kändler K., Senske J., Püchner A., Damm T., Behr J., Bals R. (2005). *Human endogenous antibiotic LL-37 stimulates airway epithelial cell proliferation and wound closure*. Am. J. Physiol. Lung Cell. Mol. Physiol. 289:L842–L848.

133. Leopold J.A., Cap A., Scribner A.W., Stanton R.C., Loscalzo J. (2001). *Glucose-6-phosphate dehydrogenase deficiency promotes endothelial oxidant stress and decreases endothelial nitric oxide bioavailability.* FASEB J. 15:1771–1773.

134. Mueller C.F., Laude K., McNally J.S., Harrison D.G. (2005). *ATVB in focus: redox mechanisms in blood vessels.* Arterioscler. Thromb. Vasc. Biol. 25:274–278.

135. Rouhanizadeh M., Hwang J., Clempus R.E., Marcu L., Lassègue B., Sevanian A., Hsiai T.K. (2005). *Oxidized-1-palmitoyl-2-arachidonoyl-sn-glycero-3-phosphorylcholine induces vascular endothelial superoxide production: implication of NADPH oxidase.* Free Rad. Biol. Med. 39:1512–1522.

136. Bianco, C., Tortora, G., Bianco, R., Caputo, R., Veneziani B. M., Caputo R., et al. (2002). *Enhancement of antitumor activity of ionizing radiation by combined treatment with the selective epidermal growth factor receptor-tyrosine kinase inhibitor ZD1839 (Iressa).* Clin. Cancer Res. 8:3250–3258.

137. Newton, J. S. (2002). *Angiotensin and epidermal growth factor receptor cross talk goes up and down.* J. Hypertens. 20:597–598.

138. Zhao Y., He, D., Saatian B., Watkins, T., Spannhake E. W., Pyne N. J., Natarajan V. (2006). *Regulation of lysophosphatidic acid-induced epidermal growth factor receptor transactivation and interleukin-8 secretion in human bronchial epithelial cells by protein kinase Cdelta, Lyn kinase, and matrix metalloproteinases.* J. Biol. Chem. 281:19501–19511.

139. Porcile C., Bajetto A., Barbieri F., Barbero S., Bonavia R., Biglieri M., Piran P., Florio T., Schettini G. (2005). *Stromal cell-derived factor-1alpha (SDF-1alpha/CXCL12) stimulates ovarian cancer cell growth through the EGF receptor transactivation.* Exp. Cell Res. 308:241–253.

140. Madarame J., Higashiyama S., Kiyota H., Madachi A., Toki F., Shimomura T., Tani N., Oishi Y., Matsuura N. (2003). *Transactivation of epidermal growth factor receptor after heparin-binding epidermal growth factor-like growth factor shedding in the migration of prostate cancer cells promoted by bombesin.* Prostate 57:187–195.

141. Vaingankar S. M., Martins-Green M. (1998). *Thrombin activation of the 9E3/CEF4 chemokine involves tyrosine kinases including c-src and the epidermal growth factor receptor.* J. Biol. Chem. 273:5226–5234.

142. Vacca F., Bagnato A., Catt K. J., Tecce R. (2000). *Transactivation of the epidermal growth factor receptor in endothelin-1-induced mitogenic signaling in human ovarian carcinoma cells.* Cancer Res. 60:5310–5317.

143. Huang J., Hu J., Bian X., Chen K., Gong W., Dunlop N. M., Howard O. M., Wang J. M. (2007). *Transactivation of the epidermal growth factor receptor by*

formylpeptide receptor exacerbates the malignant behaviour of human glioblastoma cells. Cancer Res. 67:906–5913.

144. Huang J., Chen K., Gong W., Zhou Y., Le Y., Bian X., Wang J. M. (2008). *Receptor "hijacking" by malignant glioma cells: a tactic for tumor progression.* Cancer Lett. 267:254–261.

145. Prenzel N., Zwick E., Daub H., Leserer M., Abraham R., Wallasch C., Ullrich A. (1999). *EGF receptor transactivation by G-protein-coupled receptors requires metallo-proteinase cleavage of proHB-EGF*. Nature 402:884–888.

146. Lee F. S., Chao, M. V. (2001). *Activation of Trk neurotrophin receptors in the absence of neurotrophins.* Proc. Natl Acad. Sci. U. S. A. 98:3555–3560.

147. Tanimoto T., Jin Z. G., Berk B. C. (2002). *Transactivation of vascular endothelial growth factor (VEGF) receptor Flk-1/KDR is involved in sphingosine 1-phosphate- stimulated phosphorylation of Akt and endothelial nitric-oxide synthase (eNOS)*. J. Biol. Chem. 277:42997–43001.

148. Kam A. Y., Tse T. T., Kwan D. H., Wong Y. H. (2007). *Formyl peptide receptor like 1 differentially requires mitogen-activated protein kinases for the induction of glial ﬁbrillary acidic protein and interleukin-alpha in human U87 astrocytoma cells.* Cell. Signal. 19:2106–2117.

149. Bae Y. S., Kang S. W., Seo M. S., Baines I. C., Tekle E., Chock P. B., Rhee S. G. (1997). *Epidermal growth factor (EGF)-induced generation of hydrogen peroxide: role in EGF receptor-mediated tyrosine phosphorylation*. J. Biol. Chem. 272:217–221.

150. Sundaresan M., Yu Z. X., Ferrans V. J., Irani K., Finkel T. (1995). *Requirement for generation of H2O2 for platelet-derived growth factor signal transduction.* Science 270:296–299.

151. Ushio-Fukai M., Griendling K. K., Becker P. L., Hilenski L., Halleran S., Alexander R. W. (2001). *Epidermal growth factor receptor transactivation by angiotensin II requires reactive oxygen species in vascular smooth muscle cells.* Arterioscler. Thromb. Vasc. Biol. 21:489–495.

152. Saito Y., Berk B. C. (2001). *Transactivation: a novel signaling pathway from angiotensin II to tyrosine kinase receptors*. J. Mol. Cell. Cardiol. 33:3–7.

153. Rhee S. G., Kang S. W., Jeong W., Chang T. S., Yang K., Woo H. A. (2005). *Intracellular messenger function of hydrogen peroxide and its regulation by peroxiredoxins*. Curr. Opin. Cell Biol. 17:183–189.

154. Lambeth J. D. *NOX enzymes and the biology of reactive oxygen.* Nat. Rev. Immunol. 4:181–189.

155. Bokoch G. M., Diebold B., Kim J. S., Gianni D. (2009). *Emerging evidence for the importance of phosphorylation in the regulation of NADPH oxidases.* Antioxid. Redox Signal. 10:2429–2441.

156. Lassègue B., Clempus R. E. (2003). *Vascular NAD(P)H oxidases: speci_c features, expression, and regulation.* Am. J. Physiol. Regul. Integr. Comp. Physiol. 285:R277–R297.

157. Lambeth J. D. (2007). *Nox enzymes, ROS, and chronic disease: an example of antagonistic pleiotropy*. Free Radic. Biol. Med. 43:332–347.

158. Oakley F. D., Abbott D., Li Q., Engelhardt J. F. (2009). *Signaling components of redox active endosomes: the redoxosomes.* Antioxid. Redox Signal. 11:1313–1333.

159. Gianni D., Bohl B., Courtneidge S. A., Bokoch G. M. (2008). *The involvement of the tyrosine kinase c-Src in the regulation of reactive oxygen species generation mediated by NADPH oxidase-1.* Mol. Biol. Cell 19:2984–2994.

160. Jo E. J., Lee H. Y., Kim J. I., Kang H. K., Lee Y. N. Kwak J. Y., Bae Y. S. (2004). *Activation of formyl peptide receptor like-1 by WKYMVm induces serine phosphorylation of STAT3, which inhibits its tyrosine phosphorylation and nuclear translocation induced by hydrogen peroxide.* Life Sci. 75:2217–2232.

161. Zhou Y., Bian X., Le Y., Gong W., Hu J., Zhang X., Wang L., Iribarren P., Salcedo R., Howard O. M., Farrar W., Wang J. M. (2005). *Formylpeptide receptor FPR and the rapid growth of malignant human gliomas.* J. Natl. Cancer Inst. 97:823–835.

162. Chung J., Uchida E., Grammer T. C., Blenis J. (1997). *STAT3 serine phosphorylation by ERK-dependent and -independent pathways negatively modulates its tyrosine phosphorylation.* Mol. Cell. Biol. 17:6508–6516.

163. Kim H., Park J. H., Lee E. H., Kim M. J., Park S. K., Heo S. K., Kim B. S., Min Y. J. (2006). *Granulocyte function is stimulated by a novel hexapeptide, WKYMVm, in chemotherapy-treated cancer patients*. Exp. Hematol. 34:407–413.

164. Lin C., Wei W., Zhang J., Liu S., Liu Y., Zheng D. (2007). *Formyl peptide receptor-like 1-mediated endogenous TRAIL gene expression with tumoricidal activity*. Mol. Cancer Ther. 6:2618–2625.

165. Li B. Q., Wetzel M. A., Mikovits J. A., Henderson E. E., Rogers T. J., Gong W., Le Y., Ruscetti F. W., Wang J. M. (2001). *The synthetic peptide WKYMVm attenuates the function of the chemokine receptors CCR5 and CXCR4 through activation of formyl peptide receptor-like 1*. Blood 97:2941–2947.

166. Gavins, F. N. (2010). *Are formyl peptide receptors novel targets for therapeutic intervention in ischaemia–reperfusion injury?* Trends Pharmacol. Sci. 31:266–276.

167. Le Y., Yang Y., Cui Y., Yazawa H., Gong W.; Qiu C.; Wang J. M. (2002). *Receptors for chemotactic formyl peptides as pharmacological targets*. Int. Immunopharmacol. 2:1–13.

168. Zhou C., Zhang S., Nanamori M., Zhang Y., Liu Q., Li N., Sun M., Tian J., Ye P. P., Cheng N., Ye R. D., Wang M. W. (2007). *Pharmacological characterization of a novel nonpeptide antagonist for formyl peptide receptor-like 1*. Mol. Pharmacol. 72:976–983.

169. Bae Y. S., Lee H. Y., Jo E. J., Kim J. I., Kang H. K., Ye R. D., Kwak J. Y., Ryu S. H. (2004). *Identification of peptides that antagonize formyl peptide receptor-like 1- mediated signaling*. J. Immunol. 173:607–614.

Free Radical Biology & Medicine 51 (2011) 1126–1136

Contents lists available at ScienceDirect

Free Radical Biology & Medicine

journal homepage: www.elsevier.com/locate/freeradbiomed

Original Contribution

NADPH-oxidase-dependent reactive oxygen species mediate EGFR transactivation by FPRL1 in WKYMVm-stimulated human lung cancer cells

Fabio Cattaneo [a,b], Annalisa Iaccio [a], Germano Guerra [c], Stefania Montagnani [b], Rosario Ammendola [a,*]

[a] Dipartimento di Biochimica e Biotecnologie Mediche, Università degli Studi di Napoli Federico II, 80131 Napoli, Italy
[b] Dipartimento di Scienze Biomorfologiche e Funzionali, Università degli Studi di Napoli Federico II, 80131 Napoli, Italy
[c] Dipartimento di Scienze per la Salute, Università degli Studi del Molise, 86100 Campobasso, Italy

ARTICLE INFO

Article history:
Received 11 March 2011
Revised 25 May 2011
Accepted 31 May 2011
Available online 12 June 2011

Keywords:
NADPH oxidase
Reactive oxygen species
Formyl peptide receptors
EGFR
c-Src
STAT3
Free radicals

ABSTRACT

Cross talk between unrelated cell surface receptors, such as G-protein-coupled receptors (GPCR) and receptor tyrosine kinases (RTK), is a crucial signaling mechanism to expand the cellular communication network. We investigated the ability of the GPCR formyl peptide receptor-like 1 (FPRL1) to transactivate the RTK epidermal growth factor receptor (EGFR) in CaLu-6 cells. We observed that stimulation with WKYMVm, an FPRL1 agonist isolated by screening synthetic peptide libraries, induces EGFR tyrosine phosphorylation, $p47^{phox}$ phosphorylation, NADPH-oxidase-dependent superoxide generation, and c-Src kinase activity. As a result of EGFR transactivation, phosphotyrosine residues provide docking sites for recruitment and triggering of the STAT3 pathway. WKYMVm-induced EGFR transactivation is prevented by the FPRL1-selective antagonist WRWWWW, by pertussis toxin (PTX), and by the c-Src inhibitor PP2. The critical role of NADPH-oxidase-dependent superoxide generation in this cross-talk mechanism is corroborated by the finding that apocynin or a siRNA against $p22^{phox}$ prevents EGFR transactivation and c-Src kinase activity. In addition, WKYMVm promotes CaLu-6 cell growth, which is prevented by PTX and by WRWWWW. These results highlight the role of FPRL1 as a potential target of new drugs and suggest that targeting both FPRL1 and EGFR may yield superior therapeutic effects compared with targeting either receptor separately.

The human formyl peptide receptor (FPR) and its variants, FPR-like 1 (FPRL1) and FPR-like 2 (FPRL2), belong to the G-protein-coupled seven-transmembrane receptor (GPCR) family [1]. They are all coupled to the G_i family of G proteins, as indicated by the total loss of cell response to their agonists upon exposure to pertussis toxin (PTX) [2,3]. FPR and FPRL1 were first detected in phagocytic leukocytes, and FPRL2 was found in monocytes and in dendritic cells [4]. The three receptors were subsequently identified in other cell types and tissues at the protein and/or mRNA level [2,3,5–7], suggesting that these receptors have functions in addition to those exerted in polymorphonuclear cells (PMN).

FPRL1 is less efficiently activated by *N*-formylmethionylleucylphenylalanine (N-fMLP) than FPR, as also shown by its higher binding efficiency for WKYMVm, a modified peptide isolated by screening synthetic peptide libraries [8]. A variety of other agonists also bind FPRL1 in several cell types with high affinity. These include lipoxin A_4 eicosanoid, annexin 1, uPAR, the V3 region of the HIV-1 envelope glycoprotein gp120, the acute-phase protein SAA, the 42-amino-acid form of β-amyloid, the human prion peptide, and the cathelicidin LL-37 [3,9,10]. Binding of various agonists to FPRL1 triggers the activation of intracellular signaling molecules including calcium, PKC isoforms, phospholipases A2 and D, and mitogen-activated protein kinases (MAPK), including p38MAPK [9,11]. In several cell types, PKC, ERK, and p38MAPK are involved in the phosphorylation, on multiple serine residues, of the cytosolic regulatory subunit $p47^{phox}$ of NADPH oxidase in vitro and in vivo and, in turn, in NADPH-oxidase-dependent superoxide generation [7,12–14]. In nonphagocytic cells, the deliberate and regulated generation of superoxide plays a key role in a variety of essential biological processes and is catalyzed by enzymes that belong to the NADPH oxidase (Nox) family [15]. This includes Nox1, abundant in colon, brain, and vascular cells; Nox2/$gp91^{phox}$, the classic phagocyte catalytic component of the respiratory burst oxidase, which has important roles in other tissues as well; Nox3, located in the inner ear; Nox4, a widely distributed Nox abundant in the kidney, bone, and vascular cells; Nox5, a calcium-regulated enzyme mainly expressed in lymphoid tissues and testis; and Duox1 and Duox2, dual oxidases that also contain a peroxidase-like domain [16]. Nox2, Nox3, Nox4, Duox1, and Duox2 are also expressed in a number of lung cell types, such as airway/epithelial and mesenchymal cells [17].

Abbreviations: ROS, reactive oxygen species; FPRL1, formyl peptide receptor-like 1; ERK, extracellular-signal-regulated kinase; PTX, pertussis toxin; EGFR, epidermal growth factor receptor; STAT, signal transducer and activator of transcription.

* Corresponding author. Fax: +39 817464359.
E-mail address: rosario.ammendola@unina.it (R. Ammendola).

0891-5849/$ – see front matter © 2011 Elsevier Inc. All rights reserved.
doi:10.1016/j.freeradbiomed.2011.05.040

Furthermore, homologues of $p47^{phox}$ and $p67^{phox}$, denominated NOXO1 (NOX organizing protein 1) and NOXA1 (NOX activating protein 1), respectively, have been identified [18].

Nox1 is constitutively active in unstimulated cells and this is explained by the absence of regulatory phosphorylation sites on NOXO1 and by the ability of NOXO1 to localize to the resting cell membrane [19]. However, Nox1 may be further activated by platelet-derived growth factor (PDGF) and angiotensin II in vascular smooth muscle cells [20,21] and by phorbol ester in HEK293 and COS7 cells in a cell-type-specific manner [22]. Nox2/$gp91^{phox}$ is dormant in resting cells and is stimulated by several agonists, such as N-fMLP, which induces $p47^{phox}$ phosphorylation by either proline-directed kinases or PKC [12,23]. The phosphorylated serine residues of $p47^{phox}$ expose an SH3 binding site that interacts with the proline-rich region of $p22^{phox}$ and facilitates translocation to the membrane. $p67^{phox}$ then binds to the translocated $p47^{phox}$, providing a binding site for activated Rac and forming the functional enzyme. Nox3 functions together with $p22^{phox}$ as an enzyme constitutively producing superoxide, which can be regulated by the combinatorial use of the organizers and activators [24]. Nox4 requires only the membrane subunit $p22^{phox}$ for reactive oxygen species (ROS) generation and seems to be constitutively active [23]. However, a further Nox4 activation is observed in lipopolysaccharide-stimulated HEK293 cells, insulin-stimulated adipocytes, and angiotensin II-stimulated mesangial cells [25–27]. Nox5, Duox1, and Duox2 are regulated by increased intracellular calcium levels due to the presence of calcium-binding EF-hands [15,23].

We previously showed that, in serum-deprived IMR90 human fibroblasts, exposure to growth factors stimulates a nonphagocytic NADPH oxidase, and treatment with NADPH oxidase inhibitors results in the impairment of the serum-induced signaling cascade [28]. We also demonstrated that these cells express FPRL1 and that stimulation with WKYMVm induces MEK- and PKC-dependent $p47^{phox}$ phosphorylation and NADPH-oxidase-dependent superoxide generation [7,29].

Receptor tyrosine kinases (RTK) are an important subclass of transmembrane proteins. The epidermal growth factor receptor (EGFR) is the most important member of this family, being implicated in growth stimulation in a wide variety of malignant tumors. Stimulation of the receptor by EGF results in dimerization and subsequent autophosphorylation on tyrosine residues, thereby generating phosphotyrosine docking sites that activate intracellular signaling cascades. EGFR activation can also be induced by GPCR, which are a large group of cell-surface receptors that exert a wide variety of biological functions [30]. GPCR agonists increase tyrosine phosphorylation of EGFR either by increasing the kinase activity or by inhibiting an associated phosphatase activity that is mediated by oxidants [31]. The observation that GPCR stimulation induces EGFR activation serves as a paradigm for interreceptor cross talk, because it combines the broad diversity of GPCR with the potent signaling capacities of EGFR.

One of the best known downstream targets of activated EGFR is the signal transducer and activator of transcription (STAT) 3 [32,33]. STAT3 is a latent cytoplasmic transcription factor that transduces signals from cell membrane to the nucleus and is involved in the regulation of many genes in various cell types [34]. The activity of STAT3 is associated with the phosphorylation of the Tyr705 residue that is required for STAT3 dimerization, as well as with nuclear translocation and DNA binding. The full transcriptional activity is manifested only when the Ser727 residue, in the transactivation domain, is also phosphorylated [35]. Although activation of STAT3 has generally been associated with cytokines and mitogenic growth factor signaling, several ligands for GPCR also activate STAT3 in several cell types. These include angiotensin II in vascular smooth muscle cells [36], α-melanocyte-stimulating hormone in B lymphocytes [37], WKYMVm in RBL-2H3 cells [38], and Orphanin FQ and N-fMLP in hematopoietic cells [39].

In this study, we analyzed the intracellular signaling cascade triggered by WKYMVm in the human lung cancer CaLu-6 cell line. These cells express EGFR at high levels [40] and show change in the metabolism or in the generation of superoxide in response to various stimuli [41,42]. The results show that: (i) these cells express a biologically functional FPRL1 receptor, (ii) stimulation of FPRL1 by WKYMVm induces G_i protein- and NADPH-oxidase-dependent c-Src activation and EGFR tyrosine phosphorylation, (iii) FPRL1-dependent EGFR transactivation triggers activation of the STAT3 pathway, and (iv) as a consequence of the FPRL1-induced signaling, WKYMVm promotes cell proliferation in CaLu-6 cells.

Materials and methods

Reagents and cell culture treatments

The WKYMVm and WRWWWW (WRW4) peptides were synthesized and HPLC-purified by PRIMM (Milan, Italy). SDS–PAGE reagents were from Bio-Rad (Hercules, CA, USA). Protein A/G Plus agarose, anti-active phosphorylated ERK1/2, anti-tubulin, anti-c-Src, anti-$p47^{phox}$, anti-FPRL1, anti-EGFR, anti-STAT3, anti-cyclin A, anti-p-Y, and anti-rabbit antibodies were from Santa Cruz Biotechnology (Santa Cruz, CA, USA). Anti-p-c-Src(Tyr416), anti-p-STAT3(Tyr705), and anti-p-STAT3 (Ser727) were from Cell Signaling Technology (Danvers, MA, USA). Protein A–horseradish peroxidase and anti-mouse Ig–horseradish peroxidase were from Amersham Pharmacia Biotech (Little Chalfont, Buckinghamshire, UK). PD098059, AG1478, PP2, PP3, and genistein were purchased from Calbiochem (La Jolla, CA, USA). PTX, apocynin, anti-p-Ser antibody and 3-(4,5-dimethylthiazol-2-yl)-2,5-diphenyltetrazolium bromide (MTT) were from Sigma (St. Louis, MO, USA).

$p22^{phox}$ siRNA (SI03078523) and negative control siRNA (SI03650318) were purchased from Qiagen (Hiden, Germany).

CaLu-6 cells were grown in Dulbecco's modified Eagle's medium (DMEM) containing 10% fetal bovine serum (FBS), 100 U/ml penicillin, 100 μg/ml streptomycin, 1% L-glutamine, and 1% modified Eagle's medium. Cells were cultured until they reached 80% confluence, starved in serum-free DMEM for 24 h, and successively stimulated with WKYMVm peptide at the final concentration of 10 μM for various times, as indicated in the figures. In other experiments, serum-deprived cells were preincubated with 50 μM PD098059 for 90 min, 100 ng/ml PTX for 16 h, 10 μM PP2 for 45 min, 10 μM PP3 for 45 min, 60 μM genistein for 1 h, 2 μM AG1478 for 1 h, 100 μM apocynin for 2 h, or 10 μM WRW4 for 15 min before stimulation with 10 μM WKYMVm for 2 min.

In silencing experiments 4×10^5 cells were incubated for 12 h with 5 nM siRNAs in DMEM containing 10% FBS in the presence of 20 ml HiPerFect (Qiagen). Cells were then serum-deprived for 24 h before stimulation with 10 μM WKYMVm for 2 min.

RNA preparation and RT-PCR analysis

Total RNA was extracted from CaLu-6 cells and PMN with the RNAeasy Mini kit (Qiagen) according to the manufacturer's instructions, and 0.1 μg of RNA was used as template for RT-PCR experiments. To amplify FPRL1 we designed the sequences of sense oligonucleotide 5′-AATTCACATCGTGGTGGACA-3′ and antisense primer 5′-GAGGCAGCTGTTGAAGAAGG-3′, according to the sequence of the human FPRL1 coding region. These primers generate a 688-bp fragment. For human FPR, sense primer 5′-CTCCAGTTGGACTAGCC-3′ and antisense primer 5′-CCATCACCCAGGGCCCA-3′ were used to yield a 500-bp product. For human GAPDH, sense primer 5′-CCATGGAGAAGGCTGGG-3′ and antisense primer 5′-CGCCACAGTTTCCCGGA-3′ amplified a 280-bp fragment.

Western blot and immunoprecipitation analysis

Growth-arrested cells were stimulated with 10 μM WKYMVm for various times in the presence or absence of the appropriate amount of

specific inhibitors. CaLu-6 cells were rinsed with cold phosphate-buffered saline (PBS), lysed with 0.5 ml RIPA buffer (50 mM Tris–HCl, pH 7.4, 150 mM NaCl, 1% NP-40, 1 mM EDTA, 0.25% sodium deoxycholate, 1 mM NaF, 10 μM Na_3VO_4, 1 mM phenylmethylsulfonyl fluoride, 10 μg/ml aprotinin, 10 μg/ml pepstatin, 10 μg/ml leupeptin), and incubated at 4 °C for 45 min. Protein concentration was determined using a Bio-Rad protein assay. Western blot analysis was performed as previously described [10,28,29]. Antigen–antibody complexes were detected with the ECL chemiluminescence reagent kit (Amersham Pharmacia Biotech). Nuclear protein extracts were prepared with a Qproteome nuclear protein kit (Qiagen) according to the manufacturer's instructions. In immunoprecipitation experiments, cell lysates containing equal amounts of proteins were incubated with 3 μg of either anti-EGFR or anti-$p47^{phox}$ antibody overnight at 4 °C. Immunocomplexes were mixed with 30 μl of Protein A/G Plus agarose and rotated for 45 min at 4 °C. The immunoprecipitates were then washed three times with cold PBS, resuspended in 40 μl of Laemmli buffer, boiled for 5 min, pelleted by short centrifugation, and separated by 10% SDS–PAGE. Phosphorylated protein levels were quantitatively estimated by densitometry using a Discover Pharmacia scanner equipped with a Sun Spark Classic densitometric workstation.

Assay of superoxide production

The method used to determine $O_2^{\bullet-}$ is described elsewhere [10]. Membranes and cytosol were isolated from serum-starved human lung cancer cells stimulated with 10 μM WKYMVm for various times. NADPH-dependent superoxide generation was determined as the superoxide dismutase-sensitive rate of reduction of cytochrome *c*. Briefly, combinations of 10 μg of membrane and 200 μg of cytosol proteins in PBS were incubated at room temperature in the presence of 15 μM GTPγ-S, 100 μM cytochrome *c*, and 10 μM FAD in a total volume of 1 ml. NADPH (100 μM) was then added and the production of superoxide was monitored at 550 nm. The specificity of cytochrome *c* reduction was controlled by the addition to control samples of 200 U/ml superoxide dismutase. Rates of $O_2^{\bullet-}$ production were calculated from the linear segment of the increase in absorbance at 550 nm and translated into nanomoles of $O_2^{\bullet-}$ by the extinction coefficient of cytochrome *c*, $\Delta E_{550}/\Delta t = 21.1\ mM^{-1}\ cm^{-1}$, considering that 1 mol of $O_2^{\bullet-}$ reduces 1 mol of cytochrome *c*. The Student *t* test was used to compare individual treatments with their respective control value and $p<0.05$ versus values obtained with growth-arrested CaLu-6 cells was considered significant.

In vitro kinase assay

The in vitro kinase assay for c-Src activity was performed using denatured rabbit muscle enolase (Sigma) as an exogenous substrate. c-Src was immunoprecipitated by 5 μg of anti-c-Src antibody and protein A/G–Sepharose beads overnight at 4 °C. The immunoprecipitates were washed three times with 1% Nonidet P-40 lysis buffer and twice with 25 mM Tris–HCl, pH 7.4, and 10 mM $MnCl_2$. The beads were then incubated with 20 μl of kinase buffer (50 mM Tris–HCl, pH 7.4, 10 mM $MnCl_2$, 1 mM dithiothreitol) containing 2 μg of acid-denatured enolase and 10 mCi of [γ-^{32}P]ATP (PerkinElmer Life Sciences, Waltham, MA, USA) per reaction for 10 min at 37 °C. Reactions were stopped by adding Laemmli sample buffer and resolved by SDS–PAGE followed by autoradiography. Rabbit muscle enolase was denatured with 25 mM acetic acid at 30 °C for 10 min and then added to 1/10 of the total kinase reaction volume.

Statistical analysis

All data presented are expressed as means ± SD and are representative of three or more independent experiments. Statistical analyses were assessed by Student's *t* test for paired data. Results were considered significant at $p<0.05$.

Cell viability

CaLu-6 cells were plated at 4×10^4 cells per well in 200 μl of complete culture medium containing 10 μM WKYMVm in 96-well plates (Corning USA) in the presence or absence of 100 ng/ml PTX or 10 μM WRW4 and incubated at 37 °C for 12, 24, and 36 h. MTT (5 mg/ml in PBS) was then added to each well and incubated for 4 h. After careful removal of the medium, 200 μl of dimethyl sulfoxide (DMSO) was added to each well. The absorbance of the resulting formazan salts was recorded on a microplate reader at the wavelength of 540 nm. The effect of WKYMVm on cell growth was assessed as percentage cell viability. Four independent experiments were performed.

Results

FPRL1 is a biologically functional receptor in CaLu-6 cells

We first analyzed the expression of FPR and FPRL1 in the CaLu-6 cell line by RT-PCR analysis, performed with specific primers for the coding sequences of the two receptors, and by Western blot analysis using an α-FPRL1 antibody. We observed that FPRL1 mRNA, but not FPR, is expressed in these cells (Fig. 1A) and we detected the presence of the band corresponding to FPRL1 protein at the expected molecular size in immunoblot experiments (Fig. 1B). The α-FPRL1 antibody recognized the same band in cellular lysates purified from IMR90 human fibroblasts, which express FPRL1 [7] (Fig. 1B). We previously demonstrated that, in growth-arrested IMR90 human fibroblasts, activation of FPRL1 by WKYMVm induces ERK phosphorylation, $p47^{phox}$ membrane translocation, and NADPH oxidase activation [7]. Therefore, we next evaluated the ability of WKYMVm to activate the MAPK cascade, by analyzing the effect of cell exposure to the FPRL1 agonist on the phosphorylation state of ERK. We observed in time-response experiments that this treatment induces a rapid activation of ERK, which is sustained after 10 min of exposure to WKYMVm (Fig. 2A). Furthermore, the preincubation of CaLu-6 cells either with PD098059, a selective inhibitor of MEK, or with PTX, which blocks G_i proteins in their inactive form, before WKYMVm stimulation, prevents ERK phosphorylation (Fig. 2B).

Phosphorylation and membrane translocation of the cytosolic oxidase subunits are considered key events in the assembly of phagocytic and nonphagocytic NADPH oxidase [7,43]. In IMR90 cells, $p47^{phox}$ is a substrate for ERK kinase activity, and p44MAPK/p42MAPK phosphorylation is considered a prerequisite for NADPH oxidase activation [7]. Therefore, we investigated the molecular mechanisms

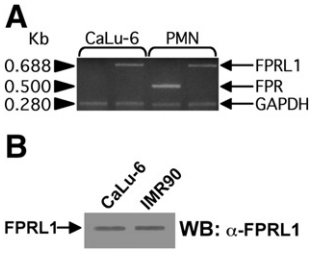

Fig. 1. Expression of FPRL1 in CaLu-6 cells. (A) Total RNAs were purified from CaLu-6 cells and PMN as a control. cDNAs were coamplified using FPR and GAPDH primers and FPRL1 and GAPDH oligonucleotides designed for human FPR, FPRL1, and GAPDH coding sequences. PCR products were separated on a 1.5% agarose gel and stained with ethidium bromide. (B) Cell lysates were purified from CaLu-6 cells and IMR90 cells as a control. A 10% SDS–PAGE gel was loaded with 50 μg of proteins and FPRL1 was detected by Western blot using a specific anti-FPRL1 antibody (α-FPRL1). The experiments were performed in triplicate.

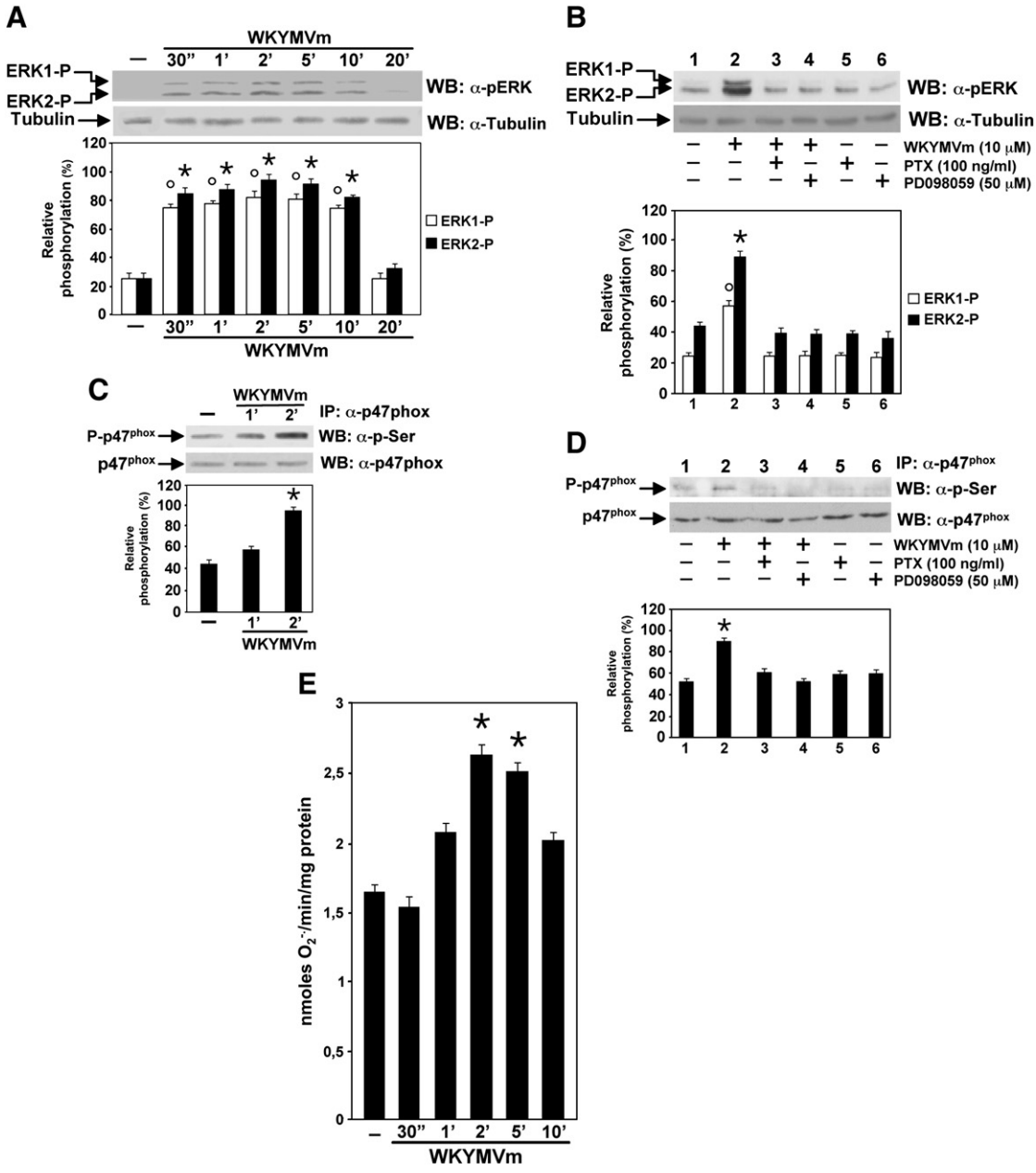

Fig. 2. ERK activation, $p47^{phox}$ phosphorylation, and NADPH-oxidase-dependent ROS generation in WKYMVm-stimulated CaLu-6 cells. (A) Cell lysates were purified from growth-arrested CaLu-6 cells stimulated for various times with 10 μM WKYMVm or (B) preincubated with the indicated concentrations of PTX or PD098059 before stimulation. Proteins (20 μg) were resolved on 10% SDS–PAGE and ERK phosphorylation was detected by Western blot with an anti-phospho-ERK antibody (α-p-ERK). An anti-tubulin antibody (α-tubulin) served as a control for protein loading. The arrows indicate the phosphorylated forms, ERK1-P and ERK2-P, of $p44^{MAPK}$ and $p42^{MAPK}$, respectively. (C) Serum-deprived CaLu-6 cells were stimulated for the indicated times with 10 μM WKYMVm or (D) preincubated with PTX or PD098059 before stimulation. One milligram of cell lysates was immunoprecipitated with an anti-$p47^{phox}$ antibody (α-$p47^{phox}$), and $p47^{phox}$ phosphorylation (P-$p47^{phox}$) was detected using an anti-phospho-serine antibody (α-p-Ser). An α-$p47^{phox}$ antibody served as a control for protein loading. All the blots are representative of at least three separate experiments of identical design. Protein expression levels were quantitatively estimated by densitometry using a Discover Pharmacia scanner equipped with a Sun Spark Classic densitometric workstation. °$p<0.05$ and *$p<0.05$ compared with unstimulated cells. (E) Ten micrograms of membrane and 200 μg of cytosolic proteins were purified from CaLu-6 cells grown in serum-free medium and stimulated with WKYMVm for the indicated times. Proteins were incubated in a NADPH oxidase activity assay and the specificity of cytochrome *c* reduction was monitored at 550 nm by using the SOD-inhibitable reduction of cytochrome *c*, as described under Materials and methods. *$p<0.05$ compared with serum-starved cells (—). The experiments were performed in triplicate.

underlying FPRL1-mediated NADPH-oxidase-dependent superoxide generation in CaLu-6 cells. Western blot analysis showed that the NADPH oxidase regulatory subunit $p47^{phox}$ is rapidly phosphorylated on serine residues upon exposure to WKYMVm (Fig. 2C) and that preincubation with PTX or PD098059 significantly prevents $p47^{phox}$ phosphorylation (Fig. 2D). Furthermore, time-response experiments showed that, consequent to activation of the NADPH oxidase regulatory subunit, stimulation of FPRL1 by WKYMVm induces NADPH-dependent superoxide generation, with maximal production occurring at 2 min (Fig. 2E). Taken together these results indicate that in CaLu-6 cells FPRL1 is a biologically functional receptor.

NADPH-oxidase-dependent superoxide generation is required for FPRL1-induced EGFR transactivation

It has been shown that in glioblastoma cells the activation of FPR by N-fMLP results in EGFR transactivation, suggesting that the two receptors synergistically cooperate to exacerbate the malignant

behavior of these tumor cells [44,45] and to produce angiogenic factors [46]. Because EGFR is expressed at high levels in CaLu-6 cells [40], we examined the ability of FPRL1 to transactivate EGFR. Fig. 3A shows that stimulation of CaLu-6 cells with 10 μM WKYMVm results in a time-dependent EGFR phosphorylation, with maximal phosphorylation of tyrosine residues occurring at 2 min. Furthermore, preincubation of cells with PTX, before stimulation with the FPRL1 agonist, results in a significant reduction in the phosphorylation level of tyrosines of EGFR, consequent to G_i-protein-specific inhibition (Fig. 3B).

A large body of evidence indicates that ROS are signaling intermediates in RTK activation [47–50]. ROS-mediated inhibition of phosphotyrosine phosphatase (PTPase) activity results in an equilibrium shift from the nonphosphorylated to the phosphorylated state of RTK. To investigate the role of NADPH-oxidase-dependent ROS generation in FPRL1-induced EGFR transactivation, we preincubated cells with the NADPH-oxidase-specific inhibitor apocynin or with a siRNA against $p22^{phox}$ before WKYMVm stimulation. We observed in immunoblot experiments that blockade of NADPH oxidase function prevents FPRL1-induced EGFR tyrosine phosphorylation (Figs. 3C and D), suggesting that NADPH oxidase activity is indeed required for EGFR transactivation.

c-Src activity is required for FPRL1-induced EGFR transactivation

Several cytosolic signal transduction proteins are implicated in the EGFR transactivation process. It has been suggested that Src-family tyrosine kinases function as both upstream and downstream mediators in GPCR-induced EGFR transactivation [51]. Inhibitor studies indicate the presence of c-Src upstream of EGFR in immortalized hypothalamic neurons [52], in LPA-stimulated COS-7 cells [53], and in vascular smooth muscle cells [54]. In contrast, in other experimental systems EGFR tyrosine phosphorylation has been reported to be independent of c-Src activity [55]. We investigated the role of c-Src in FPRL1-induced EGFR transactivation and we observed that in serum-deprived CaLu-6 cells exposed to WKYMVm, preincubation with genistein, a general tyrosine kinase inhibitor; or with the tyrphostin AG1478; or with PP2, an inhibitor of c-Src tyrosine kinase, prevents EGFR tyrosine phosphorylation (Figs. 4A and B). These results suggest that c-Src plays a key role in bridging the signals from FPRL1 to EGFR in these cells.

It has been shown that in U87 and FPRL1/CHO cells the stimulation of FPRL1 by WKYMVm increases c-Src kinase activity [56]. Therefore, we evaluated the ability of the FPRL1 agonist to activate c-Src in CaLu-6 cells in an in vitro kinase assay using enolase and [^{32}P]ATP as substrates. As shown in Fig. 5A, c-Src kinase activity was increased in cells exposed to WKYMVm for 2 min (lane 2) and was completely prevented by preincubation with PTX (lane 3).

c-Src activity is regulated by phosphorylation at two distinct tyrosine residues. Autophosphorylation of the Tyr416 residue in the kinase domain activates c-Src, whereas phosphorylation of the Tyr527 residue in the C-terminal tail by the C-terminal Src kinase blocks c-Src activity. We analyzed c-SrcTyr416 phosphorylation levels in growth-arrested CaLu-6 cells stimulated for various times with WKYMVm by using a phospho-specific antibody directed toward the phosphorylated Y416 residue of c-Src. Western blotting analysis showed that the c-SrcTyr416 phosphorylation level was regulated in a time-dependent manner, with maximal phosphorylation occurring at 2 min (Fig. 5B).

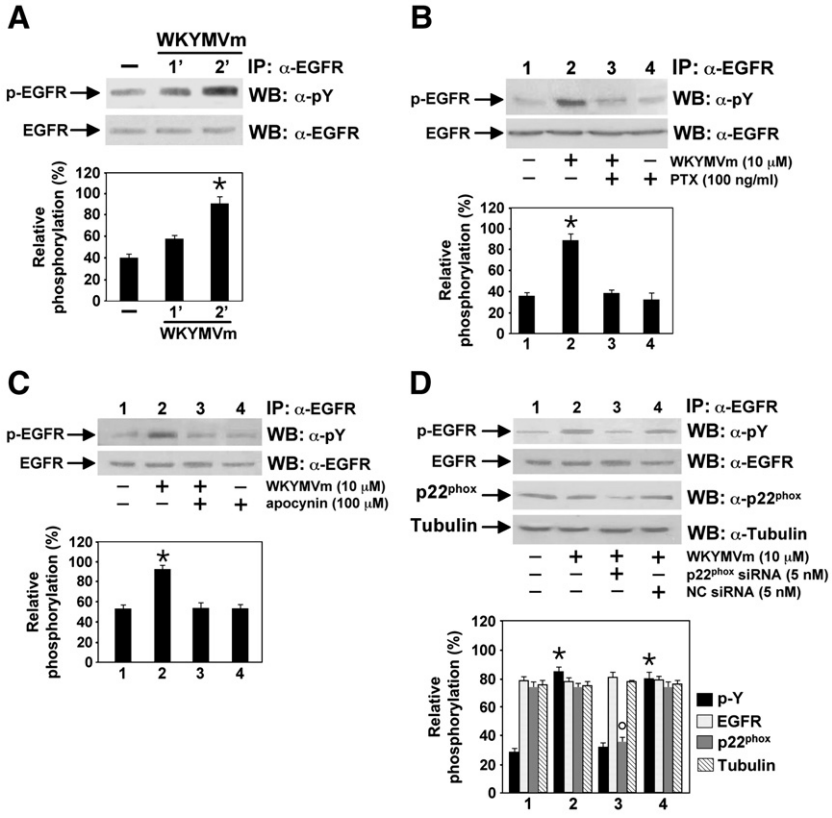

Fig. 3. FPRL1-induced EGFR transactivation depends on NADPH oxidase activation. (A) Growth-arrested CaLu-6 cells were incubated with 10 μM WKYMVm for the indicated times or preincubated with (B) 100 ng/ml PTX or (C) 100 μM apocynin before stimulation. (D) Serum-deprived cells were incubated for 12 h with 5 nM siRNA against $p22^{phox}$ ($p22^{phox}$ siRNA) or a negative control siRNA (NC siRNA) in DMEM containing 10% FBS in the presence of 20 ml HiPerFect. Cells were then serum-deprived for 24 h before stimulation with 10 μM WKYMVm for 2 min. Cell lysates containing 800 μg of proteins were incubated with 3 μg of anti-EGFR (α-EGFR) and immunocomplexes were mixed with 30 μl of Protein A/G Plus agarose. The immunoprecipitates were loaded on 10% SDS–PAGE gels and EGFR phosphorylation (p-EGFR) was detected with an anti-phospho-tyrosine antibody (α-p-Y). An α-EGFR and an α-tubulin antibody served as controls for protein loading. An α-$p22^{phox}$ antibody served as a control for interference. All the blots are representative of at least three separate experiments of identical design. Protein expression levels were quantitatively estimated by densitometry. °$p<0.05$ and *$p<0.05$ compared with unstimulated cells.

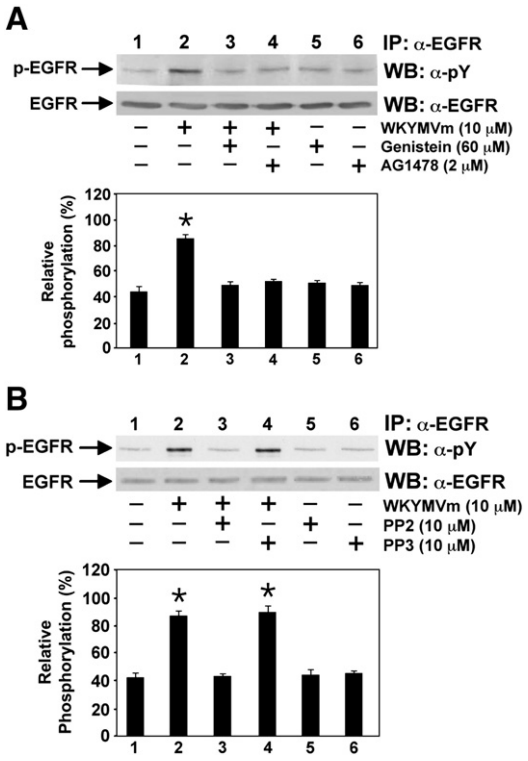

Fig. 4. General and specific tyrosine kinase inhibitors prevent FPRL1-induced EGFR phosphorylation. (A) Serum-deprived CaLu-6 cells were preincubated with genistein or AG1478 or (B) PP2 or PP3 at the indicated concentrations, before stimulation with 10 μM WKYMVm. Cell lysates (800 mg) were purified and EGFR was immunoprecipitated with an anti-EGFR antibody (α-EGFR). Proteins were resolved on 10% SDS–PAGE and EGFR phosphorylation (p-EGFR) was detected with an anti-phospho-tyrosine antibody (α-p-Y). An α-EGFR antibody served as a control for protein loading. The experiments were performed in triplicate. Phosphorylated protein levels were measured by densitometry. $^{*}p<0.05$ compared with unstimulated cells.

We also pretreated cells with PTX before WKYMVm stimulation and we found that the G_i-protein-specific inhibition significantly prevents c-SrcTyr416 phosphorylation (Fig. 5C).

c-Src is sensitive to intracellular redox conditions as demonstrated by the ROS-dependent inactivation of the PTPases that control its phosphorylation status [57]. Therefore, we investigated the role of NADPH-oxidase-dependent ROS generation in FPRL1-induced c-Src activation. We observed that pretreatment with the NADPH oxidase inhibitor apocynin or preincubation with a siRNA against $p22^{phox}$, before stimulation with WKYMVm for 2 min, prevents c-SrcTyr416 phosphorylation (Figs. 5D and E), suggesting that FPRL1-induced c-Src kinase activity requires NADPH oxidase activation.

WRW4 prevents the FPRL1-induced downstream signal transduction cascade

The peptide WRW4 antagonizes the binding of the specific FPRL1 ligand WKYMVm, thereby inhibiting intracellular calcium increase, FPRL1-induced neutrophil activation [58], and ERK phosphorylation [10]. We exposed CaLu-6 cells to WRW4 to further investigate the role of FPRL1 in the downstream signaling cascade and we observed, in dose–response experiments, that preincubation with WRW4, before WKYMVm stimulation, prevents ERK activation (Fig. 6A) and c-SrcTyr416 residue phosphorylation (Fig. 6B), with the maximal effect occurring at a concentration of 10 μM. Preincubation with 10 μM WRW4 also inhibits FPRL1-dependent EGFR transactivation (Fig. 6C) and $p47^{phox}$ phosphorylation (Fig. 6D).

FPRL1-induced EGFR transactivation triggers STAT3 activation

STAT proteins are activated as a consequence of ligand binding to cytokine and growth factor receptors such as EGFR and PDGF-R. STAT 2, 4, and 6 are activated by a small subset of cytokines, whereas STAT 1, 3, 5a, and 5b are activated also by growth factors [59]. Binding of EGF to its cognate receptor results in EGFR dimerization and phosphorylation and in the activation of receptor-associated Janus kinases (JAK). Recruitment, phosphorylation of STAT3 on the Tyr705 residue, and dimerization of STAT3 represent the trigger of the JAK/STAT3 cascade. Activated STAT3 is then translocated to the nucleus to activate target genes. Full transcriptional activity and DNA binding capacity are manifested only when the STAT3 Ser727 residue is also phosphorylated. In addition to cytokine and growth factor receptors, a number of GPCR agonists also activate STAT3 [36–39]. In glioblastoma cells N-fMLP induces a rapid and transient phosphorylation of STAT3 at the Tyr705 and Ser727 residues by binding to FPR [45] and, in RBL-2H3 cells, the Ser727 residue of STAT3 is phosphorylated consequent to the binding of WKYMVm to FPRL1 [38]. Furthermore, as a result of transmembrane signaling, uPAR activates the JAK/STAT pathway mediated by FPRL1 [60]. Therefore, we analyzed the FPRL1-induced STAT3 activation in growth-arrested CaLu-6 cells. We observed that, in time-dependent Western blot experiments, stimulation with 10 μM WKYMm rapidly induces phosphorylation of the STAT3 Tyr705 residue (Fig. 7A), the nuclear translocation of activated STAT3 (Fig. 7B), and the phosphorylation of the STAT3 Ser727 residue (Fig. 7C). Taken together the above results indicate that activation, dimerization, and nuclear translocation of STAT3 are a part of the FPRL1-dependent signaling cascade.

We next examined the molecular mechanisms involved in FPRL1-induced STAT3 activation by pretreating CaLu-6 cells with PTX, AG1478, and genistein. These experiments show that phosphorylation of the STAT3 Tyr705 residue greatly depends on FPRL1 and EGFR activation, being prevented by PTX and by general and EGFR-specific tyrosine kinase inhibitors (Fig. 8A). Furthermore, the phosphorylation of Tyr705 of STAT3 is c-Src-dependent, because it is prevented by the preincubation of CaLu-6 cells with PP2 before WKYMVm stimulation, and it is MEK-independent, as observed by the lack of effect of the MEK inhibitor PD098059 (Fig. 8B). In addition, preincubation of serum-deprived CaLu-6 cells with PTX before agonist stimulation completely prevents STAT3 Ser727 phosphorylation (Fig. 8C). The MAPK pathway plays an important role in the regulation of STAT3 signaling and, in particular, ERK were demonstrated to phosphorylate STAT3 at the Ser727 residue [61]. In CaLu-6 cells preincubation with PD098059, before WKYMVm stimulation, completely prevents the phosphorylation of STAT3 at Ser727, whereas, as expected, the general tyrosine kinase inhibitor genistein has no effect on serine phosphorylation (Fig. 8C). Consequently, ERK activity seems to be required for FPRL1-induced STAT3 Ser727 phosphorylation.

FPRL1-induced signaling cascade promotes cell proliferation

We evaluated the cellular consequences of FPRL1-induced signaling by analyzing the effects of exposure to WKYMVm on CaLu-6 cell growth. We observed that the addition of 10 μM WKMVm to the cells results in a time-dependent growth response, with the maximum level of CaLu-6 growth occurring after 24 h of exposure (Fig. 9A). Furthermore, inhibition of G_i proteins by PTX or preincubation with the FPRL1 antagonist WRW4 significantly prevents cell proliferation (Fig. 9B). This indicates that the FPRL1-dependent intracellular signaling cascades triggered by WKYMVm result in an increased growth rate of the human lung cancer CaLu-6 cell line, which can be prevented by blockade of FPRL1, highlighting the role of this receptor as a potential target of new drugs.

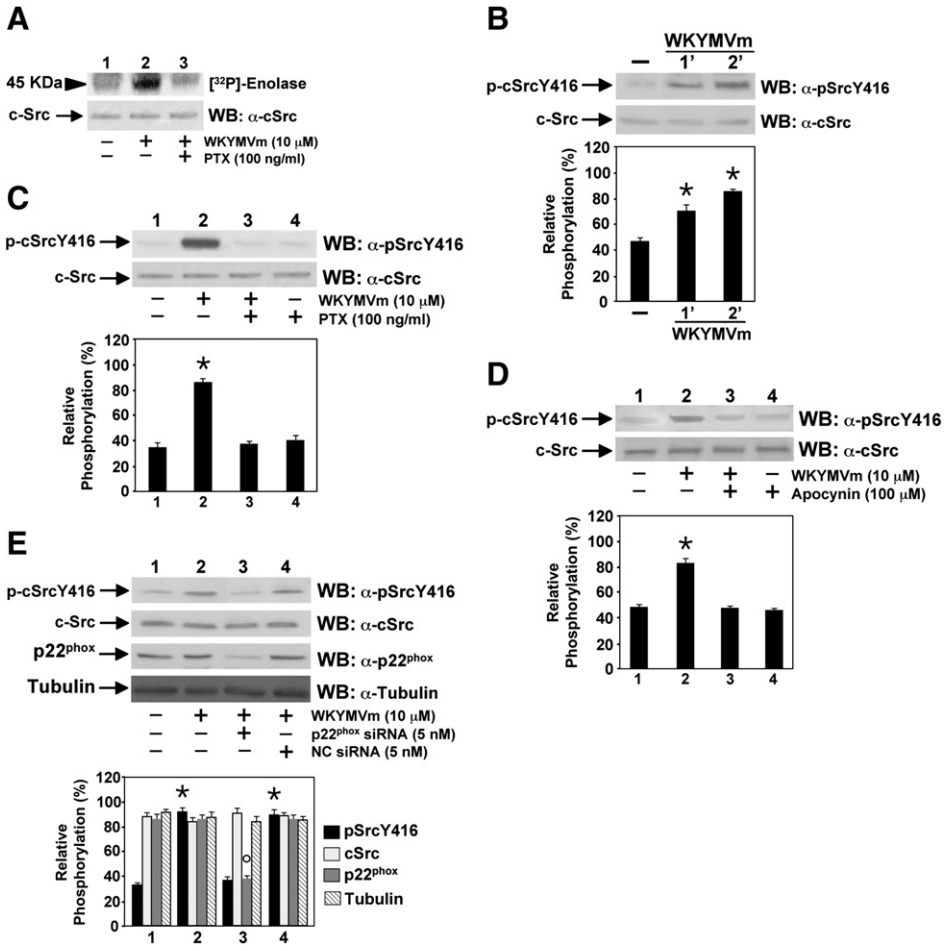

Fig. 5. FPRL1-dependent c-Src activation depends on NADPH oxidase activity. (A) The cellular activity of c-Src was detected by in vitro kinase assay. CaLu-6 cells were exposed to 10 μM WKYMVm in the presence or absence of 100 ng/ml PTX. Cell lysates were immunoprecipitated with an anti-c-Src antibody and cellular c-Src kinase activity was directly measured on protein A/G agarose beads carrying a c-Src immunocomplex in the presence of the in vitro substrate enolase and [γ-^{32}P]ATP. Samples were resolved by 10% SDS–PAGE and autoradiography. (B) Cells were exposed to 10 μM WKYMVm for the indicated times or preincubated with (C) 100 ng/ml PTX or (D) 100 μM apocynin before stimulation. Fifty micrograms of protein was loaded on 10% SDS–PAGE and c-Src Y416 phosphorylation (p-c-SrcY416) was detected with an anti-phospho-Src Y416 antibody (α-p-SrcY416). An α-c-Src antibody served as a control for protein loading. (E) Serum-deprived cells were incubated for 12 h with 5 nM siRNA against p22^{phox} (p22^{phox} siRNA) or a negative control siRNA (NC siRNA) in the presence of 20 ml HiPerFect. Cells were serum-deprived for 24 h and then exposed to 10 μM WKYMVm for 2 min. Cell lysates containing 50 μg of proteins were loaded on 10% SDS–PAGE gels and c-Src Y416 phosphorylation was detected with an α-p-SrcY416 antibody. An α-c-Src and an α-tubulin antibody served as controls for protein loading. An anti-p22^{phox} antibody (α-p22^{phox}) served as a control for interference. All the blots are representative of at least three separate experiments of identical design. Protein expression levels were quantitatively estimated by densitometry. °$p<0.05$ and *$p<0.05$ compared with unstimulated cells.

Discussion

We demonstrate that in serum-deprived CaLu-6 cells, stimulation of FPRL1 by a specific agonist results in NADPH-oxidase-dependent superoxide generation and EGFR transactivation. Furthermore, we show that ROS play a key role in bridging the signals from FPRL1 to EGFR by modulating c-Src kinase activity, as demonstrated by the effects of PP2, apocynin, and a siRNA against p22^{phox} on c-Src Y416 phosphorylation and EGFR transactivation. Our results also indicate that, as a consequence of the transphosphorylation process the phosphotyrosine residues of EGFR provide docking sites for recruitment and triggering of the STAT3 pathway. Finally, the FPRL1-induced signaling promotes an increased growth rate of CaLu-6 cells.

EGFR is a cell-surface receptor and is a member of the c-erb-B family of tyrosine kinases, known to be overexpressed in a variety of human malignant tumors and cells, including lung carcinoma and the CaLu-6 cell line [40]. In addition to activation by EGF, its cognate ligand, several GPCR can also transactivate EGFR and the cross talk between the two receptors is a crucial signaling mechanism that serves to expand the cellular communication network. In fact, the receptors for angiotensin [62], LPA [63], CXCL12 [64], bombesin [65], thrombin [66], and endothelin-1 [67] also transactivate EGFR, thereby assisting the transmission of growth signals. In glioblastoma cells EGFR transactivation is mediated by the binding of N-fMLP to FPR [44] and inhibition of EGFR phosphorylation significantly reduces FPR agonist-induced tumor cell chemotaxis and proliferation [44,68]. Thus, FPR expressed in glioblastoma cells can exploit the EGFR capacity to amplify tumor growth. In line with these results we show that, as a consequence of FPRL1-induced signaling, WKYMVm promotes an increased growth rate of CaLu-6 cells, which is prevented by blockade of FPRL1.

Much evidence suggests that GPCR-induced EGFR transactivation may involve the EGFR ligand-dependent pathway through the metalloprotease-dependent release of EGF-like ligands [69], or the EGFR ligand-independent pathway, which can involve nonreceptor tyrosine kinases such as c-Src [70,71]. In glioblastoma cells N-fMLP-induced EGFR phosphorylation requires the presence of FPR and of G_i proteins associated with the receptor and is controlled by c-Src tyrosine kinase [44]. Furthermore, stimulation of FPRL1 by WKYMVm in both U87 and FPRL1/CHO cells increases c-Src kinase activity [56]. In line with these results our study shows that FPRL1-induced signaling induces an increase in c-Src kinase activity and that c-Src plays a key role in the control of EGFR transactivation.

Another molecular mechanism that can contribute to RTK transactivation by GPCR ligands is the generation of ROS, which in

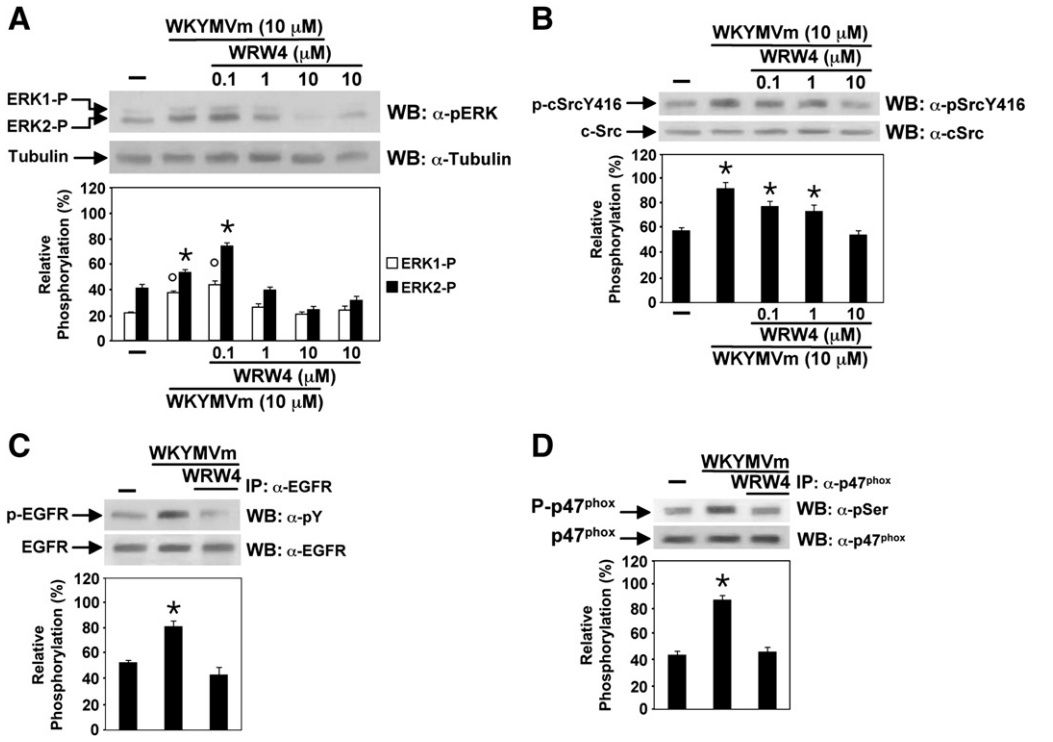

Fig. 6. WRW4 prevents the FPRL1-induced signal transduction cascade. Cell lysates were obtained from serum-deprived CaLu-6 cells exposed to 10 μM WKYMVm for 2 min in the presence or absence of increasing concentrations of WRWWWW (WRW4), as indicated. (A) Twenty micrograms of protein was resolved by 10% SDS–PAGE and subjected to immunoblotting analysis with an anti-phospho-ERK antibody (α-p-ERK). An anti-tubulin antibody (α-tubulin) served as a control for protein loading. The arrows indicate the phosphorylated forms, ERK1-P and ERK2-P, of $p44^{MAPK}$ and $p42^{MAPK}$, respectively. (B) Fifty micrograms of protein was subjected to 10% SDS–PAGE and subsequent immunoblotting by using an anti-phospho-Src Y416 antibody (α-p-SrcY416). The same filter was reprobed with an anti-c-Src antibody (α-c-Src). (C) Growth-arrested CaLu-6 cells were exposed to 10 μM WKYMVm for 2 min or preincubated with 10 μM WRW4 for 15 min before stimulation. Proteins (800 μg) were immunoprecipitated with an anti-EGFR antibody (α-EGFR) and resolved on 10% SDS–PAGE. Tyrosine phosphorylation of EGFR was detected with an anti-phospho-tyrosine (α-p-Y) antibody. An α-EGFR antibody served as a control for protein loading. (D) Cell lysates were purified from CaLu-6 cells stimulated with 10 μM WKYMVm for 2 min or preincubated with 10 μM WRW4 for 15 min before stimulation. One milligram of protein was immunoprecipitated with an anti-$p47^{phox}$ antibody (α-$p47^{phox}$) and resolved on 10% SDS–PAGE. $p47^{phox}$ phosphorylation (P-$p47^{phox}$) was detected using an anti-phospho-serine antibody (α-p-Ser). An α-$p47^{phox}$ antibody served as a control for protein loading. All the blots are representative of three separate experiments. Phosphorylated protein levels were quantitatively estimated by densitometry. $^{\circ}p<0.05$ and $^{*}p<0.05$ compared with unstimulated cells.

turn inactivate PTPases that tightly control the activity of RTK [49,50,72–75]. In fact, oxidation and reduction of protein cysteine sulfhydryl groups of PTPases may act as a molecular switch to start or to stop signaling.

Plasma membrane-associated Nox enzymes catalyze the deliberate and regulated generation of ROS. In contrast to the cytotoxic amounts of superoxide generated by phagocytes, the nonphagocytic Nox family members are recognized as producers of low levels of ROS that play critical roles in maintaining normal physiologic processes and that stimulate intracellular signaling cascades via activation of kinases and inhibition of PTPases [16]. Under physiological conditions, the intracellular production of ROS does not alter the redox state of cells, which have large reserves of reducing agents. This reducing intracellular environment allows agonist-induced increases in ROS to function as second messengers by limiting their effect in time and space [76]. A major attribute of nonphagocytic NADPH oxidases is that not only are they constitutively active but their activity is sensitively influenced by a wide variety of (patho)physiological stimuli. Several pathological conditions are associated with overproduction of ROS by Nox enzymes. They include chronic diseases that tend to appear late in life, such as Alzheimer disease, atherosclerosis, hypertension, diabetic nephropathy, lung fibrosis, and cancer. In many of these diseases overproduction of ROS also results from increased expression of Nox enzymes and/or of their regulatory subunits [77].

ROS also influence c-Src at several levels, both directly by modulating Src kinase activity and indirectly by modulating factors that regulate c-Src kinase activity [78]. We show that FPRL1-induced signaling triggers NADPH-oxidase-dependent superoxide generation, which plays a crucial role in EGFR transactivation by modulating c-Src tyrosine kinase activity, although a concomitant ligand-dependent transactivation of EGFR cannot be ruled out. On the other hand, several studies show that c-Src kinase activity influences NADPH-oxidase-dependent ROS generation at several levels by facilitating activation of the NADPH oxidase cofactors required to form the complex [78,79].

STAT3 is a member of the STAT family of cytoplasmic transcription factors. It requires extrinsic tyrosine phosphorylation to become activated and this event is induced by RTK such as EGFR, cytoplasmic c-Src tyrosine kinases, and components of the JAK family. Specific formyl peptide receptor agonists also activate STAT3 [38,45]. We found that in CaLu-6 cells exposure to WKYMVm induces FPRL1-dependent phosphorylation of STAT3 at the Y705 and S727 residues, suggesting that STAT3 activation is also a part of the FPRL1-dependent signaling cascade. We also observed MEK-dependent ERK phosphorylation in WKYMVm-stimulated CaLu-6 cells, which is consistent with our previous results obtained in IMR90 human fibroblasts [7]. It has been shown that the MAPK pathway plays an important role in the regulation of STAT3 signaling and that ERK are known to phosphorylate STAT3 at the S727 residue [61]. We demonstrate that S727 phosphorylation of STAT3 is prevented by the MEK1 inhibitor PD098059, suggesting that ERK phosphorylation is crucial for WKYMVm-induced STAT3 activation in CaLu-6 cells.

FPRL1 was initially known as a low-affinity receptor for N-fMLP. In the past few years several ligands have been identified, making FPRL1 the most promiscuous in the FPR family with respect to agonist selectivity. Interestingly, most of the newly identified agonists for FPRL1 do not share substantial sequence homology; thus, FPRL1 behaves as a “pattern recognition” receptor that can be activated by a wide variety of unrelated ligands.

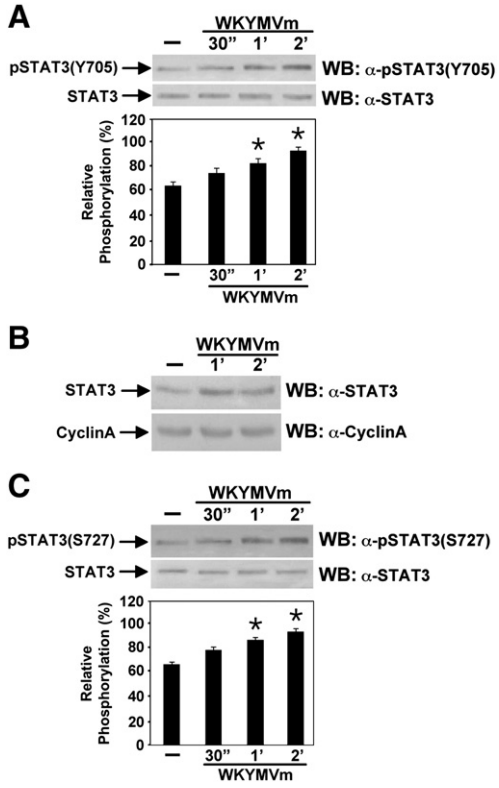

Fig. 7. FPRL1-induced EGFR transactivation triggers the STAT3 pathway. Total and nuclear cell lysates were purified from serum-starved CaLu-6 cells exposed to 10 μM WKYMVm for various times, as indicated. (A) Fifty micrograms of total protein was resolved by 10% SDS–PAGE and specific phosphorylations of STAT3 were detected with anti-phospho-STAT3 Y705 (α-p-STAT3(Y705)) or (C) anti-phospho-STAT3 S727 (α-p-STAT3(S727)) antibodies. An anti-STAT3 antibody (α-STAT3) served as a control for protein loading. (B) A 10% SDS–PAGE gel was loaded with 50 μg of nuclear extracts and STAT3 nuclear translocation was determined by Western blot with an α-STAT3 antibody. The same filter was reprobed with an anti-cyclin A antibody (α-CyclinA). All the experiments were performed in triplicate. Phosphorylated protein levels of STAT3 Y705 and STAT3 S727 were quantitatively estimated by densitometry. $^{*}p<0.05$ compared with unstimulated cells.

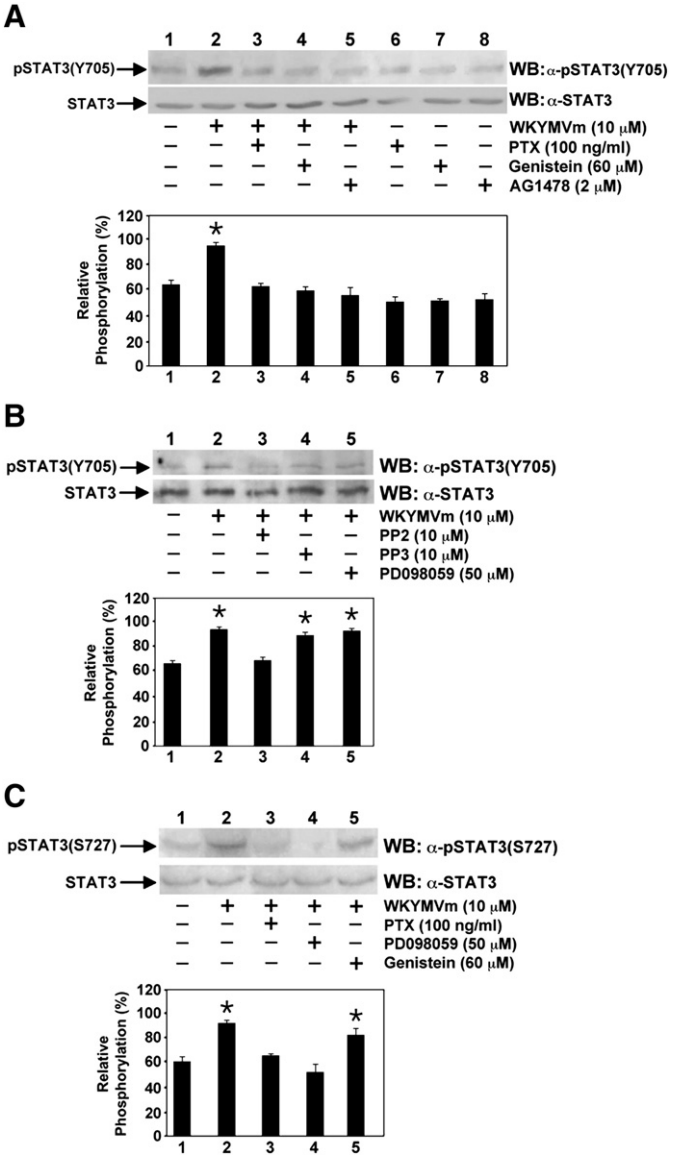

Fig. 8. FPRL1-induced STAT3 signaling requires activation of EGFR, c-Src, and MEK1. Serum-deprived CaLu-6 cells were exposed to 10 μM WKYMVm for 2 min or preincubated with the appropriate concentrations of inhibitors before stimulation, as described under Materials and methods. Total proteins (50 mg) were electrophoresed and transferred to Immobilon P membranes. (A) Cells were preincubated for 16 h with PTX, or for 1 h with genistein, or for 1 h with AG1478 at the indicated concentrations, before stimulation. The blot was incubated with a primary antibody against STAT3 phosphorylated at the Tyr705 residue (α-p-STAT3(Y705)). (B) Growth-arrested CaLu-6 cells were pretreated for 45 min with PP2, or for 45 min with PP3, or for 90 min with PD098059 at the indicated concentrations, before exposure to WKYMVm. An α-p-STAT3(Y705) antibody was used to detect STAT3 Y705 phosphorylation. (C) Human lung cancer cells were preincubated with PTX, PD098059, or genistein at the indicated concentrations, before stimulation with the FPRL1 agonist. The blot was incubated with an α-p-STAT3(S727) antibody to detect the phosphorylated form of STAT3 Ser727. Total STAT3 was detected with an antibody against nonphosphorylated STAT3 (α-STAT3). All the blots are representative of at least three separate experiments of identical design. Phosphorylated protein levels were quantitatively measured by densitometry. $^{*}p<0.05$ compared with unstimulated cells.

There have been ongoing efforts in several laboratories to study the ligand and FPRL1 interaction, in part because of the potential for FPRL1 to become a therapeutic target.

It has been shown that both agonists and antagonists for FPRL1 have therapeutic value. In fact, WKYMVm increases neutrophil bactericidal activity in chemotherapy-treated cancer patients [80] and enhances endogenous expression of TRAIL, a novel potential anticancer agent, in human monocytes and neutrophils [81]. Moreover, the administration of WKYMVm protects against death by enhanced bactericidal activity and inhibition of vital organ inflammation and immune cell apoptosis in a cecal ligation and puncture sepsis mouse model [82]. WKYMVm, activating FPRL1, also potently inhibits HIV-1 Env-mediated fusion and viral infection through heterologous desensitization of the chemokine receptors CCR5 and CXCR4, suggesting a novel approach to the development of anti-HIV-1 reagents [83].

The use of FPRL1 by SAA, Ab42, and human prion peptide suggests that this receptor may play a crucial role in proinflammatory aspects of systemic amyloidosis, Alzheimer disease, and prion diseases. This observation prompted studies in search of antagonists, which are important for delineating the signal transduction cascade associated with receptor activation and as a basis for developing anti-inflammatory therapeutic agents. Several antagonists for FPRL1 have been identified. These include the chemotaxis inhibitory protein of *Staphylococcus aureus,* the FPRL1 inhibitory protein FLIpr, the bile acids deoxycholic and chenodeoxycholic, and Quin-c7, a synthetic nonpeptide developed through chemical modification of QuinC-7 [84–86]. Moreover, W-rich peptides, such as WRW4, exert an antagonistic effect on WKYMVm-induced FPRL1 signaling, suggesting their use for the treatment of several diseases in which FPRL1 is known to play a role [58].

It should be also noted that because FPR is overexpressed in human glioblastoma cells [87], at least some members of the FPR family might

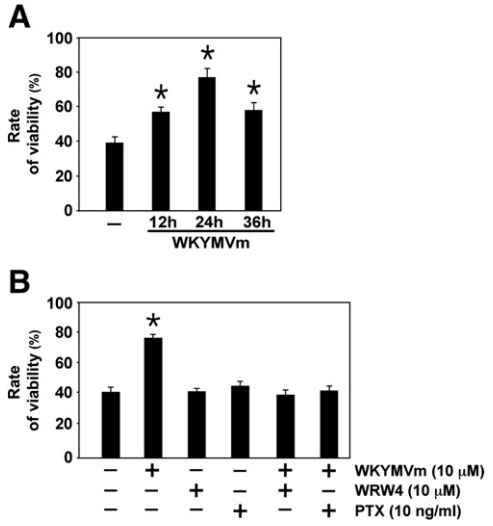

Fig. 9. FPRL1-induced signaling promotes cell growth in CaLu-6 cells. (A) CaLu-6 cells were plated at 4×10^4 cells per well in 200 μl of culture medium containing 10 μM WKYMVm in 96-well plates and incubated at 37 °C for 12, 24, and 36 h. (B) Cells were incubated for 24 h with the FPRL1 agonist in the presence or absence of PTX or WRW4 at the indicated concentrations. MTT (5 mg/ml in PBS) was added to each well and incubated for 4 h. After removal of the medium, 200 μl of DMSO was added to each well. The absorbance of the resulting formazan salts was recorded on a microplate reader at the wavelength of 540 nm. The effect of WKYMVm on cell growth was assessed as percentage of cell viability. Four independent experiments were performed. $^*p<0.05$ compared with unstimulated cells.

also be valuable biomarkers for cancer diagnosis, therefore increasing the number of available biomarkers for cancer diagnosis and staging.

The transactivation of EGFR by FPRL1 in human lung carcinoma cells may have important pathophysiological implications. The expression of FPRL1 in CaLu-6 cells could render these cells responsive not only to WKYMVm, but also to agonists contained in the environment of necrotic tumor cells. As a result of these interactions, FPRL1 could activate intracellular signaling molecules such as ROS, ERK, and c-Src that, in turn, could trigger EGFR transactivation, the STAT3 pathway, and cell growth. This suggests that clarification of the resulting signaling cascades may open the way to new drugs that interfere with the FPRL1 signaling pathway and that targeting both FPRL1 and EGFR may yield superior therapeutic effects compared with targeting either receptor separately.

Acknowledgments

This work was supported by grants from the Ministero dell'Università e della Ricerca Scientifica e Tecnologica PRIN 2007 "Attivazione dei recettori per formil-peptidi e regolazione della NADPH ossidasi in linee cellulari tumorali umane non fagocitiche." We thank Jean Ann Gilder (Scientific Communication srl) for text editing.

Refereences

[1] Prossnitz, E. R.; Ye, R. D. The N-formyl peptide receptor: a model for the study of chemoattractant receptor structure and function. *Pharmacol. Ther.* **74:**73–102; 1997.
[2] Le, Y.; Oppenheim, J. J.; Wang, J. M. Pleiotropic roles of formyl peptide receptors. *Cytokine Growth Factor Rev.* **12:**91–105; 2001.
[3] Le, Y.; Murphy, P. M.; Wang, J. M. Formyl-peptide receptors revisited. *Trends Immunol.* **23:**541–548; 2002.
[4] Durstin, M.; Gao, J. L.; Tiffany, H. L.; McDermott, D.; Murphy, P. M. Differential expression of the N-formylpeptide receptor gene cluster in human phagocytes. *Biochem. Biophys. Res. Commun.* **201:**174–179; 1994.
[5] Becker, E. L.; Forouhar, F. A.; Grunnet, M. L.; Boulay, F.; Tardif, M.; Bormann, B. J.; Sodja, D.; Ye, R. D.; Woska Jr., J. R.; Murphy, P. M. Broad immunocytochemical localization of the formylpeptide receptor in human organs, tissues and cells. *Cell Tissue Res.* **292:**129–135; 1998.
[6] Harada, M.; Habata, Y.; Hosoya, M.; Nishi, K.; Fujii, R.; Kobayashi, M.; Hinuma, S. N-formylated humanin activates both formyl peptide receptor-like 1 and 2. *Biochem. Biophys. Res. Commun.* **324:**255–261; 2004.
[7] Ammendola, R.; Russo, L.; De Felice, C.; Esposito, F.; Russo, T.; Cimino, F. Low-affinity receptor-mediated induction of superoxide by N-formyl-methionyl-leucyl-phenylalanine and WKYMVm in IMR90 human fibroblasts. *Free Radic. Biol. Med.* **36:**189–200; 2004.
[8] Baek, S. H.; Seo, J. K.; Chae, C. -B.; Suh, P. G.; Ryu, S. H. Identification of the peptides that stimulate the phosphoinositide hydrolysis and induction of superoxide generation in human neutrophils. *J. Biol. Chem.* **271:**8170–8175; 1996.
[9] Iaccio, A.; Angiolillo, A.; Ammendola, R. Intracellular signaling triggered by formyl-peptide receptors in nonphagocytic cells. *Curr. Signal Transduct. Ther.* **3:** 88–96; 2008.
[10] Iaccio, A.; Cattaneo, F.; Mauro, M.; Ammendola, R. FPRL1-mediated induction of superoxide in LL-37-stimulated IMR90 human fibroblasts. *Arch. Biochem. Biophys.* **481:**94–100; 2009.
[11] Cattaneo, F.; Guerra, G.; Ammendola, R. Expression and signaling of formyl peptide receptors in the brain. *Neurochem. Res.* **35:**2018–2026; 2010.
[12] Fontayne, A.; Dang, P. M.; Goucerot-Pocidalo, M. A.; El Benna, J. Phosphorylation of p47phox sites by PKC alpha, beta II, delta, and zeta: effect on binding to p22phox and on NADPH oxidase activation. *Biochemistry* **41:**7743–7750; 2002.
[13] Dewas, C.; Fay, M.; Gougerot-Pocidalo, M. A.; El-Benna, J. The mitogen-activated protein kinase extracellular signal-regulated kinase 1/2 pathway is involved in formyl-methionyl-leucyl-phenylalanine-induced p47phox phosphorylation in human neutrophils. *J. Immunol.* **165:**5238–5244; 2000.
[14] Lal, A. S.; Clifton, A. D.; Rouse, J.; Segal, A. W.; Cohen, P. Activation of the neutrophil NADPH oxidase is inhibited by SB 203580, a specific inhibitor of SAPK2/p38. *Biochem. Biophys. Res. Commun.* **259:**465–470; 1999.
[15] Leto, T. L.; Morand, S.; Hurt, D.; Ueyama, T. Targeting and regulation of reactive oxygen species generation by Nox family NADPH oxidase. *Antioxid. Redox Signal.* **10:**2607–2619; 2009.
[16] Bokoch, G. M.; Diebold, B.; Kim, J. S.; Gianni, D. Emerging evidence for the importance of phosphorylation in the regulation of NADPH oxidases. *Antioxid. Redox Signal.* **10:**2429–2441; 2009.
[17] Griffith, B.; Pendyala, S.; Hecker, L.; Lee, P. L.; Natarajan, V. Nox enzymes and pulmonary disease. *Antioxid. Redox Signal.* **10:**2506–2516; 2009.
[18] Takeya, R.; Ueno, N.; Kami, K.; Taura, M.; Kohjima, M.; Izaki, T.; Nunoi, H.; Sumimoto, H. Novel human homologues of p47phox and p67phox participate in activation of superoxide-producing NADPH oxidases. *J. Biol. Chem.* **278:** 25234–25246; 2003.
[19] Lambeth, J. D.; Kawahara, T.; Diebold, B. Regulation of Nox and Duox enzymatic activity and expression. *Free Radic. Biol. Med.* **43:**319–331; 2007.
[20] Suh, Y. -A.; Arnold, R. S.; Lassegue, B.; Shi, J.; Xu, X.; Sorescu, D.; Chung, A. B.; Griendling, K. K.; Lambeth, J. D. Cell transformation by the superoxide-generating oxidase Mox1. *Nature* **401:**79–82; 1999.
[21] Lassègue, B.; Sorescu, D.; Szöcs, K.; Yin, Q.; Akers, M.; Zhang, Y.; Grant, S. L.; Lambeth, J. D.; Griendling, K. K. Novel gp91phox homologues in vascular smooth muscle cells: Nox1 mediates angiotensin II-induced superoxide formation and redox-sensitive signaling pathways. *Circ. Res.* **88:**888–894; 2001.
[22] Cheng, G.; Lambeth, J. D. NOXO1, regulation of lipid binding, localization, and activation of Nox1 by the Phox homology (PX) domain. *J. Biol. Chem.* **279:** 4737–4742; 2004.
[23] Brown, D. I.; Griendling, K. K. Nox proteins in signal transduction. *Free Radic. Biol. Med.* **47:**1239–1253; 2009.
[24] Ueno, N.; Takeya, R.; Miyano, K.; Kikuchi, H.; Sumimoto, H. The NADPH oxidase Nox3 constitutively produces superoxide in a p22phox-dependent manner: its regulation by oxidase organizers and activators. *J. Biol. Chem.* **280:**23328–23339; 2005.
[25] Park, H. S.; Jung, H. Y.; Park, E. Y.; Kim, J.; Lee, W. J.; Bae, Y. S. Cutting edge: direct interaction of TLR4 with NAD(P)H oxidase 4 isozyme is essential for lipopolysaccharide-induced production of reactive oxygen species and activation of NF-kappa B. *J. Immunol.* **173:**3589–3593; 2004.
[26] Mahadev, K.; Motoshima, H.; Wu, X.; Ruddy, J. M.; Arnold, R. S.; Cheng, G. C.; Lambeth, J. D.; Goldstein, B. J. The NAD(P)H oxidase homolog Nox4 modulates insulin-stimulated generation of H_2O_2 and plays an integral role in insulin signal transduction. *Mol. Cell. Biol.* **24:**1844–1854; 2004.
[27] Gorin, Y.; Ricono, J. M.; Kim, N. H.; Bhandari, B.; Choudhury, G. G.; Abboud, H. E. Nox4 mediates angiotensin II-induced activation of Akt/protein kinase B in mesangial cells. *Am. J. Physiol. Renal Physiol.* **285:**F219–F229; 2003.
[28] Ammendola, R.; Ruocchio, M. R.; Chirico, G.; Russo, L.; De Felice, C.; Esposito, F.; Russo, T.; Cimino, F. Inhibition of NADH/NADPH oxidase affects signal transduction by growth factor receptors in normal fibroblasts. *Arch. Biochem. Biophys.* **397:** 253–257; 2002.
[29] Iaccio, A.; Collinet, C.; Montesano Gesualdi, N.; Ammendola, R. Protein kinase C-α and -δ are required for NADPH oxidase activation in WKYMVm-stimulated IMR90 human fibroblasts. *Arch. Biochem. Biophys.* **459:**288–294; 2007.
[30] Daub, H.; Wallasch, C.; Lankenau, A.; Herrlich, A.; Ullrich, A. Signal characteristics of G protein-transactivated EGF receptor. *EMBO J.* **23:**7032–7044; 1997.
[31] Knebel, A.; Rahmsdorf, H. J.; Ullrich, A.; Herrlich, A. Dephosphorylation of receptor tyrosine kinase as target of regulation by radiation, oxidants and alkylating agents. *EMBO J.* **15:**5314–5325; 1996.
[32] Zhong, Z.; Wen, Z.; Darnell Jr., J. E. Stat3: a STAT family member activated by tyrosine phosphorylation in response to epidermal growth factor and interleukin-6. *Science* **264:**95–98; 1994.
[33] Haura, E. B.; Turkson, J.; Jove, R. Mechanisms of diseases: insight into the emerging role of signal transducers and activators of transcription in cancer. *Nat. Clin. Pract. Oncol.* **2:**315–324; 2005.

[34] Levy, D. E.; Darnell Jr., J. E. Stats: transcriptional control and biological impact. *Nat. Rev. Mol. Cell Biol.* **3:**651–662; 2002.

[35] Lo, H.; Cheung, H.; Wong, Y. H. Constitutively active Galpha16 stimulates STAT3 via a c-Src/JAK and ERK-dependent mechanism. *J. Biol. Chem.* **278:**52154–52165; 2003.

[36] Liang, H.; Venema, V. J.; Wang, X.; Ju, H.; Venema, R. C.; Marrero, M. B. Regulation of angiotensin II-induced phosphorylation of STAT3 in vascular smooth muscle cells. *J. Biol. Chem.* **274:**19846–19851; 1999.

[37] Buggy, J. J. Binding of alpha-melanocyte-stimulating hormone to its G-protein-coupled receptor on B-lymphocytes activates the Jak/STAT pathway. *Biochem. J.* **331:**211–216; 1998.

[38] Jo, E. J.; Lee, H. Y.; Kim, J. I.; Kang, H. -K.; Lee, Y. -N.; Kwak, J. -Y.; Bae, Y. -S. Activation of formyl peptide receptor like-1 by WKYMVm induces serine phosphorylation of STAT3, which inhibits its tyrosine phosphorylation and nuclear translocation induced by hydrogen peroxide. *Life Sci.* **75:**2217–2232; 2004.

[39] Wu, E. H.; Lo, R. K.; Wong, Y. H. Regulation of STAT3 activity by G16-coupled receptors. *Biochem. Biophys. Res. Commun.* **303:**920–925; 2003.

[40] Bianco, C.; Tortora, G.; Bianco, R.; Caputo, R.; Veneziani, B. M.; Caputo, R.; Damiano, V.; Troiani, T.; Fontanini, G.; Raben, D.; Pepe, S.; Bianco, A. R.; Ciardiello, F. Enhancement of antitumor activity of ionizing radiation by combined treatment with the selective epidermal growth factor receptor-tyrosine kinase inhibitor ZD1839 (Iressa). *Clin. Cancer Res.* **8:**3250–3258; 2002.

[41] Han, Y. K.; Moon, H. J.; You, B. R.; Kim, S. Z.; Kim, S. H.; Park, W. H. The effects of N-acetyl cysteine on the MG132 proteasome inhibitor-treated lung cancer cells in relation to cell growth, reactive oxygen species and glutathione. *Int. J. Mol. Med.* **25:**657–662; 2010.

[42] Han, Y. K.; Moon, H. J.; You, B. R.; Kim, S. Z.; Kim, S. H.; Park, W. H. The effect of MAPK inhibitors on arsenic trioxide-treated CaLu-6 lung cells in relation to cell death, ROS and GSH levels. *Anticancer Res.* **29:**3837–3844; 2009.

[43] El-Benna, J.; Dang, P. M.; Gougerot-Pocidalo, M. A.; Marie, J. C.; Braut-Boucher, F. p47phox, the phagocyte NADPH oxidase/NOX2 organizer: structure, phosphorylation and implication in diseases. *Exp. Mol. Med.* **41:**217–225; 2009.

[44] Huang, J.; Hu, J.; Bian, X.; Chen, K.; Gong, W.; Dunlop, N. M.; Howard, O. M.; Wang, J. M. Transactivation of the epidermal growth factor receptor by formylpeptide receptor exacerbates the malignant behaviour of human glioblastoma cells. *Cancer Res.* **67:**906–5913; 2007.

[45] Zhou, Y.; Bian, X.; Le, Y.; Gong, W.; Hu, J.; Zhang, X.; Wang, L.; Iribarren, P.; Salcedo, R.; Howard, O. M.; Farrar, W.; Wang, J. M. Formylpeptide receptor FPR and the rapid growth of malignant human gliomas. *J. Natl. Cancer Inst.* **97:** 823–835; 2005.

[46] Yao, X. H.; Ping, Y. F.; Chen, J. H.; Chen, D. L.; Xu, C. P.; Zheng, J.; Wang, J. M.; Bian, X. W. Production of angiogenic factors by human glioblastoma cells following activation of the G-protein coupled formylpeptide receptor FPR. *J. Neurooncol* **86:** 47–53; 2008.

[47] Fischer, O. M.; Giordano, S.; Comoglio, P. M.; Ullrich, A. Reactive oxygen species mediate Met receptor transactivation by G protein-coupled receptors and the epidermal growth factor receptor in human carcinoma cells. *J. Biol. Chem.* **279:** 28970–28978; 2004.

[48] Catarzi, S.; Biagioni, C.; Giannoni, E.; Favilli, F.; Marcucci, T.; Iantomasi, T.; Vincenzini, M. T. Redox regulation of platelet-derived-growth-factor-receptor: role of NADPH oxidase and c-Src tyrosine kinase. *Biochim. Biophys. Acta* **1745:** 166–175; 2005.

[49] Bae, Y. S.; Kang, S. W.; Seo, M. S.; Baines, I. C.; Tekle, E.; Chock, P. B.; Rhee, S. G. Epidermal growth factor (EGF)-induced generation of hydrogen peroxide: role in EGF receptor-mediated tyrosine phosphorylation. *J. Biol. Chem.* **272:**217–221; 1997.

[50] Sundaresan, M.; Yu, Z. X.; Ferrans, V. J.; Irani, K.; Finkel, T. Requirement for generation of H_2O_2 for platelet-derived growth factor signal transduction. *Science* **270:**296–299; 1995.

[51] Fischer, O. M.; Hart, S.; Gschwind, A.; Ullrich, A. EGFR signal transactivation in cancer cells. *Biochem. Soc. Trans.* **31:**1203–1208; 2003.

[52] Shah, B. H.; Farshori, M. P.; Jambusaria, A.; Catt, K. J. Roles of Src and epidermal growth factor receptor transactivation in transient and sustained ERK1/2 responses to gonadotropin-releasing hormone receptor activation. *J. Biol. Chem.* **278:**10118–19126; 2003.

[53] Luttrell, L. M.; Della Rocca, G. J.; van Biesen, T.; Luttrell, D. K.; Lefkowitz, R. J. Gbetagamma subunits mediate Src-dependent phosphorylation of the epidermal growth factor receptor: a scaffold for G protein-coupled receptor-mediated Ras activation. *J. Biol. Chem.* **272:**4637–4644; 1997.

[54] Bokemeyer, D.; Schmitz, U.; Kramer, H. J. Angiotensin II-induced growth of vascular smooth muscle cells requires an Src-dependent activation of the epidermal growth factor receptor. *Kidney Int.* **58:**549–558; 2000.

[55] Slack, B. E. The m3 muscarinic acetylcholine receptor is coupled to mitogen-activated protein kinase via protein kinase C and epidermal growth factor receptor kinase. *Biochem. J.* **348:**381–387; 2000.

[56] Kam, A. Y.; Tse, T. T.; Kwan, D. H.; Wong, Y. H. Formyl peptide receptor like 1 differentially requires mitogen-activated protein kinases for the induction of glial fibrillary acidic protein and interleukin-alpha in human U87 astrocytoma cells. *Cell. Signal.* **19:**2106–2117; 2007.

[57] Nakashima, I.; Kato, M.; Akhand, A. A.; Suzuki, H.; Takeda, K.; Hossain, K.; Kawamoto, Y. Redox-linked signal transduction pathways for protein tyrosine kinase activation. *Antioxid. Redox Signal.* **4:**517–531; 2002.

[58] Bae, Y. S.; Lee, H. Y.; Jo, E. J.; Kim, J. I.; Kang, H. K.; Ye, R. D.; Kwak, J. Y.; Ryu, S. H. Identification of peptides that antagonize formyl peptide receptor-like 1-mediated signaling. *J. Immunol.* **173:**607–614; 2004.

[59] Silva, C. M. Role of STATs as downstream signal transducers in Src family kinase-mediated tumorigenesis. *Oncogene* **23:**8017–8023; 2004.

[60] D'Alessio, S.; Blasi, F. The urokinase receptor as an entertainer of signal transduction. *Front. Biosci.* **14:**4575–4587; 2009.

[61] Chung, J.; Uchida, E.; Grammer, T. C.; Blenis, J. STAT3 serine phosphorylation by ERK-dependent and -independent pathways negatively modulates its tyrosine phosphorylation. *Mol. Cell. Biol.* **17:**6508–6516; 1997.

[62] Newton, J. S. Angiotensin and epidermal growth factor receptor cross talk goes up and down. *J. Hypertens.* **20:**597–598; 2002.

[63] Zhao, Y.; He, D.; Saatian, B.; Watkins, T.; Spannhake, E. W.; Pyne, N. J.; Natarajan, V. Regulation of lysophosphatidic acid-induced epidermal growth factor receptor transactivation and interleukin-8 secretion in human bronchial epithelial cells by protein kinase Cdelta, Lyn kinase, and matrix metalloproteinases. *J. Biol. Chem.* **281:**19501–19511; 2006.

[64] Porcile, C.; Bajetto, A.; Barbieri, F.; Barbero, S.; Bonavia, R.; Biglieri, M.; Pirani, P.; Florio, T.; Schettini, G. Stromal cell-derived factor-1alpha (SDF-1alpha/CXCL12) stimulates ovarian cancer cell growth through the EGF receptor transactivation. *Exp. Cell Res.* **308:**241–253; 2005.

[65] Madarame, J.; Higashiyama, S.; Kiyota, H.; Madachi, A.; Toki, F.; Shimomura, T.; Tani, N.; Oishi, Y.; Matsuura, N. Transactivation of epidermal growth factor receptor after heparin-binding epidermal growth factor-like growth factor shedding in the migration of prostate cancer cells promoted by bombesin. *Prostate* **57:**187–195; 2003.

[66] Vaingankar, S. M.; Martins-Green, M. Thrombin activation of the 9E3/CEF4 chemokine involves tyrosine kinases including c-src and the epidermal growth factor receptor. *J. Biol. Chem.* **273:**5226–5234; 1998.

[67] Vacca, F.; Bagnato, A.; Catt, K. J.; Tecce, R. Transactivation of the epidermal growth factor receptor in endothelin-1-induced mitogenic signaling in human ovarian carcinoma cells. *Cancer Res.* **60:**5310–5317; 2000.

[68] Huang, J.; Chen, K.; Gong, W.; Zhou, Y.; Le, Y.; Bian, X.; Wang, J. M. Receptor "hijacking" by malignant glioma cells: a tactic for tumor progression. *Cancer Lett.* **267:**254–261; 2008.

[69] Prenzel, N.; Zwick, E.; Daub, H.; Leserer, M.; Abraham, R.; Wallasch, C.; Ullrich, A. EGF receptor transactivation by G-protein-coupled receptors requires metalloproteinase cleavage of proHB-EGF. *Nature* **402:**884–888; 1999.

[70] Lee, F. S.; Chao, M. V. Activation of Trk neurotrophin receptors in the absence of neurotrophins. *Proc. Natl Acad. Sci. U. S. A.* **98:**3555–3560; 2001.

[71] Tanimoto, T.; Jin, Z. G.; Berk, B. C. Transactivation of vascular endothelial growth factor (VEGF) receptor Flk-1/KDR is involved in sphingosine 1-phosphate-stimulated phosphorylation of Akt and endothelial nitric-oxide synthase (eNOS). *J. Biol. Chem.* **277:**42997–43001; 2002.

[72] Ushio-Fukai, M.; Griendling, K. K.; Becker, P. L.; Hilenski, L.; Halleran, S.; Alexander, R. W. Epidermal growth factor receptor transactivation by angiotensin II requires reactive oxygen species in vascular smooth muscle cells. *Arterioscler. Thromb. Vasc. Biol.* **21:**489–495; 2001.

[73] Saito, Y.; Berk, B. C. Transactivation: a novel signaling pathway from angiotensin II to tyrosine kinase receptors. *J. Mol. Cell. Cardiol.* **33:**3–7; 2001.

[74] Rhee, S. G.; Kang, S. W.; Jeong, W.; Chang, T. S.; Yang, K.; Woo, H. A. Intracellular messenger function of hydrogen peroxide and its regulation by peroxiredoxins. *Curr. Opin. Cell Biol.* **17:**183–189; 2005.

[75] Lambeth, J. D. NOX enzymes and the biology of reactive oxygen. *Nat. Rev. Immunol.* **4:**181–189; 2004.

[76] Lassègue, B.; Clempus, R. E. Vascular NAD(P)H oxidases: specific features, expression, and regulation. *Am. J. Physiol. Regul. Integr. Comp. Physiol.* **285:**R277–R297; 2003.

[77] Lambeth, J. D. Nox enzymes, ROS, and chronic disease: an example of antagonistic pleiotropy. *Free Radic. Biol. Med.* **43:**332–347; 2007.

[78] Oakley, F. D.; Abbott, D.; Li, Q.; Engelhardt, J. F. Signaling components of redox active endosomes: the redoxosomes. *Antioxid. Redox Signal.* **11:**1313–1333; 2009.

[79] Gianni, D.; Bohl, B.; Courtneidge, S. A.; Bokoch, G. M. The involvement of the tyrosine kinase c-Src in the regulation of reactive oxygen species generation mediated by NADPH oxidase-1. *Mol. Biol. Cell* **19:**2984–2994; 2008.

[80] Kim, H.; Park, J. H.; Lee, E. -H.; Kim, M. -J.; Park, S. K.; Heo, S. -K.; Kim, B. -S.; Min, Y. J. Granulocyte function is stimulated by a novel hexapeptide, WKYMVm, in chemotherapy-treated cancer patients. *Exp. Hematol.* **34:**407–413; 2006.

[81] Lin, C.; Wei, W.; Zhang, J.; Liu, S.; Liu, Y.; Zheng, D. Formyl peptide receptor-like 1-mediated endogenous *TRAIL* gene expression with tumoricidal activity. *Mol. Cancer Ther.* **6:**2618–2625; 2007.

[82] Kim, S. D.; Kim, Y. K.; Lee, H. Y.; Kim, Y. S.; Jeon, S. G.; Baek, S. H.; Song, D. K.; Ryu, S. H.; Bae, Y. S. The agonists of formyl peptide receptors prevent development of severe sepsis after microbial infection. *J. Immunol.* **185:**4302–4310; 2010.

[83] Li, B. Q.; Wetzel, M. A.; Mikovits, J. A.; Henderson, E. E.; Rogers, T. J.; Gong, W.; Le, Y.; Ruscetti, F. W.; Wang, J. M. The synthetic peptide WKYMVm attenuates the function of the chemokine receptors CCR5 and CXCR4 through activation of formyl peptide receptor-like 1. *Blood* **97:**2941–2947; 2001.

[84] Gavins, F. N. Are formyl peptide receptors novel targets for therapeutic intervention in ischaemia–reperfusion injury? *Trends Pharmacol. Sci.* **31:** 266–276; 2010.

[85] Le, Y.; Yang, Y.; Cui, Y.; Yazawa, H.; Gong, W.; Qiu, C.; Wang, J. M. Receptors for chemotactic formyl peptides as pharmacological targets. *Int. Immunopharmacol.* **2:** 1–13; 2002.

[86] Zhou, C.; Zhang, S.; Nanamori, M.; Zhang, Y.; Liu, Q.; Li, N.; Sun, M.; Tian, J.; Ye, P. P.; Cheng, N.; Ye, R. D.; Wang, M. W. Pharmacological characterization of a novel nonpeptide antagonist for formyl peptide receptor-like 1. *Mol. Pharmacol.* **72:**976–983; 2007.

[87] Huang, J.; Chen, K.; Chen, J.; Gong, W.; Dunlop, N. M.; Howard, O. M.; Gao, Y.; Bian, X. W.; Wang, J. M. The G-protein-coupled formylpeptide receptor FPR confers a more invasive phenotype on human glioblastoma cells. *Br. J. Cancer* **102:** 1052–1060; 2010.

Neurochem Res (2010) 35:2018–2026
DOI 10.1007/s11064-010-0301-5

ORIGINAL PAPER

Expression and Signaling of Formyl-Peptide Receptors in the Brain

Fabio Cattaneo · Germano Guerra · Rosario Ammendola

Accepted: 14 October 2010 / Published online: 2 November 2010

Abstract The human formyl-peptide receptor (FPR) and its variants FPRL1 and FPRL2 belong to the G-protein coupled seven transmembrane receptor (GPCR) family sensitive to pertussis toxin. FPR and FPRL1 were first detected in phagocytic leukocytes, and FPRL2 was found in monocytes and in dendritic cells. The three receptors were subsequently identified in other cell types or tissues, including neuronal cells and brain, where FPR and FPRL1 play a key role in angiogenesis, cell proliferation, protection against and cell death, as well as in neuroendocrine functions. Binding of different agonists to FPRs triggers several signaling pathways, activates NFkB and STAT3 transcriptional factors and induces the accumulation of the CDK inhibitors $p21^{waf1/cip1}$, $p16^{INK4}$ and $p27^{kip1}$. Signaling molecules, such as ERKs, JNK, PKC, p38MAPK, PLC and PLD are involved in these intracellular cascades. In this article we briefly review FPRs expression and signaling in neuronal cells.

Keywords Formyl-peptides receptors · Signal transduction · Cell cycle · Neuronal cells · Inhibitors of cyclins/CDK complexes

Special issue article in honor of Prof. Abel Lajtha.

F. Cattaneo · R. Ammendola (✉)
Dipartimento di Biochimica e Biotecnologie Mediche, Università degli Studi di Napoli Federico II, Via S. Pansini 5, 80131 Naples, Italy
e-mail: rosario.ammendola@unina.it

G. Guerra
Dipartimento di Scienze per la Salute, Università degli Studi del Molise, Località Tappino, 86100 Campobasso, Italy

Introduction

From an evolutionary perspective, the formyl-peptide receptors family has a complex history and the number of family members varies significantly between species. In human there are three genes encoding two functional receptors, FPR (formyl-peptide receptor) and FPRL1 (formyl-peptide receptor-like 1), and the putative receptor FPRL2 (formyl-peptide receptor-like 2) which encodes a putative protein with 56% amino acid sequence identity to human FPR and 83% to FPRL1 [1–3]. Although a number of functional studies of FPRs were performed by using neutrophils and monocytes, the expression of these receptors have been demonstrated in other cell types. For instance, epithelial cells, follicular cells of the thyroid, cortical cells of adrenal, hepatocytes, Kupffer cells, neurons, astrocytoma cell lines, A549 cells, brain and nervous sytem express either or/and both FPR or/and FPRL1 [4–8].

The important biological implications of FPRs in neuronal cells and tissue are illustrated by the identification of host-derived agonists that are associated with various pathophysiological settings. These agonists include β-amyloid peptide (Aβ42) [9], the prion protein fragment $PrP_{106–126}$ [10], humanin [11] and annexin I (ANXA1) [12]. All these molecules elicit pro-inflammatory responses through the use of FPRL1 as a receptor. Aβ42 and $PrP_{106–126}$ are amyloidogenic and are involved in Alzheimer's disease (AD) [13] and prion diseases [10, 14], respectively. FPRL1 has also reported to interact with a lipid metabolite lipoxin A4 (LXA4) in neuronal cells [15], showing an inhibitory effect on the expression of pro-inflammatory chemokines.

Binding to FPRs of these agonists triggers intracellular signaling cascades involved in the regulation of angiogenesis, cell proliferation, protection against apotosis and neuroendocrine functions, such as the inhibition of the

exocytosis. Unlike FPR, the signal transduction pathways mediated by FPRL1 have not been extensively studied. Following activation by ligand, FPRs undergo rapid serine and threonine phosphorylation, and are desensitized and internalized [16, 17]. However, FPRs internalization can occur in the absence of internalization, indicating that desensitization and internalization are controlled by distinct mechanisms [18, 19]. Further studies suggest that FPRs internalization is mediated by mechanisms independent by arrestin, dynamin and clathrin [20].

Recent findings have demonstrated a central role of FPRs also in the regulation of cell cycle in different cell types [20–26]. These receptors act by increasing protein levels of some inhibitors of cyclins/CDK complexes (CKI), such as $p21^{waf1/cip1}$ and $p16^{INK4A}$ and $p27^{kip1}$, in parallel with the inhibition of the expression of cyclins. Here we review and discuss some of the most significant results on: (i) the expression of FPRs in neuronal cells and tissues; (ii) the intracellular signaling triggered by these receptors; (iii) the control of the cell cycle progression exerted by some members of the FPR family.

Formyl-Peptide Receptors

The formyl-peptide receptors FPR, FPRL1 and FPRL2, expressed in human cells, belong to the G protein-coupled receptor (GPCR) family [1]. The FPR gene spans 6 kb with an intronless open reading frame interrupted by an intron in its 5'-untranslated region [27]. Both FPRL1 and FPRL2 are single-copy genes with intronless open reading frames, which co-localize with FPR in a cluster on the chromosomal region 19q13.3 [1]. FPR and FPRL1 were first detected in phagocytic leukocytes, and FPRL2 was first found in monocytes and in dendritic cells [28].

The murine FPR gene family includes at least six members: Fpr1 (mFPR1) codes for the murine orthologue of human FPR; Fpr-rs2 and Fpr-rs1 encode receptors that are strucurally and functionally similar to human FPRL1 [29]: Fpr-rs2 encodes mFPR2, which is a N-formyl-Met-Leu-Phe (N-fMLP) receptor, whereas the product of murine gene Fpr-rs1 is a receptor for lipoxin A4 (LXA4), a lipid derivative of arachidonate metabolism [30]. The other murine FPRs encode putative receptors which ligands have not been yet identified.

FPR binds N-fMLP with high efficiency, whereas FPRL1 is defined as a low-affinity N-fMLP receptor, based on its activation only by micromolecolar concentrations of formyl-peptide. FPRL1 is the only receptor whose ligands include both a formyl-peptide and a lipid, as demonstrated by the observation that it also binds LXA4 [31]. FPRL2 does not respond to formyl-peptides and it was reported to be a low affinity receptor for several FPRL1 agonists [32].

In addition to N-fMLP, several non-formylated peptides, that preferentially activate either or both FPR and FPRL1, have been identified. For instance, the synthetic hexapeptide WKYMVm (W peptide) binds FPRL1 with high efficiency, activating neutrophils and monocytes functions including chemotaxis, mobilization of complement receptor-3, cytokines release and NADPH oxidase activation [33]. We demonstrated that in IMR90 human fibroblasts, binding of WKYMVm to FPRL1, which is expressed in these cells [34], induces superoxide generation consequent to MEK- and PTX-dependent serine phosphorylation and membrane translocation of the regulatory cytosolic NADPH oxidase subunit $p47^{phox}$ [34]. In the same cells WKYMVm activates also selected protein kinase C (PKC) isoforms required for NADPH oxidase-dependent superoxide generation [35].

MMK-1, another non-formylated peptide, is a potent and very specific agonist for FPRL1, as demonstrated by its ability to induce superoxide generation in neutrophils [36] and calcium mobilization in phagocytic leukocytes [37].

In addition to exogenous agonists, many findings have been focused to identify host-derived molecules that interact with formyl-peptide receptors. A clear evidence of an endogenous agonist for FPR is represented by ANXA1 and its N-terminal domains, which specifically and significantly interfere with neutrophil transmigration [38]. Nevertheless, FPRL1 seems to interact with a greater number of host-derived agonists, including the acute-phase protein serum amloid A (SAA) [39], the 42-amino acid form of amyloid β (Aβ42) [9], the prion protein fragment $PrP_{106–126}$, [10], LXA4 [31], and LL-37, an enzymatic cleavage fragment of the cathelicidin [40]. We demonstrated that in IMR90 cells LL-37 triggers FPRL1-mediated induction of superoxide, via NADPH oxidase activation [41]. Finally, humanin, a 14–22 peptide encoded by a gene isolated from an apparently normal region from Alzheimer's disease (AD) brain, shares FPRL1 with Aβ42 on neuronal cells [11].

Formyl-Peptide Receptors Activation

FPR, FPRL1 and FPRL2 are coupled to the Gi family of G proteins, as indicated by the total loss of cell response to their agonists upon exposure to pertussis toxin (PTX) [42, 43]. FPR can also couple to G_o, $G_{\alpha 16}$ and to PTX-resistant G_z [44].

In polymorphonuclear (PMN) cells, binding of N-fMLP to FPR or FPRL1 induces an intracellular complex program that results in cell migration, reorganization of the actin cytoskeleton and NADPH oxidase activation, thereby triggering signal transduction pathways leading to a chemotactic response and superoxide generation, respectively.

After N-fMLP binding, activated heterotrimeric G-protein dissociates into α and $\beta\gamma$ subunits, thereby activating phospholipase C (PLC) and phosphoinositide 3-kinase (PI3K). This, in turn, converts the membrane phosphatidylinositol 4,5-bisphosphate (PIP2) into phosphatidylinositol 3,4,5-triphosphate (PIP3). PLC converts PIP3 in diacylglycerol (DAG) and inositol-1,4,5-triphosphate (IP3), which regulates calcium mobilization from endoplasmic reticulum stores. DAG activates PKC isoforms. PI3K (γ isoform) can also triggers the activation of the PI3K-Akt/PKB pathway. In PMN cells other intracellular effectors coupled to the signaling cascade of FPRs include phospholipases A2 and D (PLD), ERK1/2, lyn, p125FAK, Jun kinase (JNK) and p38MAPK. PKC isoforms, ERKs and p38MAPK are involved in the phosphorylation on multiple serine residues of the regulatory subunit $p47^{phox}$ of NADPH oxidase in vivo and in vitro [45]. CD38, a transmembrane glycoprotein which catalyzes the production of cyclic ADP-ribose from its substrate NAD^+, is an essential and specific transducer of N-fMLP signals in mouse neutrophils, as demonstrated by the observation that neutrophils from $CD38^{-/-}$ mice fail to migrate in response to N-fMLP [46].

Fprs Expression in Neuronal Tissues and Cells

The observation that FPR and FPRL1 have been identified in several other cell types and tissues suggests that they exert functions other than those exerted in PMN cells, probably elicited by endogenous ligands associated with human diseases.

By using immunocytochemical approaches, FPR was detected in human brain, spinal cord, anterior horn cells and hypoglossal nucleus neurons [4]. Cerebellar system, the neuropil, the sensory system, many large reticular activating system neurons, choroid plexus epithelium, ependyma, and vascular smooth muscle stained intensively. Many pyramidal cell neurons, the extrapyramidal motor system, the sympathetic portion of the autonomic nervous system, the parasympathetic system, the hippocampal neurons, many end-plate pyramidal cells, some astrocytes and pial astrocytes moderately stained with the antibody [4]. Schwann cells of the peripheral nervous system stained positively but the oligodendrocytes were negative. Interestingly, FPR antigen was not detectable in microglia, the modified macrophages of the brain [4].

By conducting a high throghput screen for GPCR expressed in mouse vomeronasal organ (VNO), which detects pheromones and other semiochemicals, 5 of 7 members of the FPR family, have been recently identified [47]. The expression patterns of the VNO-FPRs are remarkable similar to those of V1Rs and V2Rs, the two known families of chemoreceptors. Each FPR is selectively expressed in a different small subset of neurons that are highly dispersed in the neuroepithelium, consistently express $G_{\alpha i2}$ or G_0, and appear to lack other chemosensory receptors [47]. These finding suggest that VNO-FPRs are likely to function as chemosensory receptors, probably associated with the identification of pathogens, or of pathogenic states [48].

By RT-PCR analysis, mRNAs for three FPR family members, Fpr1, Fpr-rs1 and Fpr-rs2, have been identified in the mouse hippocampus, hypothalamus, anterior pituitary and adrenal gland [12]. In addition, the hypothalamus and anterior pituitary gland also express Fpr-rs6 and Fpr-rs7 mRNAs [12]. These receptors play a key role in the regulation of neuroendocrine functions mediated by ANXA1. In the pituitary gland, ANXA1 has a well defined role as a cell–cell mediator of the inhibitory effects of glucocorticoids (GC) on the secretion of corticotropin (ACTH). ANXA1 inhibits the evoked release of ACTH and this effect is mediated by Fpr-rs1 or by a closely related receptor [12]. In the mouse brain, which expresses Fpr-rs2, ANXA1 or a short ANXA1 petidomimetic ($Ac_{2–26}$) exert significant protection in the microcirculation [49]. The ANXA1-mediated cerebroprotection is associated with a marked attenuation of cell adhesion and of markers of inflammation. $Ac_{2–26}$ acts by binding Fpr-rs2, as demonstrated by displacement assays with transfected cells, in vivo experiments with transgenic mice and receptor agonists [49].

The 1321N1 human astrocyte cell line expresses a functional FPRL1 both at mRNA and protein level [15]. In these cells, LXA4, which efficiently binds FPRL1 [31], has an inhibitory effect on the expression of the proinflammatory chemokine IL-8 and adhesion molecule ICAM-1 in response to IL-1β [15]. LXA4 also regulates proliferation and differentiation of murine neural stem cells (NSC) isolated by embryo brains [26]. These cells express Fpr-rs2 and LXA4 signaling triggered by this receptor appears to tightly regulate the expansion and contraction of NSC mass by acting as "accelerator and brake" after pathological events in brain tissue [26]. These results suggest the potential therapeutic utility of LXA4 for a wide range of neuropathological disorders, wherein specifically regulating neurogenesis and neuroinflammation may be beneficial.

FPRL1 is expressed at high levels by inflammatory cells infiltrating senil plaques in brain tissues of AD patients [9], where Aβ42 can induce NADPH oxidase-dependent superoxide production via FPRL1, thus generating an oxidative stress in microglial cells [50]. The internalization of Aβ42 is mediated by FPRL1 and requires PLD in the endocytosis process [51]. By co-immunoprecipitation and fluorescence microscopy, a physical interaction between FPRL1 and MARCO (macrophage receptor with

collagenous structure) has been observed in astrocytes and in microglia [52]. The expression of FPRL1-MARCO complex increases in glial cells playing an important role for binding at cell surface and subsequent internalization of Aβ42 [52]. Stimulation of microglial cell line N9 with IFN-γ induces the expression of high levels of mFPR2 in association with increased cell migration in response to Aβ42 [53]. IFN-γ also increases the endocytosis of Aβ42 by microglial cells via mFPR2 [53]. Furthermore, an Aβ42 conformation-dependent mFPR2 overexpression is observed in mouse primary microglial cells and in murine microglial cell line MMGT12 [54]. This suggests that FPRs expression is not only constitutive but can be also induced by specific agonists.

Humanin was originally identified as an anti-apoptotic peptide that rescued neuronal cells from apoptosis induced by presenilin mutants associated with familial AD and by Aβ42 [55]. The human neuroblastoma cell lines SK-N-MC and SK-N-SK, and the mouse microglial cell line N9 express FPRL1 and the murine orthologue mFPR2, respectively [11]. In these cells the protective effect of humanin from damage by Aβ42 requires the PTX-sensitive activation of FPRL1, which is a functional receptor shared by humanin and Aβ42 [11]. Therefore, the neuroprotective activity of humanin may be attributed to its competitive occupation of FPRL1.

FPRL1 is also involved in proinflammatory processes of prion disorders which, similar to AD, include the infiltration and activation of mononuclear phagocytes in brain lesions. The 21 aminoacid fragment of the aberrant human prion protein, $PrP_{106–126}$ can form fibrils in vitro and elicits a diverse array of inflammatory responses. $PrP_{106–126}$ is an agonist for FPRL1 in glial cells [10] and induces an increase of proinflammatory cytokines, tumor necrosis factor-α and IL-6, which are implicated as neurotoxic mediators. Also in this case, PLD activity is essential for $PrP_{106–126}$-endocytosis [56] and, similar to Aβ42, in astrocytes and microglia the internalization of $PrP_{106–126}$ is mediated by FPRL1 [56]. The identification of FPRL1 as a functional receptor for Aβ42 and $PrP_{106–126}$ provides a molecular link in the chain of proinflammatory responses observed in AD and in prion diseases.

Fprs Signaling in Neuronal Tissues and Cells

In neuronal cells, binding of different agonists to FPRs triggers multiple intracellular signaling pathways necessary to regulate important biological functions. The possible involvement of FPRL1 in the regulation of astrocytosis has major biological implications, because reactive astrocytosis and brain inflammation are pathological features of many neurodegenerative diseases.

A linkage among FPRL1, MAPK, astrocytes activation and the inflammatory response has been described in U-87 cells, where the activation of FPRL1 with the highly potent agonist WKYMVm induces JNK and ERKs phosphorylation [57]. FPRL1-evoked MAPK activation depends on $G_{i/0}$ proteins and Src family tyrosine kinase activation, but is independent of PI3K and PKC. Interestingly, stimulation of FPRL1 in these cells augments the expression of glial fibrillary acidic protein (GFAP) and IL-1α, which are correlated with reactive astrocytosis [57]. Moreover, inhibition of $G_{i/0}$ proteins and JNK completely abolishes both GFAP and IL-1α up-regulations by FPRL1, while blockade of the MEK/ERK cascade exclusively suppress the GFAP production [57]. In the same cells, WKYMVm also promotes $G_{i/0}$-dependent IKK (inhibitor kB kinase) phosphorylation. This requires ERKs, PI3K and cSrc activations, but not p38MAPK, JNK or calcium mobilization [58]. PI3K activates PKB/Akt which, in turn, induces the transcriptional function of NFkB by stimulating the transactivation of RelA/p65 subunit. In U-87 cells a FPRL1-dependent NFkB-driven luciferase expression is observed [58]. Interestingly, cholesterol depletion abolishes IKK phosphorylation, denoting the important role of lipid raft integrity in the FPRL1/IKK signaling [58]. In N-fMLP- stimulated U-87 cells, the activation of signaling molecules triggered by FPR, including ERKs, p38MAPK, JNK and Akt are significantly attenuated by the lipoxygenase inhibitor Nordy [59].

The role of FPRL1 in regulating immune responses is further suggested by the observation that, in 1321N1 astrocytoma cells, LXA4 exerts anti-inflammatory effects, at least in part, via an NFkB-dependent mechanism [15]. In fact, LXA4 inhibits IL-1β-induced degradation of IkBβ and modulates IL-1β activation of NFkB-regulated reporter gene expression via FPRL1 [15].

FPRs have been also implicated in the cellular signaling regulating neuroendocrine functions. In the hypothalamo-pituitary-adrenocortical axis, ANXA1 induces the inibition of corticotrophin-release hormone (CRH)-driven ACTH secretion [60]. The signaling mechanisms used by FPRL1, the ANXA1 receptor, impinge on the CRH-driven prosecretory cascade at a late stage, compromising the SNARE proteins interaction which is critical to exocytosis [60]. At least three molecular mechanisms have been suggested for the neuroendocrine regulation of FPRL1: (i) ANXA1 activates PTX-sensitive and $G_{\alpha 1}$-mediated activation of PLC, increased intracellular calcium concentration and PLD activation; (ii) FPRL1 may couple also to G_z protein which signaling induces a long-lasting blockade of exocytosis in pituitary cells; (iii) FPRL1 signals via $\beta\gamma$ G proteins to impair exocytosis [61].

Signal transduction pathways triggered by FPRs play a key role in neurodegenerative disorders. In rat glial cells

PLD activity is essential for Aβ42 endocytosis and is required for Aβ42-induced ERKs phosphorylation [54]. The central role of ERKs in FPRL1 signaling is further supported by the observation that, in murine microglial cells, Aβ42-induced signal transduction strongly depends on phosphorylation mechanisms mediated by MAPK and that FPRL1 deactivation by antagonists or by siRNA inhibits Aβ42-induced ERKs phosphorylation [52]. The neuroprotective effect of humanin on Aβ42 requires the FPRL1-mediated activation of STAT3 transcription factor and of several tyrosine kinases [62].

FPRs signaling also partecipate in the progression of malignant tumors. In human glioblastoma cell lines U-87 and SNB75, which express FPR [63], N-fMLP induces a rapid and transient phosphorylation of ERKs, JNK, p38MAPK and Akt, as well as of STAT3 both at Tyr705 and Ser 727 residues [63]. N-fMLP-treated cells also show elevated levels of VEGF protein secreted in the medium, augmented DNA synthesis and higher levels of Bcl2. These finding suggest a contribute of FPR to glioma cell motility, proliferation and tumorigenicity. The role of FPR in these events is further supported by its ability to transactivate the Epidermal Growth Factor Receptor (EGFR), exacerbating the malignant behaviour of human glioma cells [64, 65]. In these cells N-fMLP induces PTX-sensitive EGFR phosphorylation at Tyr992 residue which is prevented by a Src tyrosine kinase inhibitor, suggesting that cSrc plays a key role in bridging the signal transduction from FPR to EGFR. These results strongly indicate that both FPR and EGFR play important roles in tumor cell growth and tumorigenesis, and that the two receptors cooperate to potentiate the proliferation of glioblastoma cells. Furthermore, the potential therapeutical implications of these findings suggest that targeting both receptors may yeld superior therapeutic effects compared with targetin either one receptor.

FPRs and Cell Cycle

Many evidences suggest that binding of specific agonists to FPRs inhibit proliferation in different cell lines. LXA4 prevents cell growth of renal mesangial cells induced by leukotriene D4 (LTD4) or platelet-derived growth factor [21]. LXA4 blocks LTD4-induced PI3K activity and triggers MEK1/ERK pathway, through which inhibition of cell proliferation is effected [21, 22].

The inhibitory effects of LXA4 on cell cycle have been also observed in human lung fibroblasts (HLF) stimulated by connective tissue growth factor (CTGF) [23]. In these cells, which express FPRL1, LXA4 supresses CTGF-stimulated phosphorylation of PI3K and PKB/Akt, modulates CTGF-activated phosphorylation of ERKs, down-regulates CTGF-evoked DNA-binding activity of STAT3 and inhibits the expression of cyclin D1. Pretreatment with PTX prevents, and over-expression of FPRL1 enhances, the inhibitory effects of LXA4 on CTGF-induced proliferation of HLF, suggesting that FPRL1 mediates the action of LXA4 on these cells [23].

A similar effect was observed in rat mesangial cells stimulated with TNFα [24]. Here, the TNFα-induced marked increments in mRNA expression and protein synthesis of cyclin E, in parallel with cell proliferation, are down-regulated by LXA4. TNFα also enhances DNA-binding activity of STAT3 and induces PKB/Akt phosphorylation at Thr308 residue, which are prevented by LXA4. Furthermore, TNFα-induced decrement in expression of $p27^{kip1}$ is ameliorated by LXA4 in a dose-dependent manner [24]. The LXA4-mediated accumulation of CDK inhibitors (CKIs) is also observed in human mesangial cells, where LXA4 significantly inhibits PDGF-stimulated proliferation [25]. In these cells lipoxins modulate PDGF-induced decrements in the levels of $p27^{kip1}$ and $p21^{waf1/cip1}$, and promotes nuclear retention of these CKIs [25].

The LXA4–induced signaling pathway also inhibits cell growth of neural stem cells [26]. LXA4-mediated alterations in cell proliferation include several molecules involved in cell cycle and growth, such as EGFR and cyclin E, which are down-regulated, and $p27^{kip1}$, which protein levels are increased [26].

We observed that the exposure to N-fMLP of human glioblastoma cell line U-87, induces $p21^{waf1/cip1}$ and $p16^{INK4}$ accumulation in a time-dependent manner (Fig. 1a). $p21^{waf1/cip1}$ has been shown to have bimodal effects on cell cycle progression and cell proliferation. In fact, $p21^{waf1/cip1}$ inhibitory activity is associated with nuclear localization, whereas cytosolic $p21^{waf1/cip1}$ increases cell cycle transit [66]. Therefore, we investigated its localization and we found that N-fMLP-induced $p21^{waf1/cip1}$ accumulation is predominantly nuclear, thus suggesting its involvement in cell cycle arrest (Fig. 1b). In several cell types the increased protein level of $p21^{waf1/cip1}$ is independent of p53 and is the consequence of the activation of Ras-ERK pathway [67]. Furthermore, many evidences demonstrate that the exposure of cells to oxidants results in the activation of the Ras-MAPK pathway. This effect is reversible, is prevented by antioxidants and is very similar to that provoked by the exposure of resting cells to growth factors [68]. We observed that, in U-87 cells N-fMLP induces ERKs phosphorylation, which is inhibited by the MEK inhibitor PD098059 (Fig. 2a) and by pre-incubation with apocynin, which prevents the translocation of $p47^{phox}$ on the membrane inhibiting the NADPH oxidase complex in phagocytic and non-phagocytic cells [69, 70] (Fig. 2a). The N-fMLP-induced $p21^{waf1/cip1}$ accumulation observed in U-87 cells is also prevented by PD098059 and apocynin

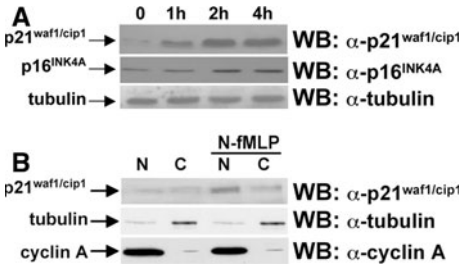

Fig. 1 N-fMLP induces CKIs accumulation. (**a**) U-87 cells (ATCC, Manassas VA) were exposed to 1 μM N-fMLP (PRIMM, Milan, Italy) for the indicated times. Cells were rinsed with phosphate-buffered saline (PBS) buffer and cell lysates were purified as previously described [34]. Protein extracts, containing 20 μg of proteins, were resolved on 10% SDS–PAGE (Bio-Rad, Richmond, CA, USA) and $p21^{waf/cip}$ and $p16^{INK4}$ were detected by using specific antibodies (Santa Cruz Biotechnology Inc, Santa Cruz, CA, USA, sc-397 and sc-65224, respectively). The same filter was reprobed with an anti-tubulin antibody (Santa Cruz Biotechnology Inc, Santa Cruz, CA, USA, sc-8035). (**b**) Cells were exposed to PBS or to 1 μM N-fMLP for 2 h and Nuclear (*N*) and cytosolic (*C*) proteins were purified by using the Nuclear/Cytosol Fractionation kit (BioVision, Inc., USA), accordingly to manufacturer's instructions. Proteins (20 μg) were resolved on 10% SDS–PAGE and subjected to immunoblotting analysis with an anti-$p21^{waf/cip}$ antibody, as previously described [34]. An anti-tubulin antibody and anti-cyclin A antibody (Santa Cruz Biotechnology Inc, Santa Cruz, CA, USA, sc-751) served as a control of cytosolic and nuclear proteins loading, respectively. Antigen–antibody complexes were detected with an ECL chemiluminescence reagent kit (Amersham Pharmacia Biotech, Little Chalfont, Buckinghamshire, UK)

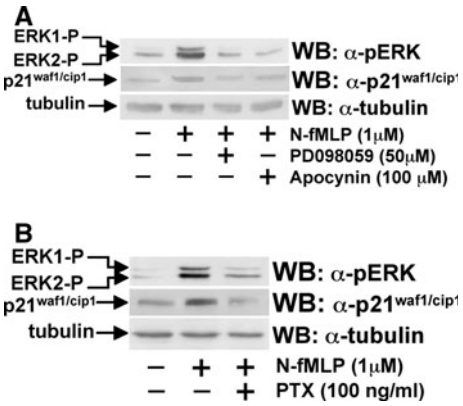

Fig. 2 N-fMLP-induced $p21^{waf/cip}$ accumulation is prevented by PD098059 and Apocynin and is mediated by FPR. (**a**) Cell lysates were purified from U-87 cells exposed to 1 μM N-fMLP for 2 h, or preincubated with 50 mM PD098059 for 90 min (Calbiochem, La Jolla, CA, USA), or with 100 mM Apocynin (Sigma, St. Louis, MO, USA) for 2 h, before stimulation. Twenty micrograms of proteins were resolved on 10% SDS–PAGE and ERKs phosphorylation and $p21^{waf/cip}$ accumulation were detected by western blot with an anti-phosphoERKs (a-pERK, Santa Cruz Biotechnology Inc, Santa Cruz, CA, USA, sc-7383) or an anti-$p21^{waf/cip}$ antibody, respectively. The same filter was reprobed with an anti-tubulin antibody, as a control of protein loading. (**b**) U-87 cells were exposed to 1 μM N-fMLP for 2 h, or preincubated with 100 ng/ml of pertussis toxin (PTX) (Sigma, St. Louis, MO, USA) for 12 h before stimulation. Total proteins (20 μg) were electrophoresed and transferred to immobilion P membranes (Millipore, Bedford, MA). The blot was incubated with an anti-phosphoERKs antibody or an anti-$p21^{waf/cip}$ antibody. An anti-tubulin antibody served as a control of protein loading. The arrows indicate the phosphorylated forms of $p44^{MAPK}$ (ERK1-P) and $p42^{MAPK}$ (ERK2-P), respectively

(Fig. 2a), suggesting that it requires the activation of MEK-ERK cascade and NADPH oxidase-dependent superoxide generation. We also examined the role of FPR in the N-fMLP-induced signalling cascade and we found that preincubation with PTX prevents both ERKs phosphorylation and $p21^{waf1/cip1}$ accumulation, as a consequence of the $G_{\alpha i}$-specific inhibition (Fig. 2b). Taken together our results suggest that in U-87 cells binding of a specific agonist to FPR inhibits cell cycle progression through increased protein levels of $p16^{INK4}$ and PTX-, NADPH oxidase- and MEK-dependent accumulation of $p21^{waf1/cip1}$.

Future Directions

During recent years, much progress has been made in the understanding of the biological roles played by formyl-peptide receptors in the brain and in neuronal cells. FPRs family has complex functional properties, partly due to their high promiscuity, but also because their activation can stimulate several signal transduction pathways depending on the ligand, its concentration and the cell type involved. FPR and FPRL1 can be activated by a wide variety of unrelated ligands that can be also generated during pathological conditions, and respond to synthetic ligands which are very useful for pharmacological studies. In particular, the use of FPRL1 by SAA, Aβ42 and $PrP_{106–126}$ suggests that this receptor may play a crucial role in pro-inflammatory aspects of systemic amyloidosis, AD and prion diseases. On the other hand, LXA4 shows inhibitory effect on the expression of pro-inflammatory chemokines via FPRL1 and may represents a strategy in the treatment of acute and chronic brain inflammation. Future research will need to address the issue of how the same receptor can bind such structurally diverse ligands, ranging from small peptides to large proteins to lipids. The understanding of the molecular mechanisms of interaction and whether the various ligands bind by shared or unique domains, is the assumption for the development of specific antagonists. The role of FPRs in the definition of different biological responses, including the FPRL1-mediated neuroendocrine responses to bacterial/viral infections and to locally generated anti-inflammatory eicosanoids (e.g., lipoxins) requires further investigations.

Further study is also required to define the relationship between the FPR expression and the progression of human primary gliomas and to identify the mechanicistic basis for the control of FPR expression in highly malignant human

glioma cells. Nevertheless, FPR and its signaling pathway may be candidate molecular target for developing novel therapeutics to treat gliomas, including the specific blockade of EGFR signaling depending on FPR transactivation by agonist. Such pharmacological strategies presumably produce less pronunced side effects than approaches based on direct EGFR inhibition by antagonists or tyrosine kinase inhibitors.

Binding of specific agonists to FPRs triggers several intracellular signaling cascades in neuronal cells, including PI3K-Akt, Ras-ERK, PKC and STAT pathways which play key role in angiogenesis, cell proliferation, protection against cell death and in the tight regulation of NADPH oxidase activity. The complete dissection of the intracellular signaling pathways triggered by different agonists will clarify the role of formyl-peptide receptors in neuronal cells in both human physiology and disease.

Acknowledgments We are greatful to the eminent scientist Prof. Abel Lajtha for being founder and Editor in Chief of Neurochemical Research, now in its 34th year. This work was supported by grants from Ministero dell'Università e della Ricerca Scientifica e Tecnologica PRIN 2007 "Attivazione dei recettori per formil-peptidi e regolazione della NADPH ossidasi in linee cellulari tumorali umane non fagocitiche". We thank Jean Ann Gilder (Scientific Communication srl) for text editing.

References

1. Bao L, Gerard NP, Eddy RL Jr et al (1992) Mapping of genes for the human C5a receptor (C5AR), human FMLP receptor (FPR), and two FMLP receptor homologue orphan receptors (FPRH1, FPRH2) to chromosome 19. Genomics 13:437–440
2. Murphy PM, Ozcelik T, Kennedy RT et al (1992) A structural homologous of the N-formyl-peptide receptor. Characterization and chromosomal mapping of a peptide chemoattractant receptor family. J Biol Chem 267:7637–7643
3. Ye RD, Cavanagh SL, Quehenberger O et al (1992) Isolation of a cDNA that encodes a novel granulocyte N-formyl peptide receptor. Biochem Biophys Res Comm 184:582–589
4. Becker EL, Forouhar FA, Grunnet ML et al (1998) Broad immunocytochemical localization of the formylpeptide receptor in human organs, tissues and cells. Cell Tissue Res 292:129–135
5. McCoy R, Haviland DL, Molmenti EP et al (1995) N-formyl-peptide and complement C5a receptors are expressed in liver cells and mediate hepatic acute phase gene regulation. J Exp Med 182:207–217
6. Rescher U, Danielczyk A, Markoff A et al (2002) Functional activation of the formyl peptide receptor by a new endogenous ligand in human lung A549 cells. J Immunol 169:1500–1504
7. Le Y, Hu J, Gong W et al (2000) Expression of functional formyl peptide receptors by human astrocytoma cell lines. J Neuroimmunol 111:102–108
8. Sozzani S, Sallusto F, Luini W et al (1995) Migration of dendritic cells in response to formylpeptides, C5a, and a distinct set of chemokines. J Immunol 155:3292–3295
9. Le Y, Gong W, Tiffany HL et al. (2001) Amyloid (beta)42 activates a G-protein-coupled chemoattractant receptor, FPR-like-1. J Neurosci 21, RC123:1–5
10. Le Y, Yazawa H, Gong W et al (2001) The neurotoxic prion peptide fragment Prp(106–126) is a chemotactic agonist for the G protein-coupled receptor formyl-peptide receptor-like1. J Immunol 166:1448–1451
11. Ying G, Iribarren P, Zhou Y et al (2004) Humanin, a newly identified neuroprotective factor, uses the G protein-coupled formylpeptide receptor-like 1 as a functional receptor. J Immunol 172:7078–7085
12. John CD, Sahni V, Mehet D et al (2007) Formyl peptide receptors and the regulation of ACTH secretion: targets for annexin A1, lipoxins, and bacterial peptides. FASEB J 21:1037–1046
13. Lambert MP, Barlow AK, Chromy BA et al (1998) Diffusible, non fibrillar ligands derived from Abeta 1–42 are potent central nervous system neurotoxins. Proc Natl Acad Sci USA 95:6448–6453
14. Brown DR, Schmidt B, Kretzschmar HA (1996) Role of microglia and host prion protein in neurotoxicity of a prion protein fragment. Nature 6:15–24
15. Decker Y, McBean G, Godson C (2009) Lipoxin A4 inhibits IL-1beta-induced IL-8 and ICAM-1 expression in 1321N1 human astrocytoma cells. Am J Physiol Cell Physiol. 296:C1420–C1427
16. Ali H, Richardson RM, Tomhave ED et al (1993) Differences in phosphorylation of formylpeptide and C5a chemoattractant receptors correlated with differences in desensitization. J Biol Chem 268:24247–24254
17. Tardif M, Mery L, Brouchon L et al (1993) Agonist-dependent phosphorylation of N-formylpeptide and activation peptide from the fifth component of C (C5a) chemoattractant receptors in HL60 cells. J Immunol 150:3534–3545
18. Prossnitz ER (1997) Desentization of N-formyl peptide receptor-mediate activation. J Biol Chem 272:15213–15219
19. Hsu MH, Chiang SC, Rd Ye et al (1997) Phosphorylation of the N-formyl peptide receptor is required for receptor internalization but not chemotaxis. J Biol Chem 272:29426–29429
20. Bennett TA, Maestas DC, Prossnitz ER (2000) Arrestin binding to G protein-coupled N-formyl peptide receptor is regulated by the conserved "DRY" sequence. J Biol Chem 32:24590–24594
21. McMahon B, Stenson C, McPhillips F et al (2000) Lipoxin antagonizes the mitogenic effects of leukotriene D4 in human renal mesangial cells. Differential activation of MAP kinases through distinct receptors. J Biol Chem 275:27566–27575
22. Mc Mahon B, Mitchell D, Shattock R et al. (2002), Lipoxin, leukotriene, and PDGF receptors cross-talk to regulate mesangial cell proliferation. FASEB J 10.1096/fj.02-0416fje
23. Wu SH, Wu XH, Lu C et al (2006) Lipoxin A4 inhibits proliferation of human lung fibroblasts induced by connective tissue growth factor. Am J Respir Cell Mol Biol 34:65–72
24. Wu SH, Lu C, Dong L et al (2005) Lipoxin A4 inhibits TNF-alpha-induced production of interleukins and proliferation of rat mesangial cells. Kideny Int 68:35–46
25. Mitchel D, Rodgers K, Hanly J et al (2004) Lipoxins inhibit Akt/PKB activation and cell cycle progression in human mesangial cells. Am J Pathol 164:937–946
26. Wada K, Arita M, Nakajima A et al (2006) Leukotriene B4 and lipoxin A4 are regulatory signals for neural stem cell proliferation and differentiation. FASEB J 20:1785–1792
27. Perez HD, Holmes R, Kelly E et al (1992) Cloning of the gene coding for the human receptor for formyl-peptides. Characterization of a promoter region and evidence for polymorphic expression. Biochemistry 31:11595–11599
28. Durstin M, Gao JL, Tiffany HL et al (1994) Differential expression of members of the N-formylpeptide receptor gene-cluster in human phagocytes. Biochem Biophys Res Commun 201:174–179
29. Hartt JK, Barish G, Murphy PM et al (1999) N-formylpeptides induce two distinct concentration optima for mouse neutrophil

chemotaxis by differential interaction with two N-formylpeptide receptor (FPR) subtypes. Molecular characterization of FPR2, a second mouse neutrophil FPR. J Exp Med 190:741–747
30. Takano T, Fiore S, Maddox JF et al (1997) Aspirin-triggered 15-epi-lipoxin A4 (LXA4) and LXA4 stable analogues are potent inhibitors of acute inflammation: evidence for anti-inflammatory receptors. J Exp Med 185:1693–1704
31. Fiore S, Maddox JF, Perez HD et al (1994) Identification of a human cDNA- encoding a functional high-affinity lipoxin A(4) receptor. J Exp Med 180:253–260
32. Le Y, Oppenheim JJ, Wang JM (2001) Pleiotropic roles of formyl peptide receptors. Cytokine Growth Factor Rev 12:91–105
33. Bae YS, Kim Y, Kim Y et al (1999) Trp-Lys-Tyr-Met-Val-D-Met is a chemoattractant for human phagocytic cells. J Leukoc Biol 66:915–922
34. Ammendola R, Russo L, De Felice C et al (2004) Low- affinity receptor-mediated induction of superoxide by N-formyl-methionyl-leucyl-phenylalanine and WKYMVm in IMR90 human fibroblasts. Free Rad Biol Med 36:189–200
35. Iaccio A, Collinet C, Montesano Gesualdi N et al (2007) Protein kinase C-α and–δ are required for NADPH oxidase activation in WKYMVm-stimulated IMR90 fibroblasts. Arch Biochem Biophys 459:288–294
36. Karlsson J, Stenfeldt AL, Rabiet MJ et al (2009) The FPR2-specific ligand MMK-1 activates the neutrophil NADPH-oxidase, but triggers no unique pathway for opening of plasma membrane calcium channels. Cell Calcium 45:431–438
37. Hu JY, Le Y, Gong W et al (2001) Synthetic peptide MMK-1 is a highly specific chemotactic agonist for leukocyte FPRL1. Leukc Biol 70:155–161
38. Walther A, Riehmann K, Gerke V et al (2000) A novel ligand of the formyl peptide receptor: annexin I regulates neutrophil extravasation by interacting with the FPR. Mol Cell 5: 831–840
39. Su SB, Gon W, Gao JL et al (1999) A seven-transmembrane, G protein-coupled receptor, FPRL1, mediates the chemotactic activity of serum amyloid A for human phagocytic. J Exp Med 189:395–402
40. De Y, Chen Q, Schmidt AP et al (2000) LL-37, the neutrophil granule- and epithelial cell-derived cathelicidin, utilizes formyl peptide receptor-like 1 (FPRL1) as a receptor to chemoattract human peripheral blood neutrophils, monocytes, and T cells. J Exp Med 192:1069–1074
41. Iaccio A, Cattaneo F, Mauro M et al (2009) FPRL1-mediated induction of superoxide in LL-37-stimulated IMR90 human fibroblast. Arch Biochem Biophys 481:94–100
42. Gierschik P, Sidoropoulos D, Jakobs KH et al (1989) Two distinct Gi-proteins mediate formyl peptide receptor signal transduction in human leukemia (HL-60) cells. J Biol Chem 264:21470–21473
43. Wentel-Seifert K, Arthur JM, Liu HY et al (1999) Quantitative analysis of formyl peptide receptor coupling to g(i)alpha(1), g(i)alpha(2), and g(i)alpha(3). J Biol Chem 264:21470–21473
44. Tsu RC, Lai HWL, Allen RA et al (1995) Differential coupling of the formyl peptide receptor to adenylate cyclase and phospholipase C by the pertussis toxin-insensitive Gz protein. Biochem J 309:331–339
45. Iaccio A, Angiolillo A, Ammendola R (2008) Intracellular signaling triggered by formyl-peptide receptors in nonphagocytic cells. Curr Sign Transd Ther 3:88–96
46. Partida-Sanchez S, Cockaine DA, Monard S et al (2001) Cyclic ADP-ribose production by CD38 regulates intracellular calcium release, extracellular calcium influx and chemotaxis in neutrophils and is required for bacterial clearance in vivo. Nat Med 7:1209–1216
47. Liberles SD, Horowitz LF, Kuang D et al (2009) Formyl peptide receptors are candidate chemosensory receptors in the vomeronasal organ. Proc Natl Acad Sci USA 106:9842–9847
48. Rivière S, Challet L, Fluegge D et al (2009) Formyl peptide receptor-like proteins are a novel family of vomeronasal chemosensors. Nature 459:574–577
49. Gavins FN, Dalli J, Flower RJ et al (2007) Activation of annexin1 counter-regulatory circuit affords protection in the mouse brain microcirculation. FASEB J 21:1751–1758
50. Tiffany HL, Lavigne MC, Cui YH et al (2001) Amyloid-beta induces chemotaxis and oxidant stress by acting at formylpeptide receptor 2, a G protein-coupled receptor expressed in phagocytes and brain. J Biol Chem 276:23645–23652
51. Brandenburg LO, Konrad M, Wruck C et al (2008) Involvement of formyl-peptide-receptor-like-1 and phospholipase D in the internalization and signal transduction of amyloid beta 1–42 in glial cells. Neuroscience 156:266–276
52. Brandenburg LO, Konrad M, Wruck CJ et al (2010) Functional and physical interactions between formyl-peptide-receptors and scavenger receptor MARCO and their involvement in amyloid beta 1–42-induced signal transduction in glial cells. J Neurochem 113:749–760
53. Chen K, Iribarren P, Huang J et al (2007) Induction of the formyl peptide receptor 2 in microglia by IFN-gamma and synergy with CD40 ligand. J Immunol 178:1759–1766
54. Heurtaux T, Michelucci A, Losciuto S et al (2010) Microglial activation depends on beta-amyloid conformation: role of the formylpeptide receptor 2. J Neurochem 114:576–586
55. Hashimoto Y, Niikura T, Tajima H et al (2001) A rescue factor abolishing neuronal cell death by a wide spectrum of familial Alzheimer's diseases genes and Aβ42. Proc Natl Acad Sci USA 98:6336–6341
56. Brandenburg LO, Koch T, Sievers J et al (2007) Internalization of PrP106–126 by the formyl-peptide-receptor-like-1 in glial cells. J Neurochem 101:718–728
57. Kam AY, Tse TT, Kwan DH et al (2007) Formyl peptide receptor like 1 differentially requires mitogen-activated protein kinase for the induction of glial fibrillare acidic protein and interleukin-1alpha in human U87 astrocytoma cells. Cell Signal 19: 2106–2117
58. Kam AY, Liu AM, Wong YH et al (2007) Formyl peptide-receptor like-1 requires lipid raft and extracellular signal-regulated protein kinase to activate inhibitor-kappa B kinase in human U87 astrocytoma cells. J Neurochem 103:1533–1566
59. Chen JH, Yao XH, Gong W et al (2007) A novel lipoxygenase inhibitor Nordy attenuates malignant human glioma cell response to chemotactic and growth stimulating factors. J Neurooncol 84:223–231
60. John CD, Gavins FN, Buss N et al (2008) Annexin-1 and the formyl peptide receptor family: neuroendocrine and metabolic aspects. Curr Opin Pharmacol 8:765–776
61. Andric SA, Zivadinovic D, Gonzales-Iglesias AE et al (2005) Endothelin-induced, long lasting, and Ca^{++} influx-independent blockade of intrinsic secretion in pituitary cells by Gz subunits. J Biol Chem 280:26896–26903
62. Hashimoto Y, Suzuki H, Aiso S et al (2005) Involvement of tyrosine kinase and STAT3 in humanin-mediated neuroprotection. Life Sci 77:3092–3104
63. Zhou Y, Bian X, Le Y et al (2005) Formylpeptide receptor FPR and the rapid growth of malignant human gliomas. J Natl Cancer Inst 97:823–835
64. Huang J, Hu J, Bian X et al (2007) Transactivation of the epidermal growth factor receptor by formylpeptide receptor exacerbates the malignant behavior of human glioblastoma cells. Cancer Res 67:5906–5913

65. Huang J, Chen K, Chen J et al (2010) The G-protein-coupled formylpeptide receptor FPR confers a more invasive phenotype on human glioblastoma cells. Br J Cancer 102:1052–1060
66. Sherr CJ, Roberts JM (1999) CDK inhibitors: positive and negative regulators of G1-phase progression. Genes Dev 13:1501–1512
67. Russo T, Zambrano N, Esposito F et al (1995) A p53-independent pathway for activation of WAF1/CIP1 expression following oxidative stress. J Biol Chem 271:4138–4142
68. Ammendola R, Ruocchio MR, Chirico G et al (2002) Inibition of NADH/NADPH oxidase affects signal transduction by growth factor receptors in normal fibroblasts. Arch Biochem Biophys 397:253–257
69. Zhang Y, Chan MMK, Andrews MC et al (2005) Apocynin but not allopurinol prevents and reverses adrenocorticotropic hormone-induced hypertension in the rat. Am J Hypertens 18: 910–916
70. Barbieri SS, Cavalca V, Eligini S et al (2004) Apocynin prevents cyclooxygenase 2 expression in human monocytes through NADPH oxidase and glutathione redox-dependent mechanisms. Free Rad Biol Med 37:156–165

Archives of Biochemistry and Biophysics 481 (2009) 94–100

Contents lists available at ScienceDirect

Archives of Biochemistry and Biophysics

journal homepage: www.elsevier.com/locate/yabbi

FPRL1-mediated induction of superoxide in LL-37-stimulated IMR90 human fibroblast

Annalisa Iaccio [b], Fabio Cattaneo [b], Martina Mauro [b], Rosario Ammendola [a,*]

[a] Dipartimento S.T.A.T., Università del Molise, Contrada Fonte Lappone, 86090 Pesche (IS), Italy
[b] Dipartimento di Biochimica e Biotecnologie Mediche, Università di Napoli Federico II, Naples, Italy

ARTICLE INFO

Article history:
Received 16 July 2008
and in revised form 16 October 2008
Available online 26 October 2008

Keywords:
Reactive oxygen species
Human fibroblasts
NADPH oxidase
FPRL1
LL-37
ERKs
p47^{phox}

ABSTRACT

Molecular mechanisms underlying the generation of reactive oxygen species in LL-37-stimulated cells are poorly understood. Previously, we demonstrated that in human fibroblasts the exposure to WKYMVm induced p47^{phox} phosphorylation and translocation and, in turn, NADPH oxidase activation. These effects were mediated by the activation of the Formyl-peptide receptor-like 1 (FPRL1) and the downstream signaling involved ERKs phosphorylation and PKCα- and PKCδ-activation. Since LL-37 uses FPRL1 as a receptor to mediate its action on several cell types, we investigated in LL-37-stimulated IMR90 cells molecular mechanisms involved in NADPH-dependent superoxide generation. The exposure to LL-37, which is expressed in fibroblasts, induced ERKs activation, p47^{phox} phosphorylation and translocation as well as NADPH oxidase activation. These effects were prevented by pertussis toxin, PD098059 and WRWWWW, a FPRL1-selective antagonist. Furthermore, the stimulation with LL-37 of HEK293 cells, transfected to stably express FPRL1, induced a rapid activation of ERKs and p47^{phox} phosphorylation.

Introduction

Fibroblasts and epithelial cells participate in the innate immune system also via the production of an arsenal of antimicrobial peptides. Among these microbicidal agents, defensins and cathelicidins play a key role in skin-mediated host defence [1]. In humans, six α-defensins, more than 30 putative β-defensin genes [2,3] and an 18-kDa human cationic antimicrobial protein (hCAP-18)[1] have been identified [4]. LL-37/hCAP18 represents the only antimicrobial peptide of the cathelicidin family expressed in human neutrophils, monocytes, NK cells, T cells, B cells [5–9], epithelial cells and skin [9,10] as well as in the gastrointestinal and in the respiratory tract [5]. Processing of LL-37 from the cathelicidin precursor is essential for activation of its biological activity. hCAP18 consists of a highly conserved preproregion of 128–143 residues, including a putative 29–30 residue signal peptide, a 99–114 residue cathelin-like domain and a COOH–terminal antimicrobial domain ranging in length from 12 to >100 amino acid residues [11]. Cleavage of hCAP18 occurs between Ala103 and Leu104 by proteinase-3, giving rise to LL-37, a 37-residue mature antimicrobial peptide with two leucine residues on its NH_2 terminus. Cathelicidins play an important role in the host defence against infection. In fact, mice deficient in the murine cathelicidin-related antimicrobial peptide suffer from more severe bacterial skin infections [12] and the deficiency of LL-37 in patients with a congenital neutropenia, known as morbus Kostmann, is an origin of severe infection in this disorder [13]. On the other hand, the overexpression of LL-37 in mice was shown to inhibit bacterial load and inflammatory response, whereas systemic gene transfer protected against endotoxemia [14].

LL-37 not only acts as an endogenous antibiotic but also displays additional roles including the regulation of inflammatory and immune responses, promotion of wound healing, re-epithelization, binding and neutralizing of lipopolysaccharides [1], as well as chemotactic activity towards neutrophils, monocytes and T cells through binding to the formyl peptide receptor-like 1 (FPRL1) [15]. LL-37 can also to chemoattract, to activate and to enhance vascular permeability of mast cells [16–18] and to stimulate dendritic cells and keratinocytes [19,20]. Furthermore, LL-37 was shown to induce the generation of reactive oxygen species (ROS) and the release of α-defensins from neutrophils [21].

To date, FPRL1 and $P2X_7$ are the only receptors described for LL-37 [15,22] and their activities include stimulation of angiogenesis [23] and cutaneous wound healing [24]. FPRL1 is the only receptor whose ligands include both a peptide and a lipid [25] and it has been identified in several human cells and tissues [26]. Interest-

* Corresponding author. Fax: +39 (0) 817464359.
E-mail address: rosario.ammendola@unimol.it (R. Ammendola).

[1] *Abbreviations used:* FPRL1, Formyl-peptide receptor-like 1; hCAP-18, 18-KDa human cationic antimicrobial protein; ERKs, extracellular signal-regulated kinases; PTX, pertussis toxin; DMEM, Dulbecco's modified Eagle medium; FBS, fetal bovine serum; PBS, phosphate-buffered saline; GPCR, G protein-coupled receptors; TLR, Toll-like receptor.

0003-9861/$ - see front matter © 2008 Elsevier Inc. All rights reserved.
doi:10.1016/j.abb.2008.10.026

ingly, the identified agonists for this receptor do not share sequence homology, which suggests that FPRL1 can be activated by a wide variety of unrelated ligands that can also be generated during pathological conditions [27].

NADPH-dependent superoxide generation may represent the downstream target of the FPRL1 activation. Phosphorylation and membrane translocation of the cytosolic regulatory subunit $p47^{phox}$ of NADPH oxidase are currently considered to be key events in the assembly and activation of this enzymatic complex. Previously, we demonstrated that IMR90 cells express on their membrane FPRL1 [28] which shows a high binding efficiency for WKYMVm, a modified peptide isolated by screening synthetic peptide libraries [29]. In serum-deprived human fibroblasts, exposure to WKYMVm induced both $p47^{phox}$ phosphorylation and translocation and NADPH-dependent superoxide generation. These effects were in large part mediated by prevention of the rapid activation of extracellular signal-regulated kinases (ERKs) with a MEK1 inhibitor and by pertussis toxin (PTX) [28]. Furthermore, preincubation with specific pharmacological inhibitors of PKCα and PKCδ isoenzymes, before stimulation with WKYMVm, prevented ERKs activation, $p47^{phox}$ phosphorylation and translocation and, in turn, NADPH oxidase activation [30].

FPRL1 shows complex functional properties, partly due to its high promiscuity, but also to the fact that its activation can stimulate several signal transduction pathways depending on the ligand, its concentration and the cell type involved [27]. In this study we investigated, in IMR90 human fibroblasts, on cell signaling triggered by binding of LL-37 on FPRL1 and on the kinase pathways involved in NADPH-dependent superoxide production. We found that LL-37 induces ROS generation via NADPH oxidase activation through a ERKs-dependent and a PKC-independent pathway mediated by FPRL1.

Materials and methods

Reagents and cell culture treatments

The LL-37 and the WRWWWW (WRW4) peptides were synthesized and HPLC purified by PAN-TECS (Tubingen, Germany) and by PRIMM (Milan, Italy), respectively. SDS–PAGE reagents were from Bio-Rad (Richmond, Ca, USA). Protein A/G plus-Agarose, anti-active phosphorylated ERK 1/2, anti-$p47^{phox}$, anti-Tubulin, and anti-PDGFR antibodies were obtained from Santa Cruz Biotechnology Inc. (Santa Cruz, CA, USA). Human anti-hCAP18/LL-37 antibody was purchased from Hycult Biotechnology, Uden, The Netherlands. Protein A-horseradish peroxidase, anti-mouse Ig-horseradish peroxidase and ECL chemiluminescent reagent kit were from Amersham Pharmacia Biotech (Little Chalfont, Buckinghamshire, UK). PD098059, GF109203X, Gö6983, BAPTA-AM, were purchased from Calbiochem (La Jolla, Ca, USA). PTX, DPI, apocynin, ferricytochrome *c*, and anti-phospho Serine antibody were obtained from Sigma (St. Louis, MO, USA).

IMR90 human fibroblasts and HEK293 cells, were obtained from ATCC (Rockville, MD, USA) and grown in Dulbecco's modified Eagle medium (DMEM) containing 10% fetal bovine serum (FBS), 100 U/ml penicillin, and 100 μg/ml streptomycin.

IMR90 cells were grown until they reached 90% confluence and then starved in serum-free DMEM. After 48 h cells were stimulated by adding the LL-37 peptide for various concentrations or times. In other experiments, serum-deprived cells were preincubated with 50 μM PD098059 for 90 min, or with 100 ng/ml PTX for 16 h, or with 25 μM BAPTA-AM for 60 min, or with 10 μM GF109203X for 10 min, or with 10 μM Gö6983 for 10 min, or with 100 μM DPI for 15 min, or with 10 μM WRW4 for 15 min, before the stimulation with 10 nM LL-37 for 1 min.

HEK293 cells and HEK293 transfected to stably express FPRL1 (FPR293) were grown until they reached 90% confluence and then starved in serum-free DMEM. After 48 h cells were stimulated by exposure to 10 nM LL-37.

Western blot analysis

Growth-arrested fibroblasts were stimulated with different concentrations of LL-37 for different times in the presence or absence of the appropriate amount of specific inhibitors. Cells were rinsed with phosphate-buffered saline (PBS) and cell lysates and Western blot analysis were performed as previously described [31]. Antigen–antibody complexes were detected with the ECL chemiluminescence reagent kit.

Phosphorylation of $p47^{phox}$

Serum-deprived IMR90 cells were stimulated with 10 nM LL-37 for 1 min in the presence or absence of the specific amounts of inhibitors and washed with ice-cold PBS. Cells were lysed as previously described [31] and $p47^{phox}$ was immunoprecipitated with a specific anti-$p47^{phox}$ antibody. Proteins were resolved on a 10% SDS–PAGE and $p47^{phox}$ phosphorylation was detected by using an anti-phospho Serine antibody. The same filter was incubated with an anti-$p47^{phox}$ antibody.

Translocation of $p47^{phox}$

Confluent IMR90 human fibroblasts were kept serum-free for 48 h and then stimulated with 10 nM LL-37 for 1 min or preincubated with the appropriate amounts of inhibitors before stimulation. Cells were washed in PBS and were broken open by freeze–thawing. The resulting lawn of plasma membrane fragments was repeatedly washed with, and then scraped into, a hypotonic medium, containing 20 mM MES pH 6, 2 mM $MgCl_2$, 5 mM KCl, and 100 mg/ml soybean trypsin inhibitor. IMR90 membranes were pelleted at 1000*g*, washed with PBS and resuspended. This technique yielded a highly purified plasma membrane fraction as previously described [28,32]. Human fibroblasts membranes were subjected to SDS–PAGE and subsequent immunoblotting by using monoclonal antibody against $p47^{phox}$. The same filters were re-probed with an anti-PDGFR antibody as a control of protein loading and membrane purification.

Assay of superoxide production

Membranes and cytosol were isolated from serum-starved fibroblasts stimulated with 1, 10 or 100 nM LL-37 for 1 min in the presence or absence of 50 μM PD098059 for 90 min, or 100 ng/ml PTX for 16 h, or 100 μM DPI for 15 min, or 100 mM apocynin for 60 min, or 25 μM BAPTA-AM for 60 min. Protein concentrations were determined by the method of Bradford [33]. NADPH-dependent superoxide production was determined as the superoxide dismutase-sensitive rate of reduction of cytochrome *c*, as previously described [28,30]. Briefly, combinations of 10 mg of membrane and 200 mg of cytosolic proteins in PBS were incubated at room temperature in the presence of 15 mM GTP-γ-S, 100 mM cytochrome *c* and 10 mM FAD in a total volume of 1 ml. NADPH (100 mM) was then added and the production of superoxide was monitored at 550 nm. The specificity of cytochrome *c* reduction was determined by the addition in control samples of 200 U/ml of superoxide dismutase (SOD). The production of superoxide anion by intact cells was measured as the SOD-inhibitable reduction of ferricytochrome *c* [34]. IMR90 cells (5×10^5 cells/well) were exposed to 10 nM LL-37 in medium containing 100 mM ferricytochrome *c* in the presence or in the absence of

60 mg/ml of SOD. The reduction of ferricytochrome *c* was followed by a change of absorbance at 550 nm every 1 min over a 5-min time corse using a Thermomax microplate reader (Molecular Devices, CA, USA). The specificity of reduction by superoxide anion was established by comparing reduction rates in the presence or in the absence of SOD. Rates of $O_2^{-\cdot}$ production were calculated from the linear segment of the increase in absorbance at 550 nm and translated into nanomoles of $O_2^{-\cdot}$ by the extinction coefficient of cytochrome *c*, $\Delta E_{550}/\Delta t = 21.1\ mM^{-1}\ cm^{-1}$, considering that 1 mole of $O_2^{-\cdot}$ reduces 1 mole of cytochrome *c*. The Student's *t* test was used to compare individual treatments with their respective control value and, in the Legend for Figures, * indicates significant differences at the $p < 0.01$ probability level as compared with the values obtained from growth-arrested fibroblasts.

RNA preparation and reverse transcription polymerase chain reaction

Total RNA from cells was extracted with the RNAeasy Mini Kit (Quiagen) according to the manufacturer's instructions and 0.1 μg of RNA was used as a template for RT-PCR experiments. To amplify hCAP18/LL-37, the sequences of sense oligonucleotide primer 5′-GAAGACCCAAAGGAATGGCC-3′ and antisense primer 5′-CAGAGCCCAGAAGCCTGAGC-3′ according to the sequence of human hCAP18/LL-37 coding region, were designed. For human GADPH, sense primer 5′-CCATGGAGAAGGCTGGG-3′ and antisense primer 5′-CGCCACAGTTTCCCGGA-3′ amplified a 280-bp fragment. For human TLR-2, sense primer 5′-CCACATACTTTGTGGATGGT-3′ and antisense primer 5′-TCTTAGTGAAGGTGTCCAT-3′ amplified a 620-bp fragment. For human TLR-4, sense primer 5′-GCTGAATTTCT ACAAAATCC-3′ and antisense primer 5′-CATTTCTAAATTCTCCCAG A-3′ amplified a 670-bp fragment. For human TLR-9 sense primer 5′-GGGTTTCTGCCGCAGC-3′ and antisense primer 5′-GTGACAG GTGGGTGAGGT-3′ amplified a 613-bp fragment.

Results

LL-37 induces NADPH oxidase activation and ERKs phosphorylation in IMR90 cells

LL-37 stimulates ROS generation in human neutrophils [21] macrophages [35] and mast cells [36]. Therefore, we first analysed the ability of this cathelicidin to stimulate NADPH oxidase-like machinery expressed in IMR90 cells [31]. To this aim human fibroblasts were serum-deprived for 48 h, exposed to different concentrations of LL-37 and membranes were incubated with cytosolic proteins in a SOD-sensitive rate of reduction of cytochrome *c* assay. As shown in Fig. 1A, we found that in dose-response experiments LL-37 significantly induced NADPH-dependent superoxide production. We also measured superoxide anion release in growth-arrested intact cells exposed to LL-37 by following the SOD-inhibitable reduction of ferricytochrome *c* at 550 nm every 1 min over a 5-min time course. We observed that stimulation for 1 min with 10 nM LL-37 induced $O_2^{-\cdot}$ generation (Fig. 1B).

Previously, we demonstrated that in IMR90 cells exposed to N-formyl peptides or WKYMVm, NADPH oxidase activation requires p42 and p44 MAPK phosphorylation [28]. Activation of MAPK by LL-37 has been reported in several cell types including neutrophils [21,22], mast cells [18], keratinocytes [19,37], epithelial cells [38] and monocytes [39]. Therefore, we next investigated in human fibroblasts the ability of LL-37 to induce ERKs phosphorylation by stimulating cells with increasing concentrations of cathelicidin and for different times. As shown in Fig. 2, incubation with 10 nM LL-37 induced ERKs activation (Panel A) and this was detectable after 30 s and significantly decreased after 5 min of exposure (Panel B).

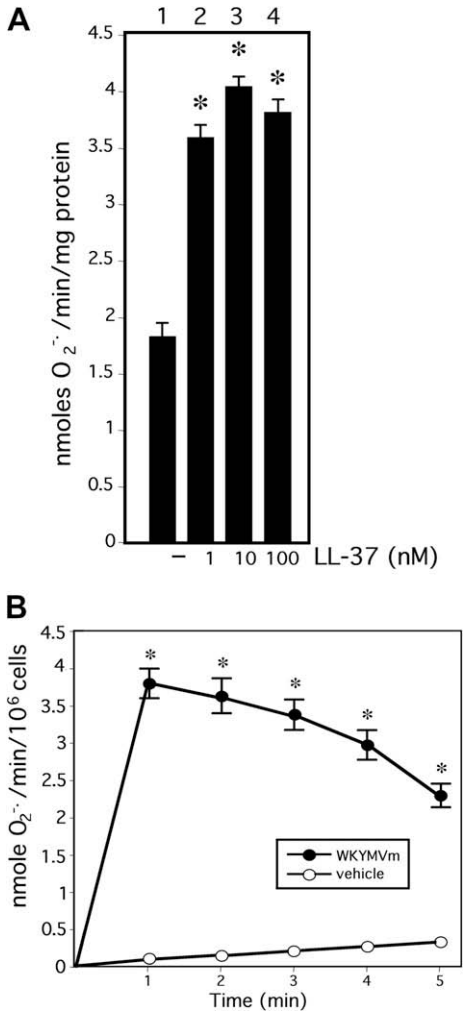

Fig. 1. LL-37 stimulates the NADPH-dependent superoxide generation in human fibroblasts. (A) Ten micrograms of membrane and 200 mg of cytosolic proteins were purified from IMR90 human fibroblasts grown in serum-free medium for 48 h and stimulated for 1 min with different concentrations of LL-37. Proteins were incubated in a NADPH oxidase activity assay in the presence of 15 mM GTP-g-S, 100 mM cytochrome *c*, 10 mM FAD, and 100 mM NADPH. The specificity of cytochrome *c* reduction was monitored at 550 nm by using the SOD-inhibitable reduction of cytochrome *c*, as described in Materials and methods. (B) Serum-deprived IMR90 cells (5×10^5 cells/well) were exposed to 10 nM LL-37 in medium containing 100 mM ferricitochrome *c* in the presence or in the absence of 60 mg/ml of SOD. The reduction of ferricytochrome *c* was followed by a change of absorbance at 550 nm every 1 min, over a 5-min time course. The specificity of the reaction was determined by comparing reduction rate in the presence or in the absence of SOD. * $p < 0.01$ when compared with serum-starved cells.

PD098059, PTX and WRW4 prevent LL-37-induced ERKs phosphorylation

In serum-deprived human fibroblasts stimulated with N-fMLP or WKYMVm, ERKs activation and superoxide generation are prevented by inhibition of MEK1 [28]. Therefore, we examined in LL-37-stimulated IMR90 cells the effects of PD098059 on signaling cascade and we observed that this treatment significantly prevented ERKs phosphorylation (Fig. 3A).

FPRL1 has been proposed to be a receptor for LL-37 on monocytes [15], neutrophils [22], T cells [15], keratinocytes [37], endothelial [23] and epithelial cells [40]. We investigated in IMR90 cells whether FPRL1 or other G protein-coupled receptors (GPCR) were involved in LL-37-induced signaling, by examining sensitivity to inhibition with pertussis toxin and we observed a significant

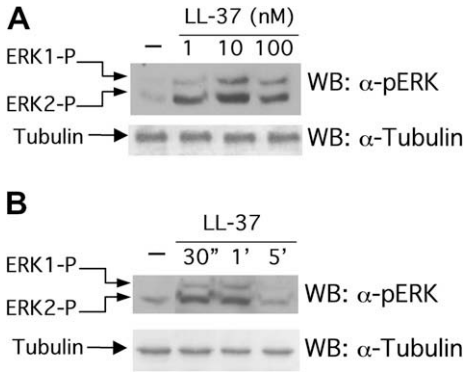

Fig. 2. LL-37 induces ERKs activation in IMR90 cells. Cell lysates, containing 20 μg of proteins, were purified from IMR90 human fibroblasts grown in serum-free medium for 48 h and then stimulated with different concentrations of LL-37 (A) and for different times (B) as indicated in the figure. Proteins were resolved by electrophoresis on 10% SDS–PAGE and transferred to a nitrocellulose membrane. ERKs phosphorylation was detected by western blotting by using an anti-phosphoERK antibody and an anti-Tubulin antibody was used as a control of protein loading. The arrows indicate the phosphorylated forms (ERK1-P and ERK2-P) of $p44^{MAPK}$ and $p42^{MAPK}$, respectively.

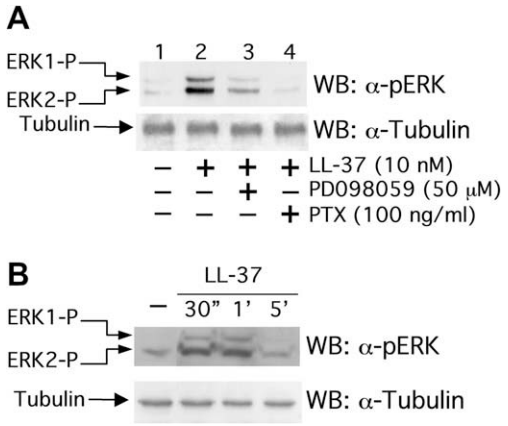

Fig. 3. LL-37-induced ERKs phosphorylation requires the activation of MEK1 and of a PTX-sensitive GPCR. (A) Proteins were extracted from growth-arrested cells stimulated with 10 nM LL-37 for 1 min or preincubated with the indicated concentrations of PD098059 or PTX before stimulation. (B) Cell lysates were obtained from serum-deprived human fibroblasts exposed to 10 nM LL-37 in the presence or absence of increasing concentrations of WRW4 as indicated. Twenty micrograms of proteins were resolved on 10% SDS–PAGE and subjected to immunoblotting analysis with an anti-phosphoERK antibody. An anti-Tubulin antibody was used as a control of protein loading. The arrows indicate the phosphorylated forms (ERK1-P and ERK2-P) of $p44^{MAPK}$ and $p42^{MAPK}$, respectively.

reduction of ERKs phosphorylation as a result of the preincubation with PTX before stimulation with LL-37 (Fig. 3A). We also analysed the effects of WRW4 [41] on LL-37-induced intracellular cascade and the results showed that in human fibroblasts the FPRL1-selective antagonist successfully inhibited ERKs activation in a dose-dependent manner (Fig. 3B).

LL-37 induces $p47^{phox}$ phosphorylation and translocation in IMR90 cells

Phosphorylation and membrane translocation of the regulatory cytosolic oxidase subunit $p47^{phox}$ are considered to be key events in the assembly of phagocytic and non-phagocytic oxidase [28,42,43]. We investigated in serum-deprived human fibroblasts stimulated with LL-37, molecular mechanisms underlying NADPH oxidase activation by analysis of $p47^{phox}$ phosphorylation and translocation. The results showed that upon incubation with the cathelicidin $p47^{phox}$ resulted phosphorylated on Serine residues (Fig. 4A) and consequently translocated on the membrane (Fig. 4B). Since in WKYMVm-induced IMR90 cells ERKs activation and PTX-sensitive GPCR are required for NADPH-dependent superoxide generation [28], we analyzed the effects of PD098059 or PTX on LL-37-induced $p47^{phox}$ phosphorylation and translocation. As shown in Fig. 4, both treatments prevented serine phosphorylation of $p47^{phox}$ (Panel A) and its compartmentalization on the membrane (Panel B).

LL-37 uses FPRL1 as its receptor in human fibroblasts

We further investigated the possibility that, in IMR90 cells, ERKs activation and $p47^{phox}$ phosphorylation and translocation observed on LL-37 exposure could be mediated by the binding of the cathelicidin to FPRL1. To this aim we used the HEK293 cell line which express NOX4, one member of the NADPH oxidase family [44] but not FPRL1 [45]. These cells were transfected to stably express FPRL1 (FPR293) and exposed to 10 nM LL-37. As shown in Fig. 5, in FPRL1-transfected HEK293 cells the incubation with LL-37 induced ERKs (Panel A) and $p47^{phox}$ phosphorylation (Panel B), whereas no activation could be detectable in parental HEK293 cells.

BAPTA-AM prevents LL-37-induced ERKs phosphorylation and NADPH oxidase activation in human fibroblasts

Other kinases pathway are activated via serpentine receptors and involved in superoxide generation. We previously demonstrated that preincubation of human fibroblasts with general and specific pharmacological inhibitors of PKC, before stimulation with WKYMVm, prevented ERKs activation and $p47^{phox}$ phosphorylation and translocation [30]. Therefore, we investigated whether in LL-37-stimulated IMR90 cells, GF109203X- and Gö6983-sensitive PKC isoforms were involved in signaling cascade leading to NADPH-dependent superoxide generation. We first explored the ability of LL-37 to activate PKC in IMR90 cells and the results

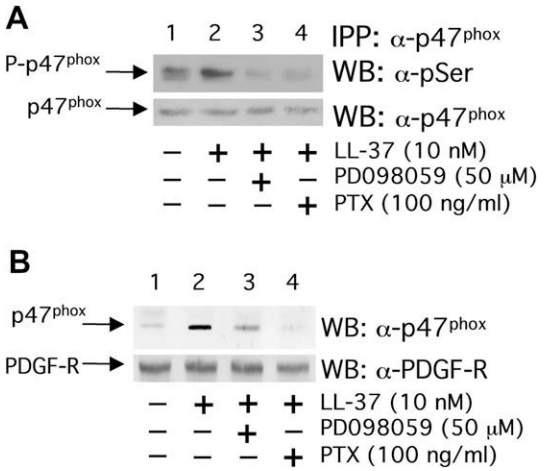

Fig. 4. LL-37 induces $p47^{phox}$ phosphorylation and translocation. (A) Serum-deprived fibroblasts were stimulated with LL-37 or preincubated with PD098059 or PTX before stimulation. One milligram of cell lysates was immunoprecipitated with an anti-$p47^{phox}$ antibody, proteins were resolved on SDS–PAGE and $p47^{phox}$ phosphorylation (P-$p47^{phox}$) was detected by using an anti-phospho Serine antibody. An anti-$p47^{phox}$ antibody was used as a control of protein loading. (B) Membranes were purified by serum-starved IMR90 cells, stimulated with LL-37 or preincubated with PD098059 or PTX before exposure to peptide. Thirty micrograms of extracts were subjected to 10% SDS–PAGE and subsequent immunoblotting by using monoclonal antibody against $p47^{phox}$. The same filter was reprobed with an anti-PDGF-R antibody.

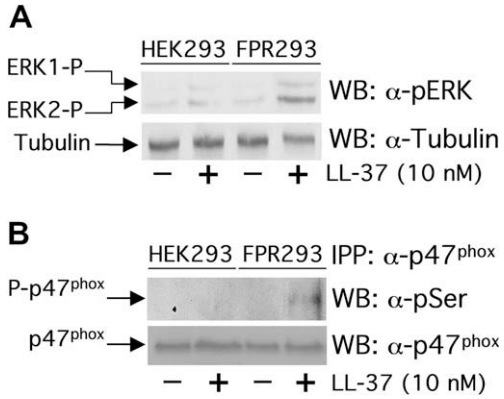

Fig. 5. LL-37-induced ERKs activation and $p47^{phox}$ phosphorylation require binding of LL-37 on FPRL1. HEK293 cells and HEK293 transfected to stably express FPRL1 (FPR293) were serum-deprived for 48 h and then stimulated with 10 nM LL-37. (A) Twenty micrograms samples of cell lysates were resolved on 10% SDS–PAGE and subjected to immunoblotting analysis with an anti-phosphoERK antibody. The same filter was reprobed with an anti-Tubulin antibody. The arrows indicate the phosphorylated forms (ERK1-P and ERK2-P) of $p44^{MAPK}$ and $p42^{MAPK}$. (B) $p47^{phox}$ was immunoprecipitated from 1 mg of total cellular extracts and proteins were resolved on 10% SDS–PAGE. $p47^{phox}$ phosphorylation (P-$p47^{phox}$) was detected by using an anti-phospho Serine antibody and an anti-$p47^{phox}$ antibody was used as a control of protein loading.

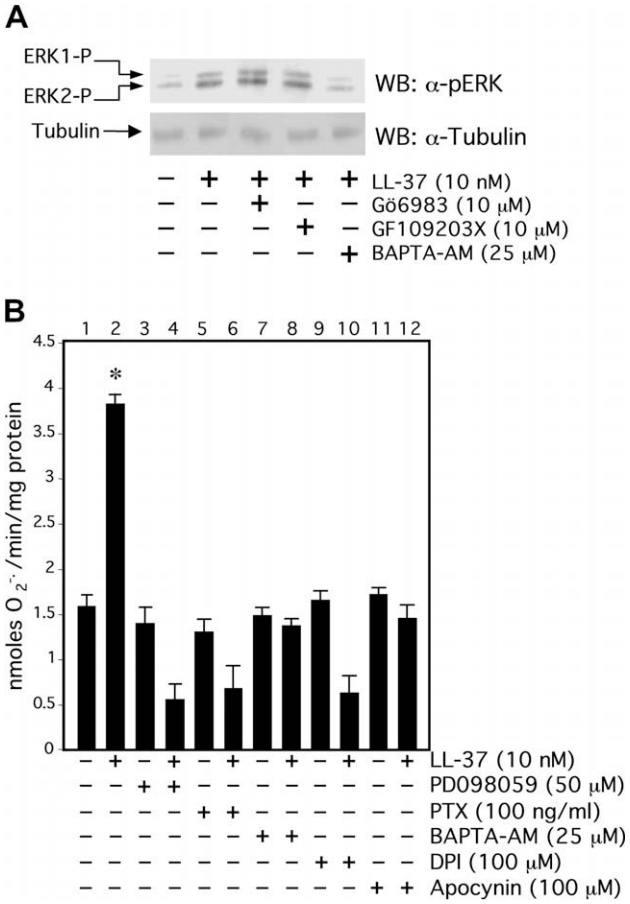

Fig. 6. BAPTA-AM prevents ERKs phosphorylation and NADPH activation. (A) Proteins were extracted from serum-deprived IMR90 fibroblasts stimulated with LL-37 or preincubated with Gö6976, or GF109203X, or BAPTA-AM to the indicated final concentrations before stimulation. ERKs phosphorylation was measured by western blotting using an anti-phosphoERK antibody. The arrows indicate the phosphorylated forms (ERK1-P and ERK2-P) of $p44^{MAPK}$ and $p42^{MAPK}$. An anti-Tubulin antibody was used as a control of protein loading. (B) Membrane and cytosol extracts were purified from IMR90 cells grown in serum-free medium for 48 h and then stimulated with LL-37 in the presence or absence of PD098059, or PTX, or BAPTA-AM, or DPI, or apocynin to the indicated final concentrations. Proteins were incubated in a NADPH oxidase activity assay and NADPH-dependent superoxide production was determined as the SOD-sensitive rate of reduction of cytochrome *c*. The experiments were performed in triplicate. $^{*}p < 0.01$ when compared with growth-arrested IMR90 cells.

showed that PKC activity, measured as ability to phosphorylate a target peptide, was undetectable (data not shown). Furthermore, preincubation with GF109203X, which acts as a competitor inhibitor for the ATP-binding site of PKC, or Gö6983, which inhibits PKC-α, -β, -γ, -δ, -ζ, before exposure to LL-37 did not attenuate ERKs phosphorylation (Fig. 6A). LL-37 induces Ca^{++} mobilization in several cell types [15,21,23] and downstream events of FPRL1 activation include increased calcium concentration [46]. Therefore, we used the intracellular calcium chelator BAPTA-AM, which has been shown to inhibit ROS in neutrophils [47], to analyse the effects of the depletion of Ca^{++} on ERKs activation and on superoxide generation. The results showed that BAPTA-AM significantly prevented LL-37-induced ERKs phosphorylation (Fig. 6A) and NADPH oxidase-like activation (Fig. 6B, bar 8). As expected, NADPH-dependent superoxide generation was also inhibited by preincubation with apocynin (Fig. 6B, bar 12), which interferes with the translocation of $p47^{phox}$, with DPI (Fig. 6B, bar 10), which blocks FAD binding to a flavin site of the oxidase, with PTX (Fig. 6B, bar 6) or with PD098059 (Fig. 6B, bar 4) before stimulation.

LL-37 is expressed in IMR90 human fibroblasts

We analyzed in IMR90 and HEK293 cells hCAP18/LL-37 mRNA by RT-PCR and the results showed that the entire coding region was expressed in these cells (Fig. 7A). We also evaluated by western blot experiments performed with a specific monoclonal antibody, the cleavage pattern and protein levels of hCAP18/LL-37. We observed that full-length hCAP18/LL-37 pro-peptide and a immunoreactive band of about 3.7 kDa, corresponding to LL-37 active peptide, was detected in both cell types (Fig. 7B). Recently, it was demonstrated that in human alveolar macrophages, monocytes, neutrophils and epithelial cells, LL-37 can be induced by stimulation through TLR-2, TLR-4 and TLR-9 [48]. Proteins encoded by these genes are members of the Toll-like receptor (TLR) family which play a key role in pathogen recognition and activation of innate immunity. They recognize pathogen-associate molecular patterns that are expressed on infectious agents, and mediate the production of cytokines necessary for the development of effective immunity. The various TLRs exhibit different pattern of expression. Therefore, we analysed the expression of these receptors in human fibroblasts and RT-PCR experiments demonstrated that mRNAs level of TLR-2, TLR-4 and TLR-9 were undetectable in IMR90 cells (Fig. 7C).

Discussion

In this study we report, for the first time, that in serum-deprived IMR90 human fibroblasts the exposure to LL-37 stimulates ROS generation via NADPH oxidase-like activation. The major lines of evidences that we provide are that incubation with LL-37 of intact fibroblasts induces: (i) MEK1-dependent, Ca^{++}-dependent and PKC-independent activation of ERKs; (ii) ERK-dependent phosphorylation and translocation of $p47^{phox}$. This signaling cascade is mediated by the binding of LL-37 to FPRL1 as demonstrated by the observation that: (i) PTX prevents ERKs activation, $p47^{phox}$ phosphorylation and translocation and NADPH oxidase activation; (ii) the FPRL1-selective antagonist WRW4 successfully inhibits LL-37-induced ERKs activation; (iii) in FPRL1-transfected HEK293 cells, the exposure to LL-37 induces ERKs activation and serine

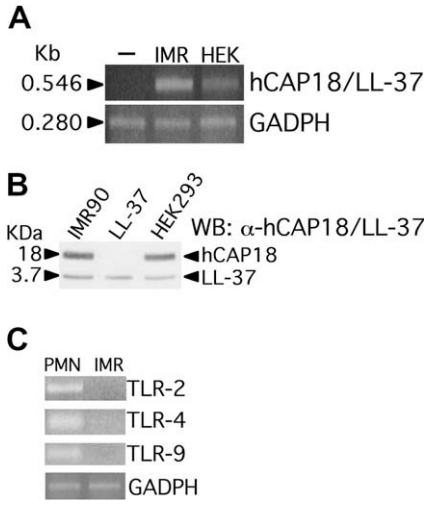

Fig. 7. Expression of LL-37 and TLRs in IMR90 and HEK293 cells. Total RNA and proteins were purified from PMNs, IMR90 and HEK293 cells. (A) Expression of hCAP18/LL-37 was determined by RT-PCR and PCR was performed by coamplifying the coding region of hCAP18/LL-37 and GADPH. Nucleotide sequence of primers is reported in Materials and methods. (B) Protein levels and the cleavage pattern of hCAP18/LL-37 were determined by western blot by using a specific anti-hCAP18/LL-37 antibody. A 10–20% SDS–PAGE was loaded with 50 mg of cell lysates or 20 ng of LL-37 peptide. Arrows indicate full-length hCAP18/LL-37 pro-peptide (18 kDa) and the 3.7 kDa LL-37 mature peptide. (C) Expression of TLRs was determined by RT-PCR and PCR was performed by coamplifyng TLRs and GADPH. PCR products were separated on 1.5% agarose gel.

phosphorylation of $p47^{phox}$, whereas no activation can be detectable in parental HEK293 cells.

NADPH-dependent superoxide generation in LL-37-stimulated phagocytic cells has been demonstrated by several studies, which show that in human macrophages antimicrobial peptide triggers respiratory burst [35] and that in neutrophils LL-37 mediates the generation of ROS most probably via NADPH oxidase, as evidenced by the inhibitory effect of DPI [21]. To date, molecular mechanisms underlying NADPH-dependent superoxide generation in LL-37-stimulated cells have not been described. Although the ability of LL-37 to induce ERKs activation has been reported by several authors in different cell types [18,19,21,22], the present study is the first report to provide evidence that in human fibroblasts LL-37-induced ERKs phosphorylation is required for $p47^{phox}$ phosphorylation and translocation and, in turn, for NADPH-dependent superoxide generation. Moreover, the observation that the depletion of intracellular Ca^{++} by BAPTA-AM markedly prevents both LL-37-induced ERKs activation and NADPH oxidase activation suggests that, in IMR90 cells, ROS generation is also dependent on intracellular Ca^{++} mobilization.

The effects of LL-37 on eukaryotic cells have been extensively studied but the mechanism(s) of interaction is(are) not yet well understood. LL-37 uses FPRL1 as a receptor to mediate its action on monocytes, human peripheral blood neutrophils, T cells [15] and endothelial cells [23]. In human keratinocyte cell line HaCaT, binding of LL-37 to FPRL1 induces the migration, the activation of transcriptional factors and of matrix metalloproteinases and the triggering of MAPK and PI3-kinase/Akt signaling pathways, which are also mediated by transactivation of EGFR [37]. In HUVECs, LL-37-induced chemotactic migration and proliferation is prevented by F2L [49], a peptide derived from heme-binding protein which has been identified as an endogenous FPRL2 ligand [50]. LL-37 is also demonstrated to promote the processing and release of IL-1β from monocytes via the activation of the nucleotide receptor $P2X_7$ [51] and to induce suppression of neutrophils apoptosis via the activation of FPRL1 and $P2X_7$ [22]. The ability of LL-37 to utilize different receptors is further supported by the observation that lung epithelial cells express high- and low-affinity receptors for LL-37 and the low-affinity appears to be FPRL1 [40]. Moreover, in primary human monocytes [39] and in airway epithelial cells [38] LL-37-induced ERKs activation was not affected by PTX treatment, indicating that the intracellular signaling cascade was not linked to the FPRL1 receptor [38,39]. In these cells, further to PTX-insensitive GPCR, ERKs phosphorylation by LL-37 requires tyrosine kinase activity of EGFR via metalloproteinase-dependent processing of EGFR ligands [38,52] suggesting that LL-37 may act on different target cells through different signaling pathways.

An open issue is the source of NADPH for the signaling cascade. The pentose phosphate pathway is the principal source of NADPH via glucose-6-phosphate dehydrogenase. In endothelial cells NADPH is required as a cofactor for NADPH oxidase and its levels reflect an increased oxidative stress state that is, in part, attributable to NADPH oxidase and/or endothelial nitric oxide synthase [53,54]. NADPH is also required as source of reducing equivalents to maintain reduced glutathione stores. In vascular endothelial cells, specific oxidized components of LDL particles, such as ox-PAPC, induce superoxide generation that appears to be mediated largely by NADPH oxidase activity [55]. Pretreatment of these cells with 2-deoxyglucose, an antimetabolite that blocks NADPH production by the pentose phosphate shunt, significantly reduces the rate of superoxide generation [55]. These finding suggest that in ox-PAPC-stimulated vascular cells, NADPH oxidase activity requires the activation of the pentose phosphate pathway as principal source of NADPH. The role of the pentose phosphate shunt of glucose metabolism in LL-37-stimulated human fibroblasts is under examination.

Our results demonstrate that ERKs phosphorylation is required for NADPH-dependent superoxide generation in LL-37-stimulated human fibroblasts and this observation evokes the question on the biological meaning of the binding of LL-37 to FPRL1. It could be hypothesized a role in the innate immune system for these cells which could be attracted into a injury to release ROS in response to LL-37 via FPRL1 activation or to begin the repair process of the damage. The detailed understanding of the LL-37-induced intracellular signaling cascade could allow the design of new drugs able to interfere on FPRL1 signaling pathway and on LL-37/FPRL1 interaction.

Taken together, our study provides insight in the role of LL-37 in the modulation of host defence of human fibroblasts and in the molecular mechanisms involved in NADPH oxidase-like regulation.

Acknowledgments

This work was supported by Grants from Ministero dell'Università e della Ricerca Scientifica e Tecnologica PRIN 2007 "Attivazione dei recettori per formil-peptidi e regolazione della NADPH ossidasi in linee cellulari tumorali umane non fagocitiche".

References

[1] F. Niyonsaba, I. Nagaoka, H. Ogawa, Crit. Rev. Immunol. 26 (2006) 545–576.
[2] H.P. Jia, B.C. Schutte, A. Schudy, R. Linzmeier, J.M. Guthmiller, G.K. Johnson, B.F. Tack, J.P. Mitros, A. Rosenthal, T. Ganz, P.B. McGray Jr., Gene 263 (2001) 211–218.
[3] B.C. Schutte, J.P. Mitros, J.A. Bartlett, J.D. Walters, H.P. Jia, M.J. Welsh, T.L. Casavant, P.B. McGray Jr., Proc. Natl. Acad. Sci. USA 99 (2002) 2129–2133.
[4] R.I. Lehrer, T. Ganz, Curr. Opin. Immunol. 11 (1999) 23–27.
[5] R. Bals, X. Wang, M. Zasloff, J.M. Wilson, Proc. Natl. Acad. Sci. USA 95 (1998) 9541–9546.
[6] B. Agerberth, J. Charo, J. Werr, B. Olsson, F. Idali, L. Lindbom, R. Kiessling, H. Jörnvall, H. Wigzell, G.H. Gudmundsson, Blood 96 (2000) 3086–3093.
[7] G.H. Gudmundsson, B. Agerberth, J. Odeberg, T. Bergman, B. Olsson, R. Salcedo, Eur. J. Biochem. 238 (1996) 325–332.
[8] J. Cowland, A. Johnsen, N. Borregaard, FEBS Lett. 368 (1995) 173–176.

[9] M. Frohm, B. Agerberth, G. Ahangari, M. Stâhle-Bäckdahl, S. Lidén, H. Wigzell, G.H. Gudmundsson, J. Biol. Chem. 272 (1997) 15258–15263.
[10] M. Frohm, H. Gunne, A.C. Bergman, B. Agerberth, T. Bergman, A. Boman, S. Lidén, H. Jörnvall, H.G. Boman, Eur. J. Biochem. 237 (1996) 86–92.
[11] M. Zanetti, R. Gennaro, D. Romeo, FEBS Lett. 374 (1995) 1–5.
[12] V. Nizet, T. Ohtake, X. Lauth, J. Trowbridge, J. Rudisill, R.A. Dorschner, V. Pestonjamasp, J. Piraino, K. Huttner, R.L. Gallo, Nature 414 (2001) 454–457.
[13] K. Pütsep, G. Carlsson, H.G. Boman, M. Andersson, Lancet 360 (2002) 1144–1149.
[14] R. Bals, D.J. Weiner, A.D. Moscioni, R.E. Meegalla, J.M. Wilson, Infect. Immun. 67 (1999) 6084–6089.
[15] D. Yang, Q. Chen, A.P. Schmidt, G.M. Anderson, J.M. Wang, J. Wooters, J.J. Oppenheim, O. Chertov, J. Exp. Med. 192 (2000) 1069–1074.
[16] F. Niyonsaba, K. Iwabuchi, A. Someya, M. Hirata, H. Matsuda, H. Ogawa, I. Nagaoka, Immunology 106 (2002) 20–26.
[17] F. Niyonsaba, A. Someya, M. Hirata, H. Ogawa, I. Nagaoka, Eur. J. Immunol. 31 (2001) 1066–1075.
[18] X. Chen, F. Niyonsaba, H. Ushio, I. Nagaoka, S. Ikeda, K. Okumura, H. Ogawa, J. Dermatol. Sci. 43 (2006) 63–66.
[19] F. Niyonsaba, H. Ushio, I. Nagaoka, K. Okumura, H. Ogawa, J. Immunol. 175 (2005) 1776–1784.
[20] F. Niyonsaba, H. Ushio, N. Nakano, W. Ng, K. Sayama, K. Hashimoto, I. Nagaoka, K. Okumura, H. Ogawa, J. Invest. Dermatol. 127 (2007) 594–604.
[21] Y. Zheng, F. Niyonsaba, H. Ushio, I. Nagaoka, S. Ikeda, R. Okamura, H. Ogawa, Brit. J. Dermatol. 157 (2007) 1124–1131.
[22] I. Nagaoka, H. Tamura, M. Hirata, J. Immunol. 176 (2006) 3044–3052.
[23] R. Koczulla, G. von Degenfeld, C. Kupatt, F. Krötz, S. Zahler, T. Gloe, K. Issbrücker, P. Unterberger, M. Zaiou, C. Lebherz, A. Karl, P. Raake, A. Pfosser, P. Boekstegers, U. Welsch, P.S. Hiemstra, C. Vogelmeier, R.L. Gallo, M. Clauss, R. Bals, J. Clin. Invest. 111 (2003) 1665–1672.
[24] J.D. Heilborn, M.F. Nilsson, G. Kratz, G. Weber, O. Sørensen, N. Borregaard, M. Ståhle-Bäckdahl, J. Invest. Dermatol. 120 (2003) 379–389.
[25] S. Fiore, J.F. Maddox, H.D. Perez, C.N. Serhan, J. Exp. Med. 180 (1994) 253–259.
[26] Y. Le, P.M. Murphy, J.M. Wang, Trends Immunol. 23 (2002) 541–548.
[27] A. Iaccio, A. Angiolillo, R. Ammendola, Curr. Sign. Transd. Therapy 3 (2008) 88–96.
[28] R. Ammendola, L. Russo, C. De Felice, F. Esposito, T. Russo, F. Cimino, Free Rad. Biol. Med. 36 (2004) 189–200.
[29] S.H. Baek, J.K. Seo, C. B Chae, P.G. Suh, S.H. Ryu, J. Biol. Chem. 271 (1996) 8170–8175.
[30] A. Iaccio, C. Collinet, N. Montesano Gesualdi, R. Ammendola, Arch. Biochem. Biophys. 459 (2007) 288–294.
[31] R. Ammendola, M.R. Ruocchio, G. Chirico, L. Russo, C. De Felice, F. Esposito, T. Russo, F. Cimino, Arch. Biochem. Biophys. 397 (2002) 253–257.
[32] L.J. Robinson, S. Pang, D.S. Harris, J. Heuser, D. James, J. Cell Biol. 117 (1992) 1181–1196.
[33] M.M. Bradford, Anal. Biochem. 72 (1976) 248–254.
[34] R. Levy, D. Rotrosen, O. Nagauker, T.L. Leto, H.L. Malech, J. Immunol. 145 (1990) 2595–2601.
[35] S.M. Zughaier, W.M. Shafer, D.S. Stephens, Cell Microbiol. 7 (2005) 1251–1262.
[36] M. von Köckritz-Blickwede, O. Goldmann, P. Thulin, K. Heinemann, A. Norrby-Teglund, M. Rohde, E. Medina, Blood 111 (2008) 3070–3080.
[37] M. Carretero, M.J. Escàmez, M. Garcìa, B. Duarte, A. Holguìn, L. Retamosa, J.L. Lorcano, M. del Rìo, F. Larcher, J. Invest. Dermatol. 128 (2008) 223–236.
[38] G.S. Tjabringa, J. Aarbiou, D.K. Ninaber, J.W. Drijfhout, O.E. Sørensen, N. Borregaard, K.F. Rabe, P.S. Hiemstra, J. Immunol. 171 (2003) 6690–6696.
[39] D.M.E. Bowdish, D.J. Davidson, D.P. Speert, R.E.W. Hancock, J. Immunol. 172 (2004) 3758–3765.
[40] Y.E. Lau, A. Rozek, M.G. Scott, D.L. Goosney, D.J. Davidson, R.E. Hancock, Infect. Immun. 73 (2005) 583–591.
[41] Y.S. Bae, H.Y. Lee, E.J. Jo, J.I. Kim, H.K. Kang, R.D. Ye, J.Y. Kwak, S.H. Ryu, J. Immunol. 173 (2004) 607–614.
[42] P.G. Heyworth, J.T. Curnutte, W.M. Nauseef, B.D. Volpp, D.W. Pearson, H. Rosen, R.A. Clark, J. Clin. Invest. 87 (1991) 352–356.
[43] M.E. Kleinberg, H.L. Malech, D.A. Miatl, T.L. Leto, Biochemistry 33 (1994) 2490–2495.
[44] A. Shiose, J. Kuroda, K. Tsuruya, M. Hirai, H. Hirakata, S. Naito, M. Hattori, Y. Sakaki, H. Sumimoto, J. Biol. Chem. 276 (2001) 1417–1423.
[45] Y. Le, J. Hu, W. Gong, W. Shen, B. Li, N.M. Dunlop, D.O. Halverson, D.G. Blair, J.M. Wang, J. Neuroimmunol. 111 (2000) 102–108.
[46] J.Y. Hu, Y. Le, W. Gong, N.M. Dunlop, J.L. Gao, P.M. Murphy, J.M. Wang, J. Leukoc. Biol. 70 (2001) 155–161.
[47] S. Devadas, L. Zaritskaya, S.G. Rhee, L. Oberley, M.S. Williams, J. Exp. Med. 195 (2002) 59–70.
[48] B. Rivas-Santiago, R. Hernandez-Pando, C. Carranza, E. Juarez, J.L. Contreras, D. Aquilar-Leon, M. Torres, M. Sada, Infect. Immun. 76 (2008) 935–941.
[49] S.Y. Lee, M.S. Lee, H.Y. Lee, S.D. Kim, J. W Shim, S.H. Jo, J.W. Lee, J.Y. Kim, Y.W. Choi, S.H. Baek, S.H. Ryu, Y.S. Bae, FEBS Lett. 582 (2008) 273–278.
[50] I. Migeotte, E. Riboldi, J.D. Franssen, F. Grégoire, C. Loison, V. Wittamer, M. Detheux, P. Robberecht, S. Costagliola, G. Vassart, S. Sozzani, M. Parmentier, D. Communi, J. Exp. Med. 201 (2005) 83–93.
[51] A. Elssner, M. Duncan, M. Gavrilin, M.D. Wewers, J. Immunol. 172 (2004) 4987–4994.
[52] R. Shaykhiev, C. Beisswenger, K. Kändler, J. Senske, A. Püchner, T. Damm, J. Behr, R. Bals, Am. J. Physiol. Lung Cell. Mol. Physiol. 289 (2005) L842–L848.
[53] J.A. Leopold, A. Cap, A.W. Scribner, R.C. Stanton, J. Loscalzo, FASEB J. 15 (2001) 1771–1773.
[54] C.F. Mueller, K. Laude, J.S. McNally, D.G. Harrison, Arterioscler. Thromb. Vasc. Biol. 25 (2005) 274–278.
[55] M. Rouhanizadeh, J. Hwang, R.E. Clempus, L. Marcu, B. Lassègue, A. Sevanian, T.K. Hsiai, Free Rad. Biol. Med. 39 (2005) 1512–1522.

Cellular Signalling 23 (2011) 1961–1971

Contents lists available at ScienceDirect

Cellular Signalling

journal homepage: www.elsevier.com/locate/cellsig

Intracellular signaling cascades triggered by the NK1 fragment of hepatocyte growth factor in human prostate epithelial cell line PNT1A ☆

Luigi Michele Pavone [a], Fabio Cattaneo [a], Silviana Rea [a,b], Valeria De Pasquale [a], Anna Spina [a,b], Elena Sauchelli [a], Vincenzo Mastellone [c], Rosario Ammendola [a,*]

[a] Department of Biochemistry and Medical Biotechnologies, University of Naples Federico II, Via S. Pansini 5, 80131 Naples, Italy
[b] Department of Biological Structures, Functions and Technologies, University of Naples Federico II, Via F. Delpino 1, 80137 Naples, Italy
[c] Department of Experimental Medicine "G. Salvatore", University of Magna Graecia, Viale Europa, Germaneto, 88100 Catanzaro, Italy

ARTICLE INFO

Article history:
Received 11 April 2011
Received in revised form 21 June 2011
Accepted 4 July 2011
Available online 12 July 2011

Keywords:
Hepatocyte growth factor
c-MET
Signal transduction
Cell growth
Prostate

ABSTRACT

Hepatocyte Growth Factor (HGF)/c-MET signaling has an emerging role in promoting cell proliferation, survival, migration, wound repair and branching in a variety of cell types. HGF plays a crucial role as a mediator of stromal–epithelial interactions in the normal prostate but the precise biological function of HGF/c-Met interaction in the normal prostate and in prostate cancer is not clear. HGF has two naturally occurring splice variants and NK1, the smallest of these HGF variants, consists of the HGF amino terminus through the first kringle domain. We evaluated the intracellular signaling cascades and the morphological changes triggered by NK1 in human prostate epithelial cell line PNT1A which shows molecular and biochemical properties close to the normal prostate epithelium. We demonstrated that these cells express a functional c-MET, and cell exposure to NK1 induces the phosphorylation of tyrosines 1313/1349/1356 residues of c-MET which provide docking sites for signaling molecules. We observed an increased phosphorylation of ERK1/2, Akt, c-Src, p125FAK, SMAD2/3, and STAT3, down-regulation of the expression of epithelial cell–cell adhesion marker E-cadherin, and enhanced expression levels of mesenchymal markers vimentin, fibronectin, vinculin, α-actinin, and α-smooth muscle actin. This results in cell proliferation, in the appearance of a mesenchymal phenotype, in morphological changes resembling cell scattering and in wound healing. Our findings highlight the function of NK1 in non-tumorigenic human prostatic epithelial cells and provide a picture of the signaling pathways triggered by NK1 in a unique cell line.

1. Introduction

Hepatocyte growth factor (HGF) and the c-MET tyrosine kinase receptor form a unique ligand-receptor signaling system. HGF is also known as a scattering factor, and its signaling through c-MET activation is involved in promoting cell proliferation, survival, migration, wound repair and cell migration in a variety of cell types [1,2]. HGF plays a crucial role as a mediator of stromal–epithelial interactions in the normal prostate; however, its specific function on c-MET-expressing epithelial cells has not been fully defined [3]. In normal prostatic epithelium c-MET expression is restricted to the basal epithelial cell layer and to a subpopulation of luminal ductal epithelial cells [4]. HGF biological activity in the conditioned medium of mouse prostatic stromal cells, in immortalized human myofibroblastic prostate stromal cells (PrSC), and in primary PrSC stimulates the scattering, motility, and collagen gel invasion of prostate cancer cells as well as the proliferation of mouse prostate epithelial cells (PrEC) [4–8]. Despite an understanding of the c-MET expression pattern in normal and malignant PrECs, the precise biological function of HGF/c-MET interaction in the normal prostate and in prostate cancer is not clear. In fact, whereas HGF stimulation of normal primary PrECs results in growth inhibition, transformed prostate cancer cells proliferate on HGF stimulation [9].

Following HGF binding, the kinase activity of c-MET is switched on by receptor dimerization and trans-phosphorylation of two catalytic tyrosine residues within the kinase activation loop. The subsequent step is the phosphorylation of two additional tyrosines in the carboxy-terminal tail (Tyr1349 and Tyr1356) which provide docking sites for phosphatidylinositol 3-kinase (PI3K), Grb2 and Gab1, as well as for other signaling molecules [10]. Gab1 is an insulin receptor substrate-1-like protein that is phosphorylated by c-MET through direct interaction with Tyr1349 and is involved in the activation of mitogen-activated protein kinase (MAPK) through the Gab1/Grb2-SOS-Ras pathway [10]. Trans-phosphorylation of the docking site of c-

☆ Contributions. L.M.P., F.C. and S.R. performed the experiments; V.D.P. and A.S. supported the experiments with technical assistance for microscopy and immunofluorescence data acquisition and analysis, E.S and V.M. have given technical supports for all the experiments; L.M.P. and R.A. designed the experiments, analyzed data and wrote the paper. All authors discussed the results and commented on the manuscript.

* Corresponding author at: Department of Biochemistry and Medical Biotechnologies, University of Naples Federico II, Via S. Pansini 5, 80131 Naples, Italy. Tel.: +39 0817463145; fax: +39 081 7464359.
E-mail address: rosario.ammendola@unina.it (R. Ammendola).

0898-6568/$ – see front matter © 2011 Elsevier Inc. All rights reserved.
doi:10.1016/j.cellsig.2011.07.005

MET induces the association of the signal transducer and activator of transcription 3 (STAT3) with its tail, followed by c-MET-dependent tyrosine phosphorylation of STAT3. This causes the dissociation of STAT3 from c-MET and its homodimerization through SH2 domains. STAT3 dimers translocate to the nucleus, where they act as transcription factors involved in the regulation of the expression of several genes [10]. All these pathways positively control c-MET-dependent cell growth, survival and migration [11].

HGF has two naturally occurring splice variants. While full-length HGF is a heterodimeric protein of 90 kDa that includes four kringle domains, the smallest of these HGF variants, NK1, consists only of the HGF amino terminus through the first kringle domain [12]. The biological activities of NK1 are not fully understood. NK1 was initially characterized as an HGF antagonist, since it was able to compete with full-length HGF for binding to c-MET but lacked intrinsic mitogenic activity in primary rat hepatocyte cultures [12]. Subsequent studies on cultured cells have shown that NK1 acts as a c-MET agonist, but requires the presence of heparan sulfate for full activity [13,14]. In vitro studies have shown, however, that there are important differences in NK1 activity that depend on the cell types used. While NK1 can act as an HGF antagonist on primary hepatocytes, it behaves as a partial agonist on mink lung epithelial cells [15], human mammary epithelial cells [12] and Chinese hamster ovary cells [16]. The discrepancy observed on the agonistic activity of NK1 may be explained by differences in the glycosaminoglycane composition of the cells, such as heparane sulfate [17,18]. In vivo studies in transgenic mice, however, have clearly established that NK1 is a potent c-MET activator [19].

The differential signaling pathways of the HGF variants in controlling cell growth and invasion have been analyzed in human breast cancer cells [20]. All the HGF variants inhibit the vigorous growth of the cancer cells, showing significative differences with full-length HGF stimulation of normal primary PrECs and transformed prostate cancer cells [9].

In this study we explored the signaling cascades triggered by the NK1 fragment of HGF in human prostate epithelial cell line PNT1A. These cells have been proved to be a good model for the analysis of cellular processes [21] and can be considered as non-tumorigenic cells showing molecular and biochemical properties close to the normal prostate epithelium [22]. The results show that PNT1A cells express a functional c-MET receptor and that stimulation with NK1 induces: i) a rapid phosphorylation of c-MET Tyr1313/1349/1356 residues which provide docking sites for the activation of extracellular signal-regulated kinases (ERKs) and STAT3 pathways; ii) PNT1A cell proliferation; iii) the expression of mesenchimal markers and the appearance of a mesenchymal phenotype; iv) the activation of PI3K/Akt signaling pathway and morphological changes resembling cell scattering; v) the activation of the focal adhesion kinase p125FAK and c-Src, and wound healing.

2. Materials and methods

2.1. Antibodies and chemicals

Primary antibodies used in this study: mouse anti-activated diphosphorylated ERK1/2 monoclonal antibody (M8159), rabbit anti-ERK1/2 polyclonal antibody (M5670), mouse anti-α-actinin monoclonal antibody (A7811), mouse anti-vinculin monoclonal antibody (V9131), mouse anti-α-smooth muscle actin (α-SMA) monoclonal antibody (A5228), mouse anti-p125FAK monoclonal antibody (F2918), rabbit anti-p125FAK polyclonal antibody (F2918), mouse anti-fibronectin monoclonal antibody (F7387) were purchased from Sigma Aldrich Chemical Co. (St. Louis, MO, USA); mouse anti-phospho-tyrosine monoclonal antibody (sc-508), rabbit anti-c-MET (sc-10) polyclonal antibody, rabbit anti-phospho-c-MET(Y1313) polyclonal antibody (sc-34085), rabbit anti-phospho-c-MET(Y1349) polyclonal antibody (sc-34086), rabbit anti-phospho-SMAD2/3 polyclonal antibody (sc-11769-R), mouse anti-SMAD2/3 monoclonal antibody (sc-133098) and mouse anti-α-tubulin monoclonal antibody (sc-8035) were from Santa Cruz Biotechnology Inc. (Santa Cruz, CA, USA); rabbit anti-phospho-Akt polyclonal antibody (#9271), rabbit anti-Akt polyclonal antibody (#9272), rabbit anti-phospho-c-Src polyclonal antibody (#2101), rabbit anti-c-Src polyclonal antibody (#2108), rabbit anti-phospho-STAT3-Y705 polyclonal antibody (#9131), rabbit anti-phospho-STAT3-S727 polyclonal antibody (#9134), rabbit anti-STAT3 polyclonal antibody (#9132) were from Cell Signaling Technology Inc. (Danvers, MA, USA); rabbit anti-phospho-c-MET(Y1356) polyclonal antibody (PAB9992) from Abnova (Walnut, CA, USA); mouse anti-E-cadherin monoclonal antibody (ab1416), and rabbit anti-vimentin polyclonal antibody (ab15248) from AbCam (Cambridge, UK).

Secondary antibodies: goat anti-rabbit IgG-FITC polyclonal antibody (F0382) was purchased from Sigma Aldrich Chemical Co.; goat anti-mouse IgG polyclonal antibody conjugated to horseradish peroxidase (HRP) (sc-2031) and goat anti-rabbit IgG-HRP polyclonal antibody (sc-3837) were from Santa Cruz Biotechnology Inc.

Chemicals: nuclear 4′,6-diamidino-2-phenylindole (DAPI) counterstaining was purchased from Santa Cruz Biotechnology Inc.; SDS-PAGE reagents were from Bio-Rad (Richmond, CA, USA); Protein-A sepharose beads (CL-4B) were from Amersham Pharmacia Biotech (Little Chalfont, Bukinghamshire, UK); the c-MET inhibitor SU11274 [(3Z)-N-(3-Chlorophenyl)-3-({3,5-dimethyl-4-[(4-methylpiperazin-1-yl)carbonyl]-1H-pyrrol-2-yl}methylene)-N-methyl-2-oxo-2,3 dihydro-1H-indole-5-sulfonamide] and fibronectin from human plasma (F2006) were from Sigma Aldrich Chemical Co; the MEK inhibitor PD098059 [2-(2′-amino-3′-methoxyphenyl)-oxanaphthalen-4-one], the PI3K inhibitor wortmannin, and anti-photo-bleaching mounting media Mowiol were from Calbiochem (La Jolla, CA, USA); the PI3K inhibitor LY294002 [2-(4-morpholinyl)-8-phenyl-4H-1-benzopyran-4- one] was purchased from Cayman Chemical (Ann Arbor, MI, USA).

The recombinant NK1 fragment of HGF was produced using a transformed methylotrophic yeast *Pichia pastoris*, GS115 strain, kindly provided by prof. E. Gherardi (Laboratory of Molecular Biology, MRC Centre, Cambridge, U.K.). The recombinant NK1 was purified by heparin affinity chromatography according to the procedure described by Chirgadze et al. [23]. The purified recombinant NK1 was diluted in sterile water for a stock solution of 1 mM.

2.2. Cell culture

Human prostate epithelial cells PNT1A were purchased from ATCC (Rockville, MD, USA). The cells were grown in RPMI supplemented with 10% heat-inactivated fetal bovine serum (FBS), 100 U/ml penicillin, 100 μg/ml streptomycin, 1% L-glutamine. Cells were stimulated with recombinant NK1, diluted in the medium to different final concentrations. In some experiments, PNT1A cells were pre-incubated with the following selective inhibitors: PD098059 (50 μM) for 90 min, or LY294002 (50 μM) for 1 h, or wortmannin (0.5 μM) for 1 h, or SU11274 (2 μM) for 16 h, before NK1 stimulation. The used concentrations of these inhibitors were not cytotoxic as assessed by trypan blue exclusion method (data not shown).

In other experiments, cells were trypsinized, washed in RPMI containing 10% FBS and re-suspended at the appropriate concentration in RPMI with the indicated FBS amount. They were plated on glass or plastic tissue culture dishes either uncoated or fibronectin-coated as indicated.

2.3. Immunofluorescence analysis

The PNT1A cells were plated into glass chamber slides (BD Bioscience, Bedford, MA, USA) and cultured until approximately 60% confluency. The cells were washed twice in phosphate buffered saline

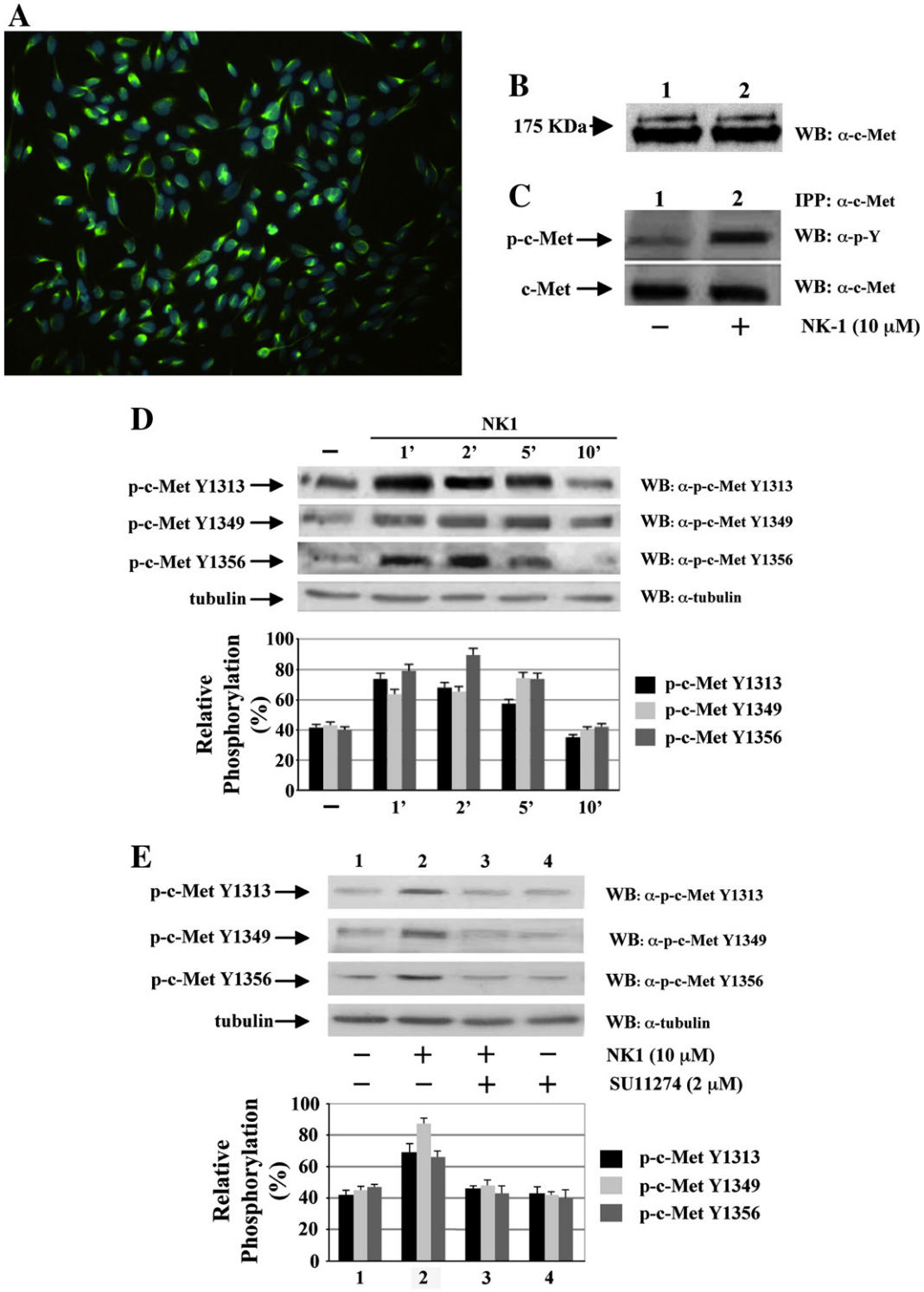

Fig. 1. c-MET expression and NK1-induced tyrosine phosphorylation of c-MET in human prostate epithelial cells PNT1A. (A) PNT1A cells were cultured until approximately 60% confluency and fixed for 30 min in 4% paraformaldehyde at 4 °C. Fixed cells were incubated overnight at 4 °C with an anti-c-MET primary antibody and then incubated with secondary fluorescein-isothiocyanate (FITC) conjugated antibody for 2 h at 4 °C. The slides were incubated with DAPI to counterstain the nuclei, observed using a Nikon Eclipse TE300 fluorescent microscope and photographed. The nuclei of PNT1A cells stained with DAPI appear in blue, whereas c-MET immunostaining appears in green. (B) Cell lysates were purified from PNT1A (lane 1) and HepG2 cells (lane 2). A 10% SDS-PAGE was loaded with 50 μg of proteins and c-MET was detected by western blot using an anti-c-MET antibody (α-c-Met). (C) Eight hundred micrograms of proteins, from untreated PNT1A cells (lane 1) and cells exposed to 10 μM NK1 for 5 min (lane 2), were immunoprecipitated (IPP) with an anti-c-MET antibody (α-c-Met) and c-MET tyrosine phosphorylation (p-c-Met) was detected by using an anti-phosphotyrosine (α-pY) antibody. An anti-c-Met antibody served as a control of protein loading. (D) Cell lysates were obtained from untreated (−) and cells exposed to 10 μM NK1 for the indicated times. Fifty micrograms of proteins were resolved on a 10% SDS-PAGE and subjected to immunoblotting analysis with anti-phospho-c-Met(Y1313) [α-p-c-Met(1313)], anti-phospho-c-Met(Y1349) [α-p-c-Met(1349)], and anti-phospho-c-Met(Y1356) [α-p-c-Met(1356)] antibodies. An anti-tubulin (α-tubulin) antibody served as a control of protein loading. (E) PNT1A cells were exposed to NK1 for 5 min either in the presence or in the absence of SU11274. Cells were also exposed only to 2 μM SU11274 (lane 4). Proteins (50 μg) were loaded on 10% SDS-PAGE and tyrosine phosphorylation was detected by using anti-phospho-c-Met(Y1313), anti-phospho-c-Met(Y1349) and anti-phospho-c-Met(Y1356) antibodies. The same filters were reprobed with an anti-tubulin antibody. All the blots are representative of at least three separate experiments of identical design.

(PBS), fixed for 30 min in 4% paraformaldehyde in PBS at 4 °C and washed three times for 5 min shaking at room temperature (RT). Fixed cells were then incubated for 1 h at RT shaking in a blocking solution of 5% bovine serum albumin (BSA) in PBS. After two washes in PBS for 5 min shaking at RT, the cells were incubated overnight at 4 °C with the anti-c-MET primary antibody diluted 1:100 in PBS. The day after, the cells were washed twice in PBS for 5 min shaking at RT. The cells were then incubated with secondary fluorescein-isothiocyanate (FITC) conjugated antibody for 2 h at 4 °C. After washing in PBS, the slides were incubated for 7 min at 4 °C with DAPI, diluted 1:500 in PBS to counterstain the nuclei and washed twice. Coverslips were mounted on slides using Mowiol mounting medium. Slides were observed using a Nikon Eclipse TE300 fluorescent microscope and photographed.

2.4. Proliferation assay

PNT1A cells were seeded in 24-well plates at a concentration of 100,000 cells per well and grown overnight in complete RPMI medium. The cells were washed and then grown for 24 h in RPMI containing 1% FBS. The cells were then incubated with NK1 diluted in the same medium at different concentrations in the range 10^{-11}–10^{-6} M. Control cells (CTR) were treated with the medium without

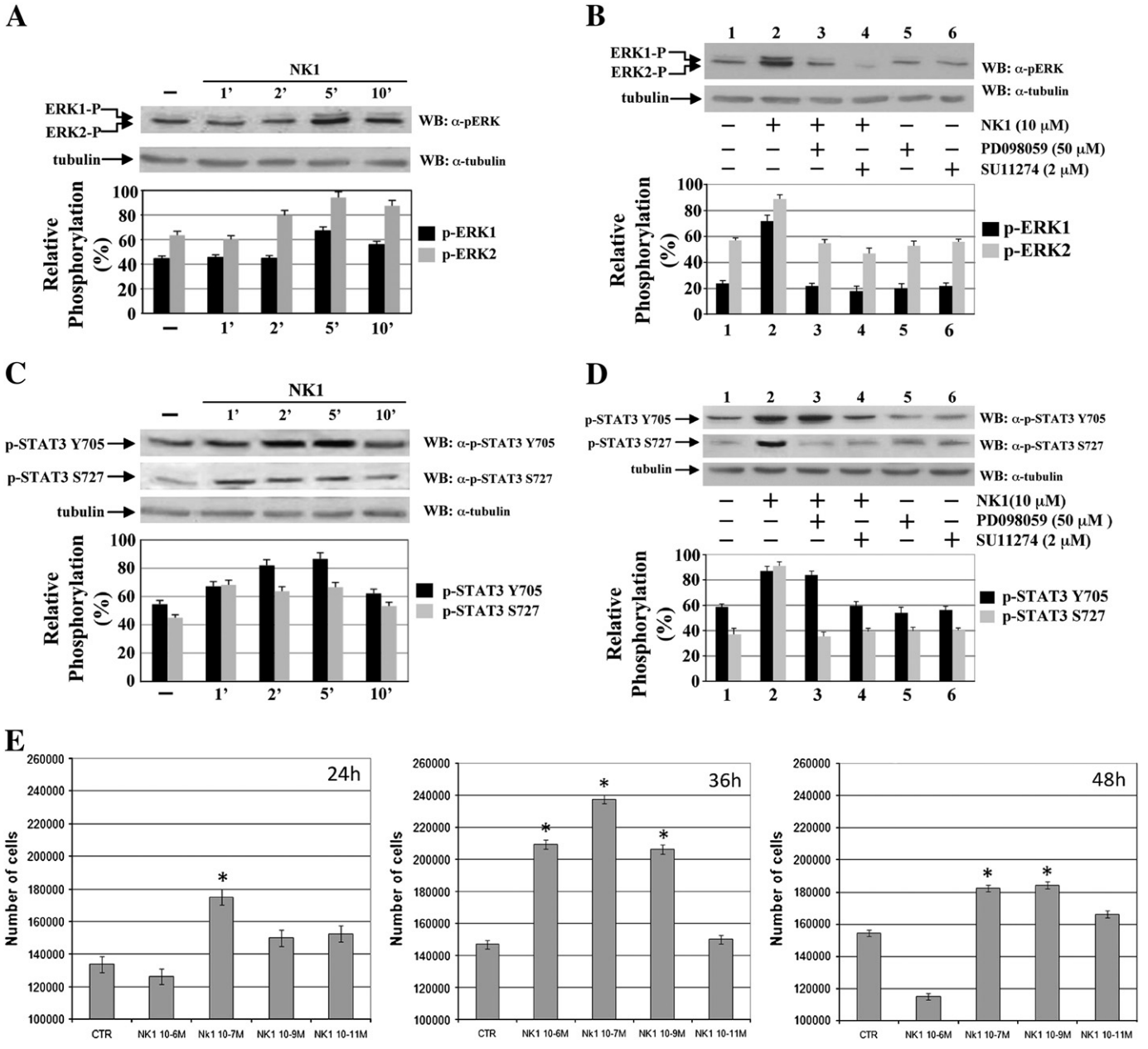

Fig. 2. NK1 triggers Ras/MAPK and STAT3 pathways and promotes cell proliferation. (A and C) Cell lysates were purified from untreated (−) and PNT1A cells exposed to 10^{-6} M NK1 for the indicated times. (B and D) PNT1A cells were exposed to NK1 for 5 min either in the absence (lane 2) or in the presence of PD098059 (lanes 3) or SU11274 (lanes 4) at the indicated concentrations. Cells were also incubated only with PD098059 (lane 5) or SU11274 (lane 6), as a control. Proteins (50 μg) were resolved on 10% SDS-PAGE. (A and B) ERKs phosphorylation was detected by western blot with an anti-phosphoERK antibody (α-pERK). The arrows indicate the phosphorylated forms (ERK1-P and ERK2-P) of $p44^{MAPK}$ and $p42^{MAPK}$, respectively. (C and D) STAT3 phosphorylation on Y705 or S727 residues was immunodetected by using an anti-phospho-STAT3 Y505 (α-p-STAT3 Y705) or an anti-phospho-STAT3 S727 (α-p-STAT3 S727) antibody, respectively. An anti-tubulin antibody served as a control of protein loading. The experiments were performed in triplicate. (E) PNT1A cells were exposed to NK1 for the indicated times and concentrations. Untreated cells (CTR) served as a control. The number of viable cells was determined by the trypan blue exclusion method. The data reported represent the mean values from three independent experiments performed in triplicate. Vertical bars indicate s. e. m. * $P<0.05$.

the addition of NK1. After 24, 36 and 48 h of incubation at 37 °C, the cells were trypsinized and the number of alive cells, resuspended in a solution of trypan blue, was determined by direct counts by using a hemocytometer. The data reported are the means of three independent experiments performed with each sample in replicates of three. Error bars indicate standard errors of the means (s. e. m.). Student's *t* test was used for statistical comparisons and differences were considered significant at $P<0.05$.

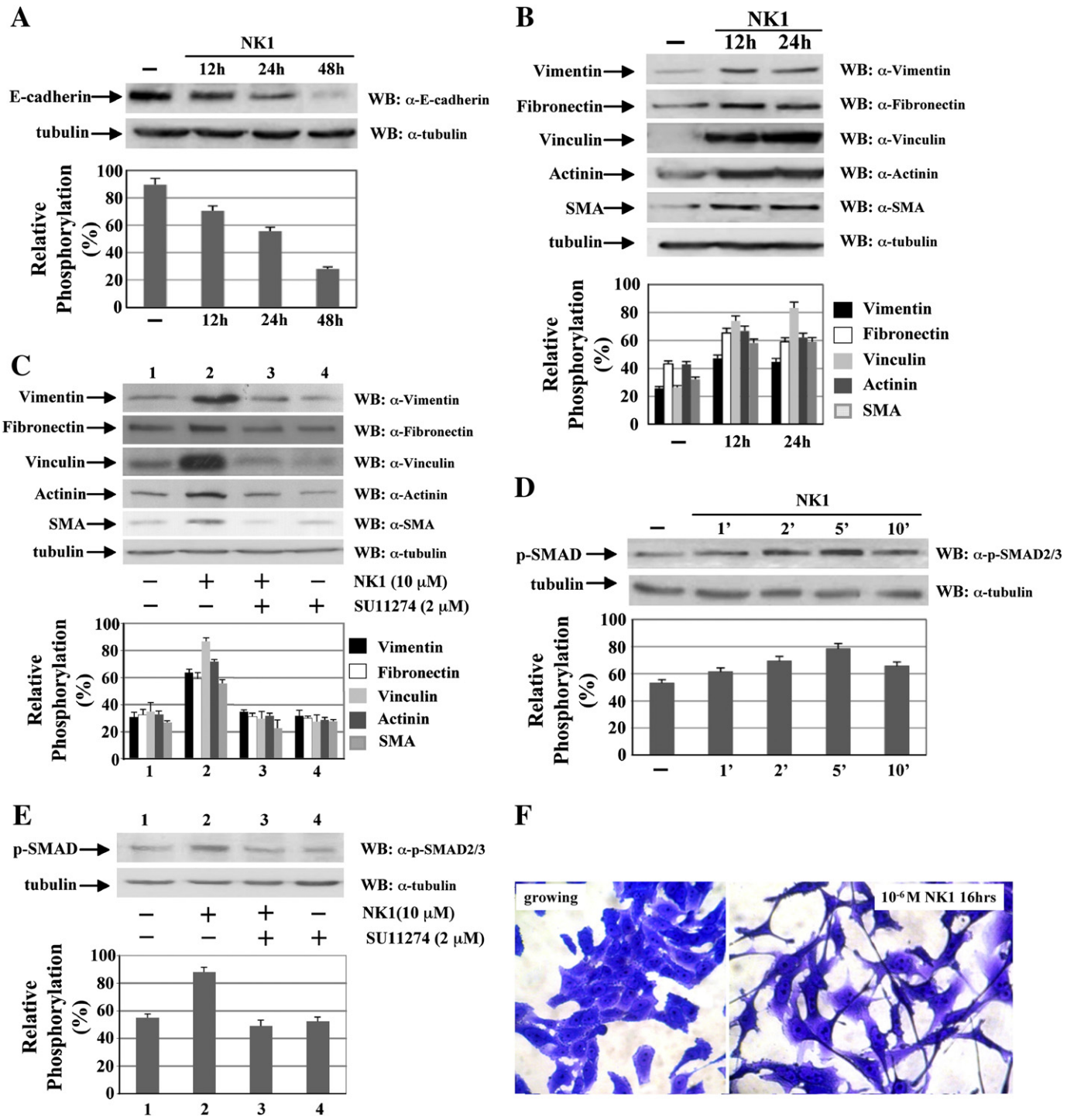

Fig. 3. NK1 promotes down-regulation of E-cadherin and expression of mesenchimal markers. (A, B and D) PNT1A cells were exposed to 10^{-6} M NK1 for the indicated times. Cell lysates (50 μg) were resolved on 10% SDS-PAGE and E-cadherin, Fibronectin, Vinculin, Actinin and SMA (A and B) or phospho-SMAD (p-SMAD2/3) (D) were immunodetected with the appropriate antibodies as indicated. (C and E) Cell lysates were obtained from PNT1A cells exposed to 10^{-6} M NK1 either in the absence (lane 2) or in the presence (lane 3) of SU11274. Cells were also incubated only with SU11274 (lane 4). A 10% SDS-PAGE was loaded with 50 μg of proteins and Fibronectin, Vinculin, Actinin and SMA (C) or phospho-SMAD (p-SMAD2/3) (E) were detected by western blot by using specific antibodies. An anti-tubulin antibody served as a control of protein loading. The blots are representative of at least three separate experiments of identical design. (F) PNT1A cells were plated in 96-well plates at a concentration of 35,000 cells/well in the absence or in the presence of 10^{-6} M NK1 for 16 h. The cells were fixed in 4% paraformaldehyde in PBS for 1 h at room temperature, then washed in PBS and stained with Coomassie brilliant blue solution for 1 h. The cells were observed under a white light microscope and photographed.

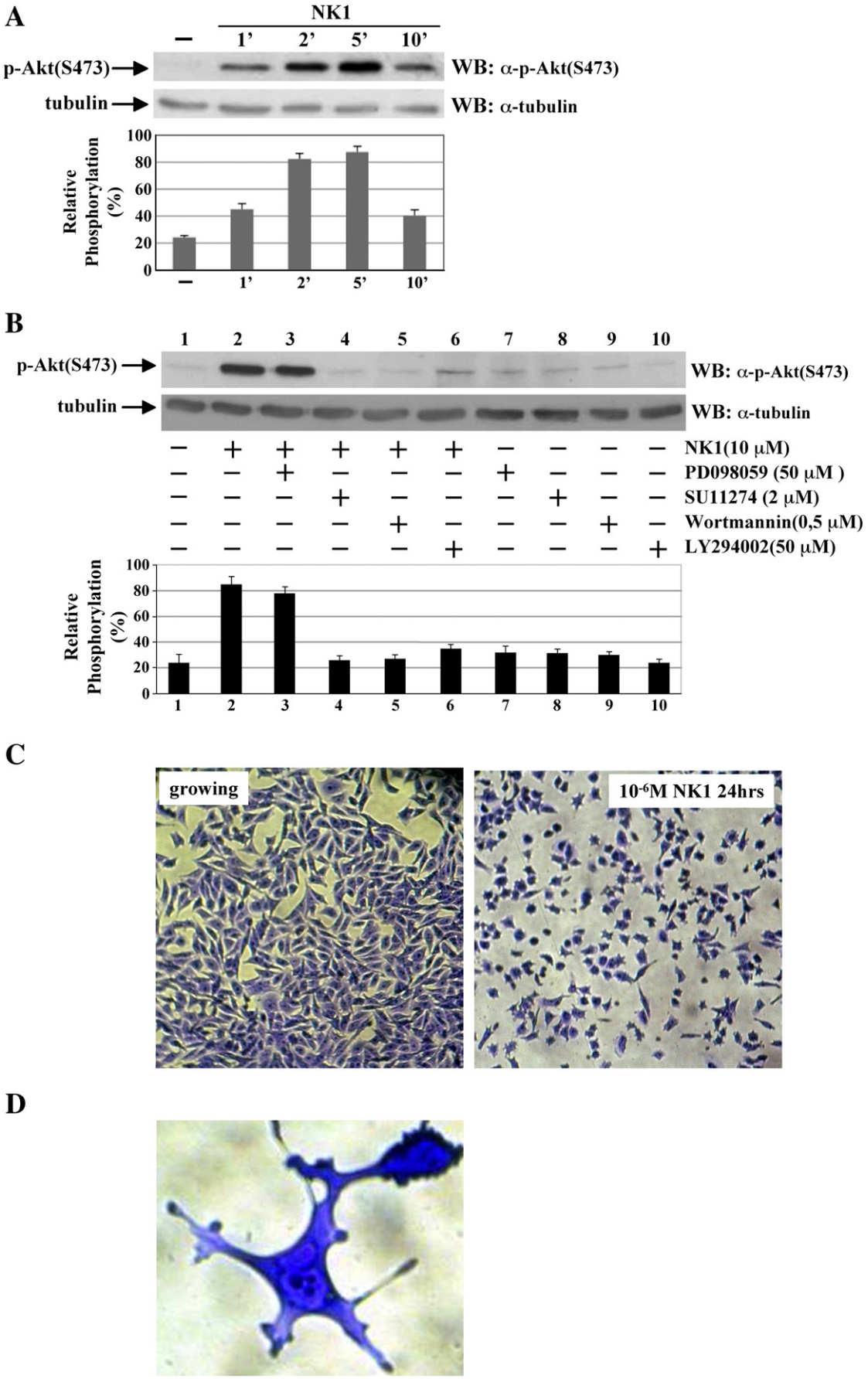
A
NK1
–
1'
2'
5'
10'
p-Akt(S473)
WB: α-p-Akt(S473)
tubulin
WB: α-tubulin
Relative Phosphorylation (%)
100
80
60
40
20
0
B
1 2 3 4 5 6 7 8 9 10
p-Akt(S473)
WB: α-p-Akt(S473)
tubulin
WB: α-tubulin
NK1(10 μM)
PD098059 (50 μM)
SU11274 (2 μM)
Wortmannin(0,5 μM)
LY294002(50 μM)
C
growing
10-6M NK1 24hrs
D

2.5. Scatter and EMT assays

PNT1A cells were plated in 96-well plates at a concentration of 35,000 cells per well in RPMI-1% FBS either in the absence or in the presence of 10 μM NK1 and grown overnight at 37 °C. The day after, the cells were washed in PBS and fixed in 4% paraformaldehyde in PBS for 1 h at RT, then washed in PBS and stained with Coomassie brilliant blue solution (0.5% Coomassie, 40% methanol, 10% acetic acid, 50% distilled water) for 1 h at RT. Next, the cells were washed in distilled water and dried up for 24 h. The cells were observed under a white light microscope and photographed.

2.6. Wound healing assay

Cells were seeded at a concentration of 100,000 cells per well in 6-well tissue culture plates uncoated or previously coated with 10 μg/ml fibronectin. The cells were grown for 24 h in RPMI supplemented with 10% FBS at 37 °C. When reaching sub-confluence, the cells were washed and grown overnight in RPMI containing 1% FBS. The day after, a wound was incised by scratching the cell monolayer using an insulin syringe needle in the middle of the plate. The cells were washed in PBS and treated with RPMI-1% FBS supplemented with 10^{-7} M NK1. After 48 h the cells were washed in PBS, fixed in 4% paraformaldehyde in PBS for 1 h at RT, then washed in PBS and stained with Coomassie brilliant blue solution for 1 h at RT. Finally, the cells were washed in distilled water and dried up for 24 h. The cells were observed under a white light microscope and photographed.

2.7. Western blotting analysis

PNT1A cells were either untreated or pre-incubated with an appropriate amount of inhibitor before stimulation with 10 μM NK1 for different times. Cells were washed in PBS and lysed with 0.5 ml RIPA buffer containing 50 mM Tris–HCl (pH 7.4), 150 mM NaCl, 1% Nonidet P40, 1 mM EDTA, 0.25% sodium deoxycholate, 10 mM NaF, 10 μM Na_3VO_4, 1 mM phenylmethylsulfonylfluoride, and a protease inhibitor cocktail (10 μg/ml aprotinin, 10 μg/ml pepstatin, 10 μg/ml leupeptin). Cell lysates were incubated at 4 °C for 45 min and centrifuged at 14,000 rpm for 15 min at 4 °C [24]. The amount of total proteins in each sample was determined by a Bio-Rad protein assay (BioRad, Hercules, CA, USA). Samples containing equal amounts of protein (50 μg) were boiled for 5 min in SDS buffer (50 mM Tris–HCl, pH 6.8, 2% SDS, 10% glycerol, 0.1% bromophenol blue, and 5% β-mercaptoethanol), separated on SDS-PAGE, and electro-transferred to Immobilion-P membrane (Millipore, Bedford, MA, USA) overnight at 4 °C. Non-specific binding was blocked with 5% dry milk in TBST (20 mM Tris–HCl, pH 7.4, 137 mM NaCl, 0.01% Tween-20) for 1 h at RT. The membranes were incubated overnight at 4 °C with the primary antibody at the appropriated dilution. After washing in TBST three times for 5 min, the membranes were incubated with the appropriate secondary antibody at RT for 45 min with constant shaking. The expression of targeted proteins was detected by an ECL kit (Amersham Pharmacia Biotech) and visualized by autoradiography [25]. Protein expression levels were quantitatively estimated by densitometry using a Discover Pharmacia scanner equipped with a sun spark classic densitometric workstation. The same blots were re-probed with anti-α-tubulin monoclonal antibody.

3. Results and discussion

3.1. PNT1A cells express a functional c-MET receptor

We first analyzed the expression of c-MET protein in non-tumorigenic prostatic epithelial cell line PNT1A. Immunofluorescence analysis shows the localization of c-MET receptor on the membrane of PNT1A cells (Fig. 1A) and by western blotting analysis we detected the presence of the band corresponding to c-MET protein at the expected molecular size of 175 kDa (Fig. 1B, lane 1). The same band is detected in lysates of human HepG2 cells which express c-MET [26] (Fig. 1B, lane 2). These results provide the first evidence of c-MET expression in the human prostate epithelial cell line PNT1A.

The mature c-MET protein may exist as an α-β complex in which the β subunit (140 kDa) is joined by disulphide bonds to a smaller α-chain of 35 kDa. c-MET activation results in the phosphorylation of several tyrosine residues which have a crucial role in the activation of signaling pathways involved in the biological activity of c-MET in response to HGF. Therefore, we next evaluated the ability of NK1 to activate c-MET in PNT1A cells and we observed that the addition of 10^{-6} M NK1 induces a rapid c-MET phosphorylation (Fig. 1C). In particular, NK1 promotes the phosphorylation of c-MET Tyr1313/1349/1356 residues in the carboxyl terminus of the receptor [27,28] within the first 5 min of stimulation (Fig. 1D). Furthermore, the NK1-induced phosphorylation of tyrosine residues of c-MET is prevented by the specific c-MET inhibitor SU11274 [29] (Fig. 1E). These results demonstrate that in PNT1A cells NK1 retains the ability of full length HGF to activate c-MET by phosphorylating critical tyrosine residues of the receptor, and support the evidence of NK1/c-MET binding [23].

3.2. NK1 promotes ERKs and STAT3 phosphorylation and cell proliferation in PNT1A cells

Phosphorylayed tyrosine residues of c-MET provide docking sites that activate intracellular signaling cascades, including MAPK and STAT pathways, which in turn lead to cell proliferation and migration [30]. HGF has been shown to activate these pathways in human cancer cell lines [31,32] and HGF stimulation of cell proliferation has been suggested to be mediated by the activation of Ras/MAPK pathway [33].

Therefore, we first evaluated the ability of NK1 to activate MAPK cascade by analyzing the effect of cell exposure to NK1 on the phosphorylation state of ERK 1/2. We observed that the treatment of PNT1A cells with 10^{-6} M NK1 induces the phosphorylation of ERK1/2 within 5 min of NK1 stimulation (Fig. 2A). The pre-incubation of PNT1A cells either with the c-MET inhibitor SU11274 or with PD098059, a selective inhibitor of MEK, before NK1 stimulation, prevents ERK1/2 phosphorylation (Fig. 2B), suggesting that in PNT1A cells the NK1-dependent activation of ERK1/2 requires c-MET phosphorylation and the subsequent activation of Ras/MAPK pathway.

Next, we evaluated the effect of NK1 on the phosphorylation of STAT3, which also actively participates in cell growth and survival processes [32]. We observed that the addition of 10^{-6} M NK1 to PNT1A cells promotes phosphorylation of STAT3 at Tyr705 and Ser727 residues (Fig. 2C), required for STAT3 dimerization/nuclear translocation and maximal transcriptional activity, respectively. The phosphorylation of Tyr705 residue of STAT3 is c-MET-dependent because it is prevented by

Fig. 4. NK1 induces the activation of PI3K/Akt signaling pathway. (A) PNT1A cells were exposed to 10^{-6} M NK1 for the indicated times and 50 μg of cell lysates were subjected to immunoblotting by using an anti-phosphoAkt(Ser473) antibody [(α-p-Akt(S473)]. (B) Cell lysates were obtained from PNT1A cells exposed to 10^{-6} M NK1 either in the absence (lane 2) or in the presence of PD098059 (lane 3), SU11274 (lane 4), wortmannin (lane 5) or LY294002 (lane 6). Cells were also incubated only with PD098059 (lane 7), or SU11274 (lane 8), or wortmannin (lane 9), or LY294002 (lane 10) as a control. Proteins (50 μg) were resolved on a 10% SDS-PAGE and phosphoAkt(Ser473) was detected by western blot with an anti-phosphoAkt(Ser473) antibody [α-p-Akt(S473)]. The same filters were reprobed with an anti-tubulin antibody (α-tubulin) to ensure equal loading of protein in all lanes. The blots are representative of at least three separate experiments of identical design. (C and D) PNT1A cells were plated in 96-well plates (35,000 cells/well) either in the absence or in the presence of 10^{-6} M NK1 for 24 h. The cells were fixed in 4% paraformaldehyde, stained with Coomassie brilliant blue solution, observed under a white light microscope and photographed.

the pre-incubation of cells with SU11274 before NK1 stimulation, and it is MEK-independent, as observed by the lack of effect of the MEK inhibitor PD098059 (Fig. 2D). By contrast, the phosphorylation of Ser727 residue of STAT3 requires both c-MET and MEK activation, as demonstrated by the effects of SU11274 or PD098059, both of which prevent STAT3 activation induced by NK1 treatment.

We also evaluated the effect of NK1 on the growth of PNT1A cells. The addition of NK1 to the cells results in a positive time- and dose-dependent growth response (Fig. 2E). NK1 induces the maximum level of PNT1A growth at the concentration of 10^{-7} M after 36 h of cell exposure. At 48 h the cells start to dye affecting the count number of proliferating cells. There is clear evidence that, whereas HGF stimulation of normal primary prostate epithelial cells results in growth inhibition, transformed prostate cancer cells proliferate on HGF stimulation [9]. Our results show that the effect of NK1 in non-tumorigenic prostate cells correlates with the proliferative activity of full length HGF in prostate cancer cells.

3.3. NK1 induces the expression of mesenchymal markers in PNT1A cells

Enhanced migratory capacity, coupled to an increased production of extracellular matrix (ECM) components, are typical of a mesenchymal

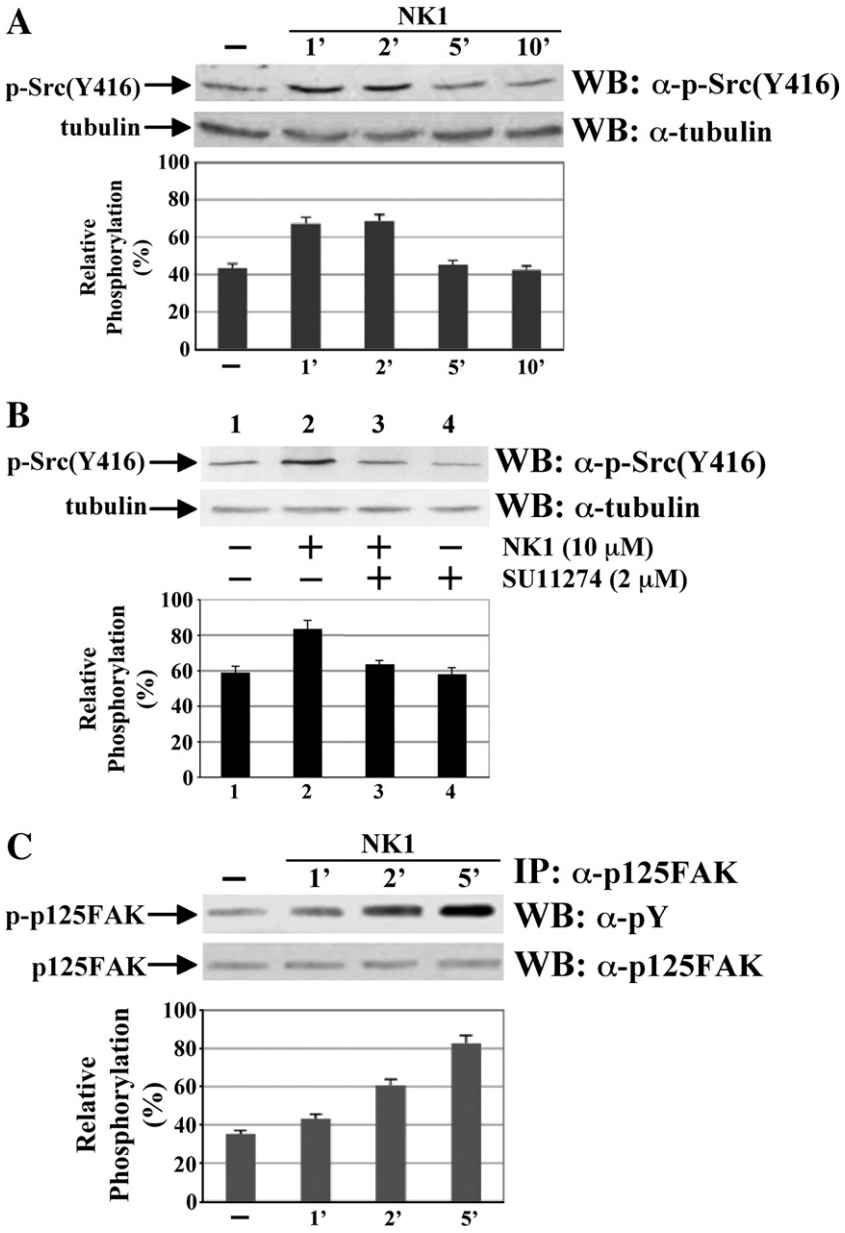

Fig. 5. NK1 activates p125FAK and c-Src and promotes wound healing in PNT1A cells. (A and C) Cells were exposed to 10^{-6} M NK1 for the indicated times. (A) Cell lysates (50 μg) were subjected to immunoblotting by using an anti-phospho-c-Src-Tyr416 antibody [α-p-Src(Y416)]. (C) Eight hundred micrograms of proteins were immunoprecipitated (IP) with an anti-p125FAK antibody (α-p125FAK). Tyrosine phosphorylation of p125FAK was detected by western blot using an anti-phospho tyrosine antibody (α-pY). (B and D) PNT1A cells were exposed to 10^{-6} M NK1 either in the absence (lane 2) or in the presence (lane 3) of SU11274. Cells were also incubated only with SU11274 (lane 4). (B) Fifty micrograms of cell lysates were resolved on a 10% SDS-PAGE and phosphorylated Tyr416 of c-Src was detected by using an anti-phospho c-Src(Tyr416) antibody [α-p-Src(Y416)]. (D) Proteins (800 μg) were immunoprecipitated (IP) with an anti-p125FAK antibody (α-p125FAK) and tyrosine phosphorylation of p125FAK was detected by western blot using an anti-phospho tyrosine antibody (α-pY). An anti-tubulin antibody (α-tubulin) served as a control of protein loading. The experiments were performed in triplicate. (E and F) Confluent cells grown in uncoated (E) or fibronectin-coated (F) plates were scratched with a plastic pipette tip. The cells were washed three times in PBS to remove detached cells, and attached cells were then cultured for 24 h in absence (left panels) or in the presence (right panels) of NK1 as indicated. Wound healing was assessed by microscopic visualization of cells that had migrated into the gap. The figure is representative of three separate experiments of identical design.

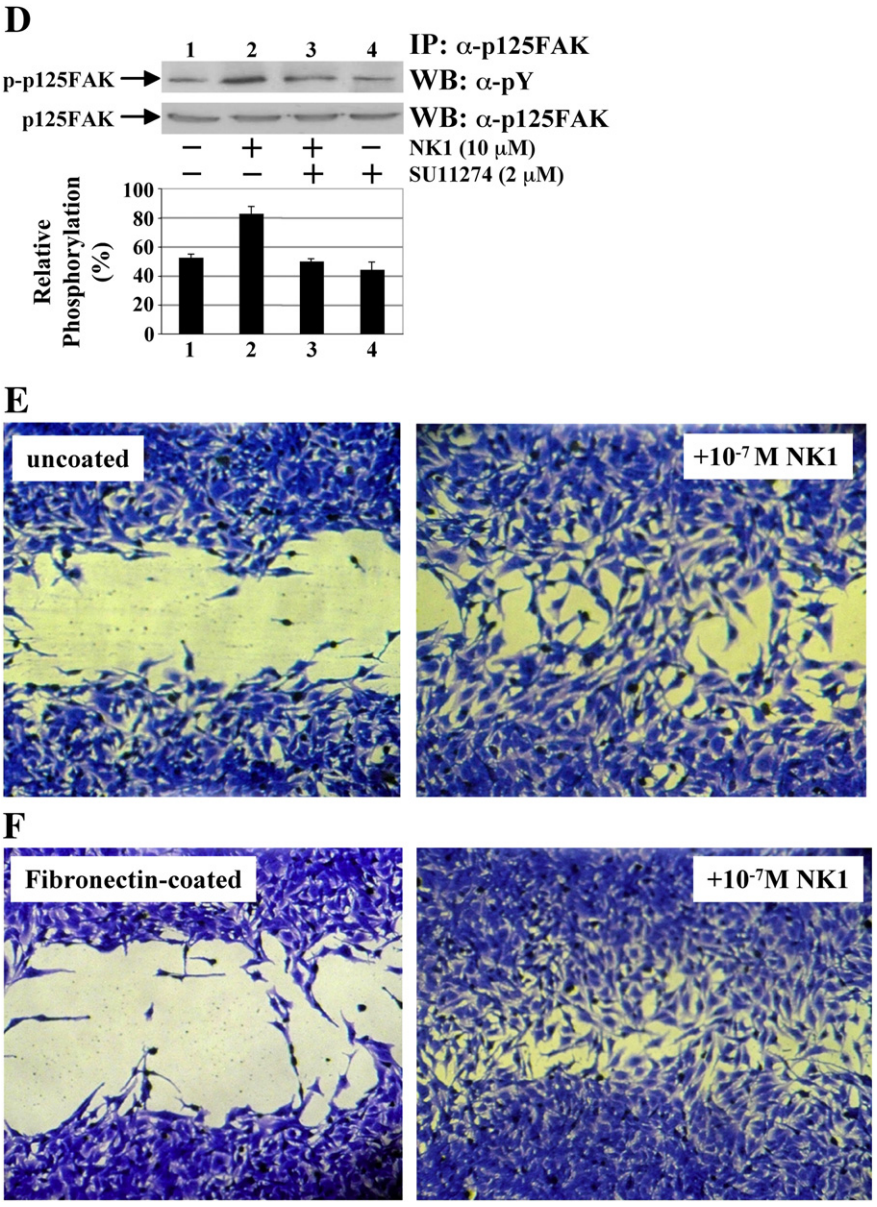

Fig. 5 (*continued*).

phenotype which cells assume as a consequence of a complex biological process which is known as Epithelial–Mesenchymal Transition (EMT) [34]. A c-MET mediated EMT has been observed in several experimental systems including human colon, breast and pancreatic cancer cell lines [35] and gastric epithelial cells [36]. Therefore, we analyzed the ability of NK1 to induce the expression of mesenchymal markers. A hallmark of EMT is the disruption of cell—cell adherens junctions which are mediated by homotypic interactions of the extracellular domains of E-cadherin. We observed a time-dependent down-regulation of E-cadherin expression after cell exposure to 10^{-6} M NK1 (Fig. 3A). Concomitant to the decreased expression of E-cadherin, NK1 treatment of PNT1A cells for 12 h promotes an increase of the expression levels of the mesenchymal markers vimentin, fibronectin and α-SMA (Fig. 3B). An increase of vinculin and α-actinin expression levels is also observed (Fig. 3B). Higher expression levels of these proteins in NK1-treated cells, as compared to control (untreated) cells, persist after 24 h. Furthermore, the pre-incubation of PNT1A cells with SU11274, before NK1 stimulation, prevents the increase of the expression levels of these markers (Fig. 3C), strongly suggesting that it requires NK1-dependent c-MET activation.

SMAD proteins are the main candidates for the induction of EMT process [37]. As NK1 induces the expression of mesenchymal markers in PNT1A cells, we evaluated the ability of NK1 to activate SMADs. The addition of 10^{-6} M NK1 promotes a time-dependent increase of SMAD2/3 phosphorylation (Fig. 3D) and this effect is prevented by the pre-incubation of the cells with the selective c-MET inhibitor SU11274 (Fig. 3E), suggesting that NK1-induced SMAD2/3 phosphorylation requires c-MET activation. The phosphorylation of SMADs occurs in response to the activation of TGF-β signaling pathway [37]. However, as also suggested by the complex phosphorylation patterns of endogenous SMADs, other kinase pathways further may regulate SMAD signaling [38]. In fact, SMAD2 phosphorylation and transcription in response to epidermal growth factor or HGF, which both act through tyrosine kinase receptors, challenge the belief that only TGF-β activates SMADs [39]. Thus, although the role of TGF-β pathway in NK1-induced expression of mesenchymal markers remains to be investigated, our results suggest that SMAD2/3 phosphorylation may represent an important point at which TGF-β and HGF pathways might converge in prostatic epithelial cells.

PNT1A cells show the normal epithelial shape appearing tightly packed in culture (Fig. 3F). After the treatment for 16 h with 10^{-6} M NK1, the cells appear to form structures that are irregular in shape and not uniform in density (Fig. 3F) showing a mesenchymal phenotype with more elongated shape, compared to epithelial cells, and result to be more loosely associated.

Thus, c-MET activation, subsequent to NK1 treatment of PNT1A cells, results in the down-regulation of E-cadherin and in the concomitant up-regulation of ECM components such as vimentin, fibronectin, α-SMA, vinculin and α-actinin, as well as the appearance of a mesenchymal phenotype.

3.4. NK1 induces the activation of PI3K/Akt signaling pathway and morphological changes resembling cell scattering

EMT and scattering are the first cellular processes typical of increased motility. Scattering correlates with the concomitant loss of E-cadherin expression and increased integrin-mediated ECM adhesion. Thus, tightly clustered epithelial cells break their cell–cell junctions and become single and migrating cells. It has been shown that HGF triggers scatter in MDCK epithelial cells [40] and that Ras/MAPK and PI3K/Akt pathways play a critical role in HGF-induced cell scattering and motility [41]. Furthermore, treatment of intact cells with wortmannin prevents HGF-induced scatter and mitogenesis in epithelial cells [42,43], suggesting that c-MET-dependent activation of PI3K is required for these activities. Therefore, we first analyzed the ability of NK1 to induce Akt activation. In our investigation, stimulation of PNT1A cells with 10^{-6} M NK1 induces a rapid increase of the phosphorylated levels of Akt at the Ser473 residue versus control (untreated) cells (Fig. 4A). The preincubation of cells with PD098059 before NK1 stimulation does not reduce Akt activation, whereas SU11274 and the highly selective P13K inhibitors wortmannin and LY294002 prevent NK1-induced Akt phosphorylation (Fig. 4B). These results suggest that the activation of PI3K/Akt pathway is a consequence of NK1/c-MET interaction and is independent from Ras/MEK/ERK signaling cascade.

We next tested the ability of NK1 to promote morphological changes resembling cell scattering. The addition of 10^{-6} M NK1 in PNT1A cells avoids their growth as a clump typical of epithelial cells giving them an un-polarized shape (Fig. 4C). Following the changes in cell-shape to an alternate morphology more prone to migration, the cells lose their apical–basal polarity and acquire a front–rear polarity (Fig. 4D), which is correlated to weak cell–cell contacts and increased motility.

3.5. NK1 activates p125FAK and c-Src and promotes wound healing in PNT1A cells

Focal adhesion kinase (FAK), a cytoplasmic kinase involved in ECM/integrin-mediated signaling pathways, has been suggested to have a crucial role for efficient cell migration in response to growth factor receptors and integrin stimulation [43]. Integrin-activated p125FAK forms a binary complex with the c-Src kinase which has been proven to be a downstream target activated by HGF engagement of c-MET receptor [44]. The complex c-Src/p125FAK can phosphorylate many other substrates and trigger multiple signaling pathways that regulate various cellular functions. Therefore, we investigated the ability of NK1 to affect the phosphorylation of c-Src and p125FAK. The addition of 10^{-6} M NK1 to PNT1A cells rapidly enhances the phosphorylation of c-Src at level of Tyr416 residue (Fig. 5A) and the tyrosine phosphorylation of p125FAK (Fig. 5C). NK1-induced phosphorylation of both c-Src and p125FAK is prevented by c-MET inhibitor SU11274 (Fig. 5B and D), thus suggesting that this signaling cascade is triggered by c-MET activation.

The signaling pathways activated by c-MET in response to NK1 stimulation of prostatic PNT1A cells are consistent with the results obtained using a global proteomics phospho-antibody array approach which demonstrated HGF-induced phosphorylation of many phospho-proteins in small cell lung cancer [45].

In order to confirm the NK1-induced migratory phenotype of PNT1A cells, we tested the ability of NK1-treated cells to repair a wound either in the absence (Fig. 5E) or in the presence (Fig. 5F) of a fibronectin coat. Confluent PNT1A cells were serum-deprived for 24 h followed by scratch wound induction. Addition of 10^{-7} M NK1 stimulates the movement of PNT1A cells towards the closure of the wound after 48 h (Fig. 5E). However, NK1-stimulated cells migrate into the artificially produced wound to a significantly greater extent in the fibronectin-coated culture dish versus uncoated dishes (Fig. 5F), indicating that cell spreading is involved as part of the mechanism for NK1-induced wound closure. Our results well correlate with the findings that epithelial wound healing can be modulated in vitro by the composition of the ECM [46]. The acquired increased capability of the cells to repair wound in the presence of NK1 further demonstrates the ability of the HGF splicing variant to promote prostate epithelial cell motility.

4. Conclusions

The biological consequences of HGF binding to c-MET and the downstream signaling have been extensively dissected in various cultured cell systems, mostly cancer cells, or cancer tissue specimens from different origin; however, they have been addressed in separate studies. Nevertheless, there is clear evidence that normal and malignant prostate epithelial cells differ in their response to HGF [9]. Here, we describe for the first time the effects induced by c-MET activation by NK1 fragment of HGF in a single non-tumorigenic cell line, namely the human prostatic epithelial cells PNT1A.

In this study, we demonstrate that in response to c-MET activation by NK1, PNT1A cells undergo morphological changes consistent with the activation of intracellular signaling cascades. We show that NK1 activates c-MET receptor expressed in PNT1A cells by phosphorylating tyrosine 1313/1349/1356 residues providing docking sites for intracellular signaling proteins, which results in the activation of the Ras/MAPK pathway, the main regulator of cellular growth processes. NK1-induced phosphorylation of c-MET also results in the activation of the STAT3 pathway which is directly involved in proliferation processes. Activation of this signaling pathway requires the phosphorylation of the Tyr705 and Ser727 residues of STAT3, as we observed in time-course experiments. Furthermore, our results also suggest that NK1-induced activation of SMADs, which are the main candidates for the induction of EMT process, requires ERK phosphorylation. In fact, SMAD2/3 phopsphorylation is prevented by the pretreatment of PNT1A cells with a specific MEK inhibitor before NK1 stimulation. Taken together, these results suggest that c-MET-dependent ERK activation could represent a key molecular signal that regulates the cellular processes of growth and of morphological changes in NK1-stimulated PNT1A cells.

Upon c-MET activation by NK1, PNT1A cells show a mesenchymal phenotype with more elongated shape compared to epithelial cells. In our investigation the migratory phenotype acquired by the PNT1A cells, after NK1 treatment and subsequent c-MET activation, is underlined by the down-regulation of E-cadherin expression and the increased levels of mesenchymal markers such as vimentin, fibronectin, vinculin, α-actinin, and α-SMA. The activation of PI3K/Akt pathway has been considered the main signaling pathway required for the induction of cell scattering and EMT [47]. In our cell system, NK1 induces Akt phosphorylation through a PI3K-dependent mechanism. Scatter and EMT are the initial processes of the cellular migration, and our results show an increased migratory capacity of PNT1A cells treated with NK1, as demonstrated by wound healing experiments. The molecular signaling that regulate cellular migration is also mediated by the activation of c-Src and p125FAK. We observed

that the activation of these two intermediate signaling molecules strongly depends on c-MET activation by NK1, as demonstrated by the pre-treatment with SU11274, which prevents c-Src Tyr416 and p125FAK phosphorylation.

Thus, our results show that stimulation of PNT1A cells with NK1 fragment of HGF promotes most of the effects reported for HGF/c-MET signaling in different cancer cell systems, but never in a normal prostate cell line and, more noticeable, all together in a single cell system.

Acknowledgments

We thank Dr. E. Cirillo for administrative help. This work was supported by grants (FISR 2005) from the Italian Department for University and Research (MIUR, Rome, Italy) and from MIUR PRIN 2007 “Attivazione dei recettori per formil-peptidi e regolazione della NADPH ossidasi in linee cellulari tumorali umane non fagocitiche”.

References

[1] C. Birchmeier, W. Birchmeier, E. Gherardi, G.F. Vande Woude, Nat. Rev. Mol. Cell Biol. 4 (2003) 915–925.
[2] N. Buchstein, D. Hoffmann, H. Smola, S. Lang, M. Paulsson, C. Niemann, T. Krieg, S.A. Eming, Am. J. Pathol. 174 (2009) 2116–2128.
[3] S.W. Hayward, G.R. Cunha, Radiol. Clin. North Am. 38 (2000) 1–14.
[4] P.A. Humphrey, X. Zhu, R. Zarnegar, P.E. Swanson, T.L. Ratliff, R.T. Vollmer, M.L. Day, Am. J. Pathol. 147 (1995) 386–396.
[5] D. Krill, M. Shuman, M.T. Thompson, M.J. Becich, S.C. Strom, Urology 49 (1997) 981–988.
[6] M. Sasaki, J. Enami, Cell Biol. Int. 23 (1999) 373–377.
[7] S.H. Lang, N.W. Clarke, N.J. George, N.G. Testa, Clin. Exp. Metastasis 17 (1999) 333–340.
[8] K. Nishimura, M. Kitamura, H. Miura, N. Nonomura, S. Takada, S. Takahara, K. Matsumoto, T. Nakamura, K. Matsumiya, Prostate 41 (1999) 145–153.
[9] G.A. Gmyrek, M. Walburg, C.P. Webb, H.M. Yu, X. You, E.D. Vaughan, G.F. Vande Woude, B.S. Knudsen, Am. J. Pathol. 159 (2001) 579–590.
[10] L. Trusolino, A. Bertotti, P.M. Comoglio, Nat. Rev. Mol. Cell. Biol. 12 (2010) 834–848.
[11] P. Accornero, L.M. Pavone, M. Baratta, Curr. Med. Chem. 17 (2010) 2699–2712.
[12] V. Cioce, K.G. Csaky, A.M.-L. Chan, D.P. Bottaro, W.G. Taylor, R. Jensen, S.A. Aaronson, J.S. Rubin, J. Biol. Chem. 271 (1996) 13110–13115.
[13] J.A. Deakin, M. Lyon, J. Cell Sci. 112 (1999) 1999–2009.
[14] D. Lietha, D.Y. Chirgadze, B. Mulloy, T.L. Blundell, E. Gherardi, EMBO J. 20 (2001) 5543–5555.
[15] R.H. Schwall, L.Y. Chang, P.J. Godowski, D.W. Kahn, K.J. Hillan, K.D. Bauer, T.F. Zioncheck, J. Cell Biol. 133 (1996) 709–718.
[16] H. Sakata, S.J. Stahl, W.G. Taylor, J.M. Rosenberg, K. Sakaguchi, P.T. Wingfield, J.S. Rubin, J. Biol. Chem. 272 (1997) 9457–9463.
[17] M. Lyon, J.A. Deakin, D. Lietha, E. Gherardi, J.T. Gallagher, J. Biol. Chem. 279 (2004) 43560–43567.
[18] J.S. Rubin, R.M. Day, D. Breckenridge, N. Atabey, W.G. Taylor, S.J. Stahl, P.T. Wingfield, J.D. Kaufman, R. Schwall, D.P. Bottaro, J. Biol. Chem. 276 (2001) 32977–32983.
[19] J.L. Jakubczak, W.J. LaRochelle, G. Merlino, Mol. Cell. Biol. 18 (1998) 1275–1283.
[20] Y.L. Yin, H.L. Chen, Acta Pharmacol. Sin. 29 (2008) 728–735.
[21] C. Avancès, V. Georget, B. Tèrouanne, F. Orio, O. Cussenot, N. Mottet, P. Costa, C. Sultan, Mol. Cell. Endocrinol. 184 (2001) 13–24.
[22] S. Mitchell, P. Abel, M. Ware, G. Stamp, E. Lalani, B.J.U. Int. 85 (2000) 932–944.
[23] D.Y. Chirgadze, J.P. Hepple, H. Zhou, R.A. Byrd, T.L. Blundell, E. Gherardi, Nat. Struct. Biol. 6 (1999) 72–79.
[24] A. Iaccio, F. Cattaneo, M. Mauro, R. Ammendola, Arch. Biochem. Biophys. 481 (2009) 94–100.
[25] F. Cattaneo, G. Guerra, R. Ammendola, Neurochem. Res. 35 (2010) 2018–2026.
[26] Q. Chen, D. Seol, B. Carr, R. Zarnegar, Hepatology 26 (1997) 59–66.
[27] P.M. Comoglio, Experientia 65 (1993) 131–165.
[28] H. Zhu, M.A. Naujokas, E.D. Fixman, K. Torossian, M. Park, J. Biol. Chem. 269 (1994) 29943–29948.
[29] X. Wang, P. Le, C. Liang, J. Chan, D. Kiewlich, T. Miller, D. Harris, L. Sun, A. Rice, S. Vasile, R.A. Blake, A.R. Howlett, N. Patel, G. McMahon, K.E. Lipson, Mol. Cancer Ther. 2 (2003) 1085–1092.
[30] E.K. Kim, E.J. Choi, Biochim. Biophys. Acta 1802 (2010) 396–405.
[31] C.F. Gao, Q. Xie, Y.L. Su, J. Koeman, S.K. Khoo, M. Gustafson, B.S. Knudsen, R. Hay, N. Shinomiya, G.F. Vande Woude, Proc. Natl. Acad. Sci. U. S. A. 102 (2005) 10528–10533.
[32] H. Yu, R. Jove, Nat. Rev. Cancer 4 (2004) 97–105.
[33] R. Paumelle, D. Tulasne, Z. Kherrouche, S. Plaza, C. Leroy, S. Reveneau, B. Vandenbunder, V. Fafeur, Oncogene 21 (2001) 2309–2319.
[34] J.P. Thiery, Nat. Rev. Cancer 2 (2002) 442–454.
[35] Q. Ma, K. Zhang, S. Guins, Mol. Cancer 9 (2010) 307–322.
[36] W. Schirrmeister, T. Gnad, Exp. Cell Res. 315 (2009) 3500–3508.
[37] J. Zavadil, E.P. Böttinger, Oncogene 24 (2005) 5764–5774.
[38] V. Ellenrieder, S.F. Hendler, W. Boeck, T. Seufferlein, A. Menke, C. Ruhland, G. Adler, T.M. Gress, Cancer Res. 61 (2001) 4222–4228.
[39] M.P. de Caestecker, W.T. Parks, C.J. Frank, P. Castagnino, D.P. Bottaro, A.B. Roberts, R.J. Lechleider, Genes Dev. 12 (1998) 1587–1592.
[40] R. Terauchi, N. Kitamura, Exp. Cell Res. 256 (2000) 411–422.
[41] S. Potempa, A.J. Ridley, Mol. Biol. Cell. 9 (1998) 2185–2200.
[42] I. Royal, M. Park, J. Biol. Chem. 46 (1995) 27780–27787.
[43] N. Rahimi, E. Tremblay, B. Elliott, J. Biol. Chem. 40 (1996) 24850–24855.
[44] J. Zhao, J.L. Guan, Cancer Metastasis Rev. 28 (2009) 35–49.
[45] P.C. Ma, M.S. Tretiakova, V. Nallasura, R. Jagadeeswaran, A.N. Husain, R. Salgia, Br. J. Cancer 97 (2007) 368–377.
[46] C. Garat, F. Kheradmand, K.H. Albertine, H.G. Folkesson, M.A. Matthay, Am. J. Physiol. Lung Cell. Mol. Physiol. 271 (1996) L844–L853.
[47] J. Okano, G. Shiota, K. Matsumoto, S. Yasui, A. Kurimasa, I. Hisatome, P. Steinberg, Y. Murawaki, Biochem. Biophys. Res. Commun. 309 (2003) 298–304.

Planta Medica

Journal of Medicinal Plant and Natural Product Research

Publishers

Georg Thieme Verlag KG
Stuttgart · New York
Rüdigerstraße 14
D-70469 Stuttgart
Postfach 30 11 20
D-70451 Stuttgart

Thieme Publishers
333 Seventh Avenue
New York, NY 10001, USA
www.thieme.com

Imbricatolic Acid from *Juniperus communis* L. Prevents Cell Cycle Progression in CaLu-6 Cells

Authors Simona De Marino[1]*, Fabio Cattaneo[2]*, Carmen Festa[1], Franco Zollo[1], Annalisa Iaccio[2], Rosario Ammendola[2], Filomena Incollingo[3], Maria Iorizzi[3]

Affiliations
[1] Dipartimento di Chimica delle Sostanze Naturali, Università degli Studi di Napoli Federico II, Napoli, Italy
[2] Dipartimento di Biochimica e Biotecnologie Mediche, Università degli Studi di Napoli Federico II, Napoli, Italy
[3] Dipartimento di Scienze e Tecnologie per l'Ambiente e il Territorio, Università degli Studi del Molise, Pesche (Isernia), Italy

Key words
- *Juniperus communis*
- Cupressaceae
- diterpenes
- dihydrobenzofuran lignan glycoside
- CDK inhibitors
- cell cycle

Abstract

Imbricatolic acid was isolated from the methanolic extract of the fresh ripe berries of *Juniperus communis* (Cupressaceae) together with sixteen known compounds and a new dihydrobenzofuran lignan glycoside named juniperoside A. Their structures were determined by spectroscopic methods and by comparison with the spectral data reported in literature.

Imbricatolic acid was evaluated for its ability to prevent cell cycle progression in p53-null CaLu-6 cells. This compound induces the upregulation of cyclin-dependent kinase inhibitors and their accumulation in the G1 phase of the cell cycle, as well as the degradation of cyclins A, D1, and E1. Furthermore, no significant imbricatolic acid-induced apoptosis was observed. Therefore, this plant-derived compound may play a role in the control of cell cycle.

Supporting information available online at http://www.thieme-connect.de/ejournals/toc/plantamedica

received July 22, 2010
revised April 4, 2011
accepted April 18, 2011

Bibliography
DOI http://dx.doi.org/10.1055/s-0030-1271104
Published online May 12, 2011
Planta Med 2011; 77: 1822–1828 © Georg Thieme Verlag KG Stuttgart · New York · ISSN 0032-0943

Correspondence
Prof. Maria Iorizzi
Dipartimento di Scienze e Tecnologie per l'Ambiente e il Territorio (DiSTAT)
Università degli Studi del Molise
Contrada Fonte Lappone
86090 Pesche (Isernia)
Italy
Phone: + 39 08 74 40 41 00
Fax: + 39 08 74 40 41 23
iorizzi@unimol.it

Introduction

Several medicinal plants, such as *Juniperus* sp. (Cupressaceae) [1], contain metabolites able to induce cell cycle arrest, playing an important role in cancer prevention. Many reports are focused on the determination of the chemical composition of the berry's essential oil [2, 3], and limited data are reported on nonvolatile components. Chemical components of the methanol extract from *Juniperus communis* berries include labdane monoterpene and megastigmane glycosides [4], labdane diterpenes [5], flavonoids, and biflavonoids [6]. Labdane diterpenes, isolated from several plant families, show a variety of biological activities [7] including the inhibition of cell proliferation in several cell lines [8]. In this study we analyzed the methanolic extract of berries from *J. communis* and focused on the bioactivity of imbricatolic acid, a labdane diterpene isolated as a major component.

Cyclin/cdk (cyclin dependent kinase) complexes facilitate progression through the cell cycle and are activated at specific checkpoints [9]. These complexes are also regulated by their binding to CDK inhibitors (CKIs) [10]. Two CKI gene families have been defined. The INK4 gene family encodes $p16^{INK4a}$, $p15^{INK4b}$, $p18^{INK4c}$, and $p19^{INK4d}$, all of which bind to CDK4 and CDK6 and inhibit kinase activities by interfering with their association with D-type cyclins [9]. In contrast, CKIs of the Cip/Kip family ($p21^{Cip1/Waf1/Sdi1}$, $p27^{Kip1}$, and $p57^{Kip2}$) bind to both cyclins and CDK subunits and can modulate the activities of cyclin D-, E-, A-, and B-CDK complexes [9]. $p21^{Cip1/Waf1/Sdi1}$ gene expression is regulated by transcriptional and posttranscriptional mechanisms. In tumor cells which lack p53 or with a mutant form of p53, $p21^{Cip1/Waf1/Sdi1}$ is activated through p53-independent pathways.

In the present paper, we report: i) the isolation and structural elucidation of a new compound and eleven known components from a methanolic extract of berries from *J. communis*, and ii) the ability of imbricatolic acid, a known labdane diterpene, to induce CKIs upregulation, accumulation in G1 phase of the cell cycle and cyclins degradation in p53-null human lung tumor cells.

* These authors contributed equally to this work.

This is a copy of the author's personal reprint

Materials and Methods

General experimental procedures

High-resolution fast atom bombardment mass spectrometry (HRFAB-MS) was recorded on a Fisons VG Prospec instrument, and electrospray ionization mass spectrometry (ESI-MS) experiments were performed on an Applied Biosystem API 2000 triple-quadrupole mass spectrometer. Optical rotations were determined on a Jasko P-2000 polarimeter. ^1H and ^{13}C NMR spectra were determined on a Varian Unity INOVA spectrometer at 500.13 and 125.77 MHz, respectively, equipped with an indirect detection probe. Chemical shifts were referenced to the solvent signals: deuterated methanol (CD_3OD). GC analyses were performed on an Agilent Technologies 6850 Series II gas chromatograph for capillary column (HP-5, 30 m × 0.25 mm, 180 °; helium carrier flow 10 mL min^{-1}) and a FID detector operated at 260 °. Droplet countercurrent chromatography (DCCC) was performed on a DCC-A apparatus (Tokyo Rikakikai Co.). HPLC was performed using a Waters 510 pump equipped with a Waters U6K injector and a Waters 401 differential refractometer as the detector, using a C_{18} μ-Bondapak column (30 cm × 3.9 mm; i.d.; flow rate 1 mL min^{-1}; Waters) and a Luna C-18 column (3 μ, 150 × 4.60 mm i.d.; flow rate 1 mL min^{-1}; Phenomenex).

Plant material

Ripe berries of *Juniperus communis* L. (Cupressaceae) were collected in the mountain areas of Isernia (Italy) in October 2008 and identified by Dr. Paola Fortini. A voucher specimen is deposited (JC-486-08) at the Herbarium of DiSTAT, University of Molise (Pesche). Berries were kept frozen at −20 °C until analyzed.

Extraction and isolation

Fresh ripe berries (400 g) were crushed and extracted with MeOH (3 × 2 L) at room temperature for 24 h. The combined extracts (170 g) were concentrated and subjected to a modified Kupchan's partition methodology as described [11]. The MeOH extract was dissolved in 10% aqueous methanol and partitioned against *n*-hexane (3 × 400 mL) yielding 1.3 g of extract. The water content (% v/v) of the MeOH extract was adjusted to 40% and partitioned against $CHCl_3$ (5 × 400 mL), yielding 1.5 g of extract; the aqueous residue was concentrated and partitioned against *n*-BuOH (3 × 500 mL) to give 2.0 g of *n*-BuOH extract. The *n*-hexane extract (1.3 g) was separated by column chromatography on SiO_2 (50 g, 230–400 mesh silica gel; 1.5 × 45 cm) and stepwise eluted using *n*-hexane/EtOAc with the ratio of 100 : 0 (300 mL), 99 : 1, 98 : 2, 80 : 20 (each 150 mL), 96 : 4, 95 : 5, 50 : 50, 0 : 100 (each 200 mL) to give 8 corresponding fractions (A–H). 150 × 10 mL tubes were collected and combined on the basis of their similar TLC behavior (SiO_2 with *n*-hexane/EtOAc 95 : 5). Fraction H (70 mg) was then purified by HPLC (C_{18} μ-Bondapak column; MeOH/H_2O 8 : 2 as eluent, flow rate 1 mL/min) to give mainly *cis*-communic acid (**6**, 2.8 mg). The $CHCl_3$ extract (1.5 g) was fractionated by DCCC using $CHCl_3$/MeOH/H_2O (7 : 13 : 8) in the ascending mode (the lower phase was the stationary phase); 320 tubes (6 mL) were collected, flow rate 18 mL/h. Fractions were combined and monitored by TLC on SiO_2 with $CHCl_3$/MeOH/H_2O (80 : 18 : 2) as eluent to give five main fractions summarized in **Table 1**. The *n*-BuOH extract (2 g) was submitted to DCCC with *n*-BuOH/Me_2CO/H_2O (3 : 1 : 5) in the descending mode (the upper phase was the stationary phase). 210 tubes (6 mL) were collected, flow rate 18 mL/h. Fractions were combined and monitored by TLC on Silica gel plates with *n*-BuOH/OHAc/H_2O (12 : 3 : 5) and $CHCl_3$/MeOH/H_2O (80 : 18 : 2). Five fractions (A–E) were obtained and purified by HPLC as summarized in **Table 1**. The purity of compounds **1**–**17** was greater than 95% determined by HPLC method (see experimental section), MS, and NMR. The bold number in brackets refers to the chemical structures indicated in **Fig. 1**. Copies of original spectra can be obtained from the author of correspondence.

Table 1 DCCC fractionation and HPLC purification of $CHCl_3$ and *n*-BuOH extracts.

Fraction	Amount (mg)	Compound	MeOH/H_2O
	$CHCl_3$ extract[a]		
1	1.2	**17**	1 : 1
2	1.5	**16**	7 : 3
2	1.7	**8**	8 : 2[b]
3	5.8	**2**	7 : 3
3	1.8	**4**	45 : 55[b]
4	3.0	**10**	8 : 2
4	1.0	**11**	8 : 2
4	1.2	**12**	8 : 2
5	1.8	**9**	75 : 25
5	1.0	**5**	75 : 25
5	2.0	**3**	75 : 25
	***n*-BuOH extract**[a]		
A	1.3	**7**	
B	1.4	**1**	4 : 6
C	3.2	**15**	1 : 1
D	1.3	**14**	8 : 2
E	3.0	**13**	1 : 1

[a] All fractions were purified on C18 μ-Bondapak column. [b] Fraction purified on a Luna C-18 column

Acid hydrolysis of 1

Compound **1** (0.5 mg) was hydrolyzed with 2N CF_3CO_2H (2 mL) at 110 ° in a sealed tube for 8 h. After cooling, the solution was diluted with H_2O (5 mL) and extracted with AcOEt (3 × 2 mL). The aqueous layer was evaporated to dryness under reduced pressure, and the residue was reacted with 0.1 M L-cysteine methyl ester hydrochloride in anhydrous pyridine (200 μL) for 1 h at 60 ° [12]. 1-(Trimethylsilyl)imidazole in pyridine was added, and the thiazolidine derivatives analyzed by GC. L-rhamnose was confirmed in **1** by comparison of the retention time of their derivatives with those of D-rhamnose (t_R = 12.60 min) and L-rhamnose (t_R = 12.14 min).

Reagents and cell culture treatments

SDS-PAGE reagents were from Bio-Rad. Anti-active phosphorylated ERK1/2, anti-tubulin, anti-PKCδ, anti-cyclinA, anti-cyclinB, anti-cyclinD1, anti-cyclinE1, anti- $p21^{Cip1/Waf1/Sdi1}$, anti-$p27^{Kip}$, anti-$p16^{INK4a}$, anti-EGFR, anti-PARP-1, anti-caspase3, and anti-rabbit antibodies were obtained from Santa Cruz Biotechnology Inc. Protein A-horseradish peroxidase and anti-mouse Ig-horseradish peroxidase were from Amersham Pharmacia. PD098059 and rottlerin were from Calbiochem. PepTag® assay for nonradioactive detection of protein kinase C was from Promega. Human anaplastic lung cancer cells CaLu-6 were purchased from ATCC and grown in Dulbecco's modified Eagle's medium (DMEM) containing 10% fetal bovine serum (FBS), 100 U/mL penicillin, 100 μg/mL streptomycin, 1% L-glutammin, and 1% modified Eagle's medium (MEM).

This is a copy of the author's personal reprint

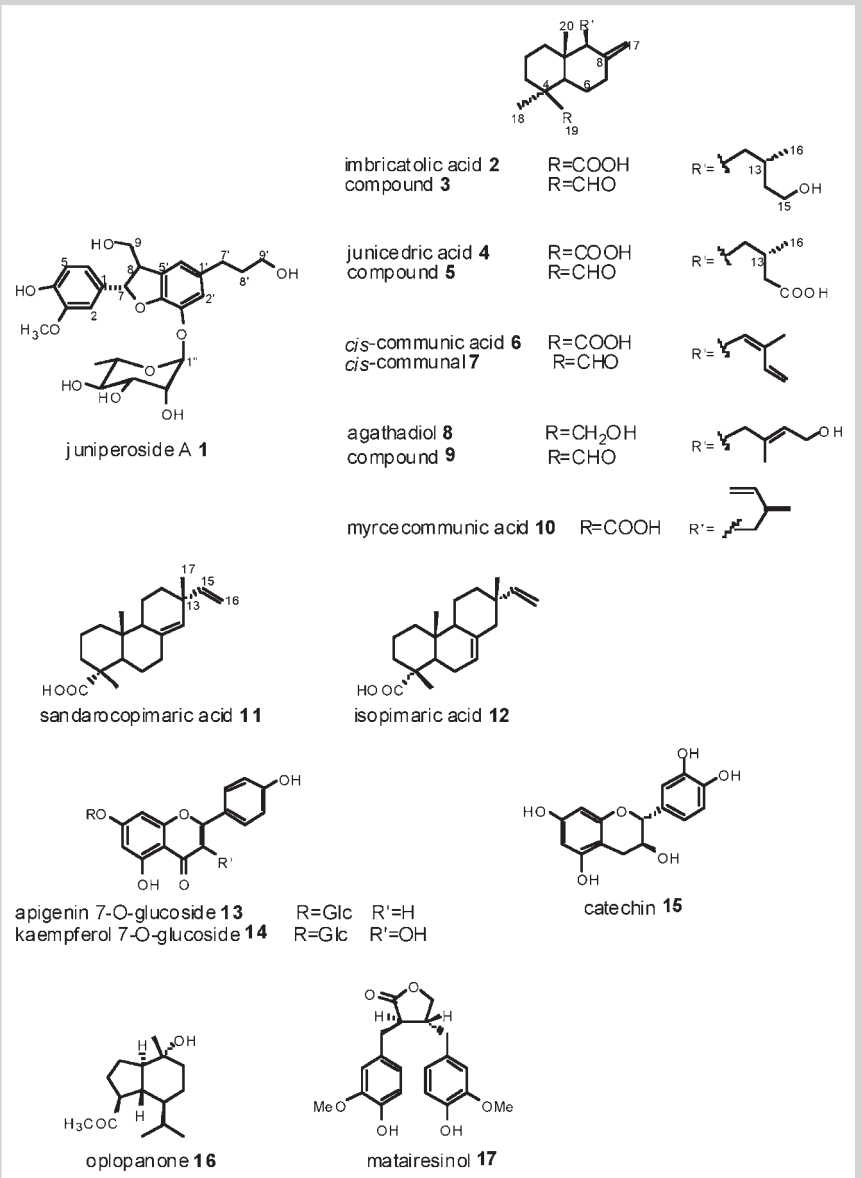

Fig. 1 Natural compounds isolated from *Juniperus communis* L. berries.

Imbricatolic acid was diluted in DMSO at a final concentration of 10 mM. Cells were grown until they reached 80% confluence and successively stimulated by imbricatolic acid at the final concentration of 10 µM for different times, as indicated in the figures. In other experiments, growing cells were preincubated with 50 µM PD098059 for 90 min, or with 1 µM rottlerin for 1 h, before the stimulation with 10 µM imbricatolic acid.

Western blot analysis and protein kinase C activity assay

Total cellular lysates and cell membranes were purified from Ca-Lu-6 cells as previously described [13]. Western blot experiments were performed in triplicate, as previously described [13]. The expression of targeted proteins was detected by an ECL kit (Amersham Biosciences) and visualized by autoradiography. Protein kinase C activity assay was performed accordingly to manufacturer's instructions (Materials and Methods **1S**, Supporting Information).

Cell viability

Calu-6 cells were placed (4×10^4 cells per well) in 96-well plates (Corning) and incubated at 37 °C in 200 µL of complete culture medium containing 10 µM imbricatolic acid or 0.1% DMSO for 3, 12, 24, 48, and 72 hrs. 3-[4,5-Dimethylthiazol-2-yl]-2,5-diphenyl tetrazoliumbromide (MTT; 5 mg/mL in PBS) was added to each well and incubated for 4 h. After removal of the medium, 0.2 mL of DMSO was added to each well. The absorbance of the resulting formazan salts was recorded on a microplate reader at the wavelength of 540 nm. The effect of imbricatolic acid on growth inhibition was assessed as percent cell viability where DMSO-treated cells were taken as 100% viable. DMSO at the concentrations used was without any effect on cell viability. Four independent experiments were performed.

Analysis of apoptosis and cell cycle

Analysis of DNA content by propidium iodide incorporation was performed in permeabilized cells, as described [14] (Materials and Methods **2S**, Supporting Information).

This is a copy of the author's personal reprint

Table 2 ^{1}H and ^{13}C NMR data (CD_3OD, 500 and 125 MHz) of compound **1**.

Position	δ_H (*J* in Hz)	δ_C	HMBC
1	–	138.8	
2	7.06 br s	110.9	C4, C6, C7
3	–	151.7	
4	–	146.1	
5	7.08 d (8.4)	119.2	C1, C3
6	6.94 d (8.4)	118.7	C2, C4, C7
7	5.57 d (5.7)	89.0	C1, C2, C6, C8, C9, C3′, C5′
8	3.47 ovl	55.6	
9	3.77 dd (9.9, 17.9), 3.88 ovl	64.8	C7, C8, C5′
1′	–	136.4	
2′	6.59 s	116.7	C4′, C6′, C7′
3′	–	146.0	
4′	–	140.7	
5′	–	129.1	
6′	6.62 s	116.3	C8, C2′
7′	2.58 d (7.3)	32.4	C1′, C2′, C6′, C8′, C9′
8′	1.80 m	35.5	C1′, C7′, C9′
9′	3.58 t (6.5)	62.0	C7′, C8′
OCH_3	3.83 s	56.0	C5
Rhamnose			
1′′	5.35 br s	101.1	C3′, C3′′, C5′′
2′′	4.08 br s	71.7	
3′′	3.90 ovl	71.9	
4′′	3.47 ovl	73.5	
5′′	3.82 ovl	70.5	
6′′	1.22 d (6.2)	17.6	C4′′, C5′′

^{1}H and ^{13}C assignments achieved by COSY, TOCSY, HSQC, and HMBC experiments

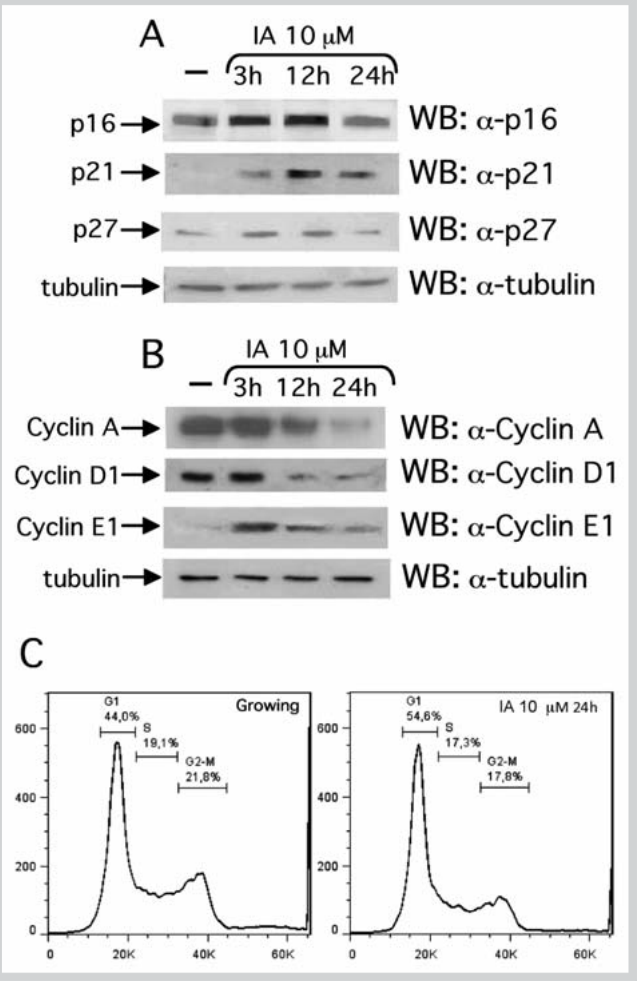

Fig. 2 CaLu-6 cells were exposed to 10 μM imbricatolic acid (IA) for the indicated times, and 40 μg of cell lysates were loaded on 12% SDS-PAGE. **A** The upregulation of $p21^{Cip1/Waf1/Sdi1}$, $p27^{Kip1}$, and $p16^{INK4a}$ and **B** degradation of cyclin A, cyclin D1, and cyclin E1 were immunodetected with specific antibodies. An anti-tubulin antibody was used as a control of protein loading. Cells were also exposed to 0.1% DMSO (–) for 12 h, as a control. **C** 5×10^6 cells were plated in 6-mm wells in the presence or absence of 10 μM imbricatolic acid (IA) for 24 h. Growing cells were incubated with 0.1% DMSO. Cells were resuspended in 300 μL of cold PBS and fixed with 1 mL of 70% ice-cold ethanol for 2 h. FACS analysis was performed as described in Materials and Methods by using a DAKA Cytomatio flow cytometer. Data were analyzed using Summit® 4.3 software. All the experiments were performed in triplicate.

Results and Discussion

Juniperus communis berries extracted with MeOH were subjected to Kupchan's methodology [11] to give *n*-hexane, $CHCl_3$, *n*-BuOH extracts, and an aqueous residue. The pure compounds were isolated, and their structures were determined by spectroscopic methods by comparison with the spectral data reported in the literature: *cis*-communic acid (**6**) [15], imbricatolic acid [15-hydroxy-labd-8(17)-en-19-oic acid] (**2**) [16], imbricatolal (**3**) [17], junicedric acid (**4**) [18], junicedral (**5**), agathadiol (**8**) [19], isoagatholal (**9**) [20], myrcecommunic acid (**10**) [21], sandarocopimaric acid (**11**) [22], isopimaric acid (**12**) [23], oplopanone (**16**) [24], and matairesinol (**17**) [25] (**Fig. 1**).

The new dihydrobenzofuran lignan glycoside, named juniperoside A (**1**) ($[\alpha]_D^{25}$ + 34.4), showed a pseudomolecular ion at *m/z* 493.2074 in its HRFABMS, and the presence of 25 carbon atoms in the ^{13}C NMR spectrum (**Table 2**) suggested the molecular formula $C_{25}H_{32}O_{10}$. In the ESI-MS (pos. ion mode) spectrum the pseudomolecular ion peak at *m/z* 515 $[M + Na]^+$ was also present. Its IR spectrum showed absorption bands at 3451 and 1660 cm^{-1} corresponding to hydroxyl and aromatic groups, respectively. The data from ^{1}H and ^{13}C NMR spectra of (**1**) were similar to those of clemastanin A [26], a glucoside isolated from *Clematis* species. Differences were detected in the sugar moiety. The ^{1}H NMR spectrum of juniperoside A showed three aromatic proton signals at δ_H 6.94, 7.06, and 7.08 which were assigned to three protons in a 1,2,4-trisubstituted benzene ring. Further two aromatic proton signals at δ_H 6.59 and 6.62 were assigned to two protons in a 1,3,4,5-tetrasubstituted benzene ring. The ^{1}H NMR spectrum also revealed proton signals due to two oxygenated methylene protons (δ_H 3.88 ovl/3.77 dd and 3.58 t), an oxygenated methine signal at δ_H 5.57 (d), and one methoxyl signal at δ_H 3.83 (s). By the aid of a ^{1}H-^{1}H COSY experiment, a propanol side chain was detected; a second spin system sequence evidenced oxygenated methylene protons (3.88/3.77) which were connected to a methine proton at δ_H 3.47. This last proton was also coupled with a proton signal at δ_H 5.57. In addition to ^{13}C NMR assignment, further HSQC experiment correlated the proton resonances of aglycone, with the relevant carbons indicating a dehydrodiconiferyl alcohol-type lignan. Significant HMBC correlations were reported in **Table 2**. The presence of a sugar moiety was deduced from the anomeric proton signal at δ_H 5.35 (br s) in the ^{1}H NMR spectrum. Starting from the anomeric proton signal, the proton resonances were assigned by ^{1}H-^{1}H COSY and TOCSY experiments. On

This is a copy of the author's personal reprint

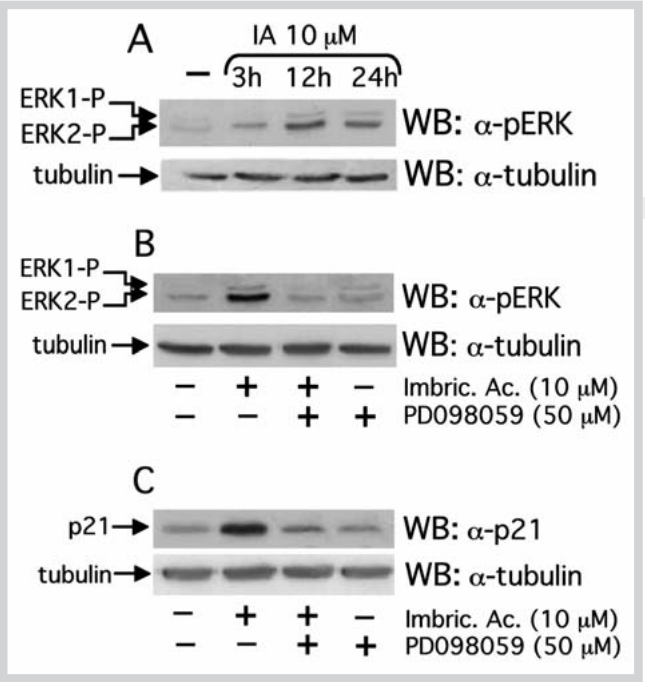

Fig. 3 Cell lysates were obtained from CaLu-6 cells exposed to 10 μM imbricatolic acid (IA) for the indicated times **A** or preincubated with PD098059 before the stimulation with 10 μM IA for 12 h (**B** and **C**). Forty micrograms of proteins were resolved by electrophoresis on 12% SDS-PAGE and transferred to a nitrocellulose membrane. ERKs phosphorylation was detected by using an anti-phosphoERK antibody (**A** and **B**). The arrows indicate the phosphorylated forms of $p44^{MAPK}$ (ERK1-P) and $p42^{MAPK}$ (ERK2-P). **C** $p21^{Cip1/Waf1/Sdi1}$ (p21) was immunodetected by using a specific antibody. An anti-tubulin antibody was used as a control of protein loading. Cells were also exposed to 0.1% DMSO (−) for 12 h. The experiments were performed in triplicate.

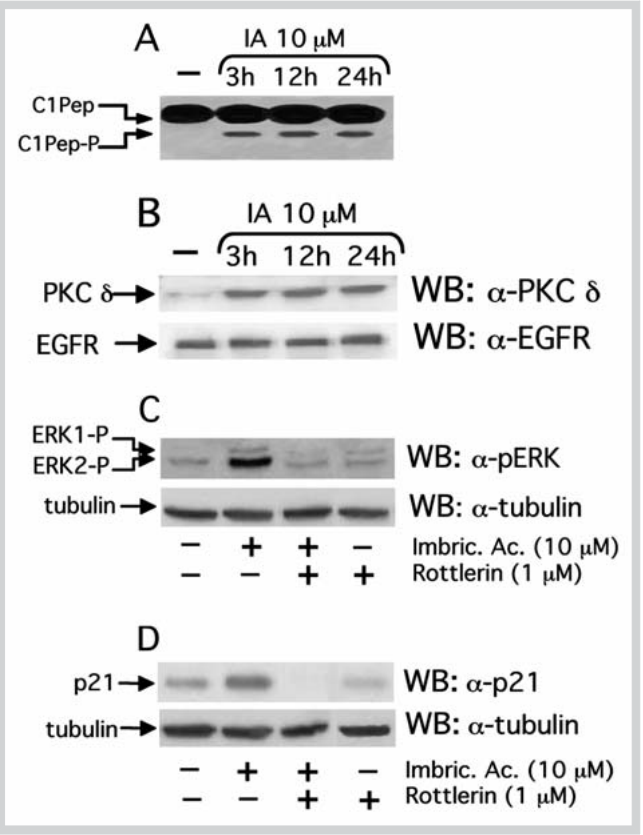

Fig. 4 **A** Assay of nonradioactive detection of PKC. 1×10^7 CaLu-6 cells were incubated with 10 μM imbricatolic acid (IA) for the indicated times or with 0.1% DMSO as a control (−). Cell lysates were purified on DEAE cellulose, and PKC assays were performed in triplicate as described in Materials and Methods. The reactions were stopped by heating to 95 °C for 10 min, and the samples were separated on a 0.8% agarose gel at 100 V for 15 min and photographed on a transilluminator. **B** Membranes were purified from CaLu-6 cells stimulated with 10 μM imbricatolic acid (IA) for the indicated times, and PKCδ was detected by a specific antibody. The same filter was incubated with anti-EGFR antibody as a control of protein loading. Cells were also exposed to 0.1% DMSO (−) for 12 h. Data is representative of three independent experiments. **C** and **D** Cellular extract were obtained from CaLu-6 cells stimulated for 12 h with 10 μM imbricatolic acid in the presence or absence of rottlerin. **C** Twenty micrograms of proteins were subjected to immunoblotting analysis with an anti-phosphoERK antibody (α-pERK). **D** Forty micrograms of proteins were electrophoresed on 12% SDS-PAGE, and the blot was incubated with an anti-$p21^{Cip1/Waf1/Sdi1}$ antibody (α-p21). The same filters were reprobed with an anti-tubulin antibody. The experiments were performed in triplicate.

acid hydrolysis with 2N CF_3CO_2H, **1** afforded rhamnose. The L configuration of rhamnose was assigned by GC analysis [12].

The connection between the rhamnopyranosyl unit to C-3′ of the aglycone was verified by the cross-peak between δ_H 5.35 (H-1″) and δ_C 146.0 (C-3′) in the HMBC experiment. HMBC cross-peaks also revealed the attachment of the methoxyl group at C-3 and the propanol side chain at C-1′ position. The stereochemistry between the hydroxymethyl and the aryl group was suggested to be *trans* by the ROESY experiment, by a coupling constant of H-7/H-8 (J = 5.7 Hz) as well as their chemical shifts. An intense ROE was observed between H-8/H-6′ (δ_H 3.47/6.62) and H-7/H_2-9 (δ_H 5.57/3.88–3.77), H-7/H-6 (δ_H 5.57/6.94), and H-7/H-2 (δ_H 5.57/7.06). Then the structure of juniperoside A **1** was determined to be 3-methoxy-3′,4,9,9′-tetrahydroxy-4′,7-epoxy-5′,8-lignan-3′-O-α-L-rhamnopyranoside.

Some labdane-type diterpenes have been shown to inhibit cell proliferation in several tumor cell lines which express functional p53 or that do not express p53 [8]. Therefore, we examined the effect of imbricatolic acid (IA) (**2**) on cell cycle inhibitory proteins $p21^{Cip1/Waf1/Sdi1}$, $p27^{Kip1}$, and $p16^{INK4a}$, as well as on cell cycle arrest, in p53-null human cancer CaLu-6 cells [27]. Cells were incubated with 10 μM IA for increasing times, and Western blot analysis showed a significant induction of these CKIs in a time-dependent manner with a maximal accumulation occurring after 12 h of treatment (**Fig. 2A**). We next evaluated the effect of IA on the protein level of cyclins. CKI of the Cip/Kip family can modulate the activities of cyclin D-, E-, and A-CDK complexes [9], which are involved in G1, G1/S, and S checkpoints, respectively. Labdane treatment of cells resulted in significant time-regulated decrease in the expression of cyclin A, D1, and E1 (**Fig. 2B**). Furthermore, DNA staining by propidium iodide showed that the exposure to 10 μM IA for 24 h induces the accumulation in G1 phase (**Fig. 2C**). We also analyzed the effects of junicedric acid (**4**) and agathadiol (**8**), which differ from IA for a carboxylic function on C15 (**4**) and for a primary alcoholic function on C19 and a double bond on C13–C14 (**8**). No effects of the two compounds on cell cycle at 10 μM were detected (data not shown).

In different cell types, the Ras/MAPK pathway mediates growth arrest by controlling cell cycle regulatory proteins [28–31]. Furthermore, in p53-null cells the accumulation of $p21^{Cip1/Waf1/Sdi1}$ is

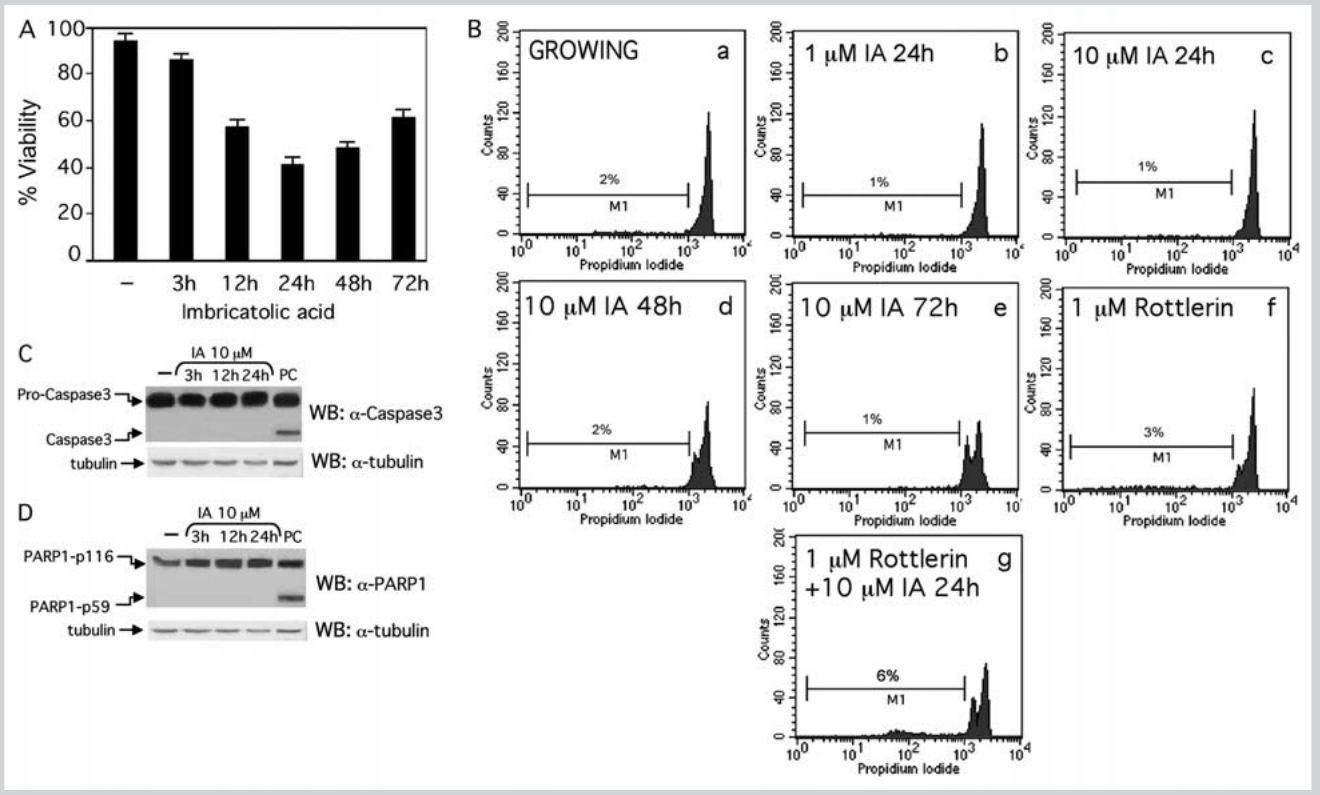

Fig. 5 **A** Cells were incubated in complete culture medium containing 10 μM imbricatolic acid or 0.1% DMSO (−) for the indicated times. MTT solution was added, and formazan crystals were then dissolved and measured at λ540 nm. Four independent experiments were performed. **B** Cells were incubated with 1 μM or 10 μM imbricatolic acid (IA) for the indicated times in the presence or absence of 1 μM rottlerin for 1 h. Growing cells were exposed to 0.1% DMSO as a control. Cells were incubated in a solution containing 50 μg/mL propidium iodide and analyzed by cytofluorimetry. The data are representative of at least three separate experiments of identical design. **C** and **D** CaLu-6 cells were exposed to 10 μM imbricatolic acid (IA) for the indicated times. Fifty micrograms of whole lysates were resolved on 10% SDS-PAGE and then incubated with specific antibodies against Caspase3 (**C**) or PARP1 (**D**). Cells were also exposed to etoposide as a positive control (PC) or to 0.1% DMSO (−) for 12 h. An anti-tubulin antibody was used as a control of protein loading. The experiments were performed in triplicate.

a consequence of the activation of Ras-ERK pathway [32]. Therefore, we investigated the molecular mechanisms underlying the upregulation of $p21^{Cip1/Waf1/Sdi1}$ by analyzing the ability of IA to activate ERKs. The incubation for increasing times with the labdane induced a sustained phosphorylation of ERKs (**Fig. 3A**) which was prevented by the MEK inhibitor PD098059 (**Fig. 3B**). We also observed that the preincubation with PD098059 prevents the IA-induced $p21^{Cip1/Waf1/Sdi1}$ accumulation (**Fig. 3C**), suggesting that this requires ERKs activation.

PKCδ is generally considered a growth inhibitor that can contribute to the p53-independent accumulation of $p21^{Cip1/Waf1/Sdi1}$ [33, 34]. We first investigated the ability of IA to activate PKC in CaLu-6 cells. **Fig. 4A** shows that PKC activity was detectable after 3 h and was sustained after 24 h of exposure to 10 μM IA. We next analyzed PKCδ activation by analyzing cellular partitioning of this isoenzyme [13]. In response to the labdane, PKCδ translocated into the membrane fraction, and a significant increase in the amount was observed within 3 h of treatment (**Fig. 4B**). We also observed that preincubation of CaLu-6 cells with 1 μM rottlerin, a selective inhibitor of PKCδ enzyme activity [35], caused a significant inhibition of IA-induced ERKs activation (**Fig. 4C**) and $p21^{Cip1/Waf1/Sdi1}$ accumulation (**Fig. 4D**). These results strongly suggest that, in CaLu-6 cells, IA induces PKCδ activation which is involved in the regulation of ERKs and, in turn, in the accumulation of a specific CKI.

To evaluate the effect of IA on cell viability of human CaLu-6 cells, we performed an MTT assay. The cells, exposed for different times with IA, showed a significant time-dependent inhibition of cell viability (**Fig. 5A**), as observed by a 89.8, 53.4, 41.4, 49.8, and 62.7% decrease after 3, 12, 24, 48, and 72 h, respectively. To test whether the decrease in cell growth was due to induction of apoptosis, we performed propidium iodide staining on CaLu-6 cells exposed for different times or concentrations to IA in the presence or absence of rottlerin. The results showed that the incubation with 1 μM or 10 μM IA for 24, 48, or 72 h (**Fig. 5B**, panels **a–e**) as well as the incubation with 1 μM rottlerin (**Fig. 5B**, panel **f**), or the pretreatment with rottlerin before IA stimulation for 24 h (**Fig. 5B**, panel **g**) did not induce any significant apoptosis. Furthermore, we performed Western blot analysis of PARP-1 and caspase3 by using specific antibodies. **Fig. 5C** shows that IA did not induce the cleavage of the 32 kDa precursor of caspase3 and, as a consequence, the 116 kDa PARP1 protein resulted not cleaved upon IA treatment (**Fig. 5D**). Taken together these data suggest that imbricatolic acid has not an apoptotic effect on CaLu-6 cells. The same results were obtained on the p53-null PC-3 cell line (data not shown).

In summary, we found that imbricatolic acid induces cell cycle arrest in CaLu-6 cells. A possible mechanism is: i) the accumulation of $p21^{Cip1/Waf1/Sdi1}$, mediated by PKCδ activation and ERKs phosphorylation; and ii) the decrease of cyclins A, D1, and E1 levels,

This is a copy of the author's personal reprint

which are considered checkpoints of S, G1, and G1/S phases transition, respectively. Further studies are in progress to evaluate the role of $p27^{Kip1}$ and $p16^{INK4a}$ in the labdane-induced cell cycle arrest.

Acknowledgements

MS and NMR spectra were provided by CSIAS, Università di Napoli Federico II, Italy. We are grateful for the financial assistance provided by the Osservatorio Ambientale Permanente della Biodiversità (Convenzione – Colli al Volturno).

Conflict of Interest

All authors declare no conflict of interest.

References

1 *Kwon HJ, Hong YK, Park C, Choi YH, Yun HJ, Lee EW, Kim BW.* Widdrol induces cell cycle arrest, associated with MCM down-regulation, in human colon adenocarcinoma cells. Cancer Lett 2010; 290: 96–103
2 *Angioni A, Barra A, Russo MT, Coroneo V, Dessi S, Cabras P.* Chemical composition of the essential oils of *Juniperus* from ripe and unripe berries and leaves and their antimicrobial activity. J Agric Food Chem 2003; 51: 3073–3078
3 *Filipowicz N, Kaminski M, Kurlenda J, Asztemborska M, Ochocka JR.* Antibacterial and antifungal activity of juniper berry oil and its selected components. Phytother Res 2003; 17: 227–231
4 *Nakanishi T, Iida N, Inatomi Y, Murata H, Inada A, Murata J, Lang FA, Iinuma M, Tanaka T, Sakagami Y.* A monoterpene glucoside and three megastigmane glycosides from *Juniperus communis* var. *depressa*. Chem Pharm Bull 2005; 53: 783–787
5 *Martin AM, Queiroz EF, Marston A, Hostettmann K.* Labdane diterpenes from *Juniperus communis* L. berries. Phytochem Anal 2006; 17: 32–35
6 *Innocenti M, Michelozzi M, Giaccherini C, Ieri F, Vincieri FF, Mulinacci N.* Flavonoids and biflavonoids in Tuscan berries of *Juniperus communis* L.: detection and quantitation by HPLC/DAD/ESI/MS. J Agric Food Chem 2007; 55: 6596–6602
7 *Demetzos C, Dimas K.* Labdane-type diterpenes: chemistry and biological activity. In: Atta-Ur-Rahman, editor. Studies in natural products chemistry of bioactive natural products, Vol. 25. Oxford: Elsevier Science; 2001: 235–292
8 *Dimas K, Papadaki M, Tsimplouli C, Hatziantoniou S, Alevizopoulos K, Pantazis P, Demetzos C.* Labd-14-ene-8,13-diol (sclareol) induces cell cycle arrest and apoptosis in human breast cancer cells and enhances the activity of anticancer drugs. Biomed Pharmacother 2006; 60: 127–133
9 *Sherr CJ, Roberts JM.* CDK inhibitors: positive and negative regulators of G1-phase progression. Genes Dev 1999; 13: 1501–1512
10 *Besson A, Dowdy SF, Roberts JM.* CDK inhibitors: cell cycle regulators and beyond. Dev Cell 2008; 14: 159–169
11 *Kupchan SM, Britton RW, Ziegler MF, Sigel CW.* Bruceantin, a new potent antileukemic simaroubolide from *Brucea antidysenterica*. J Org Chem 1973; 38: 178–179
12 *Hara S, Okabe H, Mihashi K.* Gas-liquid chromatographic separation of aldose enantiomers as trimethylsilyl ethers of methyl 2-(polyhydroxyalkyl)-thiazolidine-4-(R) carboxylates. Chem Pharm Bull 1987; 35: 501–506
13 *Iaccio A, Collinet C, Montesano Gesualdi N, Ammendola R.* Protein kinase C-alpha and -delta are required for NADPH oxidase activation in WKYMVm-stimulated IMR90 human fibroblasts. Arch Biochem Biophys 2007; 459: 288–294
14 *Romano S, D'Angelillo A, Pacelli R, Staibano S, De Luna E, Bisogni R, Eskelinen EL, Mascolo M, Calì G, Arra C, Romano MF.* Role of FK506-binding protein 51 in the control of apoptosis of irradiated melanoma cells. Cell Death Differ 2010; 17: 145–157
15 *Fang JM, Chen YC, Wang BW, Cheng YS.* Terpenes from hearthwood of *Juniperus chinensis*. Phytochemistry 1996; 41: 1361–1365
16 *Su WC, Fang JM, Cheng YS.* Labdanes from *Cryptomeria japonica*. Phytochemistry 1994; 37: 1109–1114
17 *Garbarino JA, Oyarzun M, Gambaro V.* Labdane diterpenes from *Araucari araucana*. J Nat Prod 1987; 50: 935–936
18 *Su WC, Fang JM, Cheng YS.* Diterpenoids from leaves of *Cryptomeria japonica*. Phytochemistry 1996; 41: 255–261
19 *San Feliciano A, Medarde M, Lopez JL, Del Corral M, Puebla P, Barrero AF.* Terpenoids from leaves of *Juniperus thurifera*. Phytochemistry 1988; 27: 2241–2248
20 *Hasegawa S, Hirose Y.* A diterpene glycoside and lignans from seed of *Thujopsis dolabrata*. Phytochemistry 1980; 19: 2479–2481
21 *Sakar MK, Er N, Ercil D, Del Olmo E, San Feliciano A.* (−)-Desoxypodophyllotoxin and diterpenoids from *Juniperus nana* Willd. berries. Acta Pharm Turcica 2002; 44: 213–219
22 *Fang JM, Sou YC, Chiu YH, Cheng YS.* Diterpenes from the bark of *Juniperus chinensis*. Phytochemistry 1993; 34: 1581–1584
23 *De Pascual TJ, Barrero AF, Muriel L, San Feliciano A, Grande M.* New natural diterpene acids from *Juniperus communis*. Phytochemistry 1980; 19: 1153–1156
24 *Herz W, Watanabe K.* Sesquiterpene alcohols and triterpenoids from *Liatris microcephala*. Phytochemistry 1983; 22: 1457–1459
25 *Estevez-Braun A, Estevez-Reyes R, Gonzalez AG.* ^{13}C NMR assignments of some dibenzyl-γ-butyrolactone lignans. Phytochemistry 1996; 43: 885–886
26 *Kizu H, Shimana H, Tomimori T.* Studies on the constituents of *Clematis* species. The constituents of *Clematis stans* SIEB. et ZUCC. Chem Pharm Bull 1995; 43: 2187–2194
27 *Lehman TA, Bennett WP, Metcalf RA, Welsh JA, Ecker J, Modali RV, Ullrich S, Romano JW, Appella E, Testa JR, Gerwin BI, Harris CC.* p53 mutations, ras mutations, and p53-heat shock 70 protein complexes in human lung carcinoma cell lines. Cancer Res 1991; 51: 4090–4096
28 *Serrano M, Lin AW, McCurrach ME, Beach D, Lowe SW.* Oncogenic ras provokes premature cell senescence associated with accumulation of p53 and p16INK4a. Cell 1997; 88: 593–602
29 *Groth A, Weber JD, Willumsen BM, Sherr CJ, Roussel MF.* Oncogenic Ras induces p19ARF and growth arrest in mouse embryo fibroblasts lacking p21Cip1 and p27Kip1 without activating cyclin D-dependent kinases. J Biol Chem 2000; 275: 27473–27480
30 *Roper E, Weinberg W, Watt FM, Land H.* p19ARF-independent induction of p53 and cell cycle arrest by Raf in murine keratinocytes. EMBO Rep 2001; 2: 145–150
31 *Olsen CL, Gardie B, Yaswen P, Stampfer MR.* Raf-1-induced growth arrest in human mammary epithelial cells is p16-independent and is overcome in immortal cells during conversion. Oncogene 2002; 21: 6328–6339
32 *Esposito F, Cuccovillo F, Vanoni M, Cimino F, Anderson CW, Appella E, Russo T.* Redox-mediated regulation of p21(waf1/cip1) expression involves a post-transcriptional mechanism and activation of the mitogen-activated protein kinase pathway. Eur J Biochem 1997; 245: 730–737
33 *Park JW, Jang MA, Lee YH, Passaniti A, Kwon TK.* p53-independent elevation of p21 expression by PMA results from PKC-mediated mRNA stabilization. Biochem Biophys Res Commun 2001; 280: 244–280
34 *Ryu MS, Lee MS, Hong JW, Hahn TR, Moon E, Lim IK.* TIS21/BTG2/PC3 is expressed through PKC-delta pathway and inhibits binding of cyclin B1-Cdc2 and its activity, independent of p53 expression. Exp Cell Res 2004; 299: 159–170
35 *Sheppard FR, Kelher MR, Moore EE, McLaughlin NJ, Banerjee A, Silliman CC.* Structural organization of the neutrophil NADPH oxidase: phosphorylation and translocation during priming and activation. J Leukoc Biol 2005; 78: 1025–1042

This is a copy of the author's personal reprint